GEMATON: LIVING AND DYING IN A KUSHITE TOWN ON THE NILE

Volume IV

Bioarchaeology

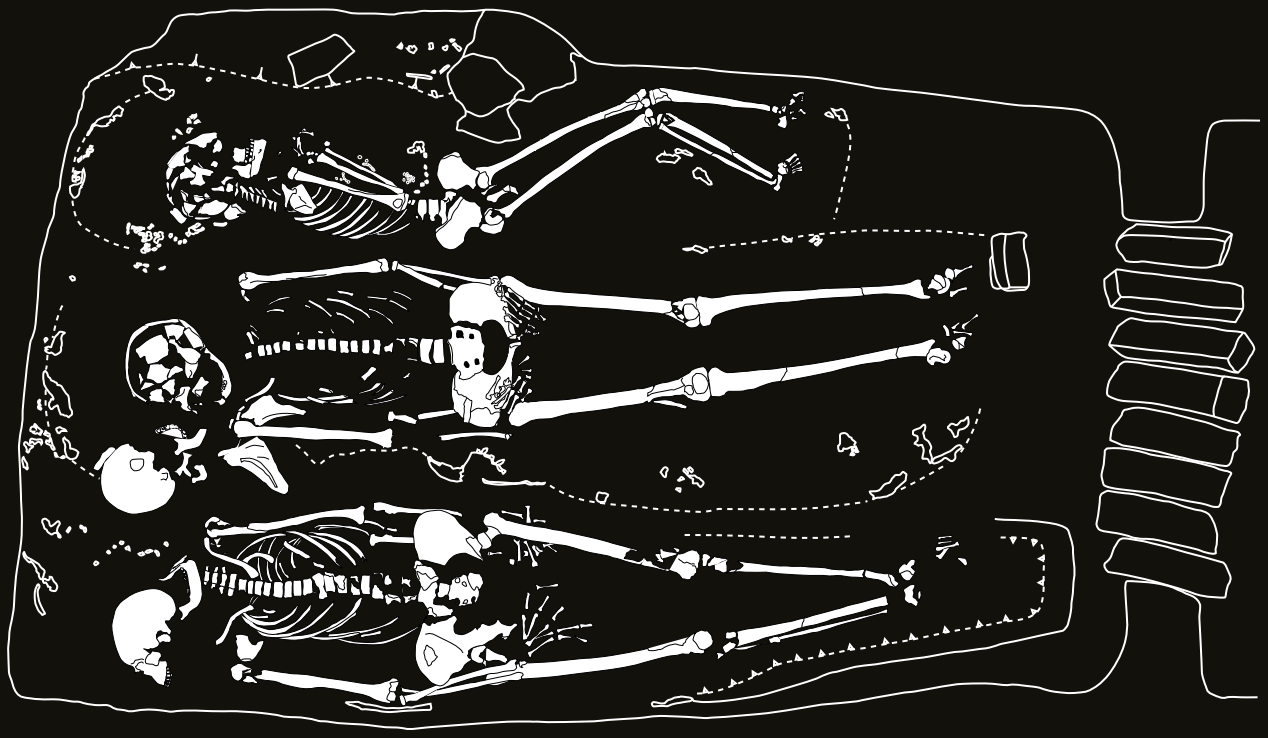

Anna M. Davies-Barrett
Tatiana Vlemincq-Mendieta
Pernille Bangsgaard

GEMATON: LIVING AND DYING IN A KUSHITE TOWN ON THE NILE

Volume IV

Archaeopress Publishing Ltd
Summertown Pavilion
18-24 Middle Way
Oxford OX2 7LG

www.archaeopress.com

Sudan Archaeological Research Society

Publication Number 30
Editor of this volume: D. A. Welsby

ISBN 978-1-80327-887-2
ISBN 978-1-80327-888-9 (e-Pdf)

Front cover: Kawa, skeletons in grave (HA2)94.
Back cover: Skeletons in the cemetery and a bucranium in Building F1.

This book is obtainable from The Sudan Archaeological Research Society
c/o Department of Egypt and Sudan, The British Museum, London WC1B 3DG
or from the Society's website http://wwww.sudarchrs.org.uk

Also available direct from Archaeopress or from our website www.archaeopress.com

SUDAN ARCHAEOLOGICAL RESEARCH SOCIETY
PUBLICATION NUMBER 30

GEMATON: LIVING AND DYING IN A KUSHITE TOWN ON THE NILE

Volume IV

Bioarchaeology

by

Anna M. Davies-Barrett
Tatiana Vlemincq-Mendieta
Pernille Bangsgaard

with contributions by

Rebecca J. Whiting
Derek A. Welsby

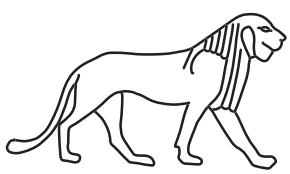

SARS
LONDON
2024

GEMATON: LIVING AND DYING IN A KUSHITE TOWN ON THE NILE

Volume IV

Bioarchaeology

Contents

List of Tables

2. The Human Remains from Kawa

3. The Faunal Remains from Kawa

List of Figures

1. Introduction

2. The Human Remains from Kawa

3. The Faunal Remains from Kawa

List of Plates

2. The Human Remains from Kawa

3. The Faunal Remains from Kawa

1. Introduction

Derek A. Welsby

It had been the intention to devote this volume to reports on the bioarchaeological material recovered during the excavations at Kawa between 1997 and 2018. Unfortunately the report on the floral remains is delayed and therefore, so as not to hold up the publication of the human and animal bone, is not included here. For a report on some of the archaeobotanical material from Kawa, published in *Sudan & Nubia,* see Fuller 2004.

The designation of graves and skeletons in the report on the human remains is in the format (grid square)context number in most cases. However a small number of graves in the cemetery, site R18, was visible on the surface and each of these was excavated individually. In those cases the number in curved brackets is the feature number relating to the survey of the site in 1993 and following the location of grave cuts on the surface during the 2000 season. All feature numbers between (1055) and (1083) were subsequently grouped into Area (HA1).

The articulated human skeletons were excavated either by the physical anthropologist present as a member of the Sudan Archaeological Research Society's team or by some of the particularly skilled local workmen under the general supervision of the anthropologist. Bodies were recorded *in situ* and lifted and bagged by the physical anthropologist, two of whom are among the authors of the report published here.

Physical anthropologists present in the field:-

2000	January-March	Margaret Judd
2000-1	December-February	Margaret Judd
2001-2	December-February	Margaret Judd
2007-8	December-February	Iwona Kozieradzka
2009-10	December-February	Emilie Gustafsson
2010-11	December-February	Natasha Kalogirou
2013	January-February	Rebecca Whiting
2013-14	December-February	Rebecca Whiting
2014-15	December-February	Bonnie Knapp
2017	January-March	Tatiana Vlemincq-Mendieta
2017-18	December-February	Tatiana Vlemincq-Mendieta

During, and on the completion of, the excavation project the skeletal material was donated to SARS by the National Corporation for Antiquities and Museums and, with its permission, passed on to the British Museum for permanent curation. Once there it was studied in detail in the Barbara Mertz Bioarchaeology Laboratory within the Department of Egypt and Sudan. The EA Number noted in the catalogue of the human bone is the object number of each skeleton accessed into the collections of the Department of Egypt and Sudan.

The animal remains were recovered during the excavation of the deposits in which they lay. Unfortunately it did not prove possible for the archaeozoologist to examine them *in situ* and their fragility in many cases resulted in considerable fragmentation of the material. An initial study of some of the material was made by Kim Burrows based in the excavation house in the 2009-10 season and by Pernille Bangsgaard in the 2008-9 and 2010-11 seasons.

In Volume I of the Kawa reports the presence of human and animal bones is recorded based on the information available immediately before the report went to press. Subsequently, during the completion of the Bioarchaeology volume, a small amount of additional material was examined. Where this material is not mentioned in Volume I attention is drawn to this fact so that this material can be taken into account when reading, in particular, the report on the excavation in the cemetery.

The sites in Sudan mentioned within the reports are located on Figure 1.1.

Dr Patricia Spencer kindly copy edited this volume. Any remaining errors are the full responsibility of the individual authors.

Figure 1.1. Sites in Sudan mentioned within the reports.

2. The Human Remains from Kawa

Anna M. Davies-Barrett and Tatiana Vlemincq-Mendieta

with contributions by Rebecca J. Whiting

1. Introduction

The association of a cemetery with a large excavated town site, such as Kawa, provides an excellent opportunity to contextualize the lived experiences of a population for which, otherwise, little may be known. Investigations of the Kushite town itself have revealed a multifaceted society, in which industry, religion and administration were performed alongside elite monument and temple building and more domestic activities. The excavation of domestic houses provides more information about the conditions in which people were living, while artefacts recovered from the site can illuminate the kinds of activities that may have been undertaken (Welsby 2023c). Analysis of human remains, particularly of a large cemetery population, when combined with archaeological knowledge of the town, allows for a greater understanding of the ways in which every-day people lived during this period and how conditions and activities in the town might have affected their health. Such information is vital for understanding the different potential lifeways of the Kushite period.

Lying to the east of the town, a large cemetery, designated as site R18, was detected in surveys in 1993. Investigation of a grave marked by a tumulus in 1993 from Area (KE5) of the cemetery recovered a middle-adult male, with a further five individuals recovered from secondary burials cut into the grave monument. The analysis of these human remains has been fully published separately (see Judd 2001, 514-515). Following the survey of the cemetery in 1993, and to gain an overview of its use, large scale excavations of four different areas within site R18 were undertaken up until 2018 (Welsby 2023b). Of the 112 graves fully excavated after the initial 1993 survey and tumulus excavation, 135 complete or semi-complete human skeletons were recovered. These graves constitute only 1% of the estimated total cemetery area, which geophysical magnetic imaging has revealed is extensive (Herbich 2023). Dating of a number of the burials has been achieved through pottery analysis (Welsby Sjöström 2023) and from a small number of other artefacts (Welsby 2023h). The results indicate that burials date to the Kushite period, from both the Napatan and Meroitic phases (*c*. 8th century BC to the 3rd century AD), with the majority of pottery recovered dating to the Meroitic period (Welsby 2023e; Welsby Sjöström 2023).

While burial positions did vary, skeletons were mainly found in an extended supine position, aligned east-west, with the head to the west. It is likely that many, if not most/all, graves were marked by monuments and a range of social strata is represented in the cemetery. The presence of the very elite within the cemetery is evidenced by the construction of dressed-stone pyramids, six of which have been excavated in Area (J), with parallels to Kushite royal burials at el-Kurru, Nuri, Meroe and Jebel Barkal (Welsby 2023h, 376-377). A total of 13 individuals were recovered from contexts associated with these pyramids, although many came from multiple simultaneous burials (e.g. grave (JE3)132 marked by Pyramid S3) and it remains difficult to identify which were the intended main occupants and which represent secondary burials. Furthermore, the status of those of more modest background also remains difficult to decipher as the monuments that likely marked the graves have long been lost to wind erosion and finds of grave goods remain modest. This is exacerbated by the fact that extensive looting has taken place across the cemetery, both in antiquity and more recently (Welsby 2023h), resulting in the disarticulation and fragmentation of skeletons and the likely loss of grave goods. Further complementary information about the grave structures, burial types, and finds are presented in Chapters 11 and 12 of Volume I of the SARS monograph series on Kawa (Welsby 2023a).

An additional human skeleton [(FP6)30], located within Room VI of Building F1, in the town (site Q3), was also recovered. As it is not known if this skeleton is contemporaneous with burials from site R18, the individual has not been included in the following population-level analysis. Instead, information on skeleton (FP6)30 can be found in section 7.

The human remains recovered from Kawa were generously donated by the National Corporation for Antiquities and Museums of Sudan (NCAM) to the Sudan Archaeological Research Society, which in turn donated them to the British Museum for permanent curation and analysis. This report presents the synthesis of skeletal analysis of the human remains excavated, providing an overview of skeletal preservation, cemetery demographics, metric and non-metric biological variation, and skeletal and oro-dental pathology. The data were recorded according to the standards established by the Barbara Mertz Bioarchaeology Laboratory at the British Museum. These methods generally follow those recommended by Buikstra and Ubelaker (1994), but also include other established methods of osteological assessment, as detailed below. The limitations of these recording methods are discussed, where appropriate. A skeletal catalogue, including data on preservation, completeness, skeletal sex, estimated age, estimated stature, and pathology for each individual, can be found in section 10. Further, raw data for all individuals included in this report can be obtained by contacting the Curator for Bioarcheology at the British Museum.

2. Preservation

The completeness of a skeleton and the preservation of the bones can have a direct impact on the information that can be obtained from them. Preservation may vary between skeletons from the same assemblage, or between

skeletal elements from the same individual. Factors such as presence or absence of bones, surface preservation, staining, fragmentation, and other taphonomic damage caused within the burial can all affect the observability of pathological changes or skeletal variations. Thus, it is vital to have an understanding of the level of preservation within an assemblage. Preservation of each skeleton from site R18 was assessed using three criteria: completeness of skeletal elements, overall taphonomic and fragmentary state of the bone, and cortical surface preservation.

The completeness of each individual was recorded in 5% increments for the following groups of skeletal elements: skull, dentition, vertebrae, ribs and sternum, upper limbs, hands, pelvis, lower limbs, and feet. The percentage scores were then averaged to produce an overall percentage of completeness for each individual. All skeletal element groups ranged in completeness from 0% to 100% across the entire assemblage, with a range of between 2% and 98% in overall completeness. Table 2.1[1] demonstrates the average percentage scores within the assemblage for each group of skeletal elements and for the overall completeness.

The taphonomic and fragmentary state of the bone was recorded according to the method used by Judd (2001), after Behrensmeyer (1978). This method provides a general assessment of the condition of the skeleton, taking into account fragmentation, weathering, and other forms of damage. The categories consisted of a numerical score with associated description:

1. Excellent: bones are solid with little or no breakage or erosion.
2. Good: bones are generally in a good condition but there is some breakage.
3. Fair: some regions of bone are missing, crushed, friable, or flaking.
4. Poor: most bones are broken, cracked, splintered, and/or weathered, with regions missing.
5. Fragments: all bones are very friable, splintered, or fragmented, with extreme weathering and little identification of morphological features possible.

The majority of skeletons ranged from between scores 2 (Good) and 4 (Poor), with an average score of 3 (Fair) (Table 2.2).

The outer cortical bone surface preservation of each skeleton was also recorded after Bello *et al*. (2006). This method assesses the estimated percentage of the cortical surface affected by weathering or other forms of post-mortem damage. The categories consisted of a numerical score conforming to the percentage of the cortical surface affected:

1. 0% of the cortical surface is sound.
2. 1-24% of the cortical surface is sound.
3. 25-49% of the cortical surface is sound.
4. 50-74% of the cortical surface is sound.
5. 75-99% of the cortical surface is sound.
6. 100% of the cortical surface is sound.

[1] For the tables see pages 99-163.

The cortical surfaces of the skeletons from site R18 were generally fairly well preserved, with an average score of 4.6, the majority of individuals having 75-99% sound cortical surfaces (Table 2.3).

While in most cases the preservation of the skeletons was fair, allowing for observation of the majority of the bone surfaces, the preservation and completeness scores demonstrate a wide variation across the cemetery. Looting of the cemetery was extensive, and this contributed in many instances towards disarticulated material, fragmentation, and exposure of the skeletons to bleaching and weathering. Additionally, there were some specific taphonomic processes observed on the skeletons from site R18. In particular, termite damage to the bone was noted in 47% (64/135) of all skeletons, targeting the medullary cavity of the long bones and in some cases causing extensive damage to the cortical surfaces, resulting in fragmentation (Plate 2.1.A). The typical appearance of termite damage can often mimic pathological changes to the bone, known as pseudopathology. Therefore, particular care was taken to differentiate alteration to the bone by termites from pathological processes. Dark mottled and purple staining, possibly related to fungal or bacterial activity, was noted on 58% (78/135) of all skeletons (Plate 2.1.B) and may have also made it difficult to observe subtle pathological changes. Similar taphonomic changes – termite damage and mottled staining – have also been observed at the *Kerma Ancien* cemetery, site H29 (Whiting 2018, 152), located within the Northern Dongola Reach 30km to the south south east of Kawa.

Plate 2.1. Taphonomic changes to the cortical surfaces of bone. A. Dark mottled staining on a fragment of right parietal [Skeleton (JE3)187]. B. Termite damage to the patellofemoral joint surface of the left femur, mimicking bone destruction caused by pathological changes [Skeleton (GD3)127].

Each element of the skeleton and, in the case of the long bones, several separate sections of each bone were also recorded for completeness. This consisted of measuring the percentage of each bone, or bone section, that was present using the following scores, after Buikstra and Ubelaker (1994):

0. Bone (or bone section) absent.
1. Greater than 75% of the bone (or bone section) present.
2. Between 25% and 75% of the bone (or bone section) present.
3. Less than 25% of the bone (or bone section) present.

Recording of the completeness of individual skeletal elements in this way allowed for a more accurate calculation of the true prevalence of pathological changes.

3. Demography

3.1 Age-at-death estimation

The estimation of age-at-death allows for a comparison of the demographic profile of cemeteries across different time periods and/or geographical locations. It also makes possible a comparison of the prevalence of pathological changes, for which age may be a contributing factor, within different age groups.

Skeletons were grouped into the following age categories:

Nonadult age estimation

Preterm: less than 37 foetal weeks.
Fullterm: 37 to 42 foetal weeks.
Infancy: from birth to less than 2 years.
Early childhood: 2 to less than 6 years.
Late childhood: 6 to less than 11 years.
Puberty: 11 to less than 16 years.
Adolescence: 16 to less than 20 years.

Adult age estimation

Young adult: 20 to less than 35 years.
Middle adult: 35 to less than 50 years.
Old adult: 50 years or greater.

Additionally, preservation did not always allow for the precise age of an individual to be estimated. In these instances, the skeleton was allocated to one of the following categories based on the developmental stage of the skeleton:

Undetermined adult: 20 years or greater.
Undetermined nonadult: less than 20 years.

These age categories are based on those proposed by Buikstra and Ubelaker (1994, 36), also taking into account nonadult groupings suggested by White *et al*. (2012, fig. 18.1).

Age-at-death of nonadults was determined using the developmental stages of the skeleton and dentition, specifically by assessing the stage of epiphyseal fusion (Schaefer *et al*. 2009, using the scoring system provided by Buikstra and Ubelaker 1994), the stage of dental development (Ubelaker 1978), and skeletal metrics (Cunningham *et al*. 2016). Dental development is considered to be affected to a lesser degree by environmental factors, when compared with skeletal development (e.g. Lewis and Flavel 2006). For example, skeletal growth and subsequent long bone lengths can be impacted by a number of environmental factors, such as malnutrition, illness or maternal health (Lewis 2007, 66-68). The reference material used to correlate skeletal metrics with age originated from various populations (Schaefer *et al*. 2009), who may have been affected by different environmental factors or genetic growth rates, although this is also true for dental development stages, which were produced using Native American populations (Ubelaker 1978). While all methods were used to establish age when preservation allowed, the stage of dental development was preferentially applied if results from each method conflicted.

Age-related degeneration of the pubic symphyses and auricular surfaces of the os coxae were used to determine adult age-at-death, using scoring methods developed by Brooks and Suchey (1990) and Lovejoy *et al*. (1985). The mean age corresponding to each pubic symphysis score and the modal age range corresponding to each auricular surface score were used to determine into which age group a skeleton should be allocated. Score 1 of the pubic symphysis method corresponded to an age group of either adolescent or young adult, depending on the accompanying epiphyseal fusion data. Scores 1, 2 and 3 of the auricular surface method and scores 2 and 3 of the pubic symphysis method corresponded to the young adult age group. Scores 4, 5 and 6 of the auricular surface method and scores 4 and 5 of the pubic symphysis method corresponded to the middle adult age group. The old adult age group consisted of pubic symphysis score 6 and auricular surface scores 7 and 8.

3.2 Nonadult age distribution

A total of 58 nonadults were present in the assemblage, making up 37% (58/135) of the collection (Table 2.4). It was not always possible to provide an exact age category for all nonadult individuals. Those that demonstrated skeletal development stages across two different age categories were allocated to the undetermined nonadult category. Within this group, one individual [(JH3)142] spanned both the late childhood and puberty categories, two individuals spanned both the puberty and adolescent categories [(GD3)86, (JE3)196], and one individual could not be assigned to any specific nonadult age group due to incompleteness [(JH4)61]. The majority of nonadults belonged to the infancy group, followed by the early childhood and late childhood categories (Figure 2.1). This is consistent with an increased risk of mortality during the early stages of life (Lewis 2007, 81-87). No preterm individuals were identified in the assemblage.

Although disarticulated remains are discussed in section 8, it is prudent to add that in graves (JF2)20 and (JD2)12 the disarticulated remains of at least one nonadult, probably infant, were discovered. As these remains could not be firmly connected to the burial contexts (in fact some fragmentary adult remains were also associated with (JF2)20), they were, therefore, not included in the overall analysis.

3.3 Adult age distribution

A total of 77 adults were identified, making up 57% (77/135) of the assemblage (Table 2.5). One individual [(1083)11] demonstrated skeletal development stages consistent with both adolescence and young adult age groups and could not be reliably allocated to either. This individual was recorded according to the methods for adult skeletons in this study and has been included in the adult group. The majority of adults belonged, fairly equally, to either the young or middle adult age categories (Figure 2.1). However, due to poor preservation in some instances, particularly of the pelves (with only an average completeness of 54%), a quarter of all adults could not be allocated an age category beyond that of undetermined adult.

Only one skeleton [(JH4)51] was allocated to the old adult age category. While this can indicate that individuals at site R18 may not have been surviving into older adulthood or were buried elsewhere in an unexcavated part of the cemetery, this may also reflect an aging bias in the methods used. The pubic symphysis and auricular surface age estimation

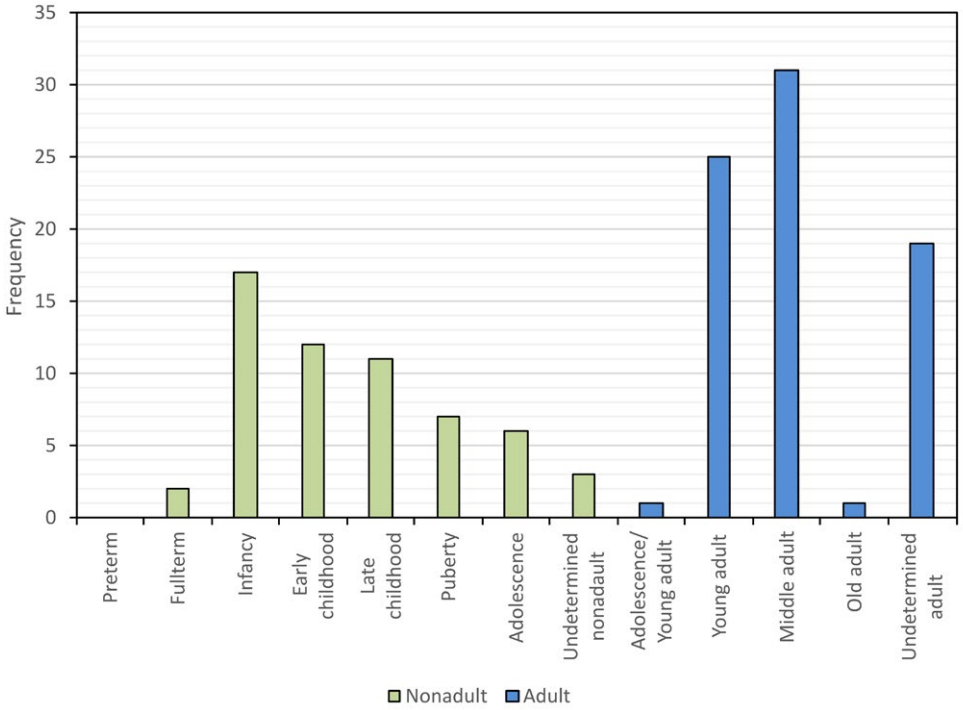

Figure 2.1. The frequency of individuals in each age category.

methods were developed using collections consisting for the large part of US black and white individuals of known-age (Brooks and Suchey 1990; Katz and Suchey 1989; Lovejoy *et al*. 1985). However, when these methods have been applied to other known-age-at-death human skeletal collections from various geographical regions, a general increase in inaccuracy with increasing age has been found (e.g. Hoppa 2000; Klepinger *et al*. 1992; Miranker 2016; Sakaue 2006; Santos 1996; Schmitt 2004). Unfortunately, as the accuracy of these age estimation methods have not been investigated using Sudanese populations with known-age data, it is not possible to tell if a bias towards under-aging using these methods was present in the current study.

3.4 Adult skeletal sex estimation

Assessing the skeletal sex of adults allows for a comparison of the demographic profiles and sex-based metric and non-metric data from different cemeteries. It also facilitates the investigation of differences in the prevalence of pathological changes between the sexes, which could highlight sex-based differences in social organisation and cultural practices.

Skeletal sex was estimated using sexually dimorphic features of the skull and pelvis (Buikstra and Ubelaker 1994). In the skull, the following morphological features were observed: nuchal crest, mastoid process, supraorbital margin, glabella, gonial angle, mandibular eminence, gonial flaring, and mandibular ramus (Acsádi and Nemeskéri 1970; Brickley 2004, 23-24; Buikstra and Ubelaker 1994, 19-20). In the pelvis, the following morphological features were observed: ventral arc, subpubic concavity, ischiopubic ramus ridge, greater sciatic notch, preauricular sulcus, composite arch, and ischiopubic proportions (Bruzek 2002; Buikstra and Ubelaker 1994, 16-19; Phenice 1969). The morphological expression of each feature was given a numerical score according to the criteria of the original method.

Based on the numerical score recorded for each feature, an individual was assigned to one of the following groups recommended by Buikstra and Ubelaker (1994):

Male: male.
Male?: probable male.
Intermediate: expressing intermediate features or a mixture of both male and female traits.
Female?: probable female.
Female: female.
Undetermined sex: unobservable features due to poor preservation.

Sexually dimorphic features of the pelvis are generally considered to be the most reliable indicators of skeletal sex, due to its reproductive function (Bass 2005, 207; Garvin *et al*. 2014; Meindl *et al*. 1985). In addition, it has been noted that skulls of Sudanese ancestry often demonstrate a far smaller range in sexual dimorphism, with a tendency towards more gracile features, producing a bias towards female sex estimation (Garvin *et al*. 2014, tab. 2). Thus, the pelvis was generally given greater weight during sex estimation. Estimation of sex in nonadults is problematic, particularly in archaeological populations for which no contemporaneous data on sexually-dimorphic variation in nonadults is available (e.g. Stull *et al*. 2020). Therefore, no attempt was made in this study to estimate the skeletal sex of nonadults.

Table 2.6 presents the total proportion of individuals in each skeletal sex group, including distribution by age. As would be expected, the majority of individuals for whom age could not be determined were also allocated to the undetermined sex group due to poor preservation of the pelvis, which is required for both age and sex estimation.

To facilitate further analysis of metric and non-metric data according to skeletal sex, throughout this report these categories have been combined into the simplified groups of male, female, and undetermined. A total of 28 individuals were assigned to the combined female group (consisting of the female and female? categories), 27 individuals to the

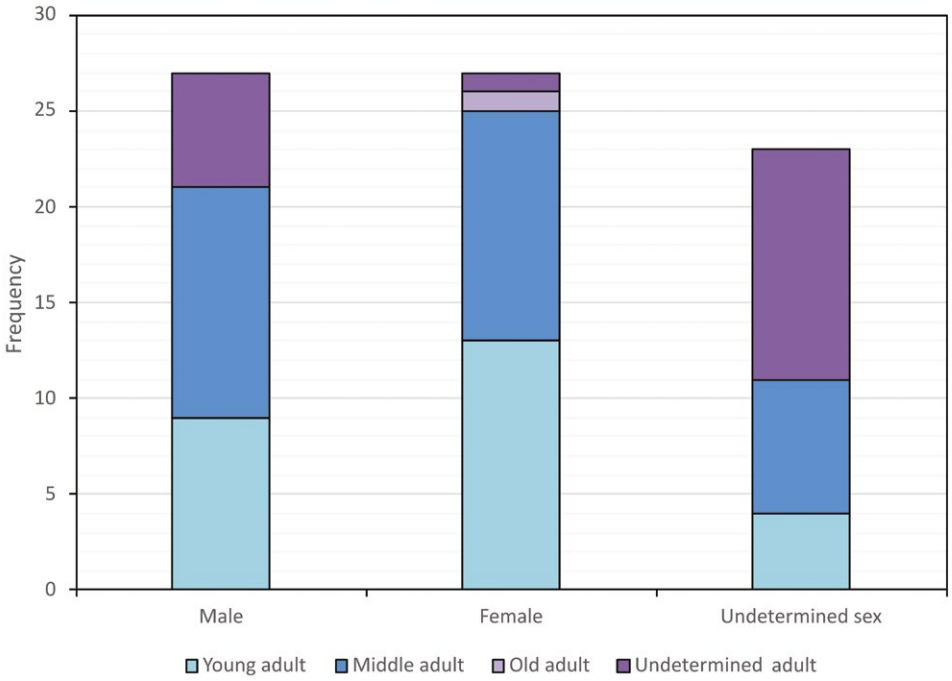

Figure 2.2. The frequency of adults in each combined skeletal sex category, according to age group.

combined male group (consisting of the male and male? categories), and 23 to the combined undetermined sex group (consisting of the intermediate and undetermined sex categories) (Figure 2.2). The frequency of male and female individuals of both young and middle adult age was relatively equal, although there was a higher number of males allocated to the undetermined adult age category.

4. Biological variation

4.1 Non-metric traits

Certain regions of the skeleton may have slight morphological variations, such as additional foramina, apertures, and cranial sutural bones, or extension or variation in the morphology of joint facets. Some of these variations, known as non-metric traits, have been linked to genetic expressions that could provide an understanding of biodistance between populations, although the development of these traits may also be affected by environment, age and sex (e.g. Buikstra and Ubelaker 1994, 85-86; Carson 2006; Stojanowski and Schillaci 2006; Trinkaus 1978; Tyrell 2000, 298-299).

The non-metric traits recorded in this study are those described by Buikstra and Ubelaker (1994, 87-94), Brothwell (1981, 90-100), Finnegan (1978) and Rose *et al*. (1991). Whilst many traits were recorded simply as present or absent, such as the sutural bones, some traits have accompanying scoring methods to measure the degree of morphological variation. When applicable, the prevalence rate for each score has been presented and the morphological descriptions associated with each score can be found in Table 2.7. As the skeleton in nonadults is still undergoing development, which may cause some confusion between the presence or absence of certain traits, only adults were systematically scored for non-metric traits.

Adults

The prevalence of cranial non-metric traits (Table 2.8), sutural bones (Table 2.9) and post-cranial non-metric traits (Table 2.10) were all recorded. Notable prevalence rates of certain non-metric traits are discussed here. The most prevalent sutural bone was the lambdoid ossicle, with 35.5% (11/31) of left lambdoid sutures and 23.3% (7/30) of right lambdoid sutures having at least one ossicle. Similar results have been found from the Meroitic site of Jebel Moya, where 44.6% of individuals were observed to have a lambdoid ossicle. This is slightly higher than in Egyptian collections, which range in prevalence from 31.6% to 37% (Berry and Berry 1972, tab. 1). However, the prevalence of this trait is lower in two sites dating to the A- and C-Group from Lower Nubia, located closest to Kawa but separated in time by over a millennium, which range from 16.3% (7/43) to 20% (1/5) (Prowse and Lovell 1995, tab. 2).

A high prevalence of septal apertures was noted in individuals from site R18, where a total of 56.9% (29/51) of left humeri and 59% (24/49) of right humeri demonstrated either a small pinhole or large perforation in the coronoid-olecranon fossa. This is similar to the situation observed in the *Kerma Ancien* cemetery at site H29, where 75% (21/28) of left and 77.3% (17/22) of right humeri demonstrated septal apertures (Whiting 2018, tab. 6.5). Other populations have presented far lower prevalence rates of this non-metric trait. For example, a range in prevalence of between 1.8% and 10.9% has been found in medieval English and modern US collections (Mays 2008, tab. 7). Many factors have been suggested to have an effect on the development of the septal aperture, including genetics, joint laxity and impingement, bone robusticity, and the morphology of the coronoid process of the ulna (Kubicka *et al*. 2015, 2031). The high prevalence of septal apertures in Sudanese groups certainly indicates that population specific factors may have been involved.

Lateral squatting facets were also highly prevalent at Kawa, affecting 67.5% (27/40) of left tibiae and 70.5% (31/44) of right tibiae. A similarly high prevalence has been found in a study of an Egyptian collection, in which 96% of skeletons exhibited lateral squatting facets (Satinoff

1972, 210-211). It has been suggested that the development of squatting facets may be associated with pressure on the ankle and hyperdorsiflexion of the joint during activities such as squatting (Trinkaus 1975, 330). Although the lateral squatting facet is frequent in many populations (Trinkaus 1975), a high prevalence has been recorded in cultures that habitually adopt the squatting posture, and a decrease in the trait has been observed over time in French and US populations corresponding to changes in internal housing structures and furnishings that no longer required the use of the squatting posture (Boulle 2001). This could indicate that squatting was a habitual posture for many of the individuals buried at site R18, although other types of activity or genetic factors related to joint development may also be involved.

Nonadults

Although the true prevalence of non-metric traits was not systematically recorded in nonadults, notable non-metric traits were observed. Two nonadults [(1058)8, (JF2)91] had apical bones and one [(GD3)114] had a supratrochlear spur on the right humerus (Plate 2.2). The latter non-metric trait was not noted in any of the adults.

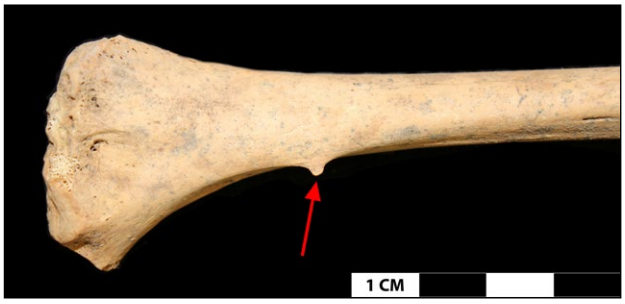

Plate 2.2. A supratrochlear spur (arrow) present on the right humerus of a nonadult [Skeleton (GD3)114].

4.2 Metric data

Metric data, such as long bone length, width or dimensions of specific bone features, can provide information on size and stature between different populations. Variations in bone growth across groups could give an indication of genetic or environmental factors, such as physiological disruption caused by nutritional levels or exposure to disease (Agarwal 2016, 133). Additionally, some changes in bone morphology such as robusticity, which can be reflected in metric data, could be an indication of activity levels (e.g. Ruff and Larsen 2014).

Measurements of nonadult skeletons, used for estimating age, were taken after Fazekas and Kósa (1978), as described in Buikstra and Ubelaker (1994, 44-46). Most measurements and anatomical landmarks for adults were taken after Buikstra and Ubelaker (1994, 69-84). Measurements of the second metacarpal were taken at the midline after Meadows and Jantz (1992) and maximum length of the metatarsals was taken following Byers *et al*. (1989), Rodríquez *et al*. (2013) and Cordeiro *et al*. (2009). All measurements are given in millimetres, unless otherwise indicated. Measurement of bones from the left side of the skeleton was favoured, unless absent or damaged. Mandibular length and mandibular angle measurements were not taken as the specific equipment required for these measurements (a mandibulometer) was unavailable.

Adult metric data

All metric measurements taken in individuals from Kawa are presented in Tables 2.11 (adults) and 2.12 (nonadults). To investigate sexual dimorphism in metric measurements, the range and mean for cranial and mandibular metric data (Table 2.13) and post-cranial metric data (Table 2.14) for males and females were also calculated. While the ranges for different measurements in males and females overlapped, males generally demonstrated a higher mean value. In particular, femoral and humeral head measurements often demonstrate population specific sexually dimorphic differences in size (e.g. Milner and Boldsen 2012). The mean maximum femoral head measurement at site R18 for females was 39mm, while the mean maximum femoral head measurements in males was 45mm. Mean measurements of the vertical diameter of the humeral head were 38mm in females and 45mm in males. Both mean measurements of humeral and femoral head diameter were significantly different according to an independent-sample T-test, which measures variance in mean values between groups (femoral head measurement: $t(45)=-9.234$, $p=<.001$; humeral head diameter: $t(31)=-6.544$, $p=<.001$). Figures 3 and 4 display box and whisker plots comparing male and female femoral and humeral head diameters, respectively. While the lowest range for males and the highest range for females in both femoral and humeral head diameter overlap, the 25th to 75th quartiles do not overlap between the sexes. Therefore, the biological sex of individuals from the undetermined sex group can be tentatively suggested based on whether their femoral or humeral head measurements fall into the 25th to 75th quartiles of either the males or the females, as demonstrated in the figures. Seven individuals of undetermined sex had either humeral or femoral head measurements that fell into the male quartiles, while four had measurements that fell into the female quartiles.

Stature

While the growth of an individual can be affected by both hereditary and environmental factors, comparison of stature between populations can give an indication of growth in different groups or time periods. Stature can be estimated using maximum measurement of the length of a complete long bone. Due to the effect of regional differences and genetic factors on growth, population specific equations for estimating stature provide the most accurate results. Stature regression formulae produced using data from ancient Egyptian skeletons (Raxter *et al*. 2008) provide the closest regional parallel to the population from site R18 and are presented in Table 2.15.

Table 2.16 presents the estimated stature of all male and female adults with available metric data for the maximum length of the femur, tibia, humerus and/or radius. Where available, stature has been calculated using the bone measurement related to the equation with the smallest standard error.

Stature in the combined female group ranged from 145.6cm to 169.3cm, with an average height of 157.7cm.

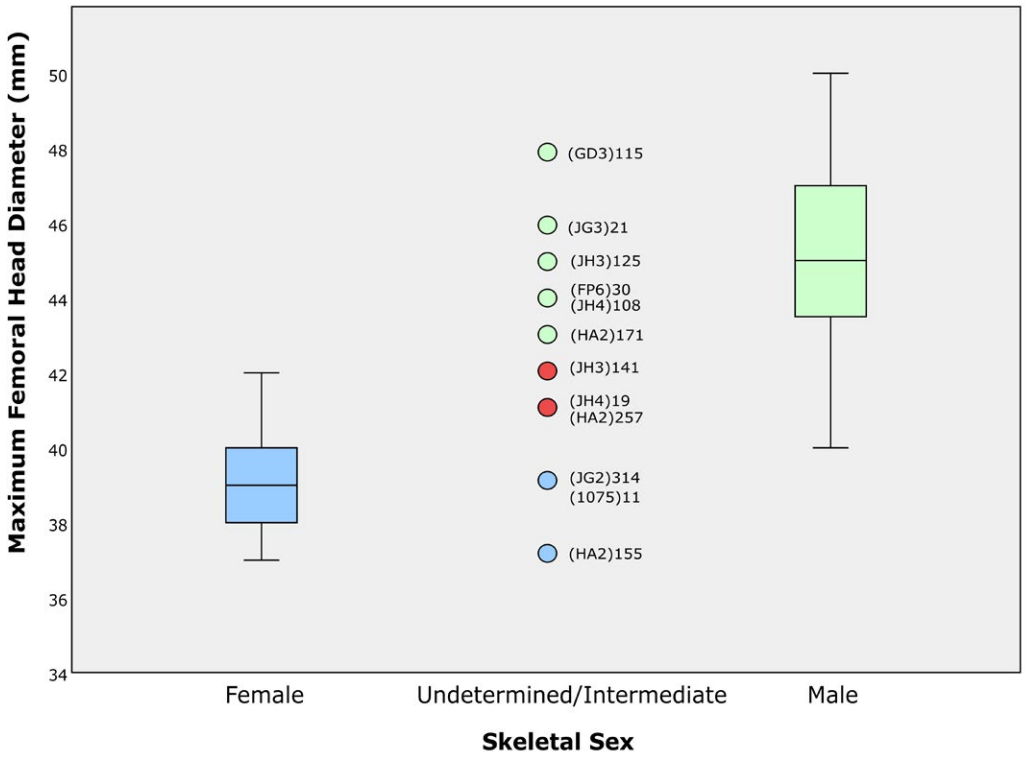

Figure 2.3. A box and whisker plot comparing femoral head diameter (mm) in female and male sex groups. The boxes represent the 25th and 75th quartiles and the whiskers represent the full range of measurements. Individuals of undetermined sex with femoral head measurements are marked on the chart separately. Those in blue represent individuals whose measurement falls below the female 75th quartile, those in green represent individuals whose measurement falls above the male 25th quartile, and those in red represent individuals whose measurement falls within the overlapping range of both male and female measurements.

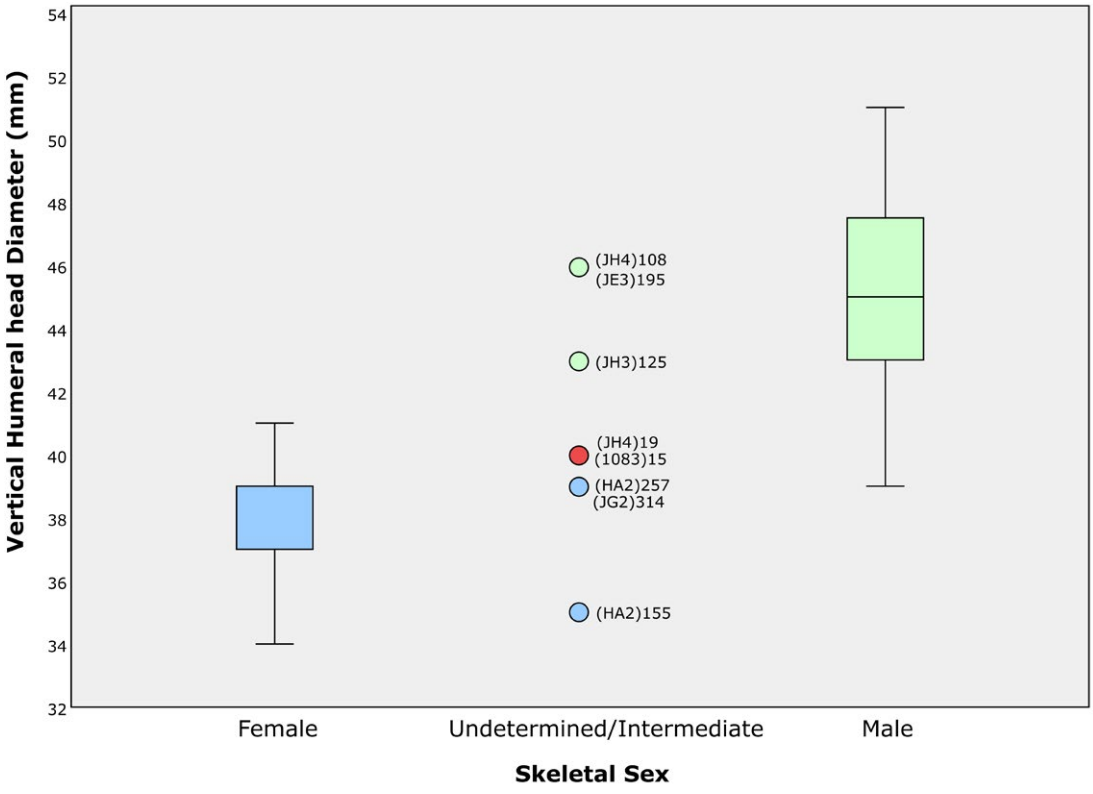

Figure 2.4. A box and whisker plot comparing humeral head diameter (mm) in female and male sex groups. The boxes represent the 25th and 75th quartiles and the whiskers represent the full range of measurements. Individuals of undetermined sex with humeral head measurements are marked on the chart separately. Those in blue represent individuals whose measurement falls below the female 75th quartile, those in green represent individuals whose measurement falls above the male 25th quartile, and those in red represent individuals whose measurement falls within the overlapping range of both male and female measurements.

The combined male group ranged in stature from 156cm to 176.5cm, with an average height of 165.9cm (Figure 2.5). The mean values of stature were significantly different between males and females (t(36)=-4.584, p=<.001) according to an independent-samples T-test. Stature estimates for males and females from site H29 correspond to the estimates from Kawa, with female and male measurements falling within the ranges presented here (150.6-162.3cm for females, 158.7-167.8cm for males), although the sample size is considerably smaller, consisting of only twelve adults (Whiting 2018, tab. 6.11). Pooled medieval Sudanese skeletons from three Fourth Cataract sites also demonstrated similar ranges, with a mean stature estimation of 156.6cm in females (ranging from 149.9cm to 163.5cm) and a mean of 168cm in males (ranging from 152.7cm to 181.3cm) (Niespodziewanski 2014). Both studies also used the regression formulae provided by Raxter *et al*. (2008).

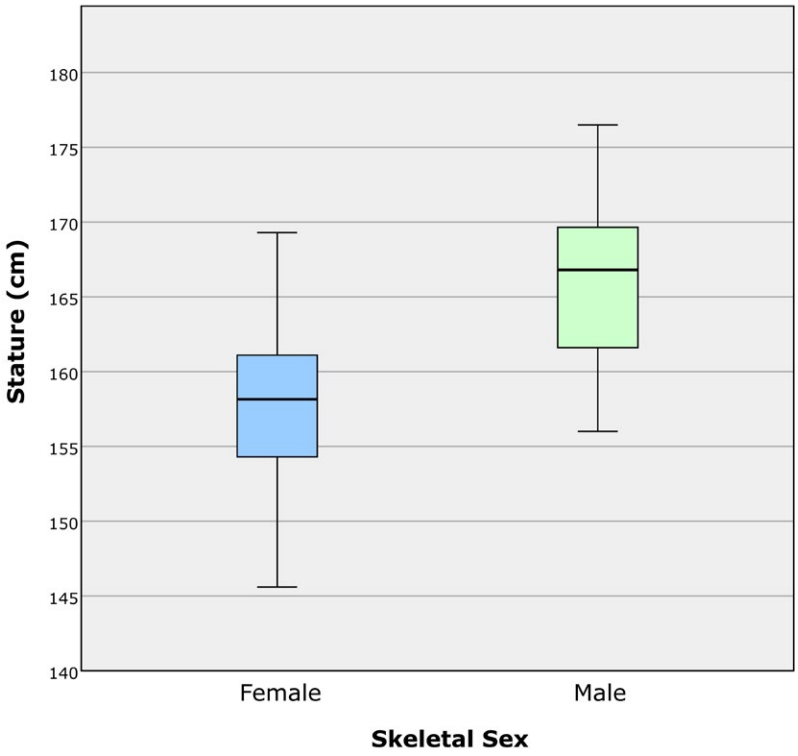

Figure 2.5. A box and whisker plot comparing stature estimates (cm) in female and male sex groups. The boxes represent the 25th and 75th quartiles and the whiskers represent the full range of stature measurements.

5. Skeletal pathology

Palaeopathological analysis of skeletons can provide insight into a host of factors affecting a population, such as diet, economy, trade, living environment, and types of activities and occupations undertaken, and allows for the investigation of the origin and development of diseases throughout human history (e.g. Roberts 2016). Comparisons of prevalence rates of pathological changes between sex or age groups can also give an indication of socio-cultural factors affecting specific members of society (e.g. Roberts and Manchester 2010, 1-20, 29-30).

Where possible, the true prevalence of pathological changes has been presented for all skeletal elements or specific bone regions that were recorded with a completeness score of either 1 or 2 (over 25% complete). As this method takes into account the fact that some skeletons may have the absence of certain skeletal elements and, thus, pathological changes may not be observable, this presents a more accurate understanding of the prevalence of pathological changes in the collection. Unfortunately, due to methods for recording completeness in some skeletal elements, it was not always possible to calculate true prevalence. Additionally, as the skeletal elements included in the calculation of true prevalence were not always 100% complete, some elements may have had missing regions that could have originally displayed pathological changes. Therefore, there will always be a bias towards lower prevalence rates.

Frequencies of pathological changes observed in skeletons from Kawa are presented below according to the type of change and the region of the skeleton affected. A brief description of the specific pathological changes related to each individual skeleton observed can be found in the Skeletal Catalogue in section 10 at the end of this report.

5.1 Joint pathology

Osteoarthritis

Degeneration of the synovial joints, known as osteoarthritis, is a common pathological condition observable in archaeological human skeletons. It develops over time and is affected, among other things, by factors such as genetics, age, body mass and activity (Weiss and Jurmain 2007). Osteoarthritis was scored as either present or absent for all observable joint surfaces according to the operational definition provided by Waldron (2021, 84). These criteria suggest that osteoarthritis should be scored as present when eburnation is observable or when at least two of the following changes to the joint are present: marginal osteophytes, new bone on the joint surface, pitting on the joint surface or alteration to the joint contour. Due to the difficulty in observing degenerative changes in developing joint surfaces, this pathology was systematically recorded in adults only. Further, joint pathology of the vertebrae is presented in section 5.2: 'Vertebral pathology'.

While many joints did not present particularly high rates of observable changes for osteoarthritis (Table 2.17, Figure 2.6), the acromioclavicular joint demonstrated the greatest prevalence, with the distal clavicular facet affected in 47.8% (22/46, left) and 35.7% (15/42, right) of individuals, and the acromial facet of the scapula affected in 31.1% (14/45, left) and 25% (12/48, right) of individuals. Acromioclavicular osteoarthritis can be caused by a number of factors, including age and genetics. However, joint stress or trauma, for example through heavy lifting, throwing, or other repetitive activities involving the joint, can be a major cause (Menge *et al*. 2014). An increased risk of acromioclavicular

osteoarthritis has been found in manual workers repeatedly lifting heavy loads (Stenlund *et al*. 1992). Additionally, males from Kawa demonstrated a far higher prevalence of acromioclavicular osteoarthritis compared to females. When right and left frequencies were combined, a statistically significant difference was observed between male and female prevalence rates of acromioclavicular osteoarthritis (Fisher's Exact Test: distal clavicular joint – p = .026; acromial joint – p = <.001). This may indicate that males were undertaking certain strenuous or traumatic activities involving the acromioclavicular joint to a greater extent than females. It should also be considered, however, that males in this population may have had a genetic predisposition to the development of acromioclavicular osteoarthritis. (e.g. Fernández-Moreno *et al*. 2008).

In addition to acromioclavicular osteoarthritis, two middle adult skeletons [(GD3)106, male; (561)21, female] demonstrated advanced bilateral impingement syndrome of the shoulder, consisting of eburnation caused by contact of the inferior surface of the acromion process with the superior surface of the humeral head (Waldron 2021, 94) (Plate 2.3). This joint disease, produced by the entrapment or 'pinching' of soft tissues during movement of the shoulder and rotator cuff damage, has been linked to repeated forceful overhead movement, among other aetiologies (Kent 2006).

Plate 2.3. Impingement syndrome of the left shoulder joint in a middle adult probable female [Skeleton (561)21]. A. Eburnation and osteophyte formation on the inferior aspect of the acromion process. B. Corresponding changes to the humeral head, including eburnation, pitting and new bone formation on the joint surface.

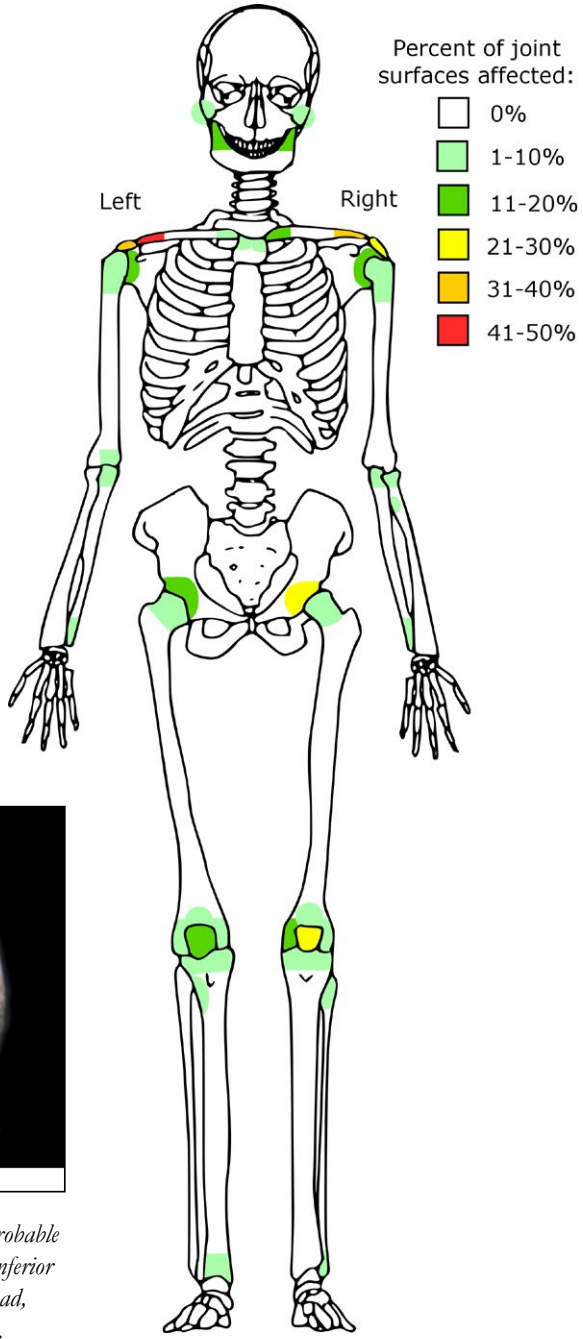

Figure 2.6. The skeletal distribution of osteoarthritis on non-vertebral joints in all adults (prevalence displayed in 10% increments). Image adapted from Buikstra and Ubelaker (1994).

The results for osteoarthritis also indicate that middle adults generally had higher prevalence rates than young adults. This reflects the influence of age as a factor in the development of osteoarthritis (Weiss and Jurmain 2007). Other joints that seemed to have slightly elevated prevalence rates of osteoarthritis include the mandibular condyle (temporomandibular joint), the glenoid fossa on the scapula (glenohumeral joint), the acetabulum of the os coxa (femoroacetabular joint) and the joint surface of the patella (patellofemoral joint) (Figure 2.6). Prevalence rates for these joint surfaces were higher in middle adults, but did not show any notable variation between males and females.

Osteochondritis dissecans

Skeleton (HA2)247, an adolescent, presented with a large circular depression on the medial condyle of the left femur. Approximately 12mm in diameter and 5mm deep, this depression had rounded margins confluent with the joint surface and a smooth floor and walls consisting of remodelled trabecular bone. In association with this lesion was a small piece of bone that rested perfectly inside the depression, known as a 'joint mouse' (Mann and Hunt 2005, 172) (Plate 2.4). The presence of a focal area of subchondral bone that has undergone necrosis, causing it to become separated from the remaining joint surface, is known as osteochondritis dissecans. Factors thought to affect the development of osteochondritis dissecans include genetic predisposition, poor blood supply caused by infection or thrombosis, abnormal ossification and repetitive microtrauma. Although

Plate 2.4. Osteochondritis dissecans of the medial condyle of the left femur, with associated 'joint mouse', in an adolescent [Skeleton (HA2)247]. Top: Joint mouse and associated divot within the medial condyle shown separately. Bottom: Joint mouse shown within divot as it would have been located anatomically in life.

rare, osteochondritis dissecans is more frequently observed in adolescents, particularly in the knee (Hixon and Gibbs 2000). A similar example of osteochondritis dissecans of the femoral condyles has been observed in a nonadult aged 13 to 15 years from a Medieval site in Croatia (Šlaus *et al*. 2010). In clinical instances involving the knee, affected adolescents are typically active in some form of sport (Hixon and Gibbs 2000), which could suggest that this individual was undertaking strenuous activity, although other causes should not be ruled out, particularly considering this individual also presented with Scheuermann's disease (section 5.2), which may have affected the types of activities they would have been able to undertake.

5.2 Vertebral pathology

The following pathological changes were recorded in the vertebrae:

Osteoarthritis – Osteoarthritis was recorded for the superior and inferior articular facets if two or more articular facets were observable, and for the atlantoaxial joint surfaces on C1 and C2. Osteoarthritis was recorded as present according to the operational definition provided by Waldron (2021, 84) (see section 5.1).

Osteophytes – Osteophytes can form around the margins of the vertebral body in response to pathological conditions such as intervertebral disc disease, spinal arthropathies, or trauma (Roberts and Manchester 2010, 139-140). This was recorded as present if new bone was observable on the superior or inferior margins of the vertebral body.

Intervertebral disc disease – Intervertebral disc disease is the result of degeneration of the intervertebral disc, causing changes to the superior and inferior surfaces of the vertebral bodies. Intervertebral disc disease was recorded according to the operational definition of Waldron (2021, 126), which requires the observation of both pitting on the inferior or superior surface of the vertebral body and marginal osteophytes for intervertebral disc disease to be recorded as present.

Schmorl's nodes – Schmorl's nodes are smooth depressions, often lined with cortical bone, on the superior and inferior surfaces of the vertebral bodies and are caused by a herniation of the intervertebral disc (Faccia and Williams 2008). A Schmorl's node was recorded as present if a smooth depression could be observed on either the superior or inferior aspect of the vertebral body.

Ligamentum flavum ossification – The ligamentum flavum is a connective tissue that runs between the laminae of adjacent vertebrae. This tissue can ossify, and such ossification has been linked to increasing age, but also with activities that require back bending or loading on the spine (Geber and Hammer 2018). Ossification of the ligamentum flavum was recorded as present when small spurs of bone were present on the superior margin or the inferior surface of the lamina between the articular facets.

Due to the difficulty in observing degenerative changes in developing joint surfaces, vertebral pathology was systematically recorded in adults only. Descriptive changes for vertebral pathology in nonadults is presented below. Only vertebrae that could be confidently allocated a precise vertebral number have been included in the results below. Table 2.18 presents the overall results for vertebral pathology and Figure 2.7 illustrates patterns in the distribution of vertebral pathology across the spine.

Whilst ossification of the ligamentum flavum most frequently affected the thoracic vertebrae, intervertebral disc disease more commonly affected the cervical, lumbar, and lower thoracic vertebrae. Schmorl's nodes were also more frequently present on the lower thoracic and lumbar vertebrae and osteoarthritis occurred relatively equally throughout the spine. The most common pathological changes of the spine were osteophytes and the ossification of the ligamentum flavum. Fusion of the vertebrae was not common, occurring in only seven skeletons.

Osteoarthritis and intervertebral disc disease were generally slightly higher in middle adults compared to young adults, while osteophytes were considerably more frequent in middle adults (Table 2.19). Little variation was present between the prevalence of Schmorl's nodes in young and middle adults. However, a higher prevalence of ligamentum flavum was observed in the upper thoracic vertebrae in young adults. Males generally demonstrated slightly higher prevalence rates of vertebral pathology than females, particularly in the cervical vertebrae (Table 2.20).

Arterial pressure defects, causing enlargement of the cervical transverse foramina and smooth walled lesions affecting the adjacent pedicle and vertebral body, were commonly observed at Kawa. Preliminary analysis by Antoine and Waldron (2023) found that 12.5% (4/29) of adults examined at Kawa displayed these defects. A further ten individuals were found to display arterial pressure defects during this full analysis, but prevalence could not be calculated due to the recording methods employed in the current report. Overall, 14 skeletons demonstrated pressure defects of the cervical vertebrae, associated with abnormality of the vertebral artery, including two nonadults in the late childhood category. These lesions can be caused by both tortuosity (bulging of an artery or vessel due to a loop, twist, or bend) or aneurysm (a bulge in an artery or

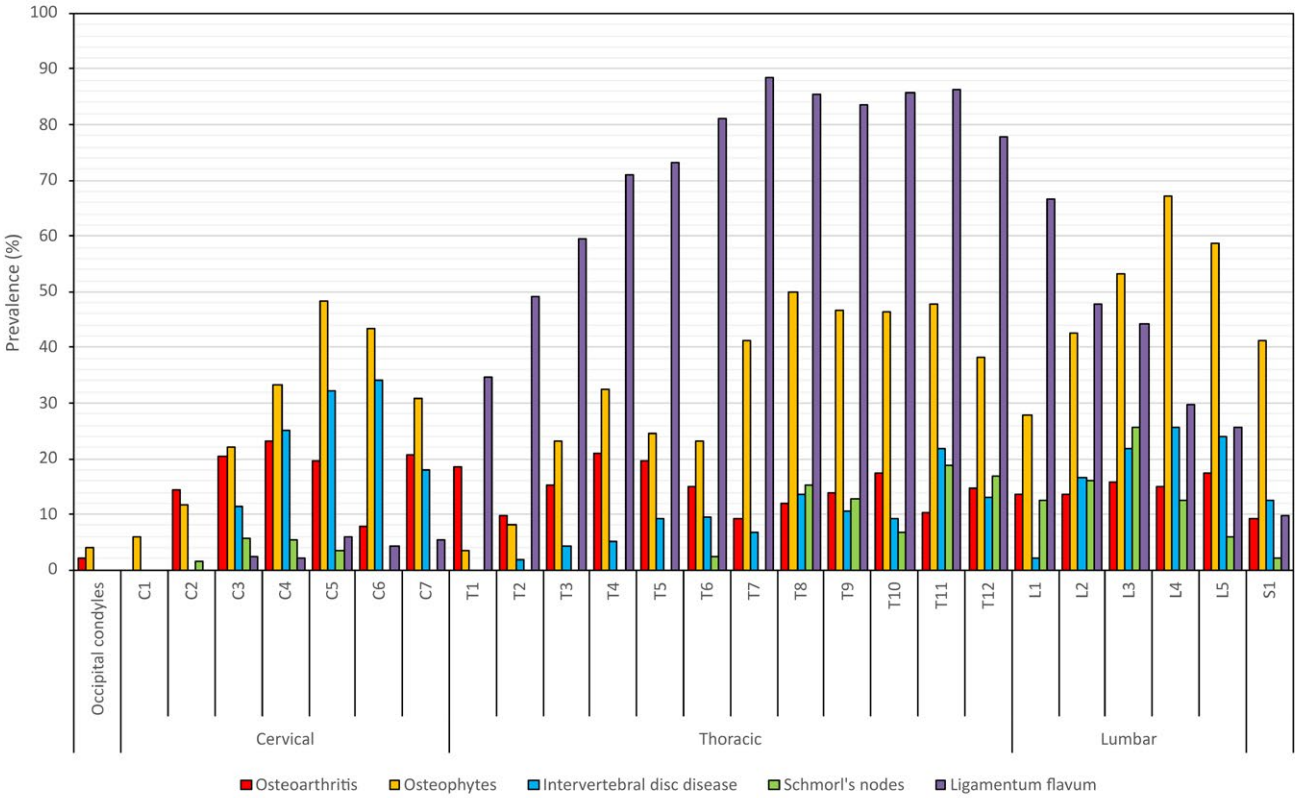

Figure 2.7. The prevalence of vertebral pathology in all adults according to vertebra, consisting of prevalence rates for osteoarthritis, osteophytes, intervertebral disc disease, Schmorl's nodes and ossification of the ligamentum flavum.

vessel due to a weakening of the vessel wall), which can both be the result of pathological changes to the arterial wall, trauma to the neck or congenital factors (Antoine and Ambers 2014). An in-depth analysis is presented by Antoine and Waldron (2023) concerning the four individuals from the preliminary dataset. This analysis suggests that all six pressure defects observed in the four individuals probably represent tortuosity. The further ten pressure defects presented here align with Antoine and Waldron's (2023) description of a tortuosity.

Seven adult skeletons demonstrated various forms of destructive lesion on the vertebrae. A middle adult female [(561)21] presented with a mixed bone reaction on the superior-anterior aspect of the fifth lumbar vertebral body, with destruction and fine woven bone formation on the majority of the right side of this vertebra. A middle adult probable male [(GD3)108] demonstrated extreme porosity and dense new bone formation on the vertebral bodies corresponding to the disc space between cervical vertebrae six and seven. While this was consistent with intervertebral disc disease, the right superior aspect of the vertebral body of the seventh cervical vertebra also had a large cavitation, with remodelled margins and an irregular floor consisting of trabecular bone. No other vertebrae were affected.

A probable female of middle adult age [(HA2)164] had multiple small cystic perforations on the superior-posterior margins of the vertebral bodies of C4 to C7, L5 and S1. These lesions had remodelled rounded margins (Plate 2.5). The twelfth thoracic vertebra of a young adult male [(HA2)124] displayed an unusual depression on the anterior margin of the superior aspect of the vertebral body, just posterior to the annular ring. This shallow lesion had an

Plate 2.5. Rounded perforations on the sixth cervical vertebra in a middle adult probable female, located on the inferior surface and posterior-inferior margin of the vertebral body [Skeleton (HA2)164].

irregular floor consisting of cortical bone, with multiple large perforations and rounded margins. The annular ring was mostly unaffected (Plate 2.6). Finally, a middle adult female [(GD3)152] presented with shallow destructive lesions on T8, T9 and L2, on the anterior region of the annular rings. The floor of these lesions consisted of trabecular bone with little remodelling, but was also accompanied by osteophyte formation on the anterior-inferior and -superior margins of the vertebral bodies and spiculated lamellar bone formation on the anterior aspects of the vertebral bodies. Destructive lesions on the vertebrae can be caused by a number of diseases,

Plate 2.6. Destruction of the twelfth thoracic vertebra in a young adult male, located on the superior aspect of the vertebral body and accompanied by porosity and remodelling [Skeleton (HA2)124].

such as tuberculosis, brucellosis, metastases, osteomyelitis, actinomycosis and sarcoidosis (Aufderheide and Rodriguez-Martin 1998, 140-141). Unfortunately, in these five instances, no distinctive pathological changes were present in either the vertebrae or the rest of the skeleton that could indicate the specific disease causing the vertebral lesions.

Two individuals demonstrated very similar isolated lesions. A middle adult of undetermined sex [(JH3)125] had unusual destruction of the superior-anterior margin of the first sacral vertebra at the midline. This shallow lesion had a remodelled porous floor and a lip of new bone around the margins, creating a clearly defined triangular-shaped region of bone loss on the superior margin and anterior surface of the vertebral body (Plate 2.7). The inferior aspect of the fifth lumbar vertebra was completely unaffected. A young adult of intermediate sex [(JH4)108] had a similar lesion on the superior-anterior margin of the fourth lumbar vertebral body, again at the midline (Plate 2.8). The inferior aspect of the third lumbar vertebra was unaffected. These types of lesions have been associated with both traumatic anterior disc herniation and with brucellar epiphysitis (Mays 2007). The lack of other pathological lesions related to brucellosis in the collection may point to anterior disc herniation as the most likely cause.

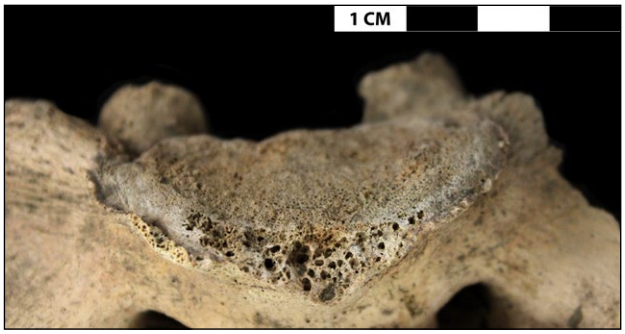

Plate 2.7. Destruction and porosity on the superior-anterior margin of the first sacral vertebra in a middle adult of unknown sex [Skeleton (JH3)125].

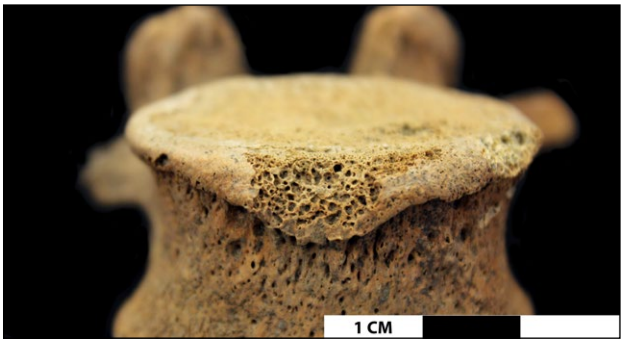

Plate 2.8. Destruction and porosity on the superior-anterior margin of the fourth lumbar vertebra in a young adult of unknown sex [Skeleton (JH4)108].

Deviation of the spine laterally from the midline is known as scoliosis and can be caused by congenital malformation of the spine such as 'wedge'-shaped vertebrae, unusual development during childhood possibly related to genetics (known as idiopathic scoliosis) or caused by pathological changes to the vertebrae, for example compression fracture (Goldberg *et al*. 2008). Three individuals, two young adult males [(HA2)124, (JG2)313] and one middle adult female [(HA2)172], demonstrated slight scoliosis of the spine in the thoracic region. In all three individuals, the cause of the scoliosis was not readily apparent, except for a slight unilateral disparity in vertebral body height, and may have represented idiopathic scoliosis, the most common form of the disease. In addition to this, two males, a young adult [(HA2)209] and a middle adult [(GD3)69], had compression fractures unilaterally affecting the height of at least one vertebral body, which likely caused at least a slight scoliotic curvature to the spine (Plate 2.9).

Plate 2.9. A compression fracture of the sixth thoracic vertebra in a young adult male, causing a height difference in the lateral aspects of the vertebral body and likely producing a slight scoliotic curve [Skeleton (HA2)209].

Diffuse idiopathic skeletal hyperostosis (DISH) is a condition that causes prolific ossification of the anterior longitudinal ligament of the spine, usually on the right side, which can take the appearance of 'melted candle wax'. This can cause fusion between vertebral bodies, although the disc space and the articular facets remain unaffected, and can also be accompanied by extraspinal bone growth, such as entheseal spurs of bone on the calca-

nei, patellae, and the superior-posterior aspect of the ulna. The condition most commonly affects men over the age of 40 years (Waldron 2021, 129-131). One male individual of undetermined age [(HA2)259] demonstrated extensive 'wax-like' osteophyte formation on the right anterior aspect of the vertebral bodies from T5 to L3, causing fusion or near fusion (osteophytes in contact but not yet fully fused) between the majority of these vertebrae (Plate 2.10). The disc space between the vertebrae was retained and the individual also demonstrated extra-spinal bone growth, in particular large entheseal spurs on the posterior aspects of the calcaneal tuberosities. This is consistent with a diagnosis of DISH (Waldron 2021, 134).

Large cavitations and increased vascularisation of the vertebral bodies were noted in three nonadults, one adolescent [(1055)6], one pubescent [(1059)8] and one of late childhood [(JF2)91]. These lesions often consisted of perforations or widened vascular foramina penetrating the anterior and lateral aspects of the thoracic, lumbar and sacral vertebral bodies (Plate 2.11). Similar cavitating lesions on the anterior and lateral bodies of the thoracic and lumbar vertebrae have been noted in two 17 to 21 year olds from Medieval Butrint, in Albania. Further molecular analysis revealed the presence of genetic material from the pathogen that causes brucellosis in samples from both these skeletons, but not from samples from individuals with no vertebral

Plate 2.10. Diffuse idiopathic skeletal hyperostosis (DISH) in an adult male of unknown age. Prolific osteophyte formation on the right anterior-lateral aspects of the thoracic and upper lumbar vertebral bodies, causing spinal fusion [Skeleton (HA2)259].

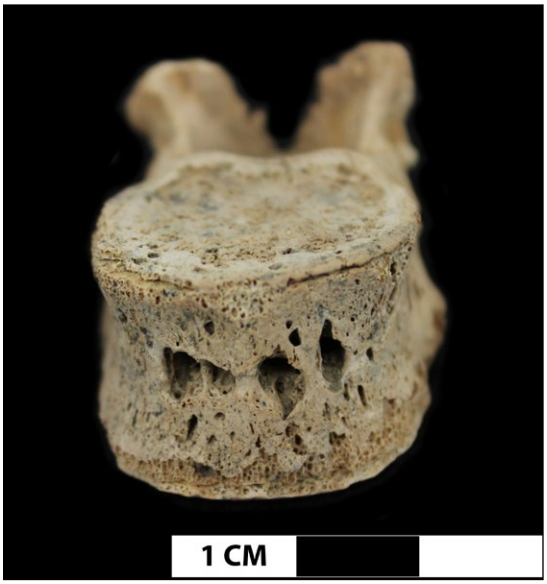

Plate 2.11. Large cavitations/hypervascularity on the anterior aspect of a thoracic vertebral body in an adolescent [Skeleton (1055)6].

lesions (Mutolo *et al*. 2012). However, Smith-Guzmán (2015b) has also noted that vertebral lesions present in a known case of brucellosis are very similar to those from individuals known to have had anaemia, suggesting that this could be due to the fact both diseases induce haemolytic anaemia. Additionally, tuberculosis can also cause cavitating lesions of the vertebral bodies, but tends to affect the vertebrae in a more irregular manner with larger and less dispersed foci (Smith-Guzmán 2015b). Enlarged cavities on the anterior vertebral bodies have also been noted as a congenital variation and may not be related to a pathological cause (Barnes 2012, 103).

An adolescent, Skeleton (HA2)247, presented with unusual changes to the vertebral bodies. Thoracic vertebrae seven to ten had rounded depressions on the inferior surfaces of the vertebral bodies, with smooth margins and a floor consisting of cortical bone, consistent with Schmorl's nodes. The fifth and sixth thoracic vertebrae had similar lesions, but with sharp margins and a floor consisting of trabecular or porous bone (Plate 2.12.A). The eleventh thoracic vertebra had a depression on the superior aspect of the vertebral body, with half of the lesion consisting of a shallow depression with rounded margins and a dense cortical floor, and

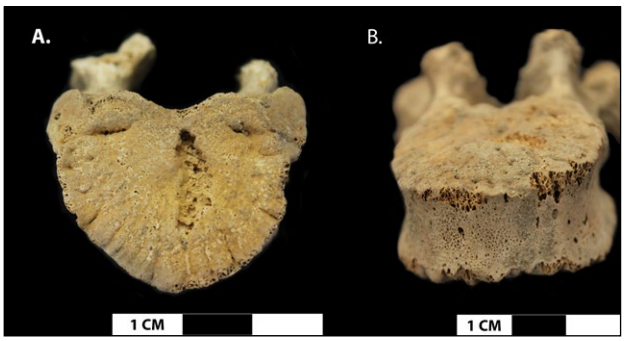

Plate 2.12. The vertebrae of an adolescent affected by Scheuermann's disease [Skeleton (HA2)247]. A. A large Schmorl's node on the inferior aspect of the sixth thoracic vertebral body. B. Fine, diffuse porosity on the anterior aspect of a thoracic vertebral body.

the other half of the lesion penetrating deeper, with sharp margins and a floor consisting of trabecular bone. From the third thoracic to the fifth lumbar vertebra, the anterior aspect of the vertebral bodies also had a fine diffuse porosity (Plate 2.12.B). This porosity may represent normal developmental bone growth or could be caused by inflammation, possibly related to the lesions described above.

The presence of multiple Schmorl's nodes in an adolescent is unusual. Scheuermann's kyphosis, in which the spine develops an abnormal curvature due to developmental wedging of the vertebral bodies, occurs in adolescents and is often accompanied by multiple Schmorl's nodes (Palazzo *et al*. 2014). Clinically, Scheuermann's disease is diagnosed when three or more contiguous vertebrae demonstrate wedging of five degrees of more (McCarthy and Frassica 2015, 142). To test for Scheuermann's disease in this individual, the degree of wedging of the thoracic and lumbar vertebral bodies was calculated using measurement landmarks and calculations from Scoles *et al*. (1991). A number of contiguous thoracic vertebrae demonstrated vertebral wedging over five degrees, with T7 demonstrating wedging of 11.4 degrees. This suggests that this individual likely had a considerable anterior kyphosis, possibly causing or related to the high number of Schmorl's nodes observed.

5.3 Trauma

Adults

Trauma was frequently observed in the human remains from site R18. The majority of the trauma was of partially healed or healed fractures caused by a high degree of force, such as a fall or a blow (Lovell 1997; Waldron 2021, 209-210). Fractures that demonstrated some form of remodelling are presented below according to the region of the skeleton affected. Where possible, true prevalence rates for trauma have also been presented. Potential perimortem trauma, in which no remodelling or callus bone formation could be observed, is discussed separately.

Skull

Nine adult individuals were noted to have healed depressions on the ectocranial surface of the cranium, possibly produced by blunt force trauma (11.5%, 9/78) (Plate 2.13). Six depression fractures were located on the frontal, three on the left parietal and one on the right parietal. Three females, four males and two individuals of undetermined sex were affected. Additionally, two males were observed to have fractures of the left temporal, one to the zygomatic process and one to the styloid process. One female and one male demonstrated nasal fractures. Table 2.21 presents the true prevalence of skull fractures in adults in the Kawa assemblage.

The true prevalence of frontal depressions was relatively high, affecting 10.5% (6/57) of all frontal bones with a completeness of over 25%. Walker (1989) suggests that a high prevalence of cranial depression fractures in skeletons from prehistoric island sites in the Santa Barbara Channel area, California, may be indicative of interpersonal violence due to intense competition over limited resources. Since this paper, a number of other studies have linked cranial depressions to inter-personal violence (e.g. Cohen *et al*. 2014; Jiménez-Brobeil *et al*. 2009; Lambert 1997; Šlaus *et al*. 2012).

Plate 2.13. A depression on the left aspect of the cranium (arrow) in the region of the coronal suture in a middle adult probable female [Skeleton (HA2)168].

This may indicate that interpersonal violence was present at Kawa. Similar cranial lesions have been noted in Nubian and Egyptian populations, for example at Semna South (Alvrus 1999), Giza and Kerma (Filer 1992; Judd and Irish 2009), and from sites O16 and P37 in the Northern Dongola Reach (Judd 2006). However, none of the depressed lesions on the ectocranial surfaces of the cranium observed at Kawa were accompanied by the retention of concentric fracture lines, diagnostic of an antemortem or perimortem fracture. Thus, these lesions may have had other causes, such as infection of the scalp, epidermoid or pilar cysts, slow growing soft tissue neoplasms or even taphonomic damage (Botham 2019; Wu *et al*. 2011).

Hands, feet, and patellae

Hand and foot fractures were fairly common in individuals from site R18. Seventeen adults (21.8%, 17/78) were observed to have fractures of the hands. This included ten metacarpal fractures, affecting seven individuals; 12 proximal phalanx fractures, affecting eight individuals; seven intermediate phalanx fractures, affecting six individuals; and three distal phalanx fractures, affecting three individuals. Males demonstrated hand fractures more frequently than females (ten males, five females, and two of undetermined sex). Twenty adults (25.6%, 20/78) were observed to have fractures of the feet. This included one individual with a fractured right cuboid; three metatarsal fractures, affecting three individuals; 12 proximal phalanx fractures, affecting 11 individuals; and ten fractures of either the intermediate or distal phalanx, affecting five individuals each. Slightly more males demonstrated fractures of the feet than females (ten males, eight females, and two of undetermined sex). No patellae were observed to have been affected by trauma (Table 2.22).

Long bones

Long bone fractures were fairly infrequent in adults (Table 2.23). Seven individuals (9%, 7/78) demonstrated long bone fractures, with the tibia and fibula being the most commonly

affected elements, affecting four and three individuals, respectively. Several skeletons had fractures of two different long bones from the same limb and were at a similar stage of bone remodelling, indicating that both fractures may have been caused by the same traumatic event. This included one individual with fractures to both the left humerus and left ulna, and three individuals with fractures of both the tibiae and fibulae from the same affected side. Involvement of both the tibia and fibula is a common occurrence in fractures of the lower leg diaphyses (Lovell 1997). All three individuals with healed fractures of the diaphyses of the tibia and fibula also demonstrated misalignment (Plate 2.14), common in archaeological populations where immobilisation of the leg for at least two to three weeks is unlikely to have taken place (Lovell 1997). Males were more commonly affected than females (five males, two females) and the left side was involved in 66.7% (8/12) of all long bone fractures.

Plate 2.14. Misaligned healed fractures of the left tibia and fibula in a middle adult male [Skeleton (HA2)169].

Post-cranial axial skeletal trauma

Rib fractures were common in skeletons from Kawa, affecting 24.4% (18/78) of adults. Many individuals had more than one rib fracture and a total of 56 rib fractures were recorded. One adult of undetermined age and sex [(HA2)155] was observed to have at least eight rib fractures and a middle adult probable male [(GD3)108] presented 12 rib fractures. Both individuals had fractures in different states of healing, suggesting multiple events involving blows to the chest. Males were more frequently affected than females (ten males, six females, three of undetermined sex).

Compression fractures of the vertebrae affected seven adult individuals (9%, 7/78). The thoracic spine was mainly affected, but one probable male [(JG2)43] demonstrated a compression fracture of the fourth cervical vertebra. Four males, two females, and one individual of undetermined sex were affected. While most skeletons exhibited a compression fracture on only a single vertebra, one female [(HA2)142] demonstrated the involvement of three thoracic vertebrae, and another female [(JF2)64] had compression fractures of the second to eighth thoracic vertebrae, likely resulting in the observed osteoarthritis of the articular facets and fusion between the third and fifth thoracic vertebrae. One male [(GD3)106] and one female [(HA2)265] demonstrated fractures of the transverse processes of the lumbar vertebrae. Additionally, a young adult male [(GD3)151] had a partially healed transverse fracture of the sacrum between the fusion points of the third and fourth sacral vertebrae.

Due to the way in which completeness was recorded in this study, true prevalence of fractures of the ribs, sacrum and vertebrae could not be presented. However, true prevalence of all other bones of the post-cranial axial skeleton could be calculated (Table 2.24). Only the sternal bodies of three individuals, two males and one female, were observed to have fractures, affecting 9.1% (3/33) of all sternal bodies with a completeness of 25% or more. A high level of direct kinetic force to the chest is required to fracture the sternum (Lovell 1997), for example from falling from a large height.

Instances of multiple traumatic injuries

While many skeletons had multiple fractures to different skeletal elements, the following individuals demonstrated a large number of fractures to various different regions of the body, which indicates that these people experienced serious or multiple traumatic injuries. Skeleton (GD3)69, a middle adult male, had healed fractures of the left temporal zygomatic process, the right fifth metatarsal, one intermediate and two proximal hand phalanges, one proximal and one intermediate foot phalanx, six fractures to the lower rib cage and a compression fracture of the eighth thoracic vertebra. Another middle adult male, Skeleton (GD3)81, had a linear fracture of the sternum, associated fractures of the right third and left second ribs, and a fractured left third metacarpal, intermediate hand phalanx and intermediate foot phalanx. Skeleton (GD3)78, a young adult male, demonstrated a healed misaligned left clavicle fracture, three healed rib fractures and fractures to three proximal hand phalanges. A probable male of middle adult age, Skeleton (GD3)108, had a healed fracture of the left humerus, a remodelling fracture of the left ulna, possible trauma causing non-union of the styloid process of the right ulna, a healed compression fracture of the twelfth thoracic vertebra, and fractures to one intermediate, one distal and two proximal hand phalanges. This individual also had 12 rib fractures, mostly on the left side of the rib cage, in different stages of healing, indicating multiple traumatic events. Skeleton (HA2)209, a young adult male, had a compression fracture of the sixth thoracic vertebral body, healed fractures of the second and third left metacarpals and of one intermediate hand phalanx, and a possible depression fracture on the left parietal. This skeleton may also have had perimortem sharp force trauma to the fourth lumbar vertebra, caused by an arrow (see subsequent section). Skeleton (HA2)169, a middle adult male, had a possible depression fracture to the frontal bone, healed fractures of the left tibia and fibula and three left rib fractures.

Numerous fractures of multiple skeletal elements were less common in women. A young adult, probable female [(HA2)142], had partially healed fractures of the sternum, tenth right rib and compression fractures of three thoracic vertebrae. All fracture calluses consisted of woven bone indicating that the traumatic injury took place not long before death and may have been a contributing factor to mortality. One young adult female [(HA2)265] had healed fractures of two left ribs, one intermediate foot phalanx and of the left transverse process of the first lumbar vertebra. Skeleton (JF2)64, a young adult female, had compression fractures of the second to eighth thoracic vertebrae and also demonstrated multiple traumatic events, with a fully healed proximal foot phalanx but three upper rib cage fractures showing the initial stages of woven bone callus formation. In general, the

higher number of men with multiple fractures compared to women (six males, three females) could indicate that men were more likely to undertake activities that involved an increased risk of traumatic injury. Gender-specific occupations may have been undertaken at Kawa, with roles leading to greater risk of injury possibly including construction or heavy lifting, or through an increased risk of interpersonal violence (e.g. Redfern 2017, 108, 120).

Perimortem trauma

Perimortem trauma is difficult to distinguish from taphonomic fracturing occurring during burial. Fractures on 'wet' bone (still containing a high organic content) produce a distinctive pattern that can be differentiated from fractures to dry bone. Wet bone fracture margins are usually of uniform colour to the rest of the bone and have bevelled edges, with irregular or sharp projections of bone (Moraitis *et al*. 2009; Moraitis and Spiliopoulou 2006). However, bone can take a long time to lose its organic content depending on the burial conditions (Kemp 2016). The majority of inhumations from site R18 were looted at some point in their past, causing disturbance and fragmentation of the burials. This looting may have taken place during the 'wet bone' phase of decomposition and, thus, it remains remarkably hard to differentiate perimortem fractures from postmortem fracturing caused by looting. Some examples of potential perimortem trauma were, however, particularly notable.

Skeleton (JG3)13, a young adult female, had several penetrating injuries that may represent perimortem sharp force trauma. The posterior aspect of the right clavicle, in the region of the medial diaphysis, had a small bevelled perforation approximately 5mm in diameter, with a possible retained inclusion from the tip of a weapon. Similarly, the right parietal also demonstrated a perforation of the ectocranial surface with associated bevelling and small internal radiating fractures, located on the posterior region of the bone, near the lambdoid and mastoparietal sutures. Finally, the left iliac blade had a circular perforation, approximately 13mm in diameter, with some bevelling on the lateral surface and depressed bone flakes on the medial surface, indicating that the direction of the force probably came from the anterior (Plate 2.15.A). The right scapula also demonstrated a possible perimortem blunt force fracture on the glenoid fossa and anterior aspect of the blade. The appearance of the perforation of the skull, with the external bevelling, is similar to that of a 'keyhole' wound (Plate 2.15.B), which occurs when a projectile strikes the cranium at a tangential angle (Berryman *et al*. 2013, 294). However, at some point this burial became highly disturbed (Plate 2.16) and such damage may have occurred during looting of the grave while bones still contained a high organic content, replicating the appearance of perimortem trauma.

When excavated, a white quartzite arrowhead was found in the region of the left side of the first thoracic vertebra of Skeleton (HA2)209, a young adult male. This skeleton was buried in a prone position but had been disturbed prior to excavation, particularly in the thoracic region (Plate 2.17). Subsequent analysis revealed possible perimortem damage to the seventh cervical vertebra on the left side, but the fact that the body had been disturbed made it difficult

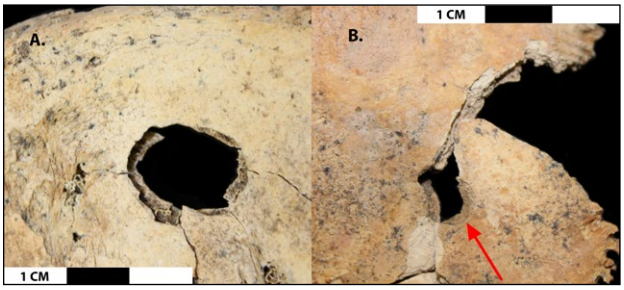

Plate 2.15. Possible perimortem sharp-force trauma in a young adult female [Skeleton (JG3)13]. A. The lateral aspect of the left iliac blade, demonstrating a circular perforation and slight bevelling. B. The ectocranial surface of the right parietal, demonstrating a 'keyhole' fracture (arrow).

Plate 2.16. The disorganised nature of Skeleton (JG3)13 within the grave when excavated, likely due to looting.

to establish if this damage was caused by the associated arrowhead or by activities related to looting. Additionally, a triangular-shaped perforation on the left inferior margin of the superior articular facet of the fourth lumbar vertebra was observed (Plate 2.18). It is possible that this perforation represents sharp force trauma caused by the recovered arrowhead, which had been subsequently disturbed, or by another weapon or other cause. Skeleton (JE3)186, a male adult of undetermined age, was also recovered with an arrowhead in the region of the upper left thigh, but no skeletal trauma was observed. It should be noted that arrowheads recovered from burials may have been present as grave furnishings.

Skeleton (JH3)133, a middle adult probable female, had an incomplete fracture of the left gonial angle, with 'peeling' or delamination of the fracture margins known as 'bone tear', highly indicative of a fracture taking place on wet bone (e.g. Moraitis *et al*. 2009). Another middle adult female [(HA2)198] had a large radiating fracture of the posterior cranium, originating from the lambda region,

Plate 2.17. The position of Skeleton (HA2)209 within the grave when excavated. Note the prone position of the skeleton and disarticulated nature of the vertebrae.

Plate 2.18. Potential sharp-force trauma in a young adult male on the left superior articular facet of the fourth lumbar vertebra (arrow) [Skeleton (HA2)209].

with outward bending (plastic deformation) of the fracture margin on the right side of the skull (Plate 2.19). The plastic deformation, in particular, is indicative of a perimortem trauma (Kranioti 2015). This was accompanied by smaller linear fractures roughly following the obliterated sagittal and coronal suture, which may have been of later postmortem origin. There were no concentric fractures or observable bevelling present.

Plate 2.19. Possible blunt force trauma in a middle adult female with plastic deformation to the posterior aspect of the cranium. [Skeleton (HA2)198].

Nonadults

Trauma was only observed in two adolescent nonadults. Skeleton (1055)6 had a remodelled compression fracture of the sixth thoracic vertebra, with a large depression on the superior aspect of the vertebral body and a marked reduction in height. The fifth thoracic vertebra also had a notable reduction in height but no evidence for a compression fracture, which had perhaps remodelled. The distal third of the right ulna of this skeleton also had a lateral curvature that was not apparent in its antimere (Plate 2.20.A). Radiography revealed a very faint linear opacity that could indicate that this individual had a healed fracture of the ulna, likely a greenstick fracture or a plastic deformation injury, at some point during childhood (Mabrey and Fitch 1989) (Plate 2.20.B). Skeleton (JE3)187 also had a possible healed

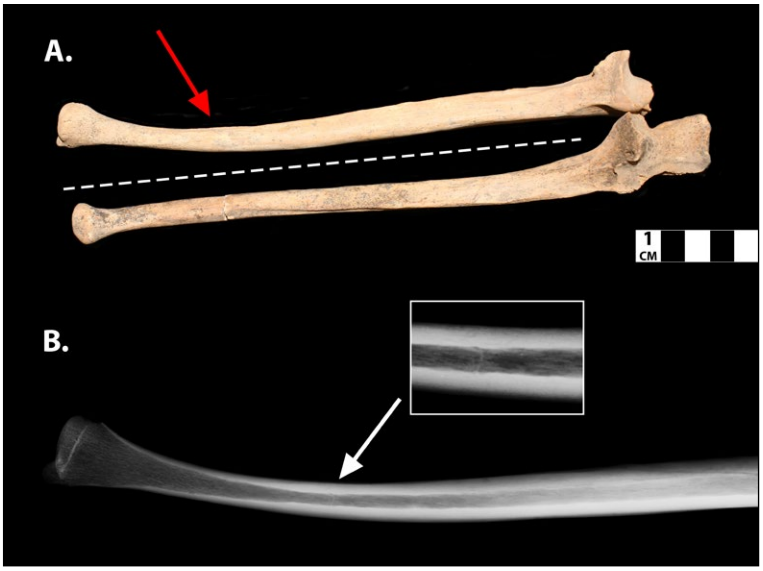

Plate 2.20. A possible childhood fracture affecting the distal third of the right ulna of an adolescent [Skeleton (1055)6]. A. Lateral curvature of the distal third of the right ulna (red arrow); not apparent on the left ulna. B. Radiograph of the right ulna with a very faint radiopaque line at the apex of the lateral curvature (white arrow and box), possibly indicating a healed childhood fracture. Radiograph by Dr Daniel O'Flynn.

fracture to the styloid process of the left radius and healed trauma to the proximal phalanx of the left first toe.

5.4 Periosteal reaction

Periosteal reaction is the formation of new layers of bone on the outer cortical surfaces of skeletal elements and is produced when the periosteum, the membrane overlying almost all surfaces of bone, reacts to pathological stimuli (Waldron 2021, 180-182; Weston 2012) (Plate 2.21). Although many bioarchaeological studies consider periosteal reaction to be the result of inflammation caused by infection of the surrounding tissue, there are numerous other causes that can trigger this new bone formation, including trauma, haemorrhage, overlying soft tissue lesions, tumours, mechanical stress and certain metabolic diseases (Rana *et al*. 2009; Waldron 2021, tab. 8.7-8.10; Weston 2012). However, the specific identification of the cause of periosteal reaction on some bones is extremely difficult (e.g. Weston 2008).

Long bones

Adults

Periosteal reaction of the long bones, particularly of the lower legs, is commonly noted in human skeletal assemblages (Marques *et al*. 2018; Weston 2008). It was observed in 26.9% (21/78) of all adults at Kawa. The tibiae and fibulae were the most common bones involved, affecting 15 individuals. The femur was involved in three individuals, the ulna in two, and the radius in one. Males were more commonly affected than females, although there were a high number of affected individuals with an undetermined sex (nine males, four females, eight of undetermined sex).

Plate 2.21. Examples of periosteal reaction on the tibiae. A. New woven bone on the proximal portion of the right tibial shaft in a middle adult probable male [Skeleton (HA2)255]. B. Remodelled porous lamellar bone on the distal portion of the left tibial shaft, causing thickening of the shaft, in a young adult of unknown sex [Skeleton (JH4)108].

Table 2.25 presents the true prevalence of periosteal reaction in the Kawa assemblage. The most frequently affected region was the middle third of the right tibia (16.4%, 9/46), but the middle and distal thirds of both left and right tibiae and fibulae were all commonly involved (Figure 2.8). The anatomy of the lower leg, including a thicker periosteum on the tibia, reduced circulatory flow, and less associated soft tissue, may increase the susceptibility of the lower leg bones to trauma and infection, as well as to ulcers, while the lower legs are also susceptible to mechanical strain and stress fractures, all of which can cause periosteal reaction (Marques *et al*. 2018).

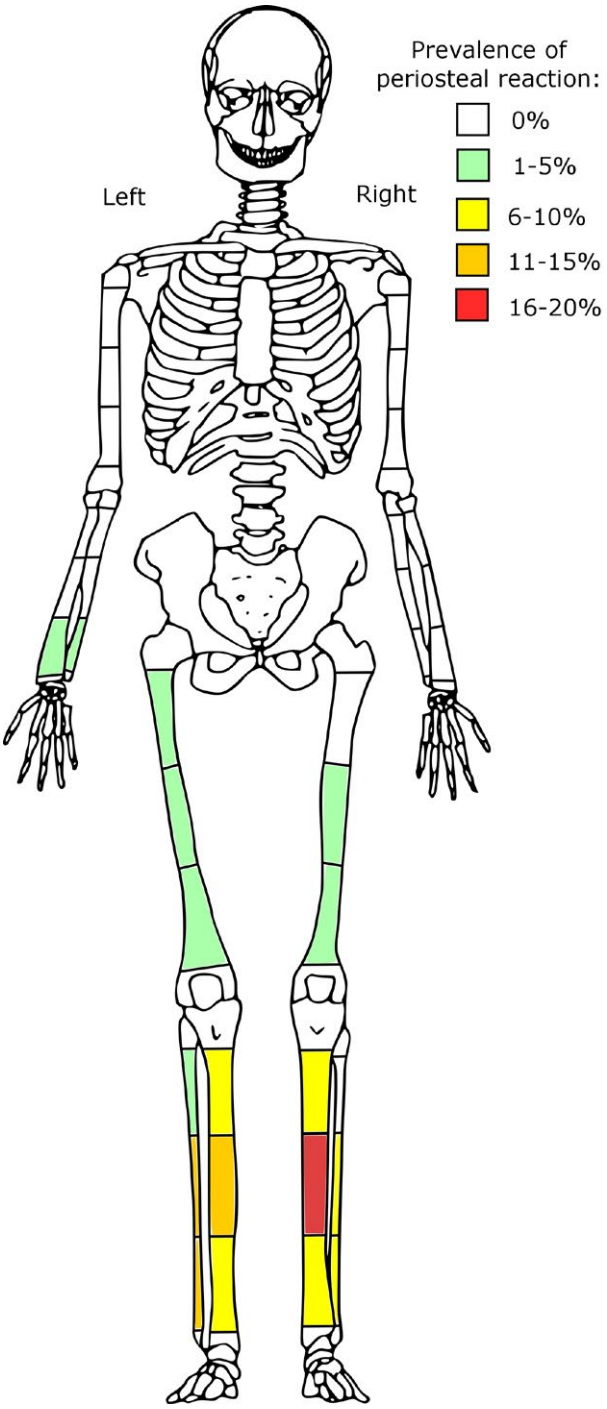

Figure 2.8. The skeletal distribution of periosteal reaction on the long bones in all adults (prevalence displayed in 5% increments). Image adapted from Buikstra and Ubelaker (1994).

Nonadults

In nonadults, periosteal reaction may be the result of a number of causes, such as vitamin C and D deficiency, infection and osteomyelitis, tuberculosis or trauma (Brickley and Ives 2006; Lewis 2007, 147; Mays *et al*. 2006; Schultz 2001). To determine the specific cause, an examination of the distribution of lesions across the entire skeleton is required. Unfortunately, nonadult skeletons from Kawa were too incomplete or did not demonstrate other lesions that would enable a specific diagnosis to be made. Periosteal reaction in nonadults is also difficult to differentiate from normal appositional growth (e.g. Rittemard *et al*. 2019). Periosteal reaction was recorded as abnormal in nonadults if it appeared disorganised, patchy and thicker than would be expected for normal growth. However, it should be considered that instances presented here as periosteal reaction due to pathological stimuli could represent normal rapid growth (Lewis 2007, 135).

The true prevalence of periosteal reaction on the long bones is presented in Table 2.26 and was fairly low among nonadults. The highest prevalence was on the midshaft of the right femur and tibia. A total of six nonadults (10.3%, 6/58) were observed to have periosteal reaction on the long bones, one infant, one nonadult of early childhood and one of late childhood, two pubescent children and one adolescent. Several skeletons had the involvement of multiple elements. As well as woven bone on the right femur, tibia and fibula, one nonadult of early childhood was also observed to have woven bone on the maxillae, mandible, ilia and right scapula. Both affected pubescent children also had involvement of multiple long bones, including elements from the upper and lower limbs. In addition to this, two other children of pubescent age demonstrated woven bone on elements of the foot, one of the third left metatarsal [(HA2)230] and one of the right calcaneus [(JH4)3] (for which true prevalence has not been presented).

Sinuses

Bony changes inside the maxillary sinuses are believed to be caused by inflammation, a condition known as sinusitis (Roberts 2007). Sinusitis can be the result of a number of factors that might trigger an inflammatory reaction within the sinuses, including viral and bacterial infection, sinus blockage, nasal obstructions, dental infection, asthma, fungal allergies and poor air quality (Brook 2009). All adults from site R18 with the presence of at least one maxillary sinus were observed for evidence of sinusitis, according to methods outlined in Davies-Barrett *et al*. (2021). Due to the recording criteria employed for the analysis of respiratory diseases at the time, nonadults were not systematically analysed for maxillary sinusitis. In total, 74.5% (41/55) of adults with one or more observable maxillary sinuses had bony changes associated with maxillary sinusitis. This affected 58.8% (30/51) of right sinuses and 60.4% (29/48) of left sinuses.

The prevalence of maxillary sinusitis at site R18 was particularly elevated and suggests that conditions in the town at Kawa may have produced a high predisposition to developing this pathological change. Prevalence rates from the nearby Kerma period site of P37 (76.6%, 23/30) and from further north at the New Kingdom/Post-New Kingdom town of Amara West (76.3%, 45/59) are equally high, particularly compared to prevalence rates from sites upriver in the Fourth Cataract region and from Gabati, which range from between 50-60% (Binder 2014, tab. 8.46; Davies-Barrett *et al*. 2021).

Ribs

Periosteal reaction on the visceral (inner) surfaces of the ribs is likely caused by pleural and pulmonary inflammation, which is commonly the result of lower respiratory tract diseases, such as tuberculosis and pneumonia, although other less common non-respiratory diseases, like cancer and pulmonary embolism, can also be involved (Davies-Barrett *et al*. 2019). Periosteal reaction on the ribs was analysed according the methods outlined by Davies-Barrett *et al*. (2019). Due to the recording criteria employed for the analysis of respiratory diseases at the time, nonadults were not systematically analysed for periosteal reaction on the visceral surfaces of the ribs. In the individuals from Kawa, 29.5% (18/61) of adults with preserved ribs demonstrated periosteal reaction on the visceral surfaces. This suggests that lower respiratory tract diseases were present in the population from Kawa, although no skeletal evidence for specific respiratory diseases, such as tuberculosis, were observed.

Adult skeletons from the New Kingdom and post-New Kingdom town of Amara West presented with a high prevalence rate of periosteal reaction on the ribs of 46.7% (49/105) (Binder 2014, tab. 8.49). Although individuals from both sites likely lived in an urban environment, where people may have been exposed to infectious diseases, poor sanitation and poor air quality, the lower prevalence in individuals from site R18 suggests that factors predisposing to lower respiratory tract disease may have differed from those at Amara West. The population from the Kerma period site P37, located within the Northern Dongola Reach, had a prevalence of 22.6% (7/31) (Davies-Barrett *et al*. 2023), which is more comparable to the result from Kawa. This suggests that regional and site-specific variations in environment, disease and sociocultural practices may have affected the prevalence of lower respiratory tract disease along the Middle Nile Valley.

5.5 Cranial lesions

Adults

Endocranial and ectocranial lesions

Not all internal cranial surfaces could be examined due to completeness of the cranium. Where this was possible, five individuals demonstrated lamellar bone formation on the endocranial surface. The cruciate eminence of the occipital was involved in two individuals, a middle adult probable female and an adult of undetermined sex and age, who also demonstrated nodular new bone formation on the endocranial surfaces of the temporals. The remaining three skeletons had porous and nodular new bone formation on the frontal bone in the region of the frontal crest. This included a middle adult male, a young adult probable female and a probable male of unknown age (Plate 2.22).

Plate 2.22. Nodular new bone formation in a probable male of unknown age on the endocranial surface of the frontal in the region of the frontal crest, possibly representing hyperostosis frontalis interna [Skeleton (JG2)43].

Bilateral thickening of the endocranial surface in the region of the frontal, including nodular bone growth, is known as hyperostosis frontalis interna (HFI) (Rühli *et al*. 2004). Possible factors causing HFI include genetics and skeletal, hormonal, and metabolic disorders (Bebel and Golijewskaja 2015). In modern samples, HFI is found overwhelmingly in post-menopausal females (Raikos *et al*. 2011), but in archaeological populations has been commonly found in males too (Rühli *et al*. 2004). The new bone formation seen on the endocranial surfaces of the frontal bones in the three individuals from Kawa could indicate the initial stages of HFI. Instances of the lesion have been recorded in other skeletons from Egypt and Sudan across time in both males and females (Bebel and Golijewskaja 2015, tab. 1). However, a number of other conditions could also cause new bone formation or thickening on the endocranial surface of the frontal (Bebel and Golijewskaja 2015; Rühli *et al*. 2004).

Diffuse porosity or porous new bone was present on the ectocranial surface of the cranial vault in 14.1% (11/78) of adults. This affected five males, five females, and one adult of undetermined sex. Middle adults appeared to be most commonly affected (six middle adults, two young adults, three adults of undetermined age). Porous lesions usually affected more than one bone making up the cranial vault. Most commonly involved was the occipital, affecting 16.9% (10/59) of all adults with an occipital bone present, but the parietals were also frequently affected (Table 2.27). The aetiology of porous lesions of the cranial vault has been highly debated, and has included vitamin D and vitamin C deficiency, osteomalacia, neoplastic conditions, infectious disease and traumatic injury (Brickley 2018). Anaemia is commonly cited as a cause of porous lesions on the cranium, but requires evidence of expansion of the diploë and thinning of the outer table of the cranium (Brickley 2018), which were not observed in any of the individuals with fragmented crania.

Enlarged arachnoid foveae

Arachnoid foveae are depressions located on the endocranial surface and are usually a normal feature (Duray and Martel 2006). However, Skeleton (HA2)171, an undetermined adult of intermediate sex, and Skeleton (JH4)50, a middle adult probable female, both presented with enlarged arachnoid foveae just lateral to the sagittal sulcus on both the left and right endocranial surfaces of the parietals, with smooth margins and a lesion floor consisting of cortical bone. The enlarged arachnoid foveae on Skeleton (JH4)50 were also accompanied by enlarged vessel impressions on the endocranial surface of the parietals. Skeleton (HA2)171 also had porous new bone formation on either side of the sagittal sulcus on the parietals and extreme maxillary and frontal sinusitis, with prolific porous new bone formation.

Skeleton (HA2)255, a middle adult probable male, had multiple lytic lesions or pressure defects on the endocranial surfaces of the frontal, occipital, both parietals and temporals, and on the greater wings of the sphenoid, particularly in regions related to the dural venus sinuses. This included what appeared to be enlarged arachnoid foveae on either side of the sagittal suture of the left and right parietals and a large lytic lesion within the cruciform eminence of the occipital and on the left greater wing of the sphenoid (Plate 2.23). The circumscribed lesions were often coalesced and variable in diameter from 1mm to 15mm, with a floor consisting of remodelled trabecular or cortical bone. Remodelling of the margins of the lesions varied, with some demonstrating smooth rounded margins and others with sharp margins and considerable undercutting. This individual also had extensive pitting on the palate and new bone formation on the right tibia and on both fibulae.

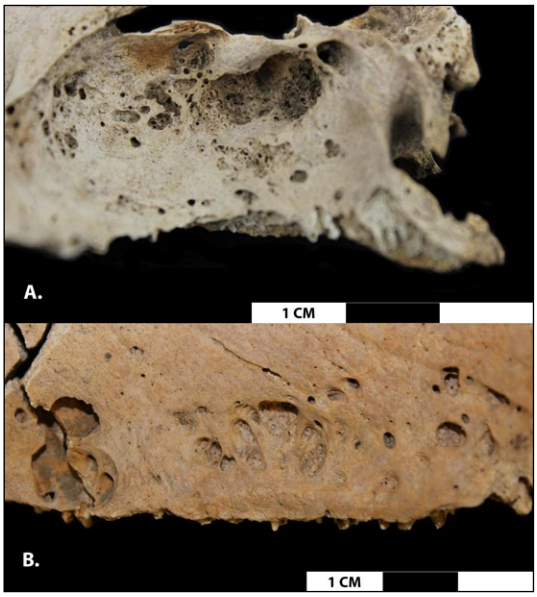

Plate 2.23. Enlarged arachnoid foveae on the endocranial surfaces in a middle adult probable male [Skeleton (HA2)255]. A. Multiple coalesced lesions on the endocranial surface of the left greater wing of the sphenoid, including a large deep cavity with remodelled rounded margins and floor. B. Multiple, sometimes coalesced, lesions on the endocranial surface of the left parietal along the sagittal sulcus. Some lesions were remodelled, with rounded margins, while others had sharp margins and undercutting.

Arachnoid foveae are common, generally asymptomatic, and can reach up to 19mm in diameter (Park *et al*. 2018; Settecase *et al*. 2014). However, they can also become enlarged

and scalloped due to elevated or fluctuating cerebrospinal fluid pressure (Settecase *et al*. 2014). Particularly in the instance of Skeleton (HA2)255, the extreme number of arachnoid foveae and the active lytic nature could represent another osteolytic disease. Pressure defects on the endocranial surface that appear similar to enlarged arachnoid foveae can be caused by meningioma, which can be identified by an enlarged vessel impression in association with pressure defects, and can also be accompanied by hyperostosis affecting both the inner and outer cranial tables (Waldron 2021, 293-294). Other diseases causing lytic lesions of the skull include metastatic carcinoma, myeloma, lymphoma, pyogenic osteomyelitis (Kaufman *et al*. 1997) and tuberculosis (Steyn and Buskes 2016). All three skeletons did not demonstrate further postcranial lesions that could aid in a differential diagnosis and, unfortunately, no radiography of the three individuals was undertaken. Further radiographic analysis may provide additional information that can aid in a differential diagnosis (Kaufman *et al*. 1997).

Nonadults

Endocranial and ectocranial lesions

Table 2.28 presents the true prevalence of cranial lesions in nonadults. Six nonadults (10.3% 6/58) had ectocranial lesions or new bone formation on the maxillae or mandible. Two individuals also had involvement of the ectocranial surfaces of the greater wings of the sphenoid. This affected two infants, two nonadults of early childhood, and two adolescents. The maxilla was involved most frequently. However, the region around the alveolar bone on both the maxilla and mandible undergoes rapid remodelling throughout childhood as the teeth develop and erupt, and the high prevalence of woven bone observed in this region may be the result of normal rapid growth (Brickley and Ives 2006). Ectocranial lesions can have a number of aetiologies in nonadults, including vitamin C and D deficiency, infection, inflammation, haematoma, meningioma and trauma (Schultz 2001, tab. 4). All ectocranial lesions appeared as porosity or new bone formation, indicative of periosteal reaction, and none had outer table cortical erosion or a distinctive hair-on-end appearance known as porotic hyperostosis, which has been related to severe genetic anaemias (Brickley 2018).

Endocranial lesions were observed most frequently on the occipital bone (Plate 2.24). Four nonadults had endocranial lesions (6.9%, 4/58), consisting of plaque-like new bone formation, all affecting the occipital bone, with variable involvement of the frontal or parietal bones, and one instance of involvement of the sphenoid. Two infants and two nonadults in early childhood were affected. A number of aetiologies for endocranial lesions have been suggested, including tearing or inflammation of the meninges caused by trauma, meningitis, tuberculosis, syphilis and vitamin deficiencies, or as the result of rapid growth (Lewis 2004). In one infant [(GD3)154], thick plaques of new bone on the endocranial surfaces of the frontal, parietals, and occipital were observed and may have been caused by endocranial pressure and inflammation due to the accumulation of fluid around the brain, related to this individual potentially having hydrocephalus (see section 5.6).

Plate 2.24. New bone formation on the endocranial surface of the occipital in a young child [Skeleton (HA2)102].

Cribra orbitalia

Porous lesions of the orbital roof, known as cribra orbitalia, are commonly observed in nonadults from archaeological populations (Plate 2.25). The aetiology of these lesions has been highly debated and includes various different anaemias, eye infection and inflammation, subperiosteal haematoma caused by vitamin C and vitamin D deficiency, haemangioma and traumatic injury (e.g. Brickley 2018; Walker *et al*. 2009; Wapler *et al*. 2004). A total of 22.4% (13/58) of nonadults had porous lesions of the orbital roof. The true prevalence of cribra orbitalia was 36% (9/25) for the left orbital roof and 39.1% (9/23) for the right orbital roof (in orbital roofs that were more than 25% complete). It was most common in nonadults in early childhood, affecting 58.3% (7/12) of all individuals in this age group, but was also present in one infant, four nonadults in late childhood, and one adolescent.

Plate 2.25. An advanced porous orbital roof lesion in the left orbit of a young child [Skeleton (HA2)102].

In Meroitic, X-Group, and Medieval individuals excavated from the Wadi Halfa region, 32% of nonadults aged between birth and 10 years had cribra orbitalia (Carlson *et al*. 1974, tab. 1), which this study attributed to iron deficiency anaemia, exacerbated by parasitic infection and weanling diarrhoea. Nonadults aged between birth and 9

years from Medieval Kulubnarti had a prevalence of cribra orbitalia of 66.2% (98/148), with the highest frequency (78%) in the age group of 4 to 6 years (Mittler and Van Gerven 1994, tab. 1), again assumed to be caused by iron deficiency anaemia. However, in a histological analysis of bone showing evidence of cribra orbitalia in Sudanese Meroitic adult skeletons from Missiminia, Wapler *et al*. (2004) found that only 43.5% of all instances of cribra orbitalia corresponded with changes linked to anaemia, while other aetiologies such as osteitis, hypervascularisation, eye infection, osteoporosis and postmortem taphonomic damage were proposed to also cause such lesions. More recently, the presence of cribra orbitalia in the Middle Nile valley has also been linked to haemolytic anaemia caused by malarial infection (Smith-Guzmán 2015a).

5.6 Congenital and developmental abnormalities

Congenital abnormalities of the skeleton are typically caused by defects in foetal development, resulting in abnormal development of skeletal elements (Lewis 2019; Roberts and Manchester 2010, 44). They can result in minor skeletal anomalies, which do not present symptoms, to severe diseases that make life beyond birth unsustainable (Roberts and Manchester 2010, 44). Causes of developmental abnormalities include genetic defects and environmental factors affecting the foetus in utero, such as exposure of the mother to infection and chemicals (Roberts and Manchester 2010, 46-48). A number of developmental abnormalities were noted in the individuals from Kawa, including those affecting the spine, cranium, hands and feet.

Vertebrae

Anomalies of the vertebrae were the most common form of congenital abnormality observed in the skeletons at Kawa and include border shifts, transitional vertebrae, cleft neural arches, and spondylolysis (Barnes 2012, 59-104). Thirteen individuals, including three nonadults, demonstrated cranial border shifts. Three of these individuals had associated cervical ribs (Plate 2.26) and four had agenesis of the twelfth rib. Caudal shifts were less common, affecting only three adult individuals. Six adult individuals also had what appeared to be an extra transitional vertebra (Barnes 2012, 70-71), although damage and absence of certain vertebrae often made it difficult to distinguish a transitional vertebra from changes caused by a vertebral border shift. The presence of a sixth lumbar vertebra was most common, occurring in four skeletons, while two demonstrated an additional sacral vertebra. Of the 48 adult skeletons with the lumbar vertebrae intact, three (6.3%) had spondylolysis, affecting L4, L5 and L6 once each (Plate 2.27). No nonadults with fully fused vertebrae were observed to have spondylolysis.

Cleft neural arches of the vertebrae were also present, affecting one adult and two nonadults. C1 was involved in two instances [(GD3)114, (JF2)64] (Plate 2.28), and C7 in one instance [(JF2)91]. One adult [(JG3)13] demonstrated a sacral arch hiatus from at least S3 to S5, although taphonomic damage prevented the observation of the neural arch of S1 and S2. Another adult [(561)25] demonstrated a neural arch hiatus of S1. Skeleton (GD3)86, who could only be aged from between 11 and 19 years of age, demonstrated complete nondevelopment of the sacral laminae, producing

Plate 2.26. The seventh cervical vertebra of a nonadult, demonstrating a cranial border shift with associated cervical ribs [Skeleton (GD3)86].

Plate 2.27. Spondylolysis of a sixth lumbar vertebra in a middle adult male [Skeleton (GD3)69].

Plate 2.28. The first cervical vertebra of a child, demonstrating a cleft posterior neural arch [Skeleton (GD3)114].

a large sacral hiatus (Plate 2.29). Often referred to as sacral spina bifida occulta, a cleft sacral arch does not generally have any clinical complications and should not be confused with neural tube defects, also known as spina bifida, which can have serious health complications (Waldron 2021, 144). While the extent of a sacral hiatus can vary from affecting one to all sacral arches, a fully open sacral hiatus is uncommon. For example, in a large sample from the Dakhleh Oasis, Egypt, 15.6% of all individuals had a sacral neural arch hiatus, but only 17.4% of this subsample had a completely open sacral neural arch (Molto *et al*. 2019, tab. 2).

Plate 2.29. A complete sacral neural arch hiatus in a nonadult [Skeleton (GD3)86].

Hydrocephalus

The skull of Skeleton (GD3)154, an infant, presented with unusual morphology. The cranium had an extremely enlarged anterior fontanelle, beginning at the superior-most point of the metopic suture, which extended no further than 20mm above the orbit, creating a large separation between the two halves of the frontal bone (Plates 2.30 & 2.31). The orbits also appeared to slope downwards inferior-laterally. The parietals had extreme bossing and, when articulated with the frontal bones, appeared enlarged laterally. The temporomandibular joint was also malformed on both the temporal bones and mandible, with medial rotation of the mandibular condyles and flattening of the temporomandibular joint on the temporal bone, likely as a result of expansion of the cranium laterally. This appearance is consistent with pathological changes related to hydrocephalus (Barnes 2012, 20; Richards and Anton 1991). This individual also presented with highly vascularised plaque-like lesions on almost all endocranial surfaces, thick deposits of woven bone on the orbital roofs, greater and lesser wings of the sphenoid, almost all surfaces of the maxillae and on the posterior surface of the right zygomatic.

Hydrocephalus is caused by accumulation of cerebrospinal fluid within the skull as a result of obstruction of the flow of fluid somewhere between the point of its production and the point of its absorption (Rekate 2009; Tully and Dobyns 2014). While it is often caused by genetic factors, it can be acquired, due to haemorrhage, infection or neoplastic disease (Tully and Dobyns 2014). In young nonadults, the resulting intracranial pressure affects the morphology of the developing cranium. Primarily, this can be observed in the form of an expanded cranial vault (Richards and Anton 1991).

Blockage in different areas of the cerebrospinal fluid pathway can affect the expression of the disease within the cranial bones (Richards and Anton 1991), and a close inspection of all available skeletal elements can help to identify the type of hydrocephalus present. In the case of Skeleton (GD3)154, the cranium was evenly expanded with

Plate 2.30. Skeleton (GD3)154, an infant, located within the grave with cranium intact, demonstrating expansion of the cranium, advanced cranial bossing, and an extremely enlarged anterior fontanelle, all likely related to the condition of hydrocephalus.

Plate 2.31. The two frontal halves of the infant with hydrocephalus, demonstrating an extremely enlarged anterior fontanelle [Skeleton (GD3)154].

a rounded appearance in the lateral view and a triangular shape when observed superiorly, partly due to extreme parietal bossing and almost inexistent frontal bossing. The anterior fontanelle was still open and was extremely enlarged. The margins of this fontanelle presented concave and sharp edges typical of hydrocephalus (Richards and Anton 1991, fig. 3), and affected the complete closure of the metopic, coronal, and sagittal sutures. These features, in addition to closed mendosal sutures and the absence of other major changes to the occipital, indicate this individual had possible non-communicating hydrocephalus (Richards and Anton 1991, tab. 3). This type of hydrocephalus is believed to be caused by a cerebrospinal fluid flow obstruction, as opposed to communicating hydrocephalus, in which there is no apparent source of obstruction (Tully and Dobyns 2014).

Endocranial impressions caused by increased intracranial pressure are also consistent with hydrocephalus (Richards and Anton 1991), but were not noted in this individual. It is possible that impressions were present but were obscured by the plaque-like new bone formation observed on the endocranial surfaces. Hydrocephalus is also often associated with a number of genetic syndromes, in particular neural tube defects (Tully and Dobyns 2014), such as spina bifida (Bell *et al*. 1980). Unfortunately, while the sacrum in Skeleton (GD3)154 was well preserved, the level of development of this individual, including incomplete fusion of the vertebral and sacral elements, precluded the identification of a neural tube defect of the sacrum.

Individual (GD3)154 is quite unique in an archaeological context since 92% of the skeleton is present and the preservation is excellent. The poor preservation of archaeological remains, particularly delicate cranial bones, is likely to be a factor in the low number of identified instances of hydrocephalus. For example, Richards and Anton (1991) reviewed 30 reports of hydrocephalus from the literature and could be certain that the correct diagnosis had been made in only seven instances, including their own. One of those instances was from the Egyptian Roman period site of Shurafa and describes a male adult of at least 30 years old with an enlarged cranium and possible partial paralysis of the left side (Derry 1913). A possible instance of hydrocephalus in a child dating to AD 350-550 from the Wadi Halfa region was reported by Armelagos (1969), but no description of the morphological changes or the criteria used for this diagnosis were provided, and the one image of the individual's cranium does not provide any conclusive evidence. The identification of an individual with hydrocephalus at Kawa is, thus, an important addition to a small but growing body of evidence for the disease in the past.

Other

Two middle adult males [(JG2)215, (JG2)312] had complete obliteration of certain cranial sutures: one of the sagittal suture and the other of both the sagittal and temporal sutures. While obliteration of the sutures occurs with increasing age and both individuals were in middle adulthood, the crania demonstrated elongation of the cranial vault from anterior to posterior, known as scaphocephaly (Plate 2.32). This occurs due to agenesis (failure to develop) or craniosynostosis (premature fusion) of the sagittal suture during development, affecting the overall morphology of the cranial vault (Barnes 2012, 11 & fig. A-1.3.1) and indicates that these two individuals likely had a developmental abnormality, rather than sutural obliteration later in life.

Plate 2.32. Agenesis or craniosynostosis of the sagittal and temporal sutures in a middle adult male, leading to elongation of the cranial vault from anterior to posterior, known as scaphocephaly [Skeleton (JG2)312].

Several congenital abnormalities were noted in the wrist. The styloid process of the ulna can form as a separate ossification centre or can be absent altogether (Barnes 2012, 140). A young adult male [(1052)3] had an absent styloid process of the right ulna, demonstrating in its place a smooth joint surface with no indication that the styloid process ever formed, although a separate ossification centre may have been overlooked during excavation. A second individual [(GD3)108], a middle adult male, had unilateral non-fusion of the styloid process of the right ulna, with the presence of the separate styloid bone and a pseudofacet between the two elements. However, non-union of the styloid process of the ulna in modern populations has been linked to trauma of the wrist in childhood (Peterson 2007, 525), and thus this instance has been recorded in the trauma section above.

Two individuals had a unilaterally absent styloid process of the third metacarpal, on the right in a probable female middle adult [(HA2)164] and on the left in an adult of undetermined sex and age [(JG3)21]. This may represent os styloideum, in which the styloid process of the third metacarpal develops as a non-unionised secondary ossification centre, which can produce pain in the wrist (Kaniewska *et al*. 2017). However, the accessory bone was not found in either instance and may have failed to ossify completely (Barnes 2012, 150). Trauma of the styloid process of the third metacarpal may also have been the cause, although no evidence for fracture, such as bone remodelling, was observed.

A middle adult male [(GD3)132] had a bipartite right trapezoid, which is one of the rarest carpals to form into bipartite sections (Barnes 2012, 144). A second individual [(JH4)50], a probable female middle adult, had ankylosis of the right lunate and triquetral, known as carpal coalition (Barnes 2012, 142-144), which was also accompanied by ankylosis of the distal interphalangeal joint of the fourth digit of the right hand. While this may have been the result

of trauma, no evidence of fracture or proliferative bone formation was observed. Ankylosis of the joints of the wrist and hand can also develop in rheumatoid arthritis, but this occurs only rarely (Leden *et al*. 2012) and the hallmark for rheumatoid arthritis, symmetrical erosive lesions of the joints of the hands and feet (Waldron 2021, 100-101), was not observed in this individual.

Symphalangism is the congenital absence of the proximal and distal interphalangeal joints (Baek and Lee 2012). It can occur in either the hands or the feet. In addition to the skeleton with the fused distal interphalangeal joint of the fourth digit of the hand, two other individuals demonstrated fused phalangeal joints of the hand: a male [(HA2)193] with fusion of the proximal interphalangeal joint of the fifth digit of the left hand, and a male [(GD3)69] with an unsided fused distal interphalangeal joint of the fifth digit. However, in both instances these skeletons had fractures of other elements in the hands, suggesting that fusion may have been the result of trauma to the joint. In the foot, 21.8% (17/78) of adults had fusion of at least one distal interphalangeal joint. Six males, five females, and six adults of undetermined sex were affected. In those phalanges that could be assigned to a specific digit, all affected joints belonged to the fifth digit and were usually bilateral. Two nonadults also had symphalangism of the foot. Unfortunately, due to the way in which completeness of the phalanges was recorded, it is not possible to provide a true prevalence. It is likely, therefore, considering how small and easily overlooked the intermediate and distal phalanges of the foot are during excavation, that the prevalence of this congenital abnormality was higher than was observable during the current analysis. For example, a high frequency of symphalangism of the fifth digit of the toe has been recorded in numerous populations from different regions of the world, ranging from 36% to 80% (Case and Heilman 2005, tab. 1). At Gabati, 30.2% of observable individuals had symphalangism of the distal interphalangeal joint (Judd 2012), suggesting that fusion of this joint may have been a common congenital anomaly in past Sudanese populations.

5.7 Possible neoplastic disease

Neoplastic disease is the uncontrolled growth of tissue, which can occur only locally, known as benign, or spread (metastasise) uncontrollably throughout the body, known as malignant (Marques 2019; Roberts and Manchester 2010, 252-253). Neoplastic disease in ancient Sudan is rare, but several instances have been reported. Whiting *et al*. (2022) describe a probable male adult from the *Kerma Ancien* site O16, located in the Northern Dongola Reach, with mixed osteolytic and osteoblastic lesions affecting the ribs, vertebrae and pelvis. This was suggested to be metastatic carcinoma of uncertain origin or other malignant neoplasm. Binder *et al*. (2014) present a young adult male from Amara West, dating to the New Kingdom period, with mainly osteolytic lesions on multiple post-cranial elements. Several bones also demonstrated new bone formation within the trabecular bone. This instance was also considered to likely represent metastatic carcinoma of uncertain origin. A Meroitic male from the Wadi Halfa region has been described as having large lytic lesions on the cranial vault, ilia, the left scapula and a lumbar vertebra, which were again suggested to be caused by metastatic cancer (Esche *et al*. 2010). There are also multiple reports of neoplastic disease across time from Egypt (Binder *et al*. 2014, tab. 1). Three instances of possible neoplastic disease were observed in the assemblage from site R18.

Skeleton (561)25

Skeleton (561)25, a middle adult male, presented with mixed reaction lesions on the superior central portion of the left iliac blade, affecting both the medial and lateral surfaces. Coalesced poorly-defined destructive lesions with rounded margins were present on both surfaces of the superior-most aspect of the blade, causing thinning of the iliac crest. These lesions were accompanied by infilling of the exposed trabeculae with dense granular or spiculated new bone, covering the floor of the lesions. Taphonomic damage to the cortical surface of other regions revealed that the trabeculae of a large portion of the superior iliac blade had been infilled with the same new bone formation (Plate 2.33). In addition, this skeleton also had new bone formation on the superior and inferior aspects of the vertebral bodies corresponding to the intervertebral discs between L4 and L5 and between L5 and S1, consisting of diffuse nodular woven bone (Plate 2.34). The only other lytic lesion noted on this skeleton was a small cavitation on the left capitate,

Plate 2.33. The lateral aspect of the iliac crest of the left ilium of a middle adult male, showing destruction of the iliac crest and blade (white arrows) and new bone formation. In regions of postmortem damage, new bone can be observed embedded within the trabeculae and extending beyond the destructive foci (red arrow) [Skeleton (561)25].

Plate 2.34. Diffuse nodular woven bone on the inferior aspect of the fifth lumbar vertebral body in a middle adult male [Skeleton (561)25].

just distal to the facet for the hamate, which could simply represent an intracarpal cyst. Radiography of the pelvis, vertebrae and ribs revealed no further lesions and, unfortunately, the remainder of the skeleton was too fragmented for imaging. The radiographs did reveal that only slight sclerotic margins were present on the lytic lesions of the iliac blade (Plate 2.35).

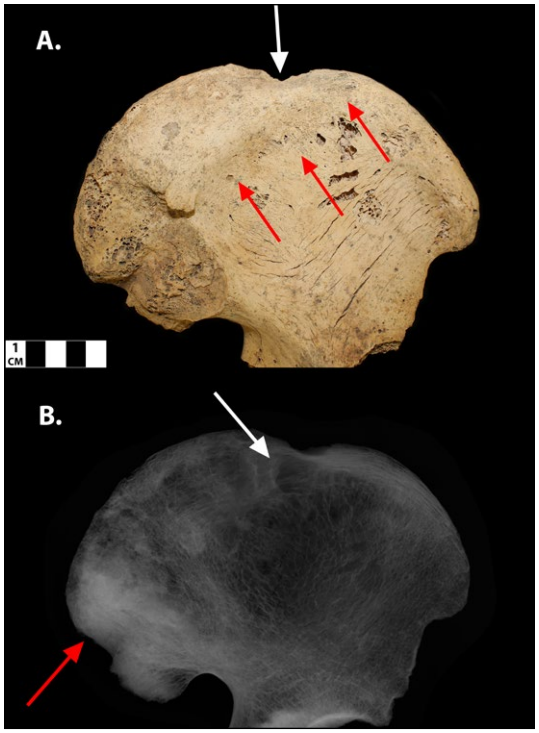

Plate 2.35. The left ilium of a middle adult male with mixed destruction and new bone formation, possibly caused by pathological changes related to metastatic cancer [Skeleton (561)25]. A. Destruction (white arrow) and the extent of visible new bone formation within the trabeculae (red arrows) on the medial surface of the ilium. B. A radiograph of the left ilium, demonstrating slight sclerotic margins around lytic lesions (white arrow). Dense radiopaque regions (red arrow) are likely caused by the infiltration of earth into the trabeculae postmortem. Radiograph by Dr Daniel O'Flynn.

A number of pathological processes can cause mixed osteoblastic and osteolytic lesions. These include osteomyelitis, mycotic infection, brucellosis and neoplastic disease. Osteomyelitis was ruled out due to the lack of cloaca and prolific new bone formation on the outer cortical surfaces (Klaus 2018). Mycotic infection is predominantly lytic in nature with no coalescence of lesions (Hershkovitz *et al*. 1998) and, while brucellosis affects the lumbar vertebrae most commonly, outside of the spine this disease affects the joints not the iliac blade (al-Shahed *et al*. 1994). An iliopsoas abscess was also considered as a cause, often occurring as a complication of tuberculosis of the spine (Roberts and Buikstra 2019). Stark *et al*. (2015) present a skeleton from an Egyptian Theban tomb with skeletal changes indicative of an abscess in the region of the pelvis, consisting of a large scalloped area of resorption, with some osteoblastic activity, on the medial surface of the left ilium. However, in the current study, the anterior-medial position of the iliopsoas muscles (e.g. Mallick *et al*. 2004, fig. 3) is not consistent with proliferative and destructive lesions being present on the lateral aspect of the ilium. The unusual infilling of the trabeculae of the ilium but a lack of new bone formation on the outer cortical surfaces is also inconsistent with an iliopsoas abscess, as the infection involved in the abscess primarily affects the muscle group rather than the bone itself.

It is possible that these lesions could represent a form of neoplastic disease such as metastatic cancer or osteosarcoma. The involvement of the haematopoietic region of the ilium, causing infilling of the trabeculae with spiculated new bone, is consistent with metastases, which invade these regions before proceeding outwards to destroy the cortical bone (Lieverse *et al*. 2014). Additionally, spiculated bone, sometimes known as a 'sunburst' reaction, within the marrow space is typical of osteosarcoma and can also occur in blastic metastases (Ragsdale *et al*. 2018). The minimal sclerotic margins of the iliac lesions when observed using radiography suggest that this lesion was relatively fast forming and the coalesced 'motheaten' appearance is typical of metastatic carcinoma (Ragsdale *et al*. 2018).

Prostate cancer typically involves an osteoblastic reaction, with a high predilection for skeletal involvement of the pelvis and lumbar vertebrae (Lieverse *et al*. 2014). Osteolysis also occurs in prostate cancer, with circumscribed or poorly defined irregular regions of bone destruction (Klaus 2018; Lieverse *et al*. 2014). Prostate cancer can also include invasion of the vertebral disc space by cancer cells, causing narrowing (Resnick 2002, 4304, 4322), which may account for the unusual new bone formation on the superior and inferior aspects of the vertebral bodies of L4, L5 and S1. Similar lesions to those observed in Skeleton (561)25 can also be reproduced in bladder, pancreatic and carcinoid tumours, but these types of tumour occur far less commonly than prostate cancer (Klaus 2018).

Similar lesions, observed both macroscopically and radiographically, can also be present in secondary osteosarcoma related to Paget's disease, which has a predilection for involvement of the pelvis (Hansen *et al*. 2006; Resnick 2002, 1971). Paget's disease is characterised by unusual bone remodelling, beginning with bone destruction and then moving on to a sclerotic stage, involving cortical thickening and coarsened trabeculae (Waldron 2021, 195). Osteosarcoma of both ilia related to Paget's disease has been observed in a British Medieval skeleton (Shaw *et al*. 2019). However, the rarity with which osteosarcoma develops in those with Paget's disease (in 1% of patients) (Hansen *et al*. 2006), and the lack of evidence for bony changes related to the disease in other elements of the skeleton, suggests that prostate metastasis may be more likely to have been responsible for the lesions observed in this individual.

Skeleton (HA2)209 and Skeleton (JG3)13

Two individuals demonstrated dense granular new bone embedded within the mandible, which was only possible to observe in both cases due to postmortem breakage. Skeleton (HA2)209, a young adult male, had a small region of dense granular new bone embedded within the cortical bone of the right gonial angle. The new bone was generally diffuse, although it appeared to be spreading from a central focus. A

second, smaller lesion, consisting of the same type of new bone, was located on the medial wall of the right maxilla, within the nasal cavity. This small lesion was embedded within the cortical bone but appeared to have eroded the external cortical surface. Skeleton (JG3)13, a young adult female, had granular, slightly porous new bone formation within the mandibular canal on the left side of the mandible. Radiography presented a faint radiopaque mass that was difficult to observe, but further CT scanning revealed a large region of bone formation within the mandible with a 'ground glass' appearance (Plate 2.36).

Plate 2.36. New bone formed within the mandibular canal on the left side of the mandible in a young adult female [Skeleton (JG3)13]. A. The granular, slightly-porous new bone is located within the mandibular canal, but is not integrated with the surrounding cortical bone. B. Image segmentation using a CT scan of the affected mandible illustrates the possible dimensions of the tumour-like new bone (orange region). CT scan and image manipulation by Dr Daniel O'Flynn.

Several types of neoplastic bone growth can occur in the jaws and can cause a radiopaque appearance on radiographs, including cementoblastoma, cemento-ossifying fibroma, fibrous dysplasia, periapical cemento-osseous dysplasia, florid cemento-osseous dysplasia and osteosarcoma (Bell and Piper 2000; El-Mofty 2014). Cementoblastoma, which is characterised by cementum formation (Huber and Folk 2009), can be ruled out in both skeletons as the appearance of the tumours in these cases were that of bone rather than cementum. Osteosarcoma can also be ruled out as this condition is very rare in the jaw and is usually seen in this region of the skeleton in older adults as a complication of Paget's disease (Bell and Piper 2000; Chaudhary and Chaudhary 2012), evidence for which was not observed in either young adult skeleton. In fibrous dysplasia, new disorganised immature bone and fibrous tissue replaces the original cortical bone (El-Mofty 2014). This is consistent with the lesion found in Skeleton (HA2)209, in which the granular new bone appears embedded within the cortical bone of the mandibular gonial angle and the medial wall of the right maxilla. Fibrous dysplasia usually occurs in the first two decades of life, but can continue to develop in later life and often occurs in the cranio-facial region (El-Mofty 2014; Rahman *et al*. 2009).

The tumour-like new bone in the young female, (JG3)13, was not merged with the cortical bone, but appeared to be sitting within the mandibular canal. This could represent cemento-ossifying fibroma, which most frequently affects adults aged 20 to 40 years, more commonly in females (Bell and Piper 2000). Consisting of bone and cemental-like tissue, it does not integrate with the cortical bone but generally consists of a well-defined lesion (El-Mofty 2014, 435). A similar lesion known as periapical cemento-osseous dysplasia usually affects females more commonly, but normally in those over 50 years of age. It occurs in the region of the mandibular incisors, and can become a large dense mass over time, consisting of fibrous tissue, bone and cemental-like tissue (Bell and Piper 2000, 268). A further condition known as florid cemento-osseous dysplasia is histologically very similar in constitution to periapical cemeto-osseous dysplasia, although it can involve large portions of the jaw and usually occurs in women of African descent of middle age or older (Daviet-Noual *et al*. 2017). Future histological analysis of the new bone may be able to help distinguish the exact form of tumour present in this individual (Bell and Piper 2000).

6. Oro-dental pathology

An investigation of dental disease, periodontal disease and dental wear can provide valuable information about diet, food preparation and oral hygiene practices (Hillson 2005, 286). In the current study, the presence of teeth, dental wear, carious lesions, dental calculus, periodontal disease and periapical lesions were all recorded.

6.1 Tooth presence

Presence and absence of teeth were scored according to the categories provided by Buisktra and Ubelaker (1994, tab. 2):

1. Present, but not in occlusion.
2. Present, development completed, in occlusion.
3. Missing, with no associated alveolar bone.
4. Missing, with alveolus resorbing or fully resorbed: antemortem loss.
5. Missing, with no alveolar resorption: postmortem loss.
6. Missing, congenital absence.
7. Present, damage renders measurement impossible, but other observations are recorded.
8. Present, but unobservable (e.g., deciduous or permanent tooth in crypt).

In total, 2,457 dental sites were scored for individuals in the adult age groups, in which 58.1% (1427/2457) of teeth were recorded as present, and 41.9% (1030/2457) as missing. Of the teeth recorded as present, 0.3% (4/1427) were not in occlusion (category 1), 74.5% (1063/1427) were fully developed and in occlusion (category 2), 25.1% (358/1427) were damaged (category 7), and 0.1% (2/1427) were unobservable because they were still in the crypt (category 8). Of the absent teeth, 66.3% (683/1030) were missing with no remaining socket (category 3), 13.6% (140/1030) were lost antemortem (category 4), 17.6% (181/1030) were lost postmortem (category 5), and 2.5% (26/1030) were congenitally absent. Category 3, whereby the tooth and associated alveolar bone is absent, consisted of 27.8% (683/2457) of all dental sites recorded. This represents a large proportion of potential information from this collection that remains

unknown, likely due to taphonomic damage and loss of alveolar bone postmortem.

The scoring and presentation of data relating to nonadult teeth is problematic, due to the presence of mixed dentitions. The presence scores for both permanent and deciduous teeth in nonadults for all observable sites is presented in Table 2.29 by age category, since it would be expected that individuals of similar age would have similar tooth development and eruption patterns. The percentage of teeth in Category 3 (missing, with no associated alveolar bone) cannot be presented for nonadults due to variations in tooth development at different ages, which makes it difficult to know how many teeth may have been present (but are now subsequently missing) in a nonadult.

6.2 Antemortem tooth loss in adults

In adults, 8% of total observable tooth sockets (140/1757) demonstrated resorption consistent with loss of the tooth prior to death (Table 2.30). This is considerably higher than at the nearby *Kerma Ancien* site H29, where antemortem tooth loss was present at 1.3% (21/1,588) of tooth sites (Whiting 2018). This could reflect changes in diet and the use of the dentition for purposes other than mastication through time. At Kawa, antemortem tooth loss was generally more prevalent across the lower dentition than across the upper dentition (Figure 2.9). Dentition on the right and left side of the jaw were roughly equally affected, except in the upper premolars. The right premolars had a slightly higher prevalence of antemortem loss. Higher prevalence rates of antemortem tooth loss at specific sites within the jaw could reflect possible use of specific dental sites for non-masticatory functions (resulting in more frequent damage and loss of these teeth) or other cultural behaviours such as intentional extraction of specific teeth (see Bolhofner 2017; Simon *et al*. 2002; Taylor and Antoine 2014). However, frequency rates and alveolar preservation levels at Kawa were too low to investigate this further.

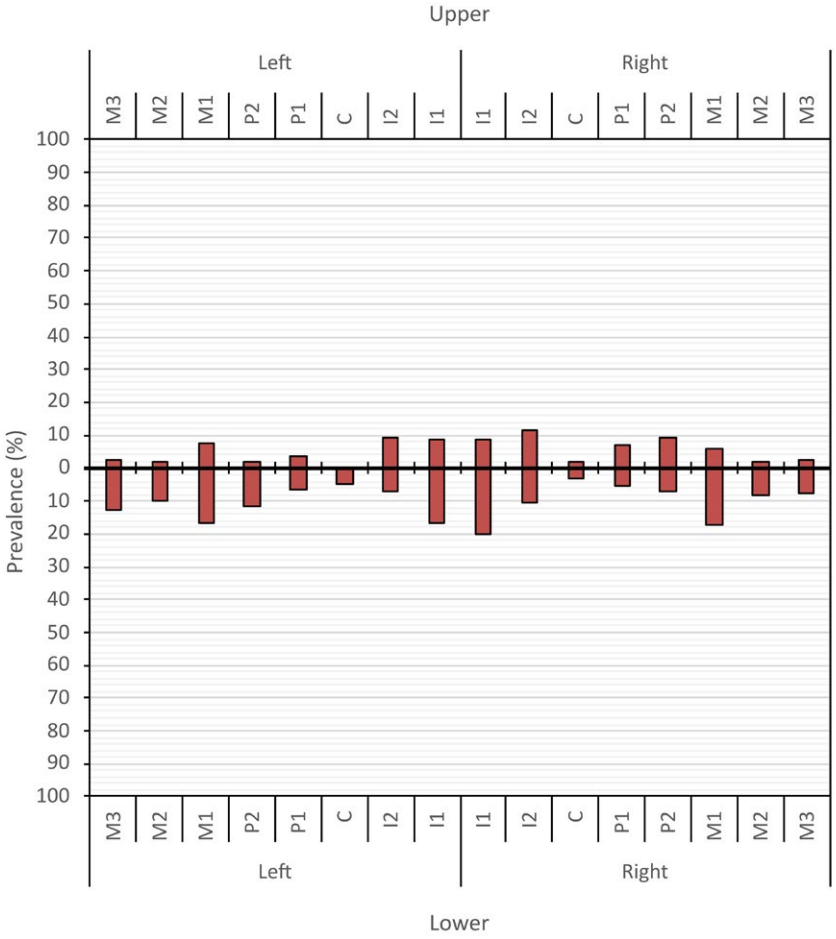

Figure 2.9. The prevalence of antemortem tooth loss by tooth site in all adults.

6.3 Dental wear

Wear was recorded in adults only. In the anterior teeth (the incisors, canines and premolars), wear was scored according to the system produced by Murphy (1959) and adapted by Smith (1984). This method requires the scoring of wear into one of eight categories, based on the amount of dentine exposure (see Buikstra and Ubelaker 1994, fig. 25). As recommended by Buikstra and Ubelaker (1994, 52), wear of the molars was recorded according to a different method produced by Scott (1979), in which each molar occlusal surface is divided into quadrants and the amount of observable enamel is scored on a scale of 1 to 10 (see Buikstra and Ubelaker 1994, fig. 26). The final score for each molar results from the sum of scores for the four quadrants, thus yielding a possible score of between 4 and 40. For teeth in which wear was unobservable, due to damage or absence of the tooth, a wear score of 0 was recorded. Although the mix of methods used here is not ideal for an accurate comparison of wear across the dentition, the wear data are presented for comparison with previously published sites and to examine general patterns of wear at Kawa.

Tables 2.31 (anterior teeth) and 2.32 (molars) demonstrate the average wear scores for each tooth in all adults, and according to sex and age groups. In general, mean wear scores in the anterior teeth according to type of tooth, side, or upper or lower dentition, were similar, ranging from an average score of 4 to 5.2, with the lowest level of wear in the anterior upper incisors (Figure 2.10). In the molars a uniform increase in wear between the first, second and third molars was evident, which is consistent with their eruption sequence (Figure 2.11). Males demonstrated a slightly higher average wear score than females particularly in the anterior dentition and, as might be expected due to the increase in wear over time, middle adults generally had higher average wear scores than young adults.

6.4 Dental caries

The demineralisation of the enamel, dentine, and cementum, known as a carious lesion or caries, results from the presence of acid-producing bacteria in the dental plaque. Persistent production of acid by these bacteria can lead to

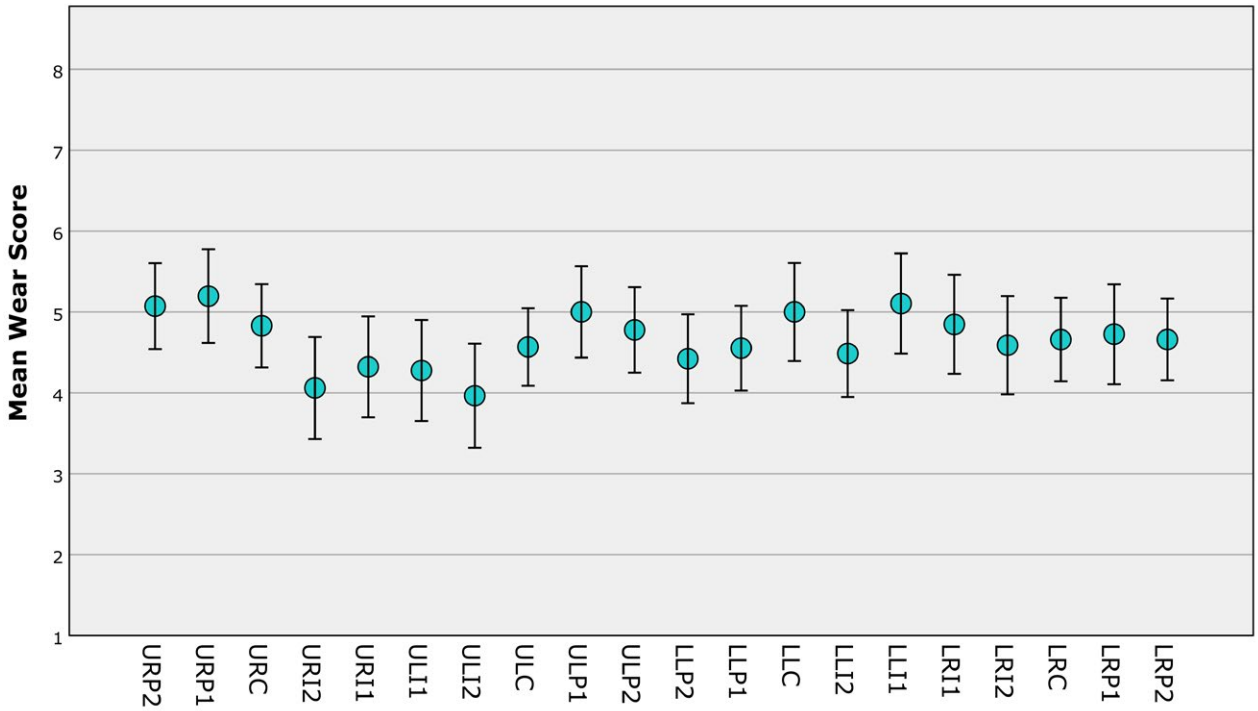

Figure 2.10. Mean wear score values for the anterior dentition (blue dots) in all adults and standard error bars.

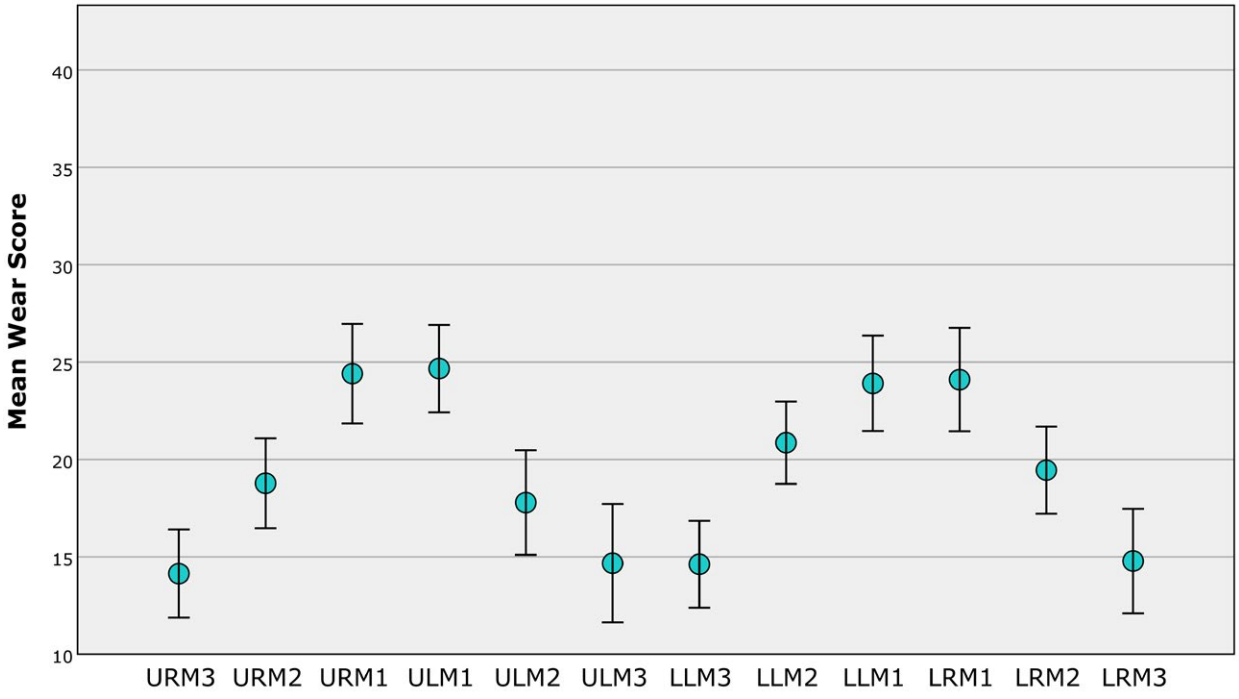

Figure 2.11. Mean wear score values for the molars (blue dots) in all adults and standard error bars.

the formation of large cavities in the crown or root surface (Lingström *et al*. 2000). An individual's susceptibility to developing dental caries appears to have some relation to genetic factors, although dental treatment and diet, particularly the intake of sugars and starches, is intimately linked to the development of these lesions (Hancock *et al*. 2020; Lingström *et al*. 2000). The longer a tooth is exposed to the oral environment, the greater the risk of developing caries. Therefore, the prevalence of carious lesions is also often seen to increase with age (Temple 2016).

Carious lesions were recorded following the method established by Moore and Corbett (1971), as recommended by Buikstra and Ubelaker (1994, 55). Dental caries were recorded for each tooth (permanent and deciduous) by the tooth surface affected, using the following scores:

0. No lesions present.

1. Occlusal surface: all grooves, pits, cusps, dentin exposures and the buccal and lingual grooves of the molars.

2. Interproximal surfaces: includes the mesial and distal cervical regions.

3. Smooth surfaces: buccal/labial and lingual surfaces other than grooves.

4. Cervical caries: originates at any cemento-enamel junction, except the interproximal regions

5. Root caries: below cemento-enamel junction.

6. Large caries: cavities that have destroyed so much of the tooth that they cannot be assigned a surface of origin.

7. Non-carious pulp exposure.

There are some issues with the recording system for dental caries employed in this study. Primarily, while the system records the prevalence of lesions on different tooth surfaces, it does not allow for the recording of the presence or absence of observable tooth surfaces, thus making a calculation of true prevalence impossible. Due to this issue, the prevalence of carious lesions is presented below by tooth affected, not by tooth surface affected. It is recommended that future studies consider employing the system produced by Hillson (2001), which takes into account the preservation of individual 'sites' on one tooth (e.g. occlusal surface, buccal surface, root surface). This provides a greater understanding of the true prevalence of carious lesions and their distribution across the dentition.

Carious lesions in adults

In general, the molars appeared to have the highest prevalence rates of carious lesions, in particular affecting females (Table 2.33, Figures 2.12 & 2.13). Males, however, showed an increased prevalence rate of caries in the upper right premolars. Although it might be expected that middle adults would have a higher prevalence of carious lesions, rates in young adults do exceed those in middle adults in some teeth, particularly the lower right molars. This may be due to the fact that subsequent increased wear in middle adults obscures the observation of caries in these teeth. The incisors demonstrate little to no carious lesions in all groups, likely due to the shape of the teeth, which somewhat inhibits the adherence of starchy foods and plaque deposits (Temple 2016).

Carious lesions in nonadults

While prevalence rates have been presented by age group in Tables 2.34 and 2.35 for nonadults, only the total prevalence for caries in all nonadults has been presented in Figure 2.14, due to the small number of observable teeth in each group. Following a similar pattern in adults, nonadults had a higher prevalence of carious lesions in the permanent molars, but, unlike adults, the anterior deciduous teeth were also affected.

6.5 Dental calculus

Dental calculus, a mineralised dental plaque that

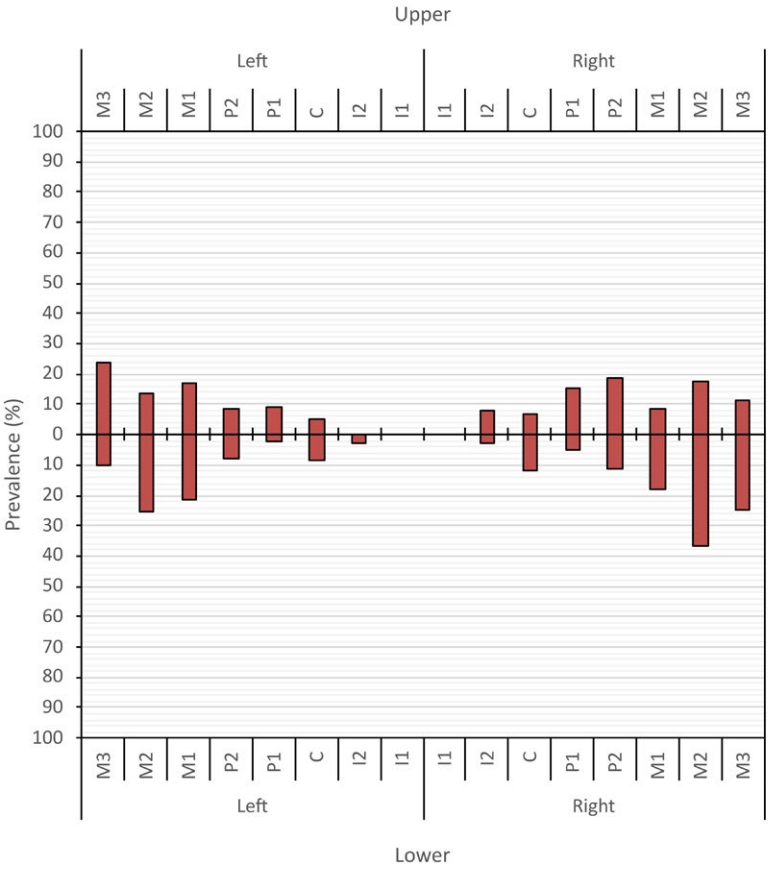

Figure 2.12. The prevalence of carious lesions by tooth in all adults.

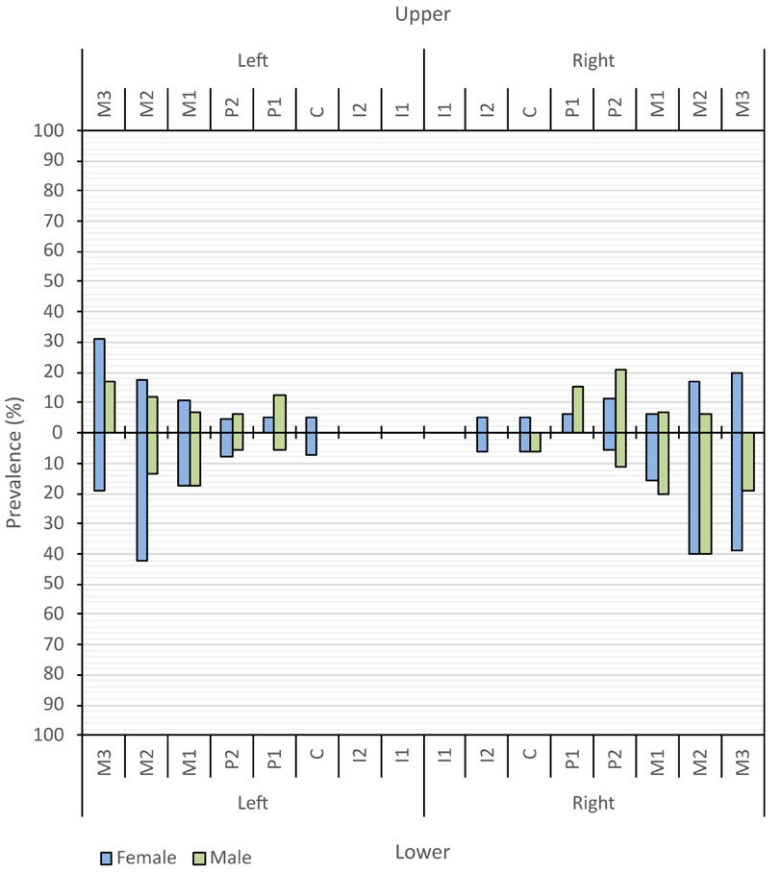

Figure 2.13. The prevalence of carious lesions by tooth in female and male sex groups.

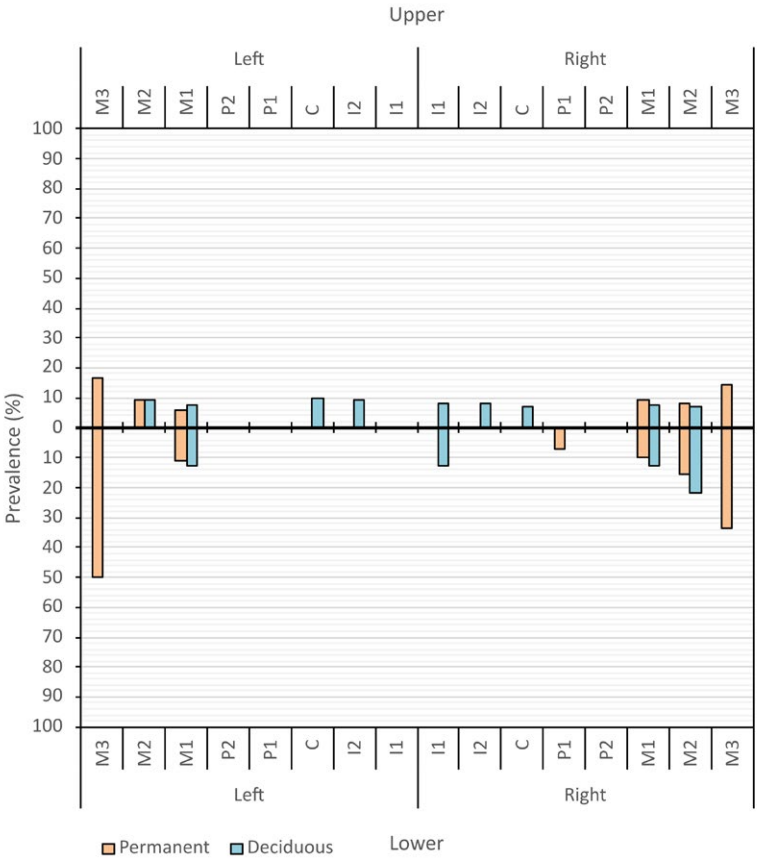

Figure 2.14. The prevalence of carious lesions by tooth in nonadults according to deciduous and permanent dentition.

forms on the exposed surfaces of teeth, is often found in archaeological skeletons (Radini *et al*. 2017). The reasons behind the quantity of calculus present and its distribution across the dentition within an individual may depend on oral hygiene, the level of carbohydrate consumption, and/or salivary flow and make-up (Jin and Yip 2002), meaning that the study of calculus may give an insight into aspects of ancient dental hygiene and diet (Buckley *et al*. 2014). As particles within the oral environment can become trapped within the mineralised plaque, calculus is also extremely useful for microscopic studies to investigate dietary inclusions and particles consumed or breathed in from the environment or during activities related to occupation (Radini *et al*. 2017).

Calculus was scored according to the method provided by Buikstra and Ubelaker (1994, 56), as follows:

0. Absent.
1. Small amount.
2. Moderate amount.
3. Large amount.

To demonstrate the suitability of the skeletons from Kawa for further calculus studies, the percentage of all individuals with calculus present on at least one observable tooth is presented in Table 2.36 according to age group. A high percentage of individuals (91%) with permanent teeth had some form of calculus present. Of the 220 deciduous teeth that could be examined, 22 (10%) had observable calculus, 100% of which demonstrated a calculus grade of 1. Of the 1,275 permanent teeth that could be examined, 899 (70.5%) had observable calculus. Of these, 77.6% (698/899) had a calculus grade of 1, 18.8% (169/899) a grade of 2 and 3.6% (32/899) a grade of 3.

6.6 Periodontal disease

Periodontal disease is the term that describes inflammation and pathological change affecting the soft and hard tissues surrounding the teeth. The changes may initially only involve inflammation of the gingivae, called gingivitis, while more advanced periodontal disease can affect the periodontal ligaments and alveolar processes (Pihlstrom *et al*. 2005). A method for scoring changes to the alveolar bone reflective of the different stages of periodontal disease has been produced by Kerr (1988). This method involves the scoring of each alveolar septum (the alveolar crest present between the teeth) into one of six categories, according to the form and textural appearance of the interdental alveolar bone (Kerr 1988):

0. Unrecordable: the tooth on either side of the septum has been lost antemortem or the septum has been damaged postmortem.
1. Normal: the septal form is characteristic of its region, with a smooth cortical surface, virtually uninterrupted by foramina, depressions, or grooves.
2. Gingivitis: the septal form is characteristic of the region, with the cortical surface showing foramina and/or grooves.
3. Acute phase of periodontal disease: the septal form shows breakdown of the contour, with bone loss in the form of a shallow depression. The bone defect is sharp and ragged.
4. Quiescent phase of periodontal disease: the septal form shows breakdown of the contour similar to score 3, but instead of a ragged bone surface it has a porous and smooth honeycomb appearance.
5. Rapidly progressive periodontal disease: the presence of a deep infra-bony defect with sides sloping at least 45 degrees and with a depth of 3mm or more. The surface may be sharp/ragged or smooth/honeycombed.

Only adults were observed for alveolar changes related to periodontal disease, due to the mixed dentitions and changes to the alveolar bone related to growth and eruption in nonadults. From the 2,310 alveolar crests that could potentially be scored, 1,524 (66%) were damaged, lost or were affected by antemortem tooth loss, and were, thus, unrecordable (score 0). The remaining 786 sites presented normal alveolar bone (score 1) in 27.7% (218/786) of cases, and slightly porous bone linked to gingivitis (score 2) in 39.1% (307/786) of instances. Scores 3, 4 and 5, all believed to be representative of changes related to periodontal disease, were present in 21.9% (172/786), 8.5% (67/786), and 2.8% (22/786) of observable sites, respectively.

Score 2 generally demonstrated the highest prevalence rates, although a large proportion of alveolar crests in association with the molars also appeared to be in the higher score categories (Table 2.37, Figure 2.15). This result is similar to that found in other Sudanese populations from

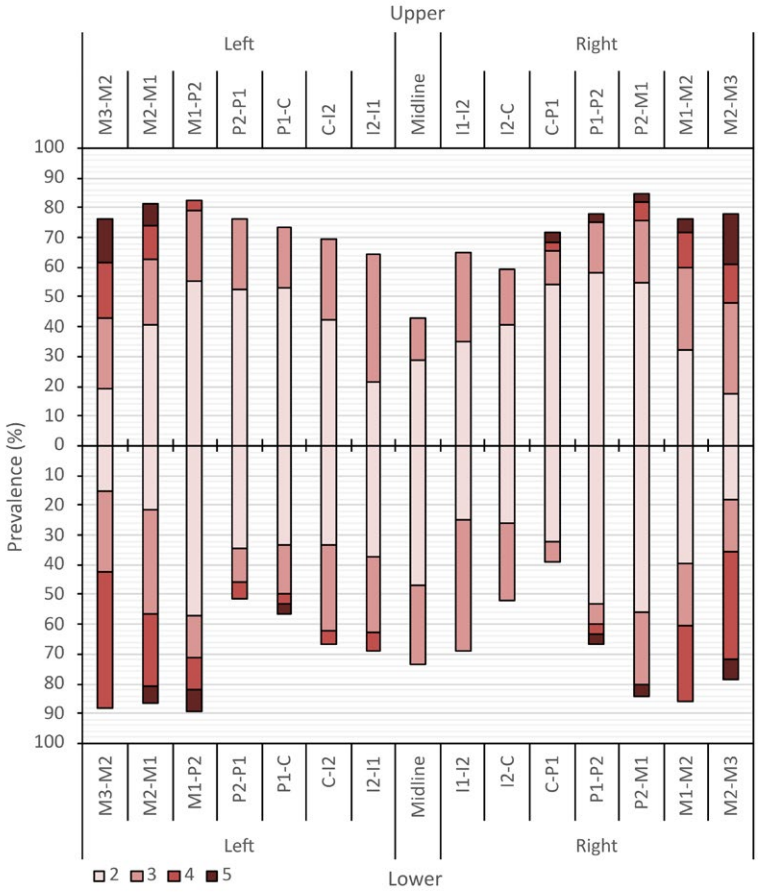

Figure 2.15. The prevalence of periodontal disease scores 2 to 5 in all adults according to alveolar crest.

the Northern Dongola Reach and Fourth Cataract regions, where prevalence rates varied between sites but consistently presented with a higher prevalence of scores 3 to 5 in the molar region of the jaws (Whiting *et al*. 2019). At Kawa, females showed slightly higher prevalence rates in the more severe scores than in males, particularly in alveolar crests related to the molars (Table 2.38). No obvious differences between young and middle adults were present, although middle adults did appear to have a greater number of alveolar crests demonstrating some form of change, in comparison to young adults who had a greater number of alveolar crests with a score of 1 (Table 2.39).

6.7 Periapical lesions

Periapical lesions, in the form of cavities, are located in the alveolar bone at the apex of the tooth root (Plate 2.37). When the pulp of the tooth is exposed, this can lead to the spread of infection down the canal and the production of pus at the apex of the root, inciting fibrous tissue formation or fluid accumulation that resorbs alveolar bone and produces periapical cavities (Hillson 2005, 307-309; Ramachandran Nair 1997). The texture of the walls of the lesion are thought to give an indication of the type of pathological process taking place. Smooth walled lesions are believed to be caused by cysts (fluid filled sacks) or granulomas (fibrous granulation tissue). A rough walled appearance may be linked to an active infective process related to pus accumulation (abscess) and may be accompanied by a sinus to drain the pus (Hillson 2005, 308-309).

Due to the mixed dentition of nonadults, only adults were observed for periapical cavities. Additionally, as periapical lesions do not always produce externally visible changes, only sites in which the apex of the socket could be observed were scored for periapical lesions (i.e., if the tooth could not be lifted from the socket, this site was recorded as unobservable). Periapical lesions were scored according to the following criteria in order to distinguish granulomas or cysts from abscesses:

0. Absent.
1. Granuloma or cyst: smooth walled lesion.
2. Abscess: rough walled lesion.

The periapical region of the first molar in both the upper and lower jaws appears to be most frequently affected (Figure 2.16). No sites related to the third molars were affected. The small number of sites observable for each tooth, when divided by age and sex categories, makes it difficult to observe differences between these groups (Table 2.40). However, females demonstrated a higher total prevalence of granulomas/cysts than males, who had a higher total prevalence of abscesses. Middle adults also had a higher total prevalence of both categories of periapical lesion than young adults. This might be expected as risk factors involved in the development of periapical lesions, such as caries and dental wear, also increase from the young to middle

Plate 2.37. A large periapical lesion (arrow) in an adult, located within the left maxillary alveolar bone in the region of the first premolar [Skeleton (HA2)171].

adult categories in this group, and have been closely linked with increasing age in other groups. For instance, in *Kerma Ancien* individuals from site H29 a higher prevalence of periapical cavities was observed in middle adults (0% in young adults, 2.7% in middle adults). However, prevalence rates in skeletons from site R18 were considerably higher than at site H29, which had a total prevalence rate of only 2.7% (25/921) (Whiting 2018), as opposed to the total prevalence rate of 9.5% (72/760) at site R18. This could indicate that differences between these two sites in the wear pattern or exposure of the pulp cavity, due to carious lesions or trauma, may have caused a greater prevalence rate at Kawa. Unfortunately, the data on other types of dental disease and tooth wear from site H29 are not comparable

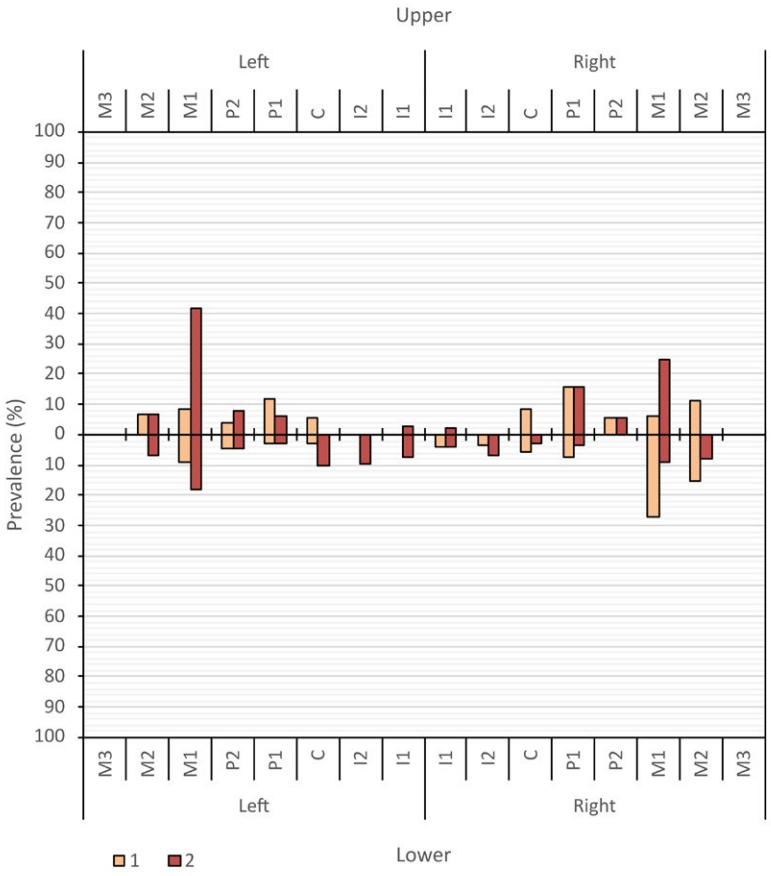

Figure 2.16. The prevalence of scores 1 (smooth-walled cavity) and 2 (rough-walled cavity) for periapical lesions in adults according to tooth site.

to the results from the current study due to differences in the methods used.

7. The skeleton from Building F1 Room VI

One articulated skeleton [(FP6)30] was recovered from Room VI of Building F1 in the town at Kawa (Plate 2.38). The placement of this individual was unusual as it was found against the south wall of the room, with no evidence for a grave cut, and may have been lain in the room to decompose during a period of abandonment (Welsby 2023f, 142). The skeleton itself was in poor condition, with a completeness of only 12%. This constituted the pelvis, lower thoracic and lumbar vertebrae and femora only. The absence of other elements may have been due to the skeleton being exposed or disturbed whilst lying within the room. The individual appeared to be that of a young adult based on epiphyseal fusion and analysis of the auricular surfaces. While poor preservation of the pelvis prevented accurate sex estimation, the femoral head diameter of this individual fell above the male 25th quartile for maximum femoral head measurements. This may suggest this individual was that of a young adult male. As it is not known when this individual was left within the room of Building F1, it is not possible to tell if it was contemporaneous with the individuals excavated from the site R18 cemetery. For this reason, the data from skeleton (FP6)30 has not been included in the analysis above. Nothing of note was observed in this individual except advanced ligamentum flavum of the surviving vertebrae and a third trochanter (non-metric trait) on the right femur.

8. The disarticulated bone

Rebecca J. Whiting

Because of the disturbed nature of many of the graves at Kawa, having been cut through by later inhumations and often robbed in antiquity, there were numerous contexts which contained disturbed, disarticulated human remains that could not be clearly associated with any one grave. All disarticulated remains recovered from Kawa are listed in Table 2.41. Only scant information could be gleaned from these remains. Of interest is the fact that Grave (JC3)12, marked by a stone pyramid, had been completely disturbed, with no human remains found within. However, the surrounding contexts, of (JC3)2, (JC3)4 and (JC3)8, contain human bone all belonging to the same young adult individual. There is no reason to believe that there is more than one individual represented here; despite some taphonomic differences in the preservation of the remains between contexts, the morphology of the skeletal elements match and there are no duplications. Additionally, the discovery of shaped ivory pieces in two of these three contexts also suggests an association between them. Conversely,

Plate 2.38. Skeleton (FP6)30 in situ *within Room VI of Building F1.*

context (JD2)10 was also associated with Grave (JC3)12 and contained the remains of a neonate or, at most, an infant between 0 to 1 years old at the time of death. Either, or both, the adult and the nonadult individuals may have been associated with Grave (JC3)12. Additionally, Grave (JF2)55 had

no remains associated with it; however, the disarticulated remains from associated context (JF2)84 suggest that this burial may have contained a neonatal individual.[2]

Another find of note is the third molar recovered from the town, site Q3 (AD5)247, within Building A4, Room D.[3] The tooth appears to be a lower left third molar with developing roots, suggesting the molar belonged to a young adult or older adolescent. A large chip to the mesial buccal cusp of the tooth was present. This trauma may have contributed to the loss of the tooth. However, wear on the edges of the chip causing smoothing of the chipped area suggests it remained *in situ* in the mouth for some time after the injury. The contexts [(AD5)246/247] appear to have been occupation layers in this building, where the only other finds were pottery. Why a human tooth might have been deposited here is unknown. The only other human remains recovered from site Q3 were that of skeleton (FP6)30, which was discovered in Building F1 Room VI and deposited in a similarly ambiguous way (section 8).

Very few pathological changes could be observed in the disarticulated remains recorded here. Osteoarthritis of the intervertebral facets was noted in several recovered vertebrae (see Table 2.41). Contexts (JE2)17[4] and (JE3)1 contained remains from two non-adults; these included long bone fragments from the humerus and femur of an older individual (11-15 years) and cranial fragments from a younger individual, all of which showed evidence of woven bone on the cortical surfaces. When the bones are still growing, a woven-bone-like appearance can be present; however, in this case, the changes appear to be pathological, although it is not possible to determine in these cases the cause of the new bone formation. As mentioned in section 5.4, this type of periosteal reaction can result from inflammation caused by infection, trauma, haemorrhage, overlying soft tissue lesions, tumours, mechanical stress and certain metabolic diseases (Rana *et al*. 2009; Waldron 2021, tab. 8.7-8.10; Weston 2012). One context, (GD3)92, contained a right femur with a healed fracture near the proximal end of the shaft, resulting in a large, disorganised swelling of the bone and apparent shortening of the shaft suggestive of a complex fracture. Some of the disarticulated dental remains showed signs of dental caries [(GD3)44, (GD3)116, (HA2)31], periapical cavities [(GD3) 116] and even non-masticatory dental wear [(GD3) 116].

9. Discussion

The 135 skeletons from the cemetery (site R18) and the single individual from the town (site Q3) represent a valuable research collection, providing an important insight into life in the Kushite period in this region. In particular, the association between the cemetery and the settlement provides a wealth of information to contextualise the lives of the inhabitants. Excavations in the town itself have uncovered numerous domestic structures: mud-brick multi-roomed dwellings containing hearths and ceramic bread ovens. Streets and disused rooms were employed as rubbish dumps and less fortunate inhabitants may also have inhabited more ephemeral housing. Administrative and industrial activities were also likely to have taken place in the town. Two large kilns have been found, and magnetic anomalies in Area B may indicate further industrial quarters (Welsby 2023c). There were also elite classes present, represented by the large stone pyramids found in the north-eastern part of the cemetery. The excavations attest a complex and vibrant town, likely made up of a number of social strata, including elite and merchant classes, agriculturalists, builders and specialist tradesmen.

Preservation and completeness of the human skeletal remains was generally fair, with good cortical preservation, although this ranged widely depending on the individual burial conditions and the level of looting. The relatively good preservation allowed for an in-depth investigation into the demographic make-up, biological variation and pathological changes present in the cemetery and attests to the suitability of the collection for further analysis. Nonadult and adult age groups were well-represented in the cemetery and followed a general attritional mortality profile, with a peak in the infancy group, declining mortality in older non-adult age groups, and a rise again in the middle adult age group category. The lack of individuals in the old adult category may indicate that people were not living beyond around 50 years of age. It is likely, however, that the aging methods utilised, which were not developed using Sudanese collections, may have an inherent bias towards placing Sudanese individuals into younger adult age categories. Males and females were also fairly equally represented, although 29.5% of adults could not be assessed for skeletal sex and 24.4% could not be assessed for age. It was also possible to assign a tentative sex estimation to a number of undetermined individuals using comparisons of humeral and femoral head measurements to those from identified male and female sex groups. The relatively equal representation of adults in the middle and young adult age groups and of males and females, as well as the large proportion of nonadult individuals, allowed for a comprehensive investigation into differences in biological variation and pathological changes between sex and age groups.

The prevalence of nonmetric traits was generally consistent with the findings of other studies in this region. In particular, the high prevalence of septal apertures on the humerii and lateral squatting facets of the tibiae have been noted in other studies from similar populations (Satinoff 1972; Whiting 2018, tab. 6.5). Metric data demonstrated a degree of sexual dimorphism, with males often having higher mean values for various different measurements. For example, using stature calculations it was possible to observe that males were on average 7cm taller than females. It was also established that measurements of the femoral head diameter and vertical humeral head diameter may be a useful tool for estimating the sex of the individuals for whom sex could not be determined using more conventional means. The mean stature estimations at site R18 were 157.7cm for females and 165.9cm for males. Overall, stature estimations were very similar to those from

[2] This data is not included in the excavation report in Volume I.

[3] Noted as coming from this context on the recording sheet, but as coming from (AD5)246 on the finds label. Both contexts are probably contemporary, (AD5)246 is in Room A4-F.

[4] It is possible that these bones come from skeleton (JE2)33.

Kerma Ancien period individuals from site H29, where mean female stature was 156.2cm and 164.5cm for males (Whiting 2018, 158). However, in individuals from Gabati dated to the Meroitic period, Judd (2012, 24) found that mean stature estimations were higher and similar between the sexes, at 161.2cm for females and 163.1cm for males. It is possible that, due to the geographical proximity of sites H29 and R18, factors such as nutrition, illness, diet and genetics played a similar role in differences in skeletal growth between males and females; as opposed to Gabati, which was located much further south where the factors affecting skeletal growth may have been quite different.

Other differences between the sexes were also noted. A statistically significant difference between the prevalence of osteoarthritis of the acromioclavicular joint in males and females was observed, with males far more likely to show evidence for the disease. Although both sexes had elevated prevalence rates of acromioclavicular osteoarthritis, the higher prevalence in males could indicate sex-specific activities that led to an increased susceptibility to the disease. While methods for recording osteoarthritis at the Meroitic-Medieval site of Gabati were different, it is still pertinent that Judd (2012, 53) found Meroitic males to invariably have a higher prevalence of osteoarthritis in major joints, particularly those of the shoulder (as well as the wrist, ankle and foot). These results, and those from site R18, could be due to strenuous or traumatic injuries related to this joint, such as repeated heavy lifting or throwing (Menge *et al*. 2014; Stenlund *et al*. 1992), although a genetic component may be present (e.g. Fernández-Moreno *et al*. 2008). Such activities would likely take place, for example, during agricultural work or in construction. The difference between males and females contrasts with observations of osteoarthritis at the *Kerma Ancien* cemetery, site H29, where both sexes presented with relatively similar prevalence rates (Whiting 2018). This could suggest that there may have been less division of gendered roles in this earlier group or that different roles were equally strenuous.

Spinal disease, such as osteoarthritis of the articular facets, osteophytes on the vertebral bodies, intervertebral disc disease and Schmorl's nodes, were all present in the adults at Kawa, with a higher prevalence, for the most part, in middle adults. The relatively high rates of different types of vertebral pathology suggest a level of spinal loading that could indicate active lifestyles and the carrying of heavy items from an early age, as noted by Tipper (2020) in an extensive study of vertebral pathology in populations from Meroitic to Medieval Sudan. The fairly high prevalence rate of intervertebral disc disease in the cervical spine in both males and females at Kawa could also indicate the effect of carrying loads, such as filled posts or baskets, on the head, which still occurs in areas of Sudan today (Tipper 2020). Other notable vertebral pathology included individuals with arterial pressure defects on the cervical vertebrae caused by tortuosity or aneurism, a number of individuals with various destructive lesions on the vertebral bodies, several instances of scoliosis, caused both by congenital developmental abnormalities and from compression fractures of the vertebral bodies, and one instance of diffuse idiopathic skeletal hyperostosis (DISH).

The high frequency of fractures in the adult individuals from Kawa also indicates an active lifestyle. However, the high prevalence of potential depression fractures on the crania, involving the frontal or parietal bones (11.5% of all adults), and the presence of nasal and other facial fractures, could also be evidence of interpersonal violence. Cranial depression fractures from individuals dating to the earlier Kerma period from the urban centre at Kerma and from rural sites P37 and O16, also located in the Northern Dongola Reach, have been interpreted as such (e.g. Judd 2006; Judd and Irish 2009). Two cases provide possible evidence for some interpersonal violence taking place at Kawa, directed towards both sexes. A young adult female presented with several potential perimortem penetrating injuries, likely related to sharp force projectile trauma, and an arrowhead recovered from the burial of a young adult male may have caused a possible sharp force trauma to the spine in this individual.[5] Neither of these burials were particularly different from those around them, nor did they contain unusual grave goods. While it is not possible to speculate on the source of this violence, the use of bows and arrows by Nubians is well attested (Bonnet 1982; Davies 2001). Possible blunt force perimortem trauma may also have been present, but was difficult to distinguish from taphonomic damage.

Other common injuries, such as those to the hands and feet, the ribs, and to the lower long bones, may have also been the result of activities related to occupation and activity, such as agricultural work or building construction. A similarly high frequency of fractures has been noted at the New Kingdom and Post-New Kingdom town of Amara West, in which 39.4% (54/137) of individuals had some form of trauma, particularly to the axial skeleton. This was attributed to potential accidental injury working in agricultural activities, including the handling of large animals (Binder and Spencer 2014). Males at Kawa also often demonstrated multiple, and at times extreme, traumatic injuries, which were much less common among females. This could point to an increased risk in males of exposure to traumatic injury, whether through activities related to occupation or through interpersonal violence.

Specific infectious diseases were difficult to identify in the skeletons from Kawa. Although destruction of the vertebral bodies was present in some individuals, none demonstrated the distinctive pathognomonic changes indicative of tuberculosis (e.g. Roberts and Buikstra 2019), and no other specific infectious diseases could be identified. Periosteal reaction on the long bones, however, was prevalent, affecting 26.9% of adults. This indicates that conditions present at Kawa were causing a relatively high prevalence of this pathology. Periosteal reaction may have been caused by infection in some instances, but other factors in its development include trauma, haemorrhage, overlying soft tissue lesions, metabolic diseases and mechanical stress (Rana *et al*. 2009; Waldron 2021, 183-184; Weston 2008; 2012). Some of these aetiologies may have resulted from a highly active lifestyle, as suggested by the rates of osteoarthritis, vertebral pathology, and trauma. The prevalence and

[5] For the stone arrowheads from Kawa see Welsby and Taylor 2024, cat. nos F-2361 to F-2382a.

distribution of periosteal reaction at site R18 can be compared with that seen in contemporary Meroitic individuals from Gabati. The highest prevalence at this site was 26.3%, recorded in the right tibia (Judd 2012), a rate very similar to the overall adult prevalence from Kawa.

That conditions at Kawa were conducive to the development of periosteal reaction is also reflected in the prevalence rates of respiratory disease in adults. In total, 29.5% of adults had periosteal reaction on the inner surface of the ribs, indicative of a lower respiratory tract disease, and 74.5% of adults had evidence for maxillary sinusitis. While both forms of pathological change can be caused by non-respiratory related diseases, such as dental disease for the sinuses and cancer or pulmonary embolism for the ribs, these prevalence rates indicate that respiratory diseases were probably a common condition for the inhabitants of Kawa. In particular, the high prevalence of maxillary sinusitis is comparable to rates from the *Kerma Ancien* and *Moyen* cemetery at site P37 in the Northern Dongola Reach and Amara West (Binder 2014, tab. 8.46; Davies-Barrett *et al*. 2021). This suggests that factors in the region were predisposing populations to the development of maxillary sinusitis. In particular, the arid environment developing in this region from the Neolithic period onwards may have had an effect on prevalence rates. Particulate matter in the air in such an environment, including dust and sand, can cause inflammation and predispose to infection in the sinuses (Davies-Barrett *et al*. 2021). Problems with sand ingress are evidenced at Kawa historically in temple inscriptions (Laming Macadam 1949, 15-16, 62) and archaeologically in the obvious encroachment of sand during the use of buildings (Welsby 2000; 2011; 2023c). However, the urban environment, including dense mud-brick housing, with hearths and ovens located indoors, and the presence of industrial quarters, are likely to have produced harmful air pollution, further increasing susceptibility to respiratory disease (Davies-Barrett *et al*. 2021; 2023).

Three adults were observed to have possible neoplastic disease. In one instance, this appeared to be a possible case of metastatic carcinoma, possibly from prostate cancer, affecting the lumbar vertebrae and left ilium. Metastatic carcinoma is rarely observed in archaeological skeletons, but individuals with evidence for the disease have also been identified at the *Kerma Ancien* cemetery, site O16, in the Northern Dongola Reach (Whiting *et al*. 2022), in a New Kingdom individual from Amara West (Binder *et al*. 2014), and in a Meroitic skeleton from the Wadi Halfa region (Esche *et al*. 2010). The inclusion of the possible instance of metastatic carcinoma from Kawa demonstrates that, although rare, this form of neoplastic disease was certainly present throughout time in the Middle Nile Valley. Two individuals also had neoplastic lesions of the jaw, both appearing to be benign.

A number of congenital and developmental abnormalities were also observed in both adult and nonadult individuals at Kawa. The vertebrae were most commonly affected and included border shifts, transitional vertebrae, cleft neural arches and spondylolysis. Other developmental abnormalities included sutural agenesis or craniosynostosis, resulting in scaphocephaly, and unusual development, or lack thereof, in the bones of the wrist, hands and feet. Of particular note is the identification of an infant with hydrocephalus, causing an enlarged cranial vault and other associated changes to the skull. This congenital disease is extremely rare to find in the archaeological record (Richards and Anton 1991), particularly so well preserved, and now adds to a small number of archaeological skeletons known to have had the disease. This infant was buried in a tomb consisting of a pit and subterranean side chamber with blocking wall, was wearing bracelets and anklets made from faience beads, and was likely buried within a coffin (Welsby 2023g, 220). This suggests that hydrocephalus, despite being a highly visible condition, did not preclude this infant from certain funerary treatments (Plate 2.39).

Plate 2.39. Skeleton (GD3)154, an infant, within the grave, demonstrating its careful burial and the inclusion of blue bead bracelets and anklets on the body when buried.

The large proportion of nonadults recovered from the site R18 cemetery also allowed for an investigation of diseases in childhood, which is not always possible in this region due to the poor representation of nonadult burials. Nonadults demonstrated a range of pathological changes, including periosteal reaction on the long bones and skull, endocranial lesions and vertebral changes, such as pressure defects of the cervical vertebrae and cavitations of the vertebral bodies. Trauma was observed in two adolescents, perhaps suggesting that nonadults in this age group began undertaking activities similar to their adult counterparts that may have exposed them to traumatic injury, although there are a range of other potential causes for fractures in nonadults. Cribra orbitalia was frequently observed in nonadults (22.4%), particularly in the early childhood category (58.3%). This is similar to rates observed in Meroitic to Medieval nonadults from the Wadi Halfa region (Carlson *et al*. 1974, tab. 1), but not as high as prevalence rates recorded from medieval Kulubnarti (Mittler and Van Gerven 1994). However, the causes of cribra orbitalia are potentially numerous and still hotly debated (Brickley 2018), making it difficult to investigate the potential causes and differences between age groups and sites. One adolescent had multiple Schmorl's nodes and anterior wedging of the vertebrae, indicative of Scheuermann's disease, which is characterised by a pronounced spinal kyphosis. Like hydrocephalus, this disease is also rarely identified in the archaeological record (Üstündağ and Deveci 2011), and has not previously been noted in

archaeological remains from Sudan. This individual also presented with osteochondritis dissecans of the left distal femur, which has been related to intense activity during adolescence, but may also be caused by a number of other factors (Hixon and Gibbs 2000).

Dental and oral diseases were common in individuals from Kawa. Of the observable permanent teeth in adults, 11.7% were affected by carious lesions, while 4.5% of permanent teeth and 7.1% of deciduous teeth were affected in nonadults. Antemortem tooth loss and periapical lesions were also relatively high, present in 8% and 9.5%, respectively, of all tooth sites observed. This is much higher than the prevalence rates observed at the *Kerma Ancien* site H29, suggesting a shift in the factors leading to antemortem tooth loss and periapical lesions between these two sites. This may be due to the relatively high prevalence of carious lesions observed at Kawa, which in advanced cases could have exposed the tooth pulp to infection and led to tooth loss. Changes to the alveolar bone indicative of periodontal disease were also present in the adults at Kawa, particularly affecting the molars, following a similar pattern to that observed in other Sudanese populations (Whiting *et al*. 2019). Both the presence of caries and periodontal disease indicates that the consumption of carbohydrates was taking place. Soft, sticky carbohydrates and sugars adhere to the teeth and encourage bacterial growth and plaque deposits, causing an increased risk of developing dental caries and periodontal disease (Hillson 2005, 302; Lingström *et al*. 2000).

The human skeletal remains from Kawa present a diverse range of information for the Kushite period, providing unique insights into life in the town. Analysis demonstrates that trauma, congenital abnormalities, and diseases of various kinds, including spinal, joint, respiratory and dental, were all present within the population. In particular, the identification of certain rare conditions, not often encountered in archaeological skeletons, provides a greater insight into the range of diseases present in the Middle Nile Valley and further demonstrates the potential of these skeletons for understanding life in this region during the Kushite period. It is likely that individuals at Kawa lived highly active lifestyles that may have increased the risk for trauma, joint disease and vertebral pathology. The town and environs in which they lived, including mud-brick housing with indoor hearths and ovens, and the arid external environment, may have also contributed to relatively high prevalence rates of respiratory diseases, as well as other pathological conditions observed. The detailed archaeological data from the town, site Q3, and from excavations within the cemetery, site R18, combined with good preservation and representation of different age and sex groups, provides the excellent opportunity for further in-depth study of life in the Kushite period in this region.

10. Kawa skeleton catalogue

Individual graves

(533)30
Area: - **Grave:** 533 **Skeleton:** 30 **EA Number:** 96531
Skeletal sex: undetermined **Age:** 20+ years **Stature:** -
Preservation:
Taphonomic score: fair *Cortical surface score:* 5 *Completeness:* 19%
Inventory:

Skull (%)	Dentition (%)	Vertebrae (%)	Ribs/sternum (%)	Upper limbs (%)	Hands (%)	Pelvis (%)	Lower limbs (%)	Feet (%)
90	25	5	5	0	0	0	40	10

Palaeopathology:
Dental disease:
Caries: ULP2.
Periapical lesion: LRI2.
Antemortem tooth loss: ULM1, LRI1.
Joint disease:
Osteoarthritis: temporomandibular joint of the right temporal.
Vertebral disease: None.
Trauma:
Possible healed depression trauma on the ectocranial surface of the frontal bone.
Inflammation: None.
Congenital:
Symphalangism of the distal interphalangeal joint of an unsided fifth foot digit.
Other: None

(561)21
Area: - **Grave:** 561 **Skeleton:** 21 **EA Number:** 96532
Skeletal sex: female? **Age:** 35-49 years **Stature:** 169.3cm $^{+}$/- 1.9cm (tibia$_{m}$)
Preservation:
Taphonomic score: poor *Cortical surface score:* 4 *Completeness:* 56%
Inventory:

Skull (%)	Dentition (%)	Vertebrae (%)	Ribs/sternum (%)	Upper limbs (%)	Hands (%)	Pelvis (%)	Lower limbs (%)	Feet (%)
10	35	40	50	40	90	70	85	85

Palaeopathology:
Dental disease:
Caries: LLM2, LRM1.
Periapical lesion: LRP1, LRM1.
Antemortem tooth loss: LLP2, LRP2.
Supernumerary or retained deciduous tooth root located between LRC and LRP1.
Joint disease:
Osteoarthritis: both mandibular condyles, distal joint of the left clavicle, glenohumeral joints of both scapulae, acromioclavicular joint of the right scapulae, glenohumeral joint of the left humerus, left acetabulum, right femoral head, patellofemoral joint of the left femur, patellofemoral joints of both patellae, medial and lateral condyles and proximal tibiofibular joint of the left tibia, metatarsophalangeal joints of both first metatarsals. Extensive rotator cuff disease of both left and right shoulder joints.
Vertebral disease:
Osteoarthritis of atlantoaxial joint: C1.
Osteophytes: C5, C6, T1, T2, L3 through to S1.
Intervertebral disc disease: C6, L3.
Schmorl's nodes: L3.
Trauma:
Partially healed fracture at the angle of a left unseriated rib.
Inflammation:
Periosteal reaction on the distal shaft of the left fibula.
Periosteal reaction on the visceral surface of a left lower-middle rib shaft.

Congenital:
Cranial vertebral border shift resulting in sacralisation of L5.
Other: None.

(561)24
Area: - **Grave:** 561 **Skeleton:** 24 **EA Number:** 96533
Skeletal sex: male **Age:** 35-49 years **Stature:** 164.1cm +/- 3.2cm ($femur_m$)
Preservation:
Taphonomic score: good *Cortical surface score:* 5 *Completeness:* 86%
Inventory:

Skull (%)	Dentition (%)	Vertebrae (%)	Ribs/sternum (%)	Upper limbs (%)	Hands (%)	Pelvis (%)	Lower limbs (%)	Feet (%)
85	80	95	90	90	80	90	85	80

Palaeopathology:
Dental disease:
Caries: URP2, LLM1, LLP2, LRP2, LRM1, LRM2.
Joint disease:
Secondary osteoarthritis of the distal interphalangeal joint due to a fracture on the distal phalanx of the first left foot digit.
Vertebral disease:
Osteophytes: C6, C7.
Intervertebral disc disease: C6, C7.
Schmorl's nodes: C3, C4, C5.
Trauma:
Healed fracture of the proximal base of the distal phalanx of the left first foot digit.
Inflammation:
Periosteal reaction on the shafts of both the left and right tibiae and fibulae.
Periosteal reaction on the shaft of the proximal phalanx of the third left foot digit.
Porous bone formation on the endocranial surface of the cranium in the region of the frontal crest.
Inflammatory bone changes present within both maxillary sinuses.
Congenital: None.
Other:
Right clavicle is 5mm shorter than left clavicle.
Possible early-stage fusion between the right lunate and triquetral articulation.

(561)25
Area: - **Grave:** 561 **Skeleton:** 25 **EA Number:** 96534
Skeletal sex: male **Age:** 20-34 years **Stature:** 173.9cm +/- 3cm ($tibia_m$)
Preservation:
Taphonomic score: Fair *Cortical surface score:* 5 *Completeness:* 82%
Inventory:

Skull (%)	Dentition (%)	Vertebrae (%)	Ribs/sternum (%)	Upper limbs (%)	Hands (%)	Pelvis (%)	Lower limbs (%)	Feet (%)
90	90	95	40	95	95	80	85	70

Palaeopathology:
Dental disease:
Periapical lesion: URP1.
Antemortem tooth loss: LLM1.
Non-masticatory wear in the form of interproximal grooves on URM1, URI2, ULM2, ULM3 and LLM2.
Joint disease:
Osteoarthritis: left temporomandibular joint on both the temporal and mandible, sternal joint of right clavicle, distal joints of both clavicles, glenohumeral joint of left scapula, acromioclavicular joints of both scapulae, both acetabula, patellofemoral surface of right patella.
Vertebral disease:
Osteoarthritis of articular facets: C1, C7, L3 through to S1.
Osteophytes: C4, C5, T3, T5 through to S1.
Intervertebral disc disease: C5, T11, T12, L4, L5, S1.
Schmorl's nodes: T11, T12, L2.
Trauma:
Depression fracture on the medial-anterior aspect of the lateral condyle of the right tibia.

Inflammation:
Inflammatory bone changes within both maxillary sinuses.
Congenital:
Neural arch hiatus of S1, S4, and S5.
Other:
Mixed reaction lesion on the superior central portion of the left ilium, affecting both anterior and posterior surfaces. Destruction of the central portion of the iliac crest, particularly on the anterior aspect. Additional destructive lesion with roughly rounded margins on posterior surface, just below iliac crest. Lytic lesions are accompanied by granular dense new bone formation, which covers the floors of the lytic lesions. Taphonomic damage also reveals that the trabecular bone of a large portion of the superior iliac blade has been infilled with the same granular dense new bone. Also present is porous, nodular woven bone formation on the superior and inferior aspects of vertebral bodies of L4, L5, and L6. In combination, lesions on the left ilium and vertebrae may indicate possible neoplastic disease. A large osteophyte just lateral to the retroauricular region on the left ilium could indicate initial fusion of the left sacroiliac joint, possibly related to destructive changes present on the left ilium.
Possible intracarpal cyst on left capitate.
Pressure defects of the right transverse foramen of C3 and the left transverse foramen of C5.

Grid square GD3

(GD3)26
Grid square: GD3 **Grave:** 3 **Skeleton:** 26 **EA Number:** 96551
Skeletal sex: undetermined **Age:** 0-1 years **Stature:** -
Preservation:
Taphonomic score: fragments *Cortical surface score:* 4 *Completeness:* 21%
Inventory:

Skull (%)	Dentition (%)	Vertebrae (%)	Ribs/sternum (%)	Upper limbs (%)	Hands (%)	Pelvis (%)	Lower limbs (%)	Feet (%)
10	20	25	10	35	10	20	40	15

Palaeopathology:
Dental disease: None.
Joint disease: None.
Vertebral disease: None.
Trauma: None.
Inflammation: None.
Congenital: None.
Other: None.

(GD3)27
Grid square: GD3 **Grave:** 16 **Skeleton:** 27 **EA Number:** 96554
Skeletal sex: female **Age:** 20-34 years **Stature:** -
Preservation:
Taphonomic score: fragments *Cortical surface score:* 4 *Completeness:* 39%
Inventory:

Skull (%)	Dentition (%)	Vertebrae (%)	Ribs/sternum (%)	Upper limbs (%)	Hands (%)	Pelvis (%)	Lower limbs (%)	Feet (%)
10	35	60	15	60	25	45	45	60

Palaeopathology:
Dental disease:
Caries: LRM2, LRM3.
Antemortem tooth loss: LLM1, LLP2, LLP1, LLC, LLI2, LLI1, LRI1, LRI2.
Unusual advanced dental wear across dentition.
Non-masticatory wear in the form of interproximal grooves on LLM3, LLM2, LRC, LRM2, LRM3, and URP1.
Joint disease: None.
Vertebral disease:
Osteoarthritis of articular facets: C4, C5, C7, T1, T6.
Osteophytes: C3, C4, C6, T7, T8, T11, T12, L3, L4, L5.
Intervertebral disc diseases: C3 through to C6, T7, T8, T11, T12, L2 through to L5.
Schmorl's node: T8.
Trauma:
Healed fracture of the shaft of the left second metatarsal.

Healed fracture of the shaft of the proximal phalanx of the left second foot digit.
Inflammation: None.
Congenital: None.
Other:
Pressure defect of the right transverse foramen of C4.

(GD3)30
Grid square: GD3 **Grave:** 7 **Skeleton:** 30 **EA Number:** 96552
Skeletal sex: undetermined **Age:** 2-5 years **Stature:** -
Preservation:
Taphonomic score: good *Cortical surface score:* 5 *Completeness:* 91%
Inventory:

Skull (%)	Dentition (%)	Vertebrae (%)	Ribs/sternum (%)	Upper limbs (%)	Hands (%)	Pelvis (%)	Lower limbs (%)	Feet (%)
95	100	100	95	85	85	100	95	60

Palaeopathology:
Dental disease:
Caries: dLRM1, dLRM2.
Joint disease: None.
Vertebral disease: None.
Trauma: None.
Inflammation:
Subtle periosteal reaction on the anterior surfaces of the maxillae and on both medial surfaces of the mandibular rami.
Periosteal reaction on the right femur, tibia, and fibula, the lateral surfaces of both ilia, and on the right scapular spine.
Possible scurvy.
Congenital: None.
Other:
Porosity of both orbital roofs.

(GD3)61
Grid square: GD3 **Grave:** 11 **Skeleton:** 61 **EA Number:** 96553
Skeletal sex: female **Age:** 20-34 years **Stature:** 154.3cm $^{+}$/- 2.7cm ($humerus_{m}$)
Preservation:
Taphonomic score: good *Cortical surface score:* 5 *Completeness:* 94%
Inventory:

Skull (%)	Dentition (%)	Vertebrae (%)	Ribs/sternum (%)	Upper limbs (%)	Hands (%)	Pelvis (%)	Lower limbs (%)	Feet (%)
90	90	95	100	95	95	95	90	95

Palaeopathology:
Dental disease:
Caries: ULM2, ULM3, LLM3, LRP2.
Antemortem tooth loss: URP1.
Joint disease:
Osteochondritis dissecans on the glenohumeral joint of the left scapula.
Vertebral disease:
Osteophytes: T11, L2 through to L5.
Trauma: None.
Inflammation:
Inflammatory bone changes within both maxillary sinuses.
Periosteal reaction on the visceral surfaces of the shafts of right ribs 4, 5 and 6.
Destruction and porosity on the base of the proximal phalanx of the left first foot digit.
New bone formation on the ectocranial surface of the right parietal.
Congenital:
Cranial vertebral border shift resulting in lumbarisation of T12, agenesis of the twelfth ribs and sacralisation of L5.
Other: None.

(GD3)62
Grid square: GD3 **Grave:** 55 **Skeleton:** 62 **EA Number:** 96560
Skeletal sex: undetermined **Age:** 0-1 years **Stature:** -
Preservation:
Taphonomic score: fragments *Cortical surface score:* 4 *Completeness:* 35%
Inventory:

Skull (%)	Dentition (%)	Vertebrae (%)	Ribs/sternum (%)	Upper limbs (%)	Hands (%)	Pelvis (%)	Lower limbs (%)	Feet (%)
35	25	55	5	30	30	30	45	60

Palaeopathology:
Dental disease: None.
Joint disease: None.
Vertebral disease: None.
Trauma: None.
Inflammation: None.
Congenital: None.
Other: None.

(GD3)65
Grid square: GD3 **Grave:** 63 **Skeleton:** 65 **EA Number:** 96562
Skeletal sex: undetermined **Age:** 2-5 years **Stature:** -
Preservation:
Taphonomic score: excellent *Cortical surface score:* 5 *Completeness:* 98%
Inventory:

Skull (%)	Dentition (%)	Vertebrae (%)	Ribs/sternum (%)	Upper limbs (%)	Hands (%)	Pelvis (%)	Lower limbs (%)	Feet (%)
100	100	100	95	95	100	100	100	90

Palaeopathology:
Dental disease:
Caries: dURI1, dULI1.
Joint disease: None.
Vertebral disease: None.
Trauma: None.
Inflammation:
Porous new bone formation on the ectocranial surface of the parietals and the occipital in the region of the lambdoid suture. Porosity present on the palate of the maxillae and on the greater wings of the sphenoid.
Congenital: None.
Other:
Cribrotic new bone formation on both orbital roofs.

(GD3)69
Grid square: GD3 **Grave:** 38 **Skeleton:** 69 **EA Number:** 96556
Skeletal sex: male **Age:** 35-49 years **Stature:** 162.2cm $^{+}$/- 3cm ($tibia_{m}$)
Preservation:
Taphonomic score: poor *Cortical surface score:* 5 *Completeness:* 76%
Inventory:

Skull (%)	Dentition (%)	Vertebrae (%)	Ribs/sternum (%)	Upper limbs (%)	Hands (%)	Pelvis (%)	Lower limbs (%)	Feet (%)
65	90	95	60	85	60	70	85	75

Palaeopathology:
Dental disease:
Periapical lesion: ULP1.
Antemortem tooth loss: URI2, URI1, ULI1, ULI2, LLC, LLI2, LRI1, LRI2, LRC.
Non-masticatory wear present as interproximal grooves between URM2 and URM1.
Antemortem chipping on distal surfaces of LLM3 and LRM3.
Joint disease:
Osteoarthritis: distal joint of the left clavicle, acromioclavicular joints of both scapulae, trochlea of the left humerus and corresponding trochlear notch of the left ulna, distal radioulnar joint of the left ulna, tarsometatarsal joint between the cuboid and fourth metatarsal of the left foot.

Possible osteochondritis dissecans on the posterior joint surfaces of both naviculars.
Vertebral disease:
Osteoarthritis of articular facets: C2 through to C7, T1, T7 through to T10, T12, L3, L6.
Osteophytes: C5, T7 through to T12, L1 though to L6.
Intervertebral disc disease: T9, T10, T11, L2, L3, L4.
Fusion between vertebral bodies of T7, T8 and T9, and between T12 and L1.
Spondylolysis of L6.
Trauma:
Healed, slightly misaligned fracture of the zygomatic process of the left temporal bone.
Healed fracture of the right fifth metatarsal.
Healed fractures of two unsided proximal hand phalanges.
Healed fracture of one unsided intermediate hand phalanx.
Healed fracture of one unsided proximal foot phalanx.
Healed fracture of one unsided intermediate foot phalanx.
Healed fractures to left ribs 7, 9, 10, and 11 and to right rib 10.
Compression fracture of the vertebral body of T8. Associated fusion between T7 to T9.
Inflammation:
New bone formation on the anterior alveolar surface of the left maxilla in the region of M1 and in the region of the infraorbital foramen.
Periosteal reaction on the medial surface of the right tibial shaft.
Porosity on the ectocranial surface of the occipital and parietals.
Congenital:
Sixth lumbar vertebra present.
Other:
Porosity on the left orbital roof.
Fusion of the distal interphalangeal joint of one unidentified hand digit. Unclear if this is trauma related.

(GD3)78
Grid square: GD3 **Grave:** 51 **Skeleton:** 78 **EA Number:** 96559
Skeletal sex: male? **Age:** 20-34 years **Stature:** 158.9cm $^{+}$/- 3.2cm (femur$_{m}$)
Preservation:
Taphonomic score: poor *Cortical surface score:* 4 *Completeness:* 51%
Inventory:

Skull (%)	Dentition (%)	Vertebrae (%)	Ribs/sternum (%)	Upper limbs (%)	Hands (%)	Pelvis (%)	Lower limbs (%)	Feet (%)
40	40	60	20	65	75	45	70	40

Palaeopathology:
Dental disease:
Caries: LLM2, LLM1, LRM1, LRM2, LRM3.
Periapical lesion: LLC.
Antemortem tooth loss: URM3, URM2, URM1, URP2, LRI1.
Non-masticatory wear in the form of interproximal grooves on LLM1, LLP1, LRP1, LRP2, and LRM2.
Joint disease:
Osteoarthritis: intermetacarpal joints between the fourth and fifth left metacarpals, metacarpophalangeal joint of the first left hand digit.
Vertebral disease:
Osteoarthritis of atlantoaxial joint: C1.
Osteoarthritis of articular facets: C2, C3, C7, T1, L1 through to S1.
Osteophytes: C3, C4, C5, L1, L2, L3, L5.
Intervertebral disc disease: C3, C4, C5.
Trauma:
Healed misaligned fracture of the sternal end of the left clavicle.
Healed fractures on two sternal rib ends and one rib shaft fragment.
Healed fractures on three unsided proximal hand phalanges.
Inflammation:
Periosteal reaction on the medial aspect of the proximal shaft of the left tibia.
Congenital:
Symphalangism of the distal interphalangeal joints of the fifth foot digits.
Other:
Pressure defects of both transverse foramina of C5.

(GD3)81

Grid square: GD3 **Grave:** 45 **Skeleton:** 81 **EA Number:** 96558

Skeletal sex: male **Age:** 35-49 years **Stature:** 169.7cm $^{+}$/- 2.9cm ($femur_m$ + $tibia_m$)

Preservation:

Taphonomic score: good *Cortical surface score:* 5 *Completeness:* 97%

Inventory:

Skull (%)	Dentition (%)	Vertebrae (%)	Ribs/sternum (%)	Upper limbs (%)	Hands (%)	Pelvis (%)	Lower limbs (%)	Feet (%)
100	90	95	100	100	100	100	90	95

Palaeopathology:

Dental disease:

Caries: URM1, URP2, URP1, ULP1, ULM1, ULM3, LRP2, LRM1, LRM2.

Periapical lesions: URM1, URP1, LRM1, LRM2.

Joint disease:

Osteoarthritis: acromioclavicular joint of both scapulae, right acetabulum.

Possible osteochondritis dissecans on the metacarpophalangeal joint surface of the proximal phalanx of the first left foot digit.

Vertebral disease:

Osteoarthritis of articular facets: T1, L1.

Osteophytes: C3, C4, C5, C7, T2, T3, T4, T6 through to T11, L1 through to S1.

Intervertebral disc disease: C3, C4, L4, L5, S1.

Schmorl's node: T8.

Pseudoarthrosis present between right transverse aspects of L5 and S1.

Trauma:

Fracture of the intermediate phalanx of the second right foot digit.

Healed fracture of the coccyx.

Healed fracture of the sternum.

Remodelling fracture of the sternal end of right rib 3.

Healed fracture of the sternal end of left rib 2.

Healed fracture of the styloid process of left third metacarpal.

Inflammation:

Periosteal reaction on the visceral surface of the shaft of left rib 5.

Congenital: None.

Other:

Pressure defect of the left jugular canal causing notable enlargement of the canal.

(GD3)86

Grid square: GD3 **Grave:** 84 **Skeleton:** 86 **EA Number:** 96563

Skeletal sex: undetermined **Age:** 11-19 years **Stature:** -

Preservation:

Taphonomic score: excellent *Cortical surface score:* 5 *Completeness:* 94%

Inventory:

Skull (%)	Dentition (%)	Vertebrae (%)	Ribs/sternum (%)	Upper limbs (%)	Hands (%)	Pelvis (%)	Lower limbs (%)	Feet (%)
95	95	100	100	85	80	90	100	100

Palaeopathology:

Dental disease:

Caries: LLM3.

Joint disease: None.

Vertebral disease: None.

Trauma: None.

Inflammation: None.

Congenital:

Cranial vertebral border shift, with thoracisation of C7, including the formation of cervical ribs.

Complete neural arch hiatus across entire sacrum.

Other:

Possible delayed development; whilst all teeth are fully erupted, skeletal fusion of epiphyses appears delayed. This may be related to an unknown congenital condition contributing to the extensive sacral neural arch hiatus present.

(GD3)89

Grid square: GD3 **Grave:** 87 **Skeleton:** 89 **EA Number:** 96564
Skeletal sex: female **Age:** 35-49 years **Stature:** -
Preservation:
Taphonomic score: fair *Cortical surface score:* 5 *Completeness:* 79%
Inventory:

Skull (%)	Dentition (%)	Vertebrae (%)	Ribs/sternum (%)	Upper limbs (%)	Hands (%)	Pelvis (%)	Lower limbs (%)	Feet (%)
100	85	60	90	95	90	40	65	85

Palaeopathology:
Dental disease:
Caries: URM3, LLM3, LLM2, LLM1, LRM3.
Periapical lesions: URM2, URM1, LLP1, LLI2, LRP1.
Antemortem tooth loss: ULM2.
Joint disease:
Osteoarthritis: acromioclavicular joint of the right scapula.
Vertebral disease:
Osteoarthritis of atlantoaxial joint: C1.
Osteoarthritis of articular facets: C2, C3, C4, T2, T5 through to T10.
Osteophytes: C2, C3, C4.
Intervertebral disc disease: C4.
Trauma:
Healed fracture of the right fifth metacarpal shaft.
Possible healed fracture of the left fourth metacarpal.
Possible healed fracture of the distal phalanx of the fourth right foot digit.
Inflammation:
Inflammatory bone changes within both maxillary sinuses.
Periosteal reaction on the visceral surfaces of left ribs 9 and 10 and right rib 6.
Congenital:
Cranial vertebral border shift, with lumbarisation of T12.
Symphalangism of both distal interphalangeal joints of the fifth foot digit.
Other:
Pressure defect of the left transverse foramen of C5.
Small pressure defect on the right dorsal aspect of the lamina of T11, causing depression of the surface.
Small erosive lesions on the dorsal aspects of the left laminae of T9 and T10. Lesions have rounded, remodelled margins and a porous floor.

(GD3)106

Grid square: GD3 **Grave:** 41 **Skeleton:** 106 **EA Number:** 96557
Skeletal sex: male **Age:** 35-49 years **Stature:** 156cm $^{+}$/- 2.9cm ($femur_m$ + $tibia_m$)
Preservation:
Taphonomic score: fair *Cortical surface score:* 5 *Completeness:* 76%
Inventory:

Skull (%)	Dentition (%)	Vertebrae (%)	Ribs/sternum (%)	Upper limbs (%)	Hands (%)	Pelvis (%)	Lower limbs (%)	Feet (%)
5	55	95	85	100	65	90	100	85

Palaeopathology:
Dental disease:
Caries: ULM3, LLP1, LRC.
Periapical lesions: LLP1, LLC, LLI1, LRI1, LRI2.
Antemortem tooth loss: LLM3, LRM2.
Joint disease:
Osteoarthritis: left mandibular condyle, distal joints of both clavicles, proximal interphalangeal joint of the second right hand digit.
Possible impingement syndrome of the left shoulder joint.
Vertebral disease:
Osteoarthritis of articular facets: C6, T8, T9, T10, T12.
Osteophytes: C3 through to C7, T8 through to S1.
Schmorl's node: T10.
Fusion present between C4 and C5.

Trauma:
Healed fractures on the left transverse processes of L3 and L4.
Inflammation:
Periosteal reaction on the visceral surfaces of the shafts of right ribs 3 and 4.
Congenital: None.
Other: None.

(GD3)108
Grid square: GD3 **Grave:** 98 **Skeleton:** 108 **EA Number:** 96566
Skeletal sex: male? **Age:** 35-49 years **Stature:** -
Preservation:
Taphonomic score: poor *Cortical surface score:* 5 *Completeness:* 69%
Inventory:

Skull (%)	Dentition (%)	Vertebrae (%)	Ribs/sternum (%)	Upper limbs (%)	Hands (%)	Pelvis (%)	Lower limbs (%)	Feet (%)
30	55	70	60	85	90	80	85	70

Palaeopathology:
Dental disease:
Antemortem tooth loss: URC, URI2, URI1, LLM3, LLM2, LLM1, LLP2, LLP1, LLC, LLI2, LLI1, LRP1, LRP2, LRM1, LRM2, LRM3.
Joint disease:
Osteoarthritis: right mandibular condyle, acromioclavicular joint of left scapula, trochlea of left humerus, distal radioulnar joints of both ulnae, metacarpophalangeal and proximal interphalangeal joints of both hands, medial condyle of the right femur, lateral condyle of the left femur, patellofemoral joints of both patellae, medial condyle of the right tibia, proximal tibiofibular joint of the right fibula, metatarsophalangeal joint of the first right foot digit.
Vertebral disease:
Osteoarthritis of articular facets: C2 through to C5, C7, T1, T2, T5, T8, T9, T11, S1.
Osteophytes: C2, C4, C6, C7, T7, T8, T9, T11, T12, L4, L5.
Intervertebral disc disease: L5. Advanced intervertebral disc disease or possible destructive lesions on the vertebral bodies of C6 and C7.
Schmorl's nodes: T9, T12, L5.
Fusion between T11 and T12 at the right articular facets, possibly as a result of trauma to T12.
Trauma:
Compression fracture of the vertebral body of T12.
Healed fractures on right rib 10 and left ribs 2, 3, 4, 11, two unseriated lower-middle left rib angles and on one unidentified left rib shaft fragment.
Partially healed fractures with woven bone on left ribs 5 and 6, and on one unidentified left rib shaft fragment.
Healed fracture at approximately midshaft of the left humerus.
Healed fracture on the distal quarter of the left ulnar shaft.
Healed fractures of the proximal phalanges of the second and fifth right hand digits, intermediate phalanx of the fifth right hand digit, and distal phalanx of the first right hand digit.
Healed fracture of the sternal body at approximately the mid-point.
Inflammation:
Inflammatory bone changes within the left maxillary sinus and frontal and sphenoidal sinuses. Fine porosity/porous new bone across the majority of the ectocranial surface of the cranium.
Periosteal reaction on the distal shaft of the left radius and periosteal reaction on the distal shaft of the left ulna. Possibly related to trauma to the left ulna.
Periosteal reaction on the lateral shafts of both tibiae.
Periosteal reaction on distal shafts of both fibulae.
Congenital:
Neural arch hiatus of S1.
Symphalangism of the distal interphalangeal joints of both fifth foot digits.
Other:
Lesion of dense, granular bone embedded within the lacrimal canal and medial wall of the left maxilla.
Non-union of the styloid process to the distal end of the right ulna. Possibly caused by trauma.

(GD3)114
Grid square: GD3 **Grave:** 109 **Skeleton:** 114 **EA Number:** 96567
Skeletal sex: undetermined **Age:** 6-10 years **Stature:** -
Preservation:
Taphonomic score: good *Cortical surface score:* 5 *Completeness:* 94%

Inventory:

Skull (%)	Dentition (%)	Vertebrae (%)	Ribs/sternum (%)	Upper limbs (%)	Hands (%)	Pelvis (%)	Lower limbs (%)	Feet (%)
90	100	95	95	90	85	100	95	95

Palaeopathology:
Dental disease: None.
Joint disease: None.
Vertebral disease: None.
Trauma: None.
Inflammation/Infection: None.
Congenital:
Neural arch hiatus of C1.
Cranial vertebral border shift, with thoracisation of C7.
Supracondylar spur (nonmetric trait) on the right humerus.
Other:
Porous lesions on both orbital roofs.
Pressure defect of the left transverse foramen of C2 and the right transverse foramen of C5.

(GD3)115
Grid square: GD3 **Grave:** 112 **Skeleton:** 115 **EA Number:** 96568
Skeletal sex: undetermined (femoral head measurement: male)
Age: 35-49 years **Stature:** -
Preservation:
Taphonomic score: poor *Cortical surface score:* 5 *Completeness:* 49%
Inventory:

Skull (%)	Dentition (%)	Vertebrae (%)	Ribs/sternum (%)	Upper limbs (%)	Hands (%)	Pelvis (%)	Lower limbs (%)	Feet (%)
5	30	80	10	55	90	15	65	90

Palaeopathology:
Dental disease:
Caries: URM3, LRC, LRP1.
Antemortem tooth loss: LRI1, LRI2, LRP2, LRM1, LRM2.
Joint disease:
Osteoarthritis: right mandibular condyle, acromioclavicular joint of the right scapula, both acetabula, articular fovea of the right radius, lateral condyles of both femora, intertarsal joints of the right talus and calcaneus.
Porosity and osteophyte formation in the radial fossae of both humeri, possibly suggesting hyperextension of the radio-humeral joints.
Vertebral disease:
Osteoarthritis of articular facets: C4, T3, T4, T9 through to T12.
Osteophytes: T6, T7, T8, T10, L4, L5.
Intervertebral disc disease: T6, T7, T8, T10.
Fusion between the vertebral bodies of L4 and L5.
Trauma:
Compression fracture of T12.
Inflammation:
Periosteal reaction on both fibulae at approximately the midshaft.
Periosteal reaction on both tibiae at approximately the midshaft.
Congenital: None.
Other:
Unusual morphology of the glenohumeral joint of the right scapula.

(GD3)127
Grid square: GD3 **Grave:** 60 **Skeleton:** 127 **EA Number:** 96561
Skeletal sex: male? **Age:** 20-34 years **Stature:** 160.1cm $^{+}$/- 2.9cm ($femur_{m}$ + $tibia_{m}$)
Preservation:
Taphonomic score: good *Cortical surface score:* 5 *Completeness:* 94%
Inventory:

Skull (%)	Dentition (%)	Vertebrae (%)	Ribs/sternum (%)	Upper limbs (%)	Hands (%)	Pelvis (%)	Lower limbs (%)	Feet (%)
80	100	100	90	95	100	90	90	100

Palaeopathology:
Dental disease:
Periapical lesion: LRM2.
Lingual wear on the crown surfaces of URI1 and ULI1.
Joint disease: None.
Vertebral disease: None.
Trauma:
Possible healed depression fracture on the ectocranial surface of the right parietal.
Healed fracture of the left fourth metacarpal.
Inflammation:
Inflammatory bone changes within the right maxillary sinus.
Congenital:
Cranial vertebral border shift, with lumbarisation of T12 and sacralisation of L5.
Other:
Porosity on the right orbital roof.

(GD3)132
Grid square: GD3 **Grave:** 130 **Skeleton:** 132 **EA Number:** 96569
Skeletal sex: male **Age:** 35-49 years **Stature:** 169.6cm $^{+}$/- 2.9cm ($femur_m$ + $tibia_m$)
Preservation:
Taphonomic score: excellent *Cortical surface score:* 6 *Completeness:* 98%
Inventory:

Skull (%)	Dentition (%)	Vertebrae (%)	Ribs/sternum (%)	Upper limbs (%)	Hands (%)	Pelvis (%)	Lower limbs (%)	Feet (%)
100	90	100	100	100	95	100	95	100

Palaeopathology:
Dental disease:
Antemortem chipping to the distal crown of ULM3.
Joint disease:
Osteoarthritis: distal joint of both clavicles, glenohumeral and acromioclavicular joints of both scapulae, right sternal notch, both acetabula, patellofemoral joints of both patellae, distal interproximal joint of the left third hand digit, both tarsometatarsal joints between the cuboid and the fourth metatarsal, metatarsophalangeal joint of the left first foot digit, interphalangeal joints of both first foot digits.
Pseudofacet present between the bases of the fourth and fifth metacarpals, possibly the result of trauma.
Vertebral disease:
Osteoarthritis of articular facets: C7, T1, T4, T5, T11 through to L4.
Osteophytes: C5, C6, C7, T7 through to T12, L2 through to L6.
Intervertebral disc disease: C5, C6, C7, T9 through to T12, L3 through to L6.
Spiculated new bone formation on the anterior aspect of the vertebral body of L5 and a small erosive lesion on the superior aspect of the vertebral body at the midline. Possibly related to intervertebral disc disease.
Schmorl's node: L4.
Trauma:
Healed fracture of the shaft of the proximal phalanx of the right fifth hand digit.
Healed fracture of the shaft of the right fifth metacarpal.
Healed fracture of the shaft of the right third metacarpal.
Healed fracture to the right cuboid on the facet for the fourth metatarsal.
Inflammation:
Inflammatory bone changes within both maxillary sinuses.
Periosteal reaction on the proximal shaft of the left femur.
Congenital:
Additional vertebra in the form of a partially sacralised L6.
Bipartite trapezoid bone in the right hand. Likely congenital, but possibly caused by trauma to the right hand.
Other:
Pressure defect of the left transverse foramen of C2.

(GD3)135
Grid square: GD3 **Grave:** 133 **Skeleton:** 135 **EA Number:** 96570
Skeletal sex: undetermined **Age:** 2-5 years **Stature:** -
Preservation:
Taphonomic score: good *Cortical surface score:* 5 *Completeness:* 7%

Inventory:

Skull (%)	Dentition (%)	Vertebrae (%)	Ribs/sternum (%)	Upper limbs (%)	Hands (%)	Pelvis (%)	Lower limbs (%)	Feet (%)
0	0	0	0	0	0	0	5	60

Palaeopathology:
Dental disease: None.
Joint disease: None.
Vertebral disease: None.
Trauma: None.
Inflammation: None.
Congenital: None.
Other: None.

(GD3)146
Grid square: GD3 **Grave:** 20 **Skeleton:** 146 **EA Number:** 96555
Skeletal sex: female **Age:** 35-49 years **Stature:** 161.5cm $^{+}$/- 1.9cm (tibia$_{m}$)
Preservation:
Taphonomic score: good *Cortical surface score:* 5 *Completeness:* 95%
Inventory:

Skull (%)	Dentition (%)	Vertebrae (%)	Ribs/sternum (%)	Upper limbs (%)	Hands (%)	Pelvis (%)	Lower limbs (%)	Feet (%)
90	100	100	95	95	100	90	90	95

Palaeopathology:
Dental disease:
Caries: LLM2.
Antemortem tooth loss: LLP2.
Transposition between LLC and LLI2 and between LRC and LRI2.
Incomplete eruption of LLC.
Joint disease:
Osteoarthritis: right mandibular condyle.
Vertebral disease:
Osteophytes: T7, T8, T10, T11, L3, L5.
Intervertebral disc disease: T11, L3.
Bilateral spondylolysis of L4.
Trauma:
Healed fracture of the shaft of the proximal phalanx of the fifth right hand digit.
Fracture of the proximal phalanx of the first left foot digit.
Fracture to the left nasal bone.
Inflammation:
Inflammatory bone changes within the right maxillary sinus.
Lamellar bone formation on the visceral surface of the neck of right rib 1 and the shaft of left rib 11.
Porosity on the ectocranial surface of the occipital.
Congenital:
Cranial vertebral border shift, with partial lumbarisation of T12 and sacralisation of L5.
Symphalangism of the distal interphalangeal joints of the fifth foot digits.
Other:
Deviation of the nasal septum to the left.

(GD3)151
Grid square: GD3 **Grave:** 138 **Skeleton:** 151 **EA Number:** 96571
Skeletal sex: male **Age:** 20-34 years **Stature:** -
Preservation:
Taphonomic score: good *Cortical surface score:* 5 *Completeness* 52%
Inventory:

Skull (%)	Dentition (%)	Vertebrae (%)	Ribs/sternum (%)	Upper limbs (%)	Hands (%)	Pelvis (%)	Lower limbs (%)	Feet (%)
45	5	40	30	65	40	85	85	70

Palaeopathology:
Dental disease: None.

Joint disease: None.
Vertebral disease:
Osteophytes: C7, T8, L4, L5.
Intervertebral disc disease: T8, L5.
Schmorl's nodes: L2 through to S1.
Trauma:
Transverse partially healed fracture across the sacrum between the alae of S3 and S4.
Inflammation: None.
Congenital: None.
Other: None.

(GD3)152
Grid square: GD3 **Grave:** 95 **Skeleton:** 152 **EA Number:** 96565
Skeletal sex: female **Age:** 35-49 years **Stature:** 160.4cm $^{+}$/- 1.9cm (tibia$_{m}$)
Preservation:
Taphonomic score: good *Cortical surface score:* 5 *Completeness:* 89%
Inventory:

Skull (%)	Dentition (%)	Vertebrae (%)	Ribs/sternum (%)	Upper limbs (%)	Hands (%)	Pelvis (%)	Lower limbs (%)	Feet (%)
90	100	100	100	100	95	95	100	20

Palaeopathology:
Dental disease:
Caries: ULM1, ULM2, ULM3.
Periapical lesion: ULM1.
Double rooted LLC (non-metric trait).
Joint disease: None.
Vertebral disease:
Osteophytes: T7 through to T10, L2, L3, L4.
Intervertebral disc disease or possible destructive lesions in the region of the annular rings of T8, T9, L2, and S1.
Trauma: None.
Inflammation:
Inflammatory bone changes within both maxillary sinuses and in the left frontal sinus. Periosteal reaction on the proximal shaft of the left fibula.
Congenital: None.
Other: None.

(GD3)154
Grid square: GD3 **Grave:** 143 **Skeleton:** 154 **EA Number:** 96572
Skeletal sex: undetermined **Age:** 0-1 years **Stature:** -
Preservation:
Taphonomic score: excellent *Cortical surface score:* 3 *Completeness*: 92%
Inventory:

Skull (%)	Dentition (%)	Vertebrae (%)	Ribs/sternum (%)	Upper limbs (%)	Hands (%)	Pelvis (%)	Lower limbs (%)	Feet (%)
100	100	100	100	100	70	100	100	60

Palaeopathology:
Dental disease:
Caries: dURI2, dULI2, dLRI1.
Joint disease: None.
Vertebral disease: None.
Trauma: None.
Inflammation: None.
Congenital:
Extremely enlarged anterior fontanelle, with non-union of the metopic suture from 2cm above the orbits, creating a large gap between the two frontal halves and at bregma between the frontal halves and the parietals. Extreme bossing of the parietals and frontals is present and the whole cranium appears enlarged laterally. Inferior angulation of the lateral corners of the orbits and distortion of the medial condyles is also present. This appearance is consistent with the congenital condition of hydrocephalus. Plaque-like porous deposits of new bone are also present across the majority of endocranial surfaces, likely related to the hydrocephalus. Porous new bone on the orbital roofs, posterior surfaces of the zygomatic bones, greater and lesser wings of the sphenoid, and majority of surfaces of the maxillae may also be related to the hydrocephalus.
Other: None.

(1052)3

Area: HA1 **Grave:** 1052 **Skeleton:** 3 **EA Number:** 96535
Skeletal sex: male **Age:** 20-34 years **Stature:** 167.3cm +/- 3cm ($tibia_m$)
Preservation:
Taphonomic score: good *Cortical surface score:* 5 *Completeness:* 93%
Inventory:

Skull (%)	Dentition (%)	Vertebrae (%)	Ribs/sternum (%)	Upper limbs (%)	Hands (%)	Pelvis (%)	Lower limbs (%)	Feet (%)
95	95	100	85	95	90	90	95	95

Palaeopathology:
Dental disease:
Caries: ULM2, LLM2, LLM1, LRM2.
Joint disease: None.
Vertebral disease:
Schmorl's node: L2.
Trauma:
Fracture on the proximal interphalangeal joint surface of a right proximal foot phalanx.
Fracture on the distal interphalangeal joint surface of a right distal foot phalanx.
Inflammation:
Periosteal reaction the shafts of both fibulae.
Extensive periosteal reaction on the visceral rib surfaces of predominantly the right side of the ribcage.
Inflammatory bone changes within the left maxillary sinus.
Congenital:
Possible congenital absence of the styloid process of the right ulna.
Symphalangism of a left distal interphalangeal foot joint.
Other:
Cyst-like circular depression on the left orbital roof (approximately 6mm in diameter and 3mm deep). The floor of the lesion consists of dense granular bone.

(1055)6

Area: HA1 **Grave:** 1055 **Skeleton:** 6 **EA Number:** 96536
Skeletal sex: undetermined **Age:** 16-19 years **Stature:** -
Preservation:
Taphonomic score: good *Cortical surface score:* 5 *Completeness:* 96%
Inventory:

Skull (%)	Dentition (%)	Vertebrae (%)	Ribs/sternum (%)	Upper limbs (%)	Hands (%)	Pelvis (%)	Lower limbs (%)	Feet (%)
100	95	100	90	95	95	95	100	90

Palaeopathology:
Dental disease:
Caries: URM3, ULM3, LLM3, LRP1, LRM2, LRM3.
Joint disease: None.
Vertebral disease:
Hypervascularisation of the anterior and lateral surfaces of the thoracic and upper lumbar vertebral bodies.
Trauma:
Possible healed childhood fracture of the right ulna. Distal third of shaft appears slightly curved laterally in comparison to the left ulnar shaft. Radiographic imaging reveals a small radiopaque line running transversely across the shaft at approximately the distal third.
Compression fracture of T6.
Possible compression fracture of T5, which has a reduction in vertebral body height.
Possible depression trauma on the ectocranial surface of the left frontal region.
Inflammation:
Small region of porosity/porous new bone formation on the ectocranial surface of the left parietal.
Congenital: None.
Other:
Porosity on the lateral aspects of both orbital roofs.

(1058)8
Area: HA1 **Grave:** 1058 **Skeleton:** 8 **EA Number:** 96537
Skeletal sex: undetermined **Age:** 6-10 years **Stature:** -
Preservation:
Taphonomic score: fair *Cortical surface score:* 3 *Completeness:* 78%
Inventory:

Skull (%)	Dentition (%)	Vertebrae (%)	Ribs/sternum (%)	Upper limbs (%)	Hands (%)	Pelvis (%)	Lower limbs (%)	Feet (%)
60	90	75	50	80	85	100	85	80

Palaeopathology:
Dental disease:
Caries: URM1, ULM2, LLM1, LRM1.
Joint disease: None.
Vertebral disease: None.
Trauma: None.
Inflammation: None.
Congenital:
Very large occipital apical bone present (non-metric trait).
Other: None.

(1059)8
Area: HA1 **Grave:** 1059 **Skeleton:** 8 **EA Number:** 96538
Skeletal sex: undetermined **Age:** 11-15 years **Stature:** -
Preservation:
Taphonomic score: good *Cortical surface score:* 4 *Completeness:* 94%
Inventory:

Skull (%)	Dentition (%)	Vertebrae (%)	Ribs/sternum (%)	Upper limbs (%)	Hands (%)	Pelvis (%)	Lower limbs (%)	Feet (%)
95	100	95	70	95	100	100	90	100

Palaeopathology:
Dental disease: None.
Joint disease: None.
Vertebral disease:
Hypervascularisation of the ventral surface of the sacrum and some vertebral bodies.
Trauma: None.
Inflammation: None.
Congenital: None.
Other: None.

(1066)8
Area: HA1 **Grave:** 1066 **Skeleton:** 8 **EA Number:** 96539
Skeletal sex: undetermined **Age:** 35-49 **Stature:** -
Taphonomic score: poor *Cortical surface score:* 3 *Completeness:* 27%
Inventory:

Skull (%)	Dentition (%)	Vertebrae (%)	Ribs/sternum (%)	Upper limbs (%)	Hands (%)	Pelvis (%)	Lower limbs (%)	Feet (%)
40	5	5	5	50	60	5	45	30

Palaeopathology:
Dental disease:
Antemortem tooth loss: LLP1.
Joint disease:
Osteoarthritis: temporomandibular joint of the right temporal.
Vertebral disease: None.
Trauma: None.
Inflammation:
Prolific inflammatory bone changes within all frontal, sphenoidal, and maxillary sinuses. Porous new bone formation also present on the anterior surfaces of the maxillae, suggesting spread of inflammation to the external facial region.
Congenital: None.
Other: None.

(1075)9
Area: HA1 **Grave:** 1075 **Skeleton:** 9 **EA Number:** 96540
Skeletal sex: female? **Age:** 20-34 years **Stature:** -
Preservation:
Taphonomic score: poor *Cortical surface score:* 5 *Completeness:* 41%
Inventory:

Skull (%)	Dentition (%)	Vertebrae (%)	Ribs/sternum (%)	Upper limbs (%)	Hands (%)	Pelvis (%)	Lower limbs (%)	Feet (%)
70	55	15	15	55	20	60	70	10

Palaeopathology:
Dental disease:
Caries: URM2.
Joint disease: None.
Vertebral disease:
Osteoarthritis of articular facets: L5.
Osteophytes: L2.
Trauma: None.
Inflammation:
Inflammatory bone changes within the left frontal sinusitis.
Congenital: None.
Other: None.

(1075)11
Area: HA1 **Grave:** 1075 **Skeleton:** 11 **EA Number:** 96541
Skeletal sex: intermediate (femoral head measurement: female)
Age: 35-49 years **Stature:** -
Preservation:
Taphonomic score: fair *Cortical surface score:* 5 *Completeness:* 36%
Inventory:

Skull (%)	Dentition (%)	Vertebrae (%)	Ribs/sternum (%)	Upper limbs (%)	Hands (%)	Pelvis (%)	Lower limbs (%)	Feet (%)
90	10	25	5	70	30	55	15	20

Palaeopathology:
Dental disease:
Periapical lesion: LLP2, LRC.
Antemortem tooth loss: URP2, URI2, ULP1, LLM3, LLM2, LLM1, LLI1, LRI1.
Joint disease:
Osteoarthritis: distal joint of right clavicle, medial condyle of right femur, patellofemoral surfaces of both patellae, metatarsophalangeal joints of both first foot digits.
Vertebral disease:
Osteoarthritis of articular facets: occipital condyles, C4, C5.
Osteophytes: C5, C6, C7.
Intervertebral disc disease: C5, C6, C7.
Trauma: None.
Inflammation:
Inflammatory bone changes within the right maxillary sinus.
Congenital: None.
Other:
Pressure defect of the left transverse foramen of C2.
Accessory facet on the conoid tubercle of the left clavicle.

(1075)16
Area: HA1 **Grave:** 1075 **Skeleton:** 16 **EA Number:** 96542
Skeletal sex: female? **Age:** 20-34 years **Stature:** 156.3cm $^{+}$/- 2.7cm (humerus$_{m}$)
Preservation:
Taphonomic score: fair *Cortical surface score:* 3 *Completeness:* 83%
Inventory:

Skull (%)	Dentition (%)	Vertebrae (%)	Ribs/sternum (%)	Upper limbs (%)	Hands (%)	Pelvis (%)	Lower limbs (%)	Feet (%)
75	100	95	70	90	90	80	55	90

Palaeopathology:
Dental disease:
Caries: LLM2, LRM2.
Joint disease: None.
Vertebral disease: None.
Trauma: None.
Inflammation:
Inflammatory bone changes within the right maxillary sinus.
Congenital:
Cranial vertebral border shift, with slight lumbarisation of T12.
Other: None.

(1075)17
Area: HA1 **Grave:** 1075 **Skeleton:** 17 **EA Number:** 96543
Skeletal sex: undetermined **Age:** 0-1 years **Stature:** -
Preservation:
Taphonomic score: good *Cortical surface score:* 5 *Completeness:* 7%
Inventory:

Skull (%)	Dentition (%)	Vertebrae (%)	Ribs/sternum (%)	Upper limbs (%)	Hands (%)	Pelvis (%)	Lower limbs (%)	Feet (%)
0	0	5	0	10	0	0	40	5

Palaeopathology:
Dental disease: None.
Joint disease: None.
Vertebral disease: None.
Trauma: None.
Inflammation: None.
Congenital: None.
Other: None.

(1083)5
Area: HA1 **Grave:** 1083 **Skeleton:** 5 **EA Number:** 96544
Skeletal sex: female **Age:** 35-49 years **Stature:** -
Preservation:
Taphonomic score: fair *Cortical surface score:* 5 *Completeness:* 47%
Inventory:

Skull (%)	Dentition (%)	Vertebrae (%)	Ribs/sternum (%)	Upper limbs (%)	Hands (%)	Pelvis (%)	Lower limbs (%)	Feet (%)
40	70	10	10	60	95	20	60	60

Palaeopathology:
Dental disease: None.
Joint disease:
Osteoarthritis: distal joint of left clavicle, trochlear notch of left ulna, patellofemoral surfaces of both patellae.
Vertebral disease: None.
Trauma: None.
Inflammation: None.
Congenital:
Symphalangism of the distal interphalangeal joints of the fifth foot digits.
Other: None.

(1083)11
Area: HA1 **Grave:** 1083 **Skeleton:** 11 **EA Number:** 96545
Skeletal sex: female **Age:** 16-19/20-34 years **Stature:** -
Preservation:
Taphonomic score: fair *Cortical surface score:* 3 *Completeness:* 45%
Inventory:

Skull (%)	Dentition (%)	Vertebrae (%)	Ribs/sternum (%)	Upper limbs (%)	Hands (%)	Pelvis (%)	Lower limbs (%)	Feet (%)
85	50	10	40	80	5	50	80	5

Palaeopathology:
Dental disease:
Caries: URM3, LLM2, LRM2, LRM3.
Joint disease: None.
Vertebral disease: None.
Trauma: None.
Inflammation: None.
Congenital: None.
Other:
Pressure defect of the right transverse foramen of C5.

(1083)15
Area: HA1 **Grave:** 1083 **Skeleton:** 15 **EA Number:** 96546
Skeletal sex: undetermined **Age:** 20+ years **Stature:** female: 157.7cm $^{+}$/- 2.7cm;
male: 163.5cm $^{+}$/- 4.2cm (humerus$_{m}$)

Preservation:
Taphonomic score: poor *Cortical surface score:* 5 *Completeness:* 57%
Inventory:

Skull (%)	Dentition (%)	Vertebrae (%)	Ribs/sternum (%)	Upper limbs (%)	Hands (%)	Pelvis (%)	Lower limbs (%)	Feet (%)
90	65	50	20	80	90	5	30	80

Palaeopathology:
Dental disease:
Caries: URM2, URP2, URP1, URC, URI2, ULC, ULP1, ULP2, ULM1, LLM2, LLM1, LLP2, LLC, LLI2, LRC, LRP1, LRP2, LRM2.
Periapical lesions: URM1, URP1, URC, ULC, ULM2, LLM2, LLM1, LLI1.
Antemortem tooth loss: LRM1.
Joint disease:
Osteoarthritis: both temporomandibular joints of the temporal bones, left mandibular condyle, distal joint of the right clavicle, glenohumeral joint of the right scapula, left sternal notch, carpometacarpal joint of the left first hand digit, patellofemoral joint of the right patella.
Vertebral disease:
Osteoarthritis of articular facets: C7.
Trauma: None.
Inflammation:
Inflammatory bone changes within both maxillary sinuses and the right frontal and left sphenoidal sinuses.
Thick periosteal reaction on the visceral surfaces of the left upper ribs.
Plaque-like new bone formation on the endocranial surfaces of the occipital and temporal.
Porous new bone formation on an unsided distal hand phalanx.
Periosteal reaction on the distal shaft of the left fibula.
Periosteal reaction on the distal shaft of the right tibia.
Periosteal reaction on the medial surface of the right calcaneus.
Congenital: None.
Other:
Small region of dense granular new bone formation embedded within the cortical bone at the left supraorbital margin of the frontal.
Porosity of the left orbital roof.

(1084)8
Area: HA1 **Grave:** 1084 **Skeleton:** 8 **EA Number:** 96547
Skeletal sex: undetermined **Age:** 0-1 years **Stature:** -
Preservation:
Taphonomic score: fair *Cortical surface score:* 5 *Completeness:* 12%
Inventory:

Skull (%)	Dentition (%)	Vertebrae (%)	Ribs/sternum (%)	Upper limbs (%)	Hands (%)	Pelvis (%)	Lower limbs (%)	Feet (%)
5	0	15	25	50	0	0	10	5

Palaeopathology:
Dental disease: None.
Joint disease: None.
Vertebral disease: None.

Trauma: None
Inflammation: None
Congenital: None.
Other: None.

(1093)8
Area: HA1 **Grave:** 1093 **Skeleton:** 8 **EA Number:** 96548
Skeletal sex: undetermined **Age:** 20+ years **Stature:** -
Preservation:
Taphonomic score: poor *Cortical surface score:* 5 *Completeness:* 20%
Inventory:

Skull (%)	Dentition (%)	Vertebrae (%)	Ribs/sternum (%)	Upper limbs (%)	Hands (%)	Pelvis (%)	Lower limbs (%)	Feet (%)
0	0	0	0	0	45	0	55	80

Palaeopathology:
Dental disease: None.
Joint disease:
Osteoarthritis: proximal interphalangeal joint of one unsided proximal phalanx.
Vertebral disease: None.
Trauma: None.
Inflammation:
Periosteal reaction on the distal shaft of the left fibula.
Congenital:
Symphalangism of both distal interphalangeal joints of the fifth foot digits.
Other: None.

(1096)7
Area: HA1 **Grave:** 1096 **Skeleton:** 7 **EA Number:** 96549
Skeletal sex: undetermined **Age:** 0-1 years **Stature:** -
Preservation:
Taphonomic score: fair *Cortical surface score:* 5 *Completeness:* 35%
Inventory:

Skull (%)	Dentition (%)	Vertebrae (%)	Ribs/sternum (%)	Upper limbs (%)	Hands (%)	Pelvis (%)	Lower limbs (%)	Feet (%)
40	25	35	40	70	15	30	30	30

Palaeopathology:
Dental disease: None.
Joint disease: None.
Vertebral disease: None.
Trauma: None.
Inflammation: None.
Congenital: None.
Other: None.

(1097)7
Area: HA1 **Grave:** 1097 **Skeleton:** 7 **EA Number:** 96550
Skeletal sex: undetermined **Age:** 2-5 years **Stature:** -
Preservation:
Taphonomic score: fair *Cortical surface score:* 5 *Completeness:* 67%
Inventory:

Skull (%)	Dentition (%)	Vertebrae (%)	Ribs/sternum (%)	Upper limbs (%)	Hands (%)	Pelvis (%)	Lower limbs (%)	Feet (%)
60	75	50	40	80	60	80	95	60

Palaeopathology:
Dental disease:
Caries: dURC.
Alveolar socket for a supernumerary left central lower incisor is present, although the tooth has been lost.
Joint disease: None.
Vertebral disease: None.
Trauma: None.

Inflammation: None.
Congenital: None.
Other: None.

Grid square HA2

(HA2)102
Grid square: HA2 **Grave:** 96 **Skeleton:** 102 **EA Number:** 96595
Skeletal sex: undetermined **Age:** 2-5 years **Stature:** -
Preservation:
Taphonomic score: fair *Cortical surface score:* 5 *Completeness*: 85%
Inventory:

Skull (%)	Dentition (%)	Vertebrae (%)	Ribs/sternum (%)	Upper limbs (%)	Hands (%)	Pelvis (%)	Lower limbs (%)	Feet (%)
95	100	100	90	85	40	100	95	60

Palaeopathology:
Dental disease: None.
Joint disease: None.
Vertebral disease: None.
Trauma: None.
Inflammation:
New bone formation and porosity on the endocranial surfaces of the frontal crest and cruciform eminence.
Congenital: None.
Other:
Advanced porosity and trabecular expansion of both orbital roofs.
Slight expansion of the cranial diploë.

(HA2)124
Grid square: HA2 **Grave:** 119 **Skeleton:** 124 **EA Number:** 96598
Skeletal sex: male **Age:** 20-34 years **Stature:** 170cm $^{+}$/- 2.9cm (femur $_{m}$ + tibia $_{m}$)
Preservation:
Taphonomic score: good *Cortical surface score:* 5 *Completeness*: 95%
Inventory:

Skull (%)	Dentition (%)	Vertebrae (%)	Ribs/sternum (%)	Upper limbs (%)	Hands (%)	Pelvis (%)	Lower limbs (%)	Feet (%)
95	95	100	95	100	95	95	100	80

Palaeopathology:
Dental disease:
Caries: LRM3.
Joint disease: None.
Vertebral disease:
Schmorl's nodes: T8, T11, T12, L2, L3, L4.
Asymmetrical lateral vertebral body height of T3 and T6, possibly resulting in slight scoliosis.
Unusual shallow destruction of the anterior margin of the superior surface of the vertebral body of T12. Floor is remodelled, but demonstrates multiple large perforations/pores. The annular ring is completely unaffected.
Trauma:
Possible healed trauma to both nasal bones.
Inflammation: None.
Congenital: None.
Other:
Pressure defect of the right transverse foramen of C4.
Notable 'swelling', confluent with the cortical surface, of the right side of the mandibular body. No new bone formation or evidence for dental disease is present. Radiography did not show any apparent underlying bone changes.

(HA2)129
Grid square: HA2 **Grave:** 112 Skeleton 129 **EA Number:** 96597
Skeletal sex: undetermined **Age:** 0-1 years **Stature:** -
Preservation:
Taphonomic score: fair *Cortical surface score:* 4 *Completeness*: 52%

Inventory:

Skull (%)	Dentition (%)	Vertebrae (%)	Ribs/sternum (%)	Upper limbs (%)	Hands (%)	Pelvis (%)	Lower limbs (%)	Feet (%)
85	60	75	80	85	0	20	60	5

Palaeopathology:
Dental disease: None.
Joint disease: None.
Vertebral disease: None.
Trauma: None.
Inflammation:
Plaque-like woven bone beyond that of normal nonadult bone growth on the endocranial surfaces of the frontal, sphenoid, and occipital and on the lateral aspect of the left mandibular body.
Congenital: None.
Other: None.

(HA2)142
Grid square: HA2 **Grave:** 58 **Skeleton:** 142 **EA Number:** 96574
Skeletal sex: female? **Age:** 20-34 years **Stature:** 145.6cm $^{+}$/- 1.9cm (tibia$_{m}$)
Preservation:
Taphonomic score: good *Cortical surface score:* 5 *Completeness*: 64%
Inventory:

Skull (%)	Dentition (%)	Vertebrae (%)	Ribs/sternum (%)	Upper limbs (%)	Hands (%)	Pelvis (%)	Lower limbs (%)	Feet (%)
90	95	25	50	85	85	15	95	35

Palaeopathology:
Dental disease:
Caries: URP2, ULM1, LLC, LRM1, LRM2, LRM3.
Periapical lesions: URP1, ULM1, LRM1.
Antemortem tooth loss: LLI1.
Joint disease:
Osteoarthritis: both acetabula, both patellofemoral joints of the patellae, one unsided proximal interphalangeal foot joint.
Vertebral disease:
Osteoarthritis of atlantoaxial joint: C1, C2.
Osteoarthritis of articular facets: C5.
Osteophytes: T12.
Trauma:
Partially healed fracture of the sternum.
Partially healed fracture on the angle of right rib 10.
Partially healed compression fractures of the vertebral bodies of T12 and two unseriated thoracic vertebrae.
Inflammation:
Inflammatory bone changes within the left maxillary sinus.
Congenital: None.
Other:
Deposits of lamellar bone on the endocranial surface of the frontal in the region of the frontal crest. Possible hyperostosis frontalis interna.
Large oval-shaped pressure defect on the endocranial surface of the parietals, midway along the sagittal sulcus.

(HA2)154
Grid square: HA2 **Grave:** 94 **Skeleton:** 154 **EA Number:** 96588
Skeletal sex: undetermined **Age:** 6-10 years **Stature:** -
Preservation:
Taphonomic score: fair
Cortical surface score: 5
Completeness: 78%
Inventory:

Skull (%)	Dentition (%)	Vertebrae (%)	Ribs/sternum (%)	Upper limbs (%)	Hands (%)	Pelvis (%)	Lower limbs (%)	Feet (%)
90	100	70	90	95	55	90	90	20

Palaeopathology:
Dental disease:
Periapical lesions: LLP2, LLI1, LRI1.
Joint disease: None.
Vertebral disease: None.
Trauma: None.
Inflammation: None.
Congenital: None.
Other:
Pressure defect of the right transverse foramen of C4.

(HA2)155
Grid square: HA2 **Grave:** 100 **Skeleton:** 155 **EA Number:** 96596
Skeletal sex: undetermined (humeral and femoral head measurements: female)
Age: 20+ **Stature:** -
Preservation:
Taphonomic score: poor *Cortical surface score:* 5 *Completeness*: 51%
Inventory:

Skull (%)	Dentition (%)	Vertebrae (%)	Ribs/sternum (%)	Upper limbs (%)	Hands (%)	Pelvis (%)	Lower limbs (%)	Feet (%)
70	40	85	40	85	80	15	35	10

Palaeopathology:
Dental disease:
Caries: ULM1.
Periapical lesions: LLC, LLI2, LRI2, LRC.
Antemortem tooth loss: URP1, LLI2, LLI1, LRI1, LRI2, LRP1.
Joint disease:
Osteoarthritis: distal joints of both clavicles, glenohumeral joint of left scapula, acromioclavicular joints of both scapulae, left acetabulum, medial condyles of both femora.
Vertebral disease:
Osteoarthritis of atlantoaxial joint: C1, C2.
Osteoarthritis of articular facets: C2, C3, C5, C7.
Osteophytes: C3 through to C6, T3, T4, T5, T7 through to T10, T12, L3.
Intervertebral disc disease: C3 through to C6, T4, T5, T8, T9, T10, T12.
Trauma:
Partially healed fractures on right ribs 4, 10, and 12, and on an unseriated right lower-middle rib and two unidentified right rib shaft fragments.
Healed fractures on left rib shaft fragment and on an unsided rib shaft fragment.
At least two healed rib fractures and six partially healed fractures are present.
Inflammation:
Inflammatory bone changes within the right sphenoidal sinus.
Congenital: None.
Other:
Pressure defect on the endocranial surface of the right greater wing of the sphenoid, causing a large smooth surfaced depression.

(HA2)157
Grid square: HA2 **Grave:** 94 **Skeleton:** 157 **EA Number:** 96589
Skeletal sex: undetermined **Age:** 16-19 years **Stature:** -
Preservation:
Taphonomic score: good *Cortical surface score:* 5 *Completeness*: 54%
Inventory:

Skull (%)	Dentition (%)	Vertebrae (%)	Ribs/sternum (%)	Upper limbs (%)	Hands (%)	Pelvis (%)	Lower limbs (%)	Feet (%)
0	5	80	80	75	80	95	70	5

Palaeopathology:
Dental disease: None.
Joint disease: None.
Vertebral disease: None.
Trauma: None.

Inflammation: None.
Congenital: None.
Other: None.

(HA2)164
Grid square: HA2 **Grave:** 94 **Skeleton:** 164 **EA Number:** 96590
Skeletal sex: female? **Age:** 35-49 years **Stature:** 162cm +/- 1.9cm ($tibia_m$)
Preservation:
Taphonomic score: good *Cortical surface score:* 5 *Completeness*: 87%
Inventory:

Skull (%)	Dentition (%)	Vertebrae (%)	Ribs/sternum (%)	Upper limbs (%)	Hands (%)	Pelvis (%)	Lower limbs (%)	Feet (%)
95	80	95	60	95	95	80	95	90

Palaeopathology:
Dental disease:
Caries: URI2.
Periapical lesion: ULC.
Antemortem tooth loss: URP2, URP1, ULI1, ULI2, ULP1, ULP2, LLM3, LLM2, LLM1, LLP2, LLI1, LRI1, LRI2, LRC, LRP1, LRM3.
Joint disease:
Osteoarthritis: both mandibular condyles, circumferential articulation of the right radius, right femoral head, lateral condyle of the right femur, proximal and distal interphalangeal joints of both feet.
Dense lamellar new bone formation and pitting on the anterior surface of the radial fossa of the left humerus, possibly indicating hyperextension of the radiohumeral joint.
Vertebral disease:
Osteophytes: C5, L4, L5, S1.
Intervertebral disc disease: C5, L4, L5, S1.
Small circular destructive lesions on the superior and inferior surfaces of the vertebral bodies of C4, C5, C6, C7, L4, L5 and S1. These may be related to intervertebral disc disease or an infectious process.
Trauma:
Healed fracture on the proximal interphalangeal joint surface of the intermediate phalanx of the second left hand digit.
Healed fracture on the proximal interphalangeal joint surface of the intermediate phalanx of the fourth right foot digit.
Healed fractures on the shafts of left ribs 2, 3 and 4 and right rib 7.
Inflammation:
Inflammatory bone changes within both maxillary sinuses.
Periosteal reaction on the visceral surfaces of the necks of left ribs 7, 8 and 9.
Congenital:
Absence of the styloid process of the right third metacarpal, indicating possible non-union of the styloid ossification centre. May also be trauma related.
Symphalangism of the distal interphalangeal joints of both fifth foot digits.
Other:
Fine porosity across the posterior aspect of the ectocranial surface of the cranium.
Porosity on the endocranial surface of the left greater wing of the sphenoid.
Erosion of the medial surface of the right triquetral, resulting in a large depression on the surface. Other carpals on both hands demonstrate similar erosions, depressions, or cyst-like cavities to a lesser degree around the joint margins.
Small circular perforation with remodelled, rounded margins on the superior margin of the glenoid fossa on both the left and right scapulae.

(HA2)165
Grid square: HA2 **Grave:** 94 **Skeleton:** 165 **EA Number:** 96591
Skeletal sex: undetermined **Age:** 11-15 years **Stature:** -
Preservation:
Taphonomic score: fair *Cortical surface score:* 5 *Completeness*: 88%
Inventory:

Skull (%)	Dentition (%)	Vertebrae (%)	Ribs/sternum (%)	Upper limbs (%)	Hands (%)	Pelvis (%)	Lower limbs (%)	Feet (%)
80	100	100	95	90	95	90	80	65

Palaeopathology:
Dental disease:
Caries: LRM2.

Multiple instances of enamel hypoplasia and antemortem enamel chipping on the dentition.
Joint disease: None.
Vertebral disease: None.
Trauma: None.
Inflammation:
Inflammatory bone changes within the maxillary sinuses.
Periosteal reaction on the distal shaft of the left radius.
Periosteal reaction on the posterior surfaces of the midshafts of both tibiae.
Periosteal reaction on the proximal shaft of the left femur.
Congenital: None.
Other: None.

(HA2)168
Grid square: HA2 **Grave:** 90 **Skeleton:** 168 **EA Number:** 96586
Skeletal sex: female? **Age:** 35-49 years **Stature:** 152.7cm $^{+}$/- 4.1cm (radius $_{m}$)
Preservation:
Taphonomic score: poor *Cortical surface score:* 4 *Completeness*: 66%
Inventory:

Skull (%)	Dentition (%)	Vertebrae (%)	Ribs/sternum (%)	Upper limbs (%)	Hands (%)	Pelvis (%)	Lower limbs (%)	Feet (%)
90	50	75	25	65	80	60	90	60

Palaeopathology:
Dental disease:
Caries: URP2.
Antemortem tooth loss: ULM1, LLM2, LLM1, LRM1.
Joint disease:
Osteoarthritis: distal joint of the right clavicle, glenohumeral joints of both scapulae, glenohumeral joint of the right humerus, distal radioulnar joint of the right ulna, right acetabulum, patellofemoral joints of both patellae, distal interphalangeal joints of the right hand, distal interphalangeal joints of both feet.
Vertebral disease:
Osteoarthritis of atlantoaxial joint: C2.
Osteoarthritis of articular facets: T12, L1.
Osteophytes: C4, C5, C6, S1.
Intervertebral disc disease: C4, C5, C6.
Schmorl's nodes: T11, two unidentified thoracic vertebrae.
Trauma:
Possible healed depression fracture on the ectocranial surface of the left side of the cranium in the region of the coronal suture.
Inflammation:
Inflammatory bone changes within both maxillary sinuses.
Porous lamellar bone formation on the endocranial surface in the region of the cruciform eminence of the occipital.
Congenital:
Symphalangism of the distal interphalangeal joints of both fifth foot digits.
Other: None.

(HA2)169
Grid square: HA2 **Grave:** 90 **Skeleton:**169 **EA Number:** 96587
Skeletal sex: male **Age:** 35-49 years **Stature:** 156.7cm $^{+}$/- 3.2cm (femur $_{m}$)
Preservation:
Taphonomic score: fair *Cortical surface score:* 5 *Completeness*: 83%
Inventory:

Skull (%)	Dentition (%)	Vertebrae (%)	Ribs/sternum (%)	Upper limbs (%)	Hands (%)	Pelvis (%)	Lower limbs (%)	Feet (%)
65	95	95	70	85	80	80	90	85

Palaeopathology:
Dental disease:
Caries: URP1, ULP1, LRM2.
Antemortem tooth loss: LLM1, LRM1.
Unusual wear on the lingual crown surfaces of URC, URI2, URI1, ULI1, ULI2 and ULC.

Joint disease:
Osteoarthritis: sternal joint of the right clavicle, distal joints of both clavicles, acromioclavicular joints of both scapulae, right sternal notch.
Vertebral disease:
Osteoarthritis of articular facets: T5, T10, L1.
Osteophytes: C3, C5, C6, T10, L1 through to L5.
Intervertebral disc disease: C5, C6, L2.
Schmorl's nodes: T6, T8, T9.
Trauma:
Possible depression fracture on the ectocranial surface of the frontal bone.
Healed misaligned fracture of the distal third of the left tibial shaft.
Healed misaligned fracture of the proximal quarter of the left fibular shaft.
Possible healed fracture of the shaft of the right fifth metacarpal.
Healed fractures on the shafts of left ribs 2, 9, and 10.
Inflammation:
Small region of periosteal reaction on the midshaft of the right tibia.
Congenital: None.
Other:
Slight porosity on the ectocranial surface of the parietals.

(HA2)171
Grid square: HA2 **Grave:** 94 **Skeleton:** 171 **EA Number:** 96592
Skeletal sex: intermediate (femoral head measurement: male)
Age: 20+ **Stature:** -
Preservation:
Taphonomic score: fair *Cortical surface score:* 5 *Completeness*: 72%
Inventory:

Skull (%)	Dentition (%)	Vertebrae (%)	Ribs/sternum (%)	Upper limbs (%)	Hands (%)	Pelvis (%)	Lower limbs (%)	Feet (%)
80	85	70	80	70	90	60	70	40

Palaeopathology:
Dental disease:
Caries: URM2, URI2, ULM1, LLM1, LLC, LRC, LRM2.
Periapical lesions: ULP2, ULM1, LLC, LLI2, LRC, LRM2.
Antemortem tooth loss: URM1, URP2, ULM2, ULM3, LRM1.
Joint disease:
Osteoarthritis: distal joint of the left clavicle.
Pitting is also present on the inferior surface of the right acromion process, suggestive of impingement syndrome of the right shoulder.
Vertebral disease:
Osteoarthritis of articular facets: C3, C4, C5, C7, T1.
Osteophytes: C2 through to C6, T4 through to T10, S1.
Intervertebral disc disease: C5, C6.
Schmorl's node: T8.
Trauma:
Healed fractures on the shafts of right ribs 4 and 5.
Possible healed depression trauma on the distal end of the proximal phalanx of the left second hand digit, causing fusion of the distal interphalangeal joint
Inflammation:
Prolific inflammatory bone changes within both maxillary sinuses and right frontal sinus.
Periosteal reaction on the distal shaft of the left tibia.
Periosteal reaction on the distal shaft of the left fibula.
Congenital: None.
Other:
Enlarged arachnoid granulations on either side of the sagittal sulcus on the endocranial surfaces of the parietals. Porous lamellar bone formation is also present within the sagittal sulcus.

(HA2)172
Grid square: HA2 **Grave:** 94 **Skeleton:** 172 **EA Number:** 96593
Skeletal sex: female **Age:** 35-49 years **Stature:** 155.3cm $^{+}$/- 1.9cm (tibia $_{m}$)
Preservation:
Taphonomic score: good *Cortical surface score:* 5 *Completeness*: 88%
Inventory:

Skull (%)	Dentition (%)	Vertebrae (%)	Ribs/sternum (%)	Upper limbs (%)	Hands (%)	Pelvis (%)	Lower limbs (%)	Feet (%)
90	90	100	85	90	80	80	100	80

Palaeopathology:
Dental disease:
Caries: LLM2, LLM1, LRM2.
Apical lesion: ULI1.
Antemortem tooth loss: LRP2.
Joint disease:
Osteoarthritis: distal joints of both clavicles, patellofemoral surfaces of both the right femur and right patella, lateral condyle of the left femur, carpometacarpal joint of the left first metacarpal, distal interphalangeal joint of the left first hand digit.
Vertebral disease:
Osteoarthritis of articular facets: C4, T2 through to T6, L5, S1.
Osteophytes: C5, C6, C7, T4 through to T11, L3 through to S1.
Intervertebral disc disease: C6, T5, T6, L5, S1.
Slight scoliosis, curving to the right, of the vertebral bodies from T2 to T6, likely related with advanced osteoarthritis of the articular facets of T2 to T6.
Lamellar bone formation on the anterior surface of the vertebral body of T4.
Trauma:
Healed fracture on the interphalangeal joint surface of the distal phalanx of the right first foot digit.
Inflammation: None.
Congenital:
Cranial vertebral border shift resulting in lumbarisation of T12, agenesis of the twelfth ribs, and the presence of a sixth sacral vertebra.
Other:
Cyst-like lesion on the palmar aspect of the right scaphoid.
Pressure defect of the left transverse foramen of C2.

(HA2)192
Grid square: HA2 **Grave:** 67 **Skeleton:** 192 **EA Number:** 96577
Skeletal sex: Female **Age:** 35-49 years **Stature:** -
Preservation:
Taphonomic score: fair *Cortical surface score:* 5 *Completeness*: 31%
Inventory:

Skull (%)	Dentition (%)	Vertebrae (%)	Ribs/sternum (%)	Upper limbs (%)	Hands (%)	Pelvis (%)	Lower limbs (%)	Feet (%)
60	10	45	5	50	10	30	50	20

Palaeopathology:
Dental disease:
Caries: LRM3.
Joint disease: None.
Vertebral disease:
Osteoarthritis of articular facets: T2.
Trauma: None.
Inflammation: None.
Congenital: None.
Other: None.

(HA2)193
Grid square: HA2 **Grave:** 31 **Skeleton:** 193 **EA Number:** 96600
Skeletal sex: male **Age:** 35-49 years **Stature:** 161cm $^{+}$/- 3.2cm (femur $_{m}$)
Preservation:
Taphonomic score: good *Cortical surface score:* 5 *Completeness*: 91%

Inventory:

Skull (%)	Dentition (%)	Vertebrae (%)	Ribs/sternum (%)	Upper limbs (%)	Hands (%)	Pelvis (%)	Lower limbs (%)	Feet (%)
100	95	100	95	95	85	100	90	60

Palaeopathology:

Dental disease:

Caries: URP2, ULP2.

Periapical lesions: URP2, URC, URI1, ULP1, ULP2, LLP2.

Antemortem tooth loss: LLM1, LRM1, LRM3.

Joint disease:

Osteoarthritis: temporomandibular joint of the left temporal, sternal joint of the left clavicle, glenohumeral and acromioclavicular joints of both scapulae, glenohumeral joint of the right humerus, right acetabulum, all joints of both femora, patellofemoral joint of the right patella, medial and lateral condyles of both tibiae, talofibular joint of the right fibula, talar intertarsal joint of the navicular, metacarpo/metatarsophalangeal and proximal interphalangeal joints of the hands and feet.

Vertebral disease:

Osteoarthritis of articular facets: C2 through to C5, T8 through to L1, L5.

Osteophytes: C3 through to C7, T4 through to S1.

Intervertebral disc disease: C4 through to C7, T4 through to S1.

Trauma:

Possible healed depression traumas on the ectocranial surface of the frontal and the left parietal.

Healed fracture of the shaft of an unsided proximal foot phalanx.

Inflammation:

Inflammatory bone changes within both maxillary sinuses.

Congenital:

Neural arch hiatus of S1 and S2.

Other:

Small region of dense granular new bone formation embedded within the medial wall of the left maxilla.

Pressure defect of the left transverse foramen of C6.

Fusion of the proximal interproximal joint of the left fifth hand digit. No evidence for trauma as a cause of the fusion, but may be related to osteoarthritis or congenital symphalangism.

(HA2)195

Grid square: HA2 **Grave:** 79 **Skeleton:** 195 **EA Number:** 96581

Skeletal sex: female **Age:** 20-34 years **Stature:** 153.2cm $^{+}$/- 2.5cm (femur$_{m}$)

Preservation:

Taphonomic score: fair *Cortical surface score:* 5 *Completeness*: 52%

Inventory:

Skull (%)	Dentition (%)	Vertebrae (%)	Ribs/sternum (%)	Upper limbs (%)	Hands (%)	Pelvis (%)	Lower limbs (%)	Feet (%)
20	65	45	15	70	70	50	90	40

Palaeopathology:

Dental disease:

Caries: URM3, URM2, URM1, ULM2, LRI2, LRC, LRM1, LRM3.

Periapical lesions: URM2, URM1, ULM1.

Antemortem tooth loss: LLM2, LLP2, LLI1, LRI1.

Non-masticatory wear present in the form of interproximal grooves on URM3, URM1, URP1, URC, ULP1, ULM2, ULM3, and LRM1.

Joint disease:

Osteoarthritis: both acetabula, medial condyles of both femora, lateral condyles of both tibiae, talocrural joint of the left tibia, carpometacarpal joint of the right first metacarpal, metatarsophalangeal joints of the right third and fifth metatarsals.

Vertebral disease:

Osteophytes: C4, T4.

Intervertebral disc disease: C4.

Trauma:

Healed fracture of the shaft of an unsided proximal phalanx of the fifth hand digit.

Healed fracture of the proximal joint facet of the left fibula.

Healed misaligned fracture of the proximal quarter of the left fibular shaft.

Healed misaligned fracture of the proximal quarter of the left tibial shaft.

Inflammation:

Inflammatory bone changes within the right maxillary sinus and sphenoidal sinus.

Congenital: None.
Other: None.

(HA2)198
Grid square: HA2 **Grave:** 83 **Skeleton:** 198 **EA Number:** 96585
Skeletal sex: female **Age:** 35-49 years **Stature:** 163.9cm $^{+}$/- 1.9cm (tibia$_{m}$)
Preservation:
Taphonomic score: good *Cortical surface score:* 5 *Completeness*: 86%
Inventory:

Skull (%)	Dentition (%)	Vertebrae (%)	Ribs/sternum (%)	Upper limbs (%)	Hands (%)	Pelvis (%)	Lower limbs (%)	Feet (%)
100	90	85	95	95	95	80	90	45

Palaeopathology:
Dental disease:
Caries: URM2.
Periapical lesion: LRI1.
Joint disease: None.
Vertebral disease:
Osteoarthritis of atlantoaxial joint: C1.
Osteoarthritis of articular facets: L2.
Osteophytes: C6, T4 through to S1.
Trauma:
Unusual large radiating fracture on the posterior aspect of the cranium, originating from approximately lambda and radiating outwards. No apparent concentric fractures or bevelling are observable, but plastic deformation is present. Possibly represents perimortem trauma.
Possible small healed depression fracture on the ectocranial surface of the frontal bone.
Inflammation:
Periosteal reaction on left ribs 1 and 5.
Congenital: None.
Other:
Slight porosity on the ectocranial surface of the cranium in the region of the external occipital protuberance.

(HA2)209
Grid square: HA2 **Grave:** 39 **Skeleton:** 209 **EA Number:** 96573
Skeletal sex: male **Age:** 20-34 years **Stature:** 171cm $^{+}$/- 3.4cm (humerus$_{m}$ + radius$_{m}$)
Preservation:
Taphonomic score: good *Cortical surface score:* 5 *Completeness*: 89%
Inventory:

Skull (%)	Dentition (%)	Vertebrae (%)	Ribs/sternum (%)	Upper limbs (%)	Hands (%)	Pelvis (%)	Lower limbs (%)	Feet (%)
95	90	100	95	90	95	70	80	90

Palaeopathology:
Dental disease:
Caries: URP1.
Antemortem tooth loss: ULI1, ULI2, ULM1.
Joint disease:
Osteoarthritis: distal joints of both clavicles, acromioclavicular joint of the left scapula.
Vertebral disease:
Osteophytes: C5, C7, L2 through to L5.
Schmorl's nodes: C2, C3, C4, T12.
Trauma:
Compression fracture of the vertebral body of T6.
Possible sharp force/projectile perimortem trauma on the left superior articular facet of L4, consisting of a small triangular shaped, sharp-margined perforation.
Healed fractures to the shafts of the left second and third metacarpals.
Healed fracture on the distal interphalangeal joint of an unsided intermediate hand phalanx.
Possible healed depression trauma present on the ectocranial surface of the left parietal.
Inflammation:
Plaque-like lamellar bone formation on the shafts of both second metatarsals.

Congenital:
Sixth sacral vertebra present.
Symphalangism of both distal interproximal phalangeal joints of the fifth foot digits.
Other:
Dense granular new bone embedded within the cortical bone (observable due to post-mortem damage) of the gonial angle of the right mandibular ramus. Generally diffuse, although spreading out from a central focus. The right maxilla also presents with dense granular new bone embedded within the medial wall.
Pressure defect of the right transverse foramen of C2.
This skeleton demonstrates unusual fracturing that may have taken place perimortem or postmortem *in situ*. Although difficult to differentiate from more recent postmortem damage, there are unusual fractures to the right gonial angle of the mandible and to the right ulnar shaft. There are also sharp, triangular shaped perforations to the right suprascapular fossa and left humerus (anterior surface, just above medial epicondyle) that could represent sharp force trauma.

(HA2)230
Grid square: HA2 **Grave:** 67/229 **Skeleton:** 230 **EA Number:** 96578
Skeletal sex: undetermined **Age:** 11-15 years **Stature:** -
Preservation:
Taphonomic score: good *Cortical surface score:* 5 *Completeness*: 96%
Inventory:

Skull (%)	Dentition (%)	Vertebrae (%)	Ribs/sternum (%)	Upper limbs (%)	Hands (%)	Pelvis (%)	Lower limbs (%)	Feet (%)
95	100	100	95	95	90	100	95	90

Palaeopathology:
Dental disease:
Caries: URM2, URM1.
Joint disease: None.
Vertebral disease: None.
Trauma: None.
Inflammation:
Small region of periosteal reaction on the midshaft of the left third metatarsal.
Congenital: None.
Other: None.

(HA2)232
Grid square: HA2 **Grave:** 79 **Skeleton:** 232 **EA Number:** 96583
Skeletal sex: female **Age:** 20-34 years **Stature:** -
Preservation:
Taphonomic score: fair *Cortical surface score:* 5 *Completeness*: 57%
Inventory:

Skull (%)	Dentition (%)	Vertebrae (%)	Ribs/sternum (%)	Upper limbs (%)	Hands (%)	Pelvis (%)	Lower limbs (%)	Feet (%)
30	0	70	60	65	90	40	85	70

Palaeopathology:
Dental disease: None.
Joint disease:
Osteoarthritis: glenohumeral joint of the left scapula, metatarsophalangeal joint of the left third metatarsal.
Vertebral disease:
Osteoarthritis of articular facets: L3, L4, L5.
Osteophytes: T3, T4, T9 through to T12, L2 through to S1.
Intervertebral disc disease: L2 through to L5.
Trauma: None.
Inflammation:
Periosteal reaction on the dorsal surface of the right lateral cuneiform, possibly associated with the erosive lesion described below.
Congenital: None.
Other:
Possible intratarsal cysts or erosive lesions at the margins of intra-tarsal joint surfaces on the left navicular and both lateral cuneiforms.

(HA2)237

Grid square: HA2 **Grave:** 207 **Skeleton:** 237 **EA Number:** 96601

Skeletal sex: male? **Age:** 20+ years **Stature:** 168.5cm $^{+}$/- 3.7cm ($radius_{m}$)

Preservation:

Taphonomic score: fair *Cortical surface score:* 5 *Completeness*: 36%

Inventory:

Skull (%)	Dentition (%)	Vertebrae (%)	Ribs/sternum (%)	Upper limbs (%)	Hands (%)	Pelvis (%)	Lower limbs (%)	Feet (%)
0	30	5	5	60	80	20	90	35

Palaeopathology:

Dental disease:

Caries: LRM2.

Joint disease:

Osteoarthritis: sternal and distal joints of the left clavicle, right acetabulum, patellofemoral surfaces of both patellae, distal interphalangeal joint of one right hand digit.

Bone changes within the radial fossae of both humeri, possibly representing hyperextension of the radiohumeral joints.

Vertebral disease:

Osteophytes: C2.

Trauma:

Healed fracture on the shaft of the proximal phalanx of the fifth right hand digit.

Periosteal reaction on the lateral surfaces in the region of the midshaft on both tibiae.

Periosteal reaction in the region of the midshaft on the right fibula.

Inflammation: None.

Congenital: None.

Other: None.

(HA2)239

Grid square: HA2 **Grave:** 94 **Skeleton:** 239 **EA Number:** 96594

Skeletal sex: undetermined **Age:** 16-19 years **Stature:** -

Preservation:

Taphonomic score: fair *Cortical surface score:* 5 *Completeness*: 88%

Inventory:

Skull (%)	Dentition (%)	Vertebrae (%)	Ribs/sternum (%)	Upper limbs (%)	Hands (%)	Pelvis (%)	Lower limbs (%)	Feet (%)
85	100	85	90	95	85	70	95	90

Palaeopathology:

Dental disease:

Caries: LLM3, LRM3.

Joint disease: None.

Vertebral disease: None.

Trauma: None.

Inflammation: None.

Congenital:

Cranial vertebral border shift, resulting in complete lumbarisation of T12, agenesis of twelfth ribs, and partial sacralisation of L5.

Symphalangism of the distal interphalangeal joint of the right fifth foot digit.

Other: None.

(HA2)247

Grid square: HA2 **Grave:** 161 **Skeleton:** 247 **EA Number:** 96599

Skeletal sex: undetermined **Age:** 16-19 years **Stature:** -

Preservation:

Taphonomic score: good *Cortical surface score:* 4 *Completeness*: 88%

Inventory:

Skull (%)	Dentition (%)	Vertebrae (%)	Ribs/sternum (%)	Upper limbs (%)	Hands (%)	Pelvis (%)	Lower limbs (%)	Feet (%)
85	90	95	85	85	70	80	100	100

Palaeopathology:

Dental disease: None.

Joint disease:
Osteochondritis dissecans on the medial condyle of the left femur.
Vertebral disease:
Schmorl's nodes: T5 to T11, L2, in various stages of remodelling.
Measurement of the thoracic vertebral body heights indicates pronounced wedging of the vertebral bodies, resulting in Scheuermann's kyphosis. Very fine porosity on the anterior aspects of the vertebral bodies is also present and may be related.
Trauma: None.
Inflammation:
Inflammatory bone changes within both maxillary sinuses.
Congenital: None.
Other: None.

(HA2)255
Grid square: HA2 **Grave:** 215 **Skeleton:** 255 **EA Number:** 96603
Skeletal sex: male? **Age:** 35-49 years **Stature:** 168.3cm $^{+}$/- 3.7cm (radius $_{m}$)
Preservation:
Taphonomic score: fair *Cortical surface score:* 5 *Completeness*: 77%
Inventory:

Skull (%)	Dentition (%)	Vertebrae (%)	Ribs/sternum (%)	Upper limbs (%)	Hands (%)	Pelvis (%)	Lower limbs (%)	Feet (%)
95	65	70	60	85	85	70	95	70

Palaeopathology:
Dental disease:
Caries: URM2.
Antemortem tooth loss: LRM1.
Joint disease:
Osteoarthritis: distal joint of the left clavicle, acromioclavicular joint of the left scapula, glenohumeral joint of the left humerus.
Vertebral disease:
Osteoarthritis of articular facets: C2, C3.
Osteophytes: C5, C6, T11, T12.
Intervertebral disc disease: C5.
Schmorl's node: T11.
Vascular impressions, new bone formation, and vascular cavitations on the lateral surfaces of the vertebral body of T11.
Trauma:
Healed fracture on the sternal end of left rib 9.
Inflammation:
Inflammatory bone changes within both maxillary sinuses.
Periosteal reaction on the distal shaft of the right femur.
Periosteal reaction on the distal shafts of both fibulae and the midshaft of the left fibula.
Thick periosteal reaction on the right tibial shaft.
Congenital: None.
Other:
Porosity and pitting on the palate of the maxillae.
Multiple lytic lesions on the endocranial surfaces of the frontal, parietals, occipital, sphenoid and temporals, particularly in regions of high vascularisation. The lesions are circumscribed, with sharp margins, often undercutting the inner table and expanding into the diploë. In some lesions, remodelling and slight rounding of the margins has taken place. Some lesions are coalesced or are made up of multiple fine pits. Particularly large examples are present on the cruciform eminence of the occipital and on the left greater wing of the sphenoid. These may represent enlarged arachnoid fovea but may also be related to another disease process, such as meningioma.

(HA2)257
Grid square: HA2 **Grave:** 213 **Skeleton:** 257 **EA Number:** 96602
Skeletal sex: intermediate (humeral head measurement: female)
Age: 35-49 years **Stature:** -
Preservation:
Taphonomic score: good *Cortical surface score:* 5 *Completeness*: 91%

Inventory:

Skull (%)	Dentition (%)	Vertebrae (%)	Ribs/sternum (%)	Upper limbs (%)	Hands (%)	Pelvis (%)	Lower limbs (%)	Feet (%)
100	90	100	100	95	95	80	95	60

Palaeopathology:
Dental disease: None.
Joint disease: None.
Vertebral disease:
Osteoarthritis of articular facets: T3, T4.
Osteophytes: C5, C6, T10, T11, T12, L2, L4, L5.
Intervertebral disc disease: C5.
Trauma: None.
Inflammation: None.
Congenital:
Cranial vertebral border shift resulting in slight lumbarisation of T12.
Other: None.

(HA2)259
Grid square: HA2 **Grave:** 58 **Skeleton:** 259 **EA Number:** 96575
Skeletal sex: male **Age:** 20+ years **Stature:** 165.6cm $^{+}$/- 3.4cm ($humerus_{m}$ + $radius_{m}$)
Preservation:
Taphonomic score: fair *Cortical surface score:* 5 *Completeness*: 85%
Inventory:

Skull (%)	Dentition (%)	Vertebrae (%)	Ribs/sternum (%)	Upper limbs (%)	Hands (%)	Pelvis (%)	Lower limbs (%)	Feet (%)
90	90	100	70	90	95	80	80	70

Palaeopathology:
Dental disease:
Caries: URP2, ULM3.
Apical lesion: ULM1.
Antemortem tooth loss: URM1, ULI2.
Joint disease:
Osteoarthritis: sternal joint of the right clavicle, distal joint of both clavicles, glenohumeral and acromioclavicular joints of both scapulae, glenohumeral joints of both humeri, both acetabula, patellofemoral joint of the right patella, one unsided distal interphalangeal fifth foot digit.
Eburnation present on an unsided sesamoid bone of the foot.
Vertebral disease:
Osteoarthritis of atlantoaxial joint: C1, C2.
Osteoarthritis of articular facets: C2 through to C5, T6, L2 through to L5.
Osteophyte formation: C5, C6, C7, T3, T5 through to S1. The large wax-like osteophytes run continuously down the right anterior-lateral side of the vertebral bodies, causing complete or partial fusion of the vertebral bodies from T5 to L3. Disc space is retained between the vertebral bodies and entheseal ossification has occurred elsewhere in the skeleton, including large calcaneal spurs. This likely indicates this individual had diffuse idiopathic skeletal hyperostosis (DISH).
Fusion also present between C5 and C6.
Intervertebral disc disease: C5, C6, C7.
Trauma:
Healed fracture of the left styloid process of the temporal.
Healed fracture of the shaft of left rib 10.
Healed/healing fracture on the distal interphalangeal joint surface of an unsided distal foot phalanx.
Inflammation:
Inflammatory bone changes within the left maxillary sinus and right frontal sinus.
Localised periosteal reaction in a roughly oval shape on the posterior-lateral aspect of the midshafts of both radii.
Congenital:
Caudal vertebral border shift, causing lumbarisation of S1.
Other:
Fusion between the left trapezoid and second metacarpal at the dorsal margin of the carpometacarpal joint. No apparent trauma present. May be congenital or caused by osteoarthritis.

(HA2)265

Grid square: HA2 **Grave:** 79 **Skeleton:** 265 **EA Number:** 96584
Skeletal sex: female **Age:** 20-34 years **Stature:** 151cm $^{+}$/- 1.9cm (tibia$_{m}$)
Preservation:
Taphonomic score: fair *Cortical surface score:* 5 *Completeness*: 55%
Inventory:

Skull (%)	Dentition (%)	Vertebrae (%)	Ribs/sternum (%)	Upper limbs (%)	Hands (%)	Pelvis (%)	Lower limbs (%)	Feet (%)
0	0	75	75	50	60	85	85	65

Palaeopathology:
Dental disease: None.
Joint disease:
Osteoarthritis: sternal joint of the right clavicle, glenohumeral joint of the right scapula. Eburnation is present on the inferior surface of the right acromion process, suggesting impingement syndrome of the right shoulder may have been present.
Vertebral disease:
Osteoarthritis of articular facets: L2.
Osteophytes: L4, L5.
Trauma:
Healed fractures of the shafts of left rib 3 and an unseriated left middle rib.
Healed fracture on the proximal interphalangeal joint surface of a right intermediate foot phalanx.
Possible healed fracture on the left transverse process of L1.
Inflammation: None.
Congenital: None.
Other: None.

(HA2)278

Grid square: HA2 **Grave:** 71 **Skeleton:** 278 **EA Number:** 96579
Skeletal sex: undetermined **Age:** 20+ years **Stature:** -
Preservation:
Taphonomic score: fair *Cortical surface score:* 5 *Completeness*: 19%
Inventory:

Skull (%)	Dentition (%)	Vertebrae (%)	Ribs/sternum (%)	Upper limbs (%)	Hands (%)	Pelvis (%)	Lower limbs (%)	Feet (%)
0	0	20	15	25	10	10	35	60

Palaeopathology:
Dental disease: None.
Joint disease: None.
Vertebral disease:
Osteophytes: L3.
Trauma: None.
Inflammation:
Periosteal reaction on the visceral surface of the neck of right rib 3 and on an unseriated left upper-middle rib.
Periosteal reaction on the distal shaft of the right fibula.
Congenital: None.
Other: None.

(HA2)279

Grid square: HA2 **Grave:** 71 **Skeleton:** 279 **EA Number:** 96580
Skeletal sex: undetermined **Age:** 37-42 weeks **Stature:** -
Preservation:
Taphonomic score: fair *Cortical surface score:* 5 *Completeness*: 12%
Inventory:

Skull (%)	Dentition (%)	Vertebrae (%)	Ribs/sternum (%)	Upper limbs (%)	Hands (%)	Pelvis (%)	Lower limbs (%)	Feet (%)
10	10	5	5	25	0	30	20	0

Palaeopathology:
Dental disease: None.
Joint disease: None.
Vertebral disease: None.

Trauma: None.
Inflammation: None.
Congenital: None.
Other: None.

(HA2)280
Grid square: HA2 **Grave:** 58 **Skeleton:** 280 **EA Number:** 96576
Skeletal sex: undetermined **Age:** 20+ years **Stature:** -
Preservation:
Taphonomic score: fair *Cortical surface score:* 5 *Completeness*: 15%
Inventory:

Skull (%)	Dentition (%)	Vertebrae (%)	Ribs/sternum (%)	Upper limbs (%)	Hands (%)	Pelvis (%)	Lower limbs (%)	Feet (%)
10	40	25	10	40	0	0	10	0

Palaeopathology:
Dental disease:
Caries: LRP2.
Joint disease:
Osteoarthritis: distal joint of the left clavicle, glenohumeral joint of the right scapula, acromioclavicular joint of the left scapula, patellofemoral joint of both patellae.
Vertebral disease:
Osteophytes: C4, C5, C6.
Intervertebral disc disease: C4, C5, C6.
Trauma: None.
Inflammation: None.
Congenital: None.
Other:
Erosive, cyst-like lesion located on the lateral margin of the left mandibular condyle.
Slight bone resorption and undercutting of joint surfaces around the margins of the superior articular facets of C1 and possibly on a number of other vertebral articular facets.
Possible shallow, diffuse erosive lesions on the superior aspects of both left and right acromion processes.

(HA2)281
Grid square: HA2 **Grave:** 79 **Skeleton:** 281 **EA Number:** 96582
Skeletal sex: undetermined **Age:** 37-42 weeks **Stature:** -
Preservation:
Taphonomic score: good *Cortical surface score:* 5 *Completeness*: 16%
Inventory:

Skull (%)	Dentition (%)	Vertebrae (%)	Ribs/sternum (%)	Upper limbs (%)	Hands (%)	Pelvis (%)	Lower limbs (%)	Feet (%)
10	0	5	10	60	0	0	60	0

Palaeopathology:
Dental disease: None.
Joint disease: None.
Vertebral disease: None.
Trauma: None.
Inflammation: None.
Congenital: None.
Other: None.

Grid square JE2

(JE2)33
Grid square: JE2 **Grave:** 14 (Pyramid: M8) **Skeleton:** 33 **EA Number:** 96604
Skeletal sex: undetermined **Age:** 11-15 years **Stature:** -
Preservation:
Taphonomic score: fair *Cortical surface score:* 2 *Completeness*: 73%
Inventory:

Skull (%)	Dentition (%)	Vertebrae (%)	Ribs/sternum (%)	Upper limbs (%)	Hands (%)	Pelvis (%)	Lower limbs (%)	Feet (%)
70	100	95	70	80	80	80	75	10

Palaeopathology:
Dental disease: None.
Joint disease: None.
Vertebral disease: None.
Trauma: None.
Inflammation:
Periosteal reaction on the shafts of the right clavicle, left humerus, and right and left femora.
Congenital: None.
Other: None.

Grid square JE3

(JE3)88
Grid square: JE3 **Grave:** 69 (Pyramid: S1) **Skeleton:** 88 **EA Number:** 96605
Skeletal sex: undetermined **Age:** 0-1 years **Stature:** -
Preservation:
Taphonomic score: fair *Cortical surface score:* 5 *Completeness*: 64%
Inventory:

Skull (%)	Dentition (%)	Vertebrae (%)	Ribs/sternum (%)	Upper limbs (%)	Hands (%)	Pelvis (%)	Lower limbs (%)	Feet (%)
40	20	75	45	75	65	95	90	75

Palaeopathology:
Dental disease: None.
Joint disease: None.
Vertebral disease: None.
Trauma: None.
Inflammation: None.
Congenital: None.
Other: None.

(JE3)89
Grid square: JE3 **Grave:** 69 (Pyramid: S1) **Skeleton:** 89 **EA Number:** 96606
Skeletal sex: undetermined **Age:** 0-1 years **Stature:** -
Preservation:
Taphonomic score: poor *Cortical surface score:* 4 *Completeness*: 16%
Inventory:

Skull (%)	Dentition (%)	Vertebrae (%)	Ribs/sternum (%)	Upper limbs (%)	Hands (%)	Pelvis (%)	Lower limbs (%)	Feet (%)
20	30	10	10	10	15	0	30	20

Palaeopathology:
Dental disease: None.
Joint disease: None.
Vertebral disease: None.
Trauma: None.
Inflammation: None.
Congenital: None.
Other: None.

(JE3)90
Grid square: JE3 **Grave:** 69 (Pyramid: S1) **Skeleton:** 90 **EA Number:** 96607
Skeletal sex: undetermined **Age:** 0-1 years **Stature:** -
Preservation:
Taphonomic score: good *Cortical surface score:* 5 *Completeness*: 74%
Inventory:

Skull (%)	Dentition (%)	Vertebrae (%)	Ribs/sternum (%)	Upper limbs (%)	Hands (%)	Pelvis (%)	Lower limbs (%)	Feet (%)
85	80	80	75	70	65	70	70	75

Palaeopathology:
Dental disease: None.
Joint disease: None.

Vertebral disease: None.
Trauma: None.
Inflammation: None.
Congenital: None.
Other:
Slight flaring of the sternal rib ends.

(JE3)184
Grid square: JE3 **Grave:** 132 (Pyramid: S3) **Skeleton:** 184 **EA Number:** 96610
Skeletal sex: undetermined **Age:** 6-10 years **Stature:** -
Preservation:
Taphonomic score: fair
Cortical surface score: 5
Completeness: 58%
Inventory:

Skull (%)	Dentition (%)	Vertebrae (%)	Ribs/sternum (%)	Upper limbs (%)	Hands (%)	Pelvis (%)	Lower limbs (%)	Feet (%)
75	85	70	75	45	20	70	75	10

Palaeopathology:
Dental disease: None.
Joint disease: None.
Vertebral disease: None.
Trauma: None.
Inflammation:
Woven new bone on the greater wings and pterygoid plates of the sphenoid. May be related to normal nonadult growth.
Congenital: None.
Other:
Porosity on the right orbital roof.

(JE3)185
Grid square: JE3 **Grave:** 132 (Pyramid: S3) **Skeleton:** 185 **EA Number:** 96611
Skeletal sex: female? **Age:** 20-34 years **Stature:** 160.6cm $^{+}$/- 2.7cm (humerus $_{m}$)
Preservation:
Taphonomic score: fair *Cortical surface score:* 5 *Completeness*: 73%
Inventory:

Skull (%)	Dentition (%)	Vertebrae (%)	Ribs/sternum (%)	Upper limbs (%)	Hands (%)	Pelvis (%)	Lower limbs (%)	Feet (%)
80	90	80	85	75	40	65	75	70

Palaeopathology:
Dental disease:
Antemortem tooth loss: LRI1.
Incomplete eruption of the third molars.
Mesial rotation of ULP2.
Joint disease: None.
Vertebral disease: None.
Trauma: None.
Inflammation:
Inflammatory bone changes within both maxillary sinuses.
Congenital: None.
Other: None.

(JE3)186
Grid square: JE3 **Grave:** 132 (Pyramid: S3) **Skeleton:** 186 **EA Number:** 96612
Skeletal sex: male **Age:** 20+ years **Stature:** 166.3cm $^{+}$/- 4.2cm (humerus $_{m}$)
Preservation:
Taphonomic score: fair *Cortical surface score:* 5 *Completeness*: 78%
Inventory:

Skull (%)	Dentition (%)	Vertebrae (%)	Ribs/sternum (%)	Upper limbs (%)	Hands (%)	Pelvis (%)	Lower limbs (%)	Feet (%)
75	85	90	70	75	80	75	75	80

Palaeopathology:
Dental disease:
Caries: LLM2, LRM2, LRM3.
Antemortem tooth loss: LLI1.
Joint disease:
Osteoarthritis: glenohumeral joint of both scapulae.
Possible osteochondritis dissecans of the glenohumeral joint of the left scapula.
Vertebral disease: None.
Trauma:
Possible healed fracture of the coccyx.
Healed fracture of the proximal and distal phalanges of the left first foot digit.
Inflammation:
Inflammatory bone formation within the left maxillary sinus.
Congenital:
Symphalangism of both left and right fifth distal interphalangeal foot joints.
Other:
Porosity on the endocranial surface of the frontal in the region of the supraorbital margins, squamous portion of the occipital, and posterior aspects of parietals.
Enthesophyte present posterior-inferior to the head of the left second metacarpal.

(JE3)187
Grid square: JE3 **Grave:** 132 (Pyramid: S3) **Skeleton:** 187 **EA Number:** 96613
Skeletal sex: Male? **Age:** 16-19 years **Stature:** -
Preservation:
Taphonomic score: fair *Cortical surface score:* 5 *Completeness*: 82%
Inventory:

Skull (%)	Dentition (%)	Vertebrae (%)	Ribs/sternum (%)	Upper limbs (%)	Hands (%)	Pelvis (%)	Lower limbs (%)	Feet (%)
70	90	80	90	90	90	65	80	85

Palaeopathology:
Dental disease: None.
Joint disease: None.
Vertebral disease: None.
Trauma:
Healed fracture of the left radial styloid process.
Possible healed fracture of the coccyx.
Healed fractures of the proximal and distal phalanges of the left first foot digit.
Inflammation:
Periosteal reaction on the proximal shaft of the left tibia.
Congenital: None.
Other:
Porosity on the frontal bone in the region of the left supraorbital margin.
Torsion of the left humerus, causing lateral curvature of the shaft.

(JE3)188
Grid square: JE3 **Grave:** 132 (Pyramid: S3) **Skeleton:** 188 **EA Number:** 96614
Skeletal sex: undetermined **Age:** 0-1 years **Stature:** -
Preservation:
Taphonomic score: poor *Cortical surface score:* 5 *Completeness*: 16%
Inventory:

Skull (%)	Dentition (%)	Vertebrae (%)	Ribs/sternum (%)	Upper limbs (%)	Hands (%)	Pelvis (%)	Lower limbs (%)	Feet (%)
20	50	20	15	0	5	5	25	5

Palaeopathology:
Dental disease: None.
Joint disease: None.
Vertebral disease: None.
Trauma: None.
Inflammation: None.
Congenital: None.
Other: None.

(JE3)189
Grid square: JE3 **Grave:** 132 (Pyramid: S3) **Skeleton:** 189 **EA Number:** 96615
Skeletal sex: undetermined **Age:** 6-10 years **Stature:** -
Preservation:
Taphonomic score: poor *Cortical surface score:* 5 *Completeness*: 57%
Inventory:

Skull (%)	Dentition (%)	Vertebrae (%)	Ribs/sternum (%)	Upper limbs (%)	Hands (%)	Pelvis (%)	Lower limbs (%)	Feet (%)
50	75	85	50	35	5	70	80	60

Palaeopathology:
Dental disease: None.
Joint disease: None.
Vertebral disease: None.
Trauma: None.
Inflammation: None.
Congenital: None.
Other: None.

(JE3)190
Grid square: JE3 **Grave:** 132 (Pyramid: S3) **Skeleton:** 190 **EA Number:** 96616
Skeletal sex: undetermined **Age:** 2-5 years **Stature:** -
Preservation:
Taphonomic score: fair *Cortical surface score:* 5 *Completeness*: 61%
Inventory:

Skull (%)	Dentition (%)	Vertebrae (%)	Ribs/sternum (%)	Upper limbs (%)	Hands (%)	Pelvis (%)	Lower limbs (%)	Feet (%)
70	85	85	80	60	5	75	70	15

Palaeopathology:
Dental disease: None.
Joint disease: None.
Vertebral disease: None.
Trauma: None.
Inflammation: None.
Congenital: None.
Other:
Porosity on both orbital roofs.

(JE3)195
Grid square: JE3 **Grave:** 115 (Pyramid: S2) **Skeleton:** 195 **EA Number:** 96608
Skeletal sex: undetermined (humeral head measurement: male)
Age: 20+ years **Stature:** -
Preservation:
Taphonomic score: poor *Cortical surface score:* 5 *Completeness*: 7%
Inventory:

Skull (%)	Dentition (%)	Vertebrae (%)	Ribs/sternum (%)	Upper limbs (%)	Hands (%)	Pelvis (%)	Lower limbs (%)	Feet (%)
10	0	10	5	10	5	0	10	10

Palaeopathology:
Dental disease:
Antemortem tooth loss: URI2, URI1.
Joint disease: None.
Vertebral disease: None.
Trauma: None.
Inflammation: None.
Congenital: None.
Other: None.

(JE3)196
Grid square: JE3 **Grave:** 115 (Pyramid: S2) **Skeleton:** 196 **EA Number:** 96609
Skeletal sex: undetermined **Age:** 11-19 years **Stature:** -
Preservation:
Taphonomic score: poor *Cortical surface score:* 5 *Completeness*: 7%
Inventory:

Skull (%)	Dentition (%)	Vertebrae (%)	Ribs/sternum (%)	Upper limbs (%)	Hands (%)	Pelvis (%)	Lower limbs (%)	Feet (%)
10	0	5	0	10	5	5	10	15

Palaeopathology:
Dental disease: None.
Joint disease: None.
Vertebral disease: None.
Trauma: None.
Inflammation: None.
Congenital: None.
Other: None.

Grid square JF2

(JF2)64
Grid square: JF2 **Grave:** 26 **Skeleton:** 64 **EA Number:** 96618
Skeletal sex: female **Age:** 20-34 years **Stature:** -
Preservation:
Taphonomic score: fair *Cortical surface score:* 4 *Completeness*: 78%
Inventory:

Skull (%)	Dentition (%)	Vertebrae (%)	Ribs/sternum (%)	Upper limbs (%)	Hands (%)	Pelvis (%)	Lower limbs (%)	Feet (%)
75	80	95	70	95	95	60	95	40

Palaeopathology:
Dental disease:
Apical lesion: ULM2.
Congenital absence of LLI1.
Non-masticatory wear on the lingual surface of URI2.
Large deposits of calculus on URM3 and LRM3.
Joint disease: None.
Vertebral disease:
Osteoarthritis of articular facets: T5, T6, T7.
Osteophytes: T3, T4, T5, T7, T8, T10, T11, L3, L4, L5.
Intervertebral disc disease: T3, T11.
Fusion between the articular facets of T3, T4, and T5.
Trauma:
Healed fracture on the metatarsophalangeal joint of the proximal phalanx of the left first foot digit.
Healed/healing compression fractures of the vertebral bodies of T2 through to T8. Likely the cause of the fusion between vertebrae T3, T4, and T5.
Partially healed fractures on the shaft of right rib 2 and two unsided upper-middle ribs.
Inflammation:
Inflammatory bone changes within the left maxillary sinus.
Localised periosteal reaction on the right tibia at approximately midshaft.
Congenital:
Caudal vertebral border shift, including slight lumbarisation of S1.
Neural arch hiatus of C1.
Other:
Cyst-like destructive lesion on the right lateral cuneiform on the joint surface for the third metatarsal.

(JF2)75
Grid square: JF2 **Grave:** 27 **Skeleton:** 75 **EA Number:** 96619
Skeletal sex: undetermined **Age:** 0-1 years **Stature:** -
Preservation:
Taphonomic score: poor *Cortical surface score:* 4 *Completeness*: 48%

Inventory:

Skull (%)	Dentition (%)	Vertebrae (%)	Ribs/sternum (%)	Upper limbs (%)	Hands (%)	Pelvis (%)	Lower limbs (%)	Feet (%)
50	100	80	20	70	40	40	30	5

Palaeopathology:
Dental disease:
Caries: dLLM1, dLRM1.
Joint disease: None.
Vertebral disease: None.
Trauma: None.
Inflammation: None.
Congenital: None.
Other: None.

(JF2)88
Grid square: JF2 **Grave:** 79 **Skeleton:** 88 **EA Number:** 96620
Skeletal sex: undetermined **Age:** 0-1 years **Stature:** -
Preservation:
Taphonomic score: fair *Cortical surface score:* 4 *Completeness*: 50%
Inventory:

Skull (%)	Dentition (%)	Vertebrae (%)	Ribs/sternum (%)	Upper limbs (%)	Hands (%)	Pelvis (%)	Lower limbs (%)	Feet (%)
30	95	90	40	45	20	15	95	20

Palaeopathology:
Dental disease: None.
Joint disease: None.
Vertebral disease: None.
Trauma: None.
Inflammation: None.
Congenital: None.
Other: None.

(JF2)91
Grid square: JF2 **Grave:** 2 **Skeleton:** 91 **EA Number:** 96617
Skeletal sex: undetermined **Age:** 6-10 years **Stature:** -
Preservation:
Taphonomic score: fair *Cortical surface score:* 3 *Completeness*: 89%
Inventory:

Skull (%)	Dentition (%)	Vertebrae (%)	Ribs/sternum (%)	Upper limbs (%)	Hands (%)	Pelvis (%)	Lower limbs (%)	Feet (%)
85	95	95	95	95	95	100	100	40

Palaeopathology:
Dental disease: None.
Joint disease: None.
Vertebral disease:
Vascular cavitations of the lateral and anterior aspects of the vertebral bodies of the thoracic, lumbar, and sacral vertebral bodies.
Trauma: None.
Inflammation: None.
Congenital:
Neural arch hiatus of C7.
Apical occipital bone present (non-metric trait).
Other:
Porosity on both orbital roofs.

Grid square JG1

(JG1)34
Grid square: JG1 **Grave:** 12 **Skeleton:** 34 **EA Number:** 96621
Skeletal sex: undetermined **Age:** 20+ years **Stature:** -
Preservation:
Taphonomic score: poor *Cortical surface score:* 4 *Completeness*: 33%
Inventory:

Skull (%)	Dentition (%)	Vertebrae (%)	Ribs/sternum (%)	Upper limbs (%)	Hands (%)	Pelvis (%)	Lower limbs (%)	Feet (%)
70	45	15	5	65	30	5	60	5

Palaeopathology:
Dental disease:
Caries: URM1, URP1, URC, ULM1, ULM3.
Periapical lesions: URP2, URP1, URC.
Antemortem tooth loss: URI1, ULI2, ULC.
Unusual wear on the buccal surfaces of URM1, ULM1, LLM1, LLP2, LLP1, LLC, and LRM3 and on the lingual surfaces of LLP1, LLC, LRI2, and LRC, possibly related to a non-masticatory wear process.
Joint disease:
Osteoarthritis: sternal joint of the left clavicle.
Vertebral disease:
Osteoarthritis of the atlantoaxial joint: C2.
Osteoarthritis of superior articular facets: an unidentified thoracic vertebra.
Osteophytes: two unidentified thoracic vertebrae.
Trauma: None.
Inflammation:
Inflammatory bone changes within the right maxillary sinus.
Thick periosteal reaction on the distal shafts of both femora.
Congenital: None.
Other: None.

(JG1)51
Grid square: JG1 **Grave:** 31 **Skeleton:** 51 **EA Number:** 96622
Skeletal sex: male? **Age:** 20-34 years **Stature:** -
Preservation:
Taphonomic score: poor *Cortical surface score:* 2 *Completeness*: 46%
Inventory:

Skull (%)	Dentition (%)	Vertebrae (%)	Ribs/sternum (%)	Upper limbs (%)	Hands (%)	Pelvis (%)	Lower limbs (%)	Feet (%)
0	0	40	10	25	85	70	90	90

Palaeopathology:
Dental disease: None.
Joint disease: None.
Vertebral disease:
Schmorl's nodes: T9, T11, T12, L1, L3, L4.
Bilateral spondylolysis of L5.
Trauma: None.
Inflammation: None.
Congenital: None.
Other: None.

Grid square JG2

(JG2)23
Grid square: JG2 **Grave:** 2 **Skeleton:** 23 **EA Number:** 96623
Skeletal sex: female? **Age:** 20+ **Stature:** -
Preservation:
Taphonomic score: fair *Cortical surface score:* 5 *Completeness*: 11%

Inventory:

Skull (%)	Dentition (%)	Vertebrae (%)	Ribs/sternum (%)	Upper limbs (%)	Hands (%)	Pelvis (%)	Lower limbs (%)	Feet (%)
80	15	0	0	0	0	0	5	0

Palaeopathology:
Dental disease:
Periapical lesion: URM1.
Joint disease: None.
Vertebral disease: None.
Trauma: None.
Inflammation:
Inflammatory bone changes within both maxillary sinuses.
Congenital: None.
Other:
Porosity on the ectocranial surface and thickening of the cranial vault in the region of the frontal, parietal, and occipital squamae.

(JG2)35
Grid square: JG2 **Grave:** 2 **Skeleton:** 35 **EA Number:** 96624
Skeletal sex: undetermined **Age:** 2-5 years **Stature:** -
Preservation:
Taphonomic score: poor *Cortical surface score:* 4 *Completeness*: 26%
Inventory:

Skull (%)	Dentition (%)	Vertebrae (%)	Ribs/sternum (%)	Upper limbs (%)	Hands (%)	Pelvis (%)	Lower limbs (%)	Feet (%)
20	20	40	40	40	25	30	10	5

Palaeopathology:
Dental disease:
Enamel hypoplasia observable on unerupted crowns of LRI1, LRI2, LRC, LRM1 and ULC.
Joint disease: None.
Vertebral disease: None.
Trauma: None.
Inflammation:
New bone formation on the endocranial surface of the occipital squama.
Congenital: None.
Other:
Porosity on the left orbital roof.

(JG2)43
Grid square: JG2 **Grave:** 2 **Skeleton:** 43 **EA Number:** 96625
Skeletal sex: male? **Age:** 20+ years **Stature:** -
Preservation:
Taphonomic score: fair *Cortical surface score:* 5 *Completeness*: 43%
Inventory:

Skull (%)	Dentition (%)	Vertebrae (%)	Ribs/sternum (%)	Upper limbs (%)	Hands (%)	Pelvis (%)	Lower limbs (%)	Feet (%)
80	65	75	30	75	10	20	20	10

Palaeopathology:
Dental disease:
Antemortem tooth loss: URI2, URI1, LRI1.
Joint disease:
Osteoarthritis: right temporomandibular joint of both the temporal and mandible, trochlear notch of the left ulna (likely secondary osteoarthritis related to trauma), patellofemoral surface and medial condyle of the right femur.
Vertebral disease:
Osteoarthritis of atlantoaxial joint: C1.
Osteoarthritis of articular facets: C5, C6, L3, L4.
Osteophytes: C2, C4 through to C7, T3, T7, T10 through to L1, L3 through to S1.
Intervertebral disc disease: C4, C6, C7.

Trauma:
Healed misaligned fracture of the olecranon process of the left ulna.
Compression fracture of the vertebral body of C4.
Inflammation:
Inflammatory bone changes within the right maxillary sinus.
Periosteal reaction on the visceral surface of the neck of right rib 1 and on the angle of a lower-middle right rib.
Congenital: None.
Other:
Nodular lamellar bone formation on the endocranial surface of the frontal. Possible hyperostosis frontalis interna.

(JG2)64
Grid square: JG2 **Grave:** 150 **Skeleton:** 64 **EA Number:** 96626
Skeletal sex: male? **Age:** 20+ **Stature:** -
Preservation:
Taphonomic score: poor *Cortical surface score:* 4 *Completeness*: 21%
Inventory:

Skull (%)	Dentition (%)	Vertebrae (%)	Ribs/sternum (%)	Upper limbs (%)	Hands (%)	Pelvis (%)	Lower limbs (%)	Feet (%)
10	0	20	15	35	25	10	50	20

Palaeopathology:
Dental disease:
Antemortem tooth loss: LLM3, LLM2, LLM1, LLP2, LLP1.
Joint disease: None.
Vertebral disease:
Osteoarthritis of articular facets: C7.
Osteophytes: C4, C5, C7, three unidentified thoracic vertebrae.
Trauma:
Healed fracture of the shaft of the left fifth metacarpal.
Inflammation:
Periosteal reaction on the shaft of a lower left rib.
Congenital: None.
Other: None.

(JG2)65
Grid square: JG2 **Grave:** 150 **Skeleton:** 65 **EA Number:** 96627
Skeletal sex: undetermined **Age:** 0-1 years **Stature:** -
Preservation:
Taphonomic score: poor *Cortical surface score:* 5 *Completeness*: 7%
Inventory:

Skull (%)	Dentition (%)	Vertebrae (%)	Ribs/sternum (%)	Upper limbs (%)	Hands (%)	Pelvis (%)	Lower limbs (%)	Feet (%)
10	0	5	5	15	5	10	15	0

Palaeopathology:
Dental disease: None.
Joint disease: None.
Vertebral disease: None.
Trauma: None.
Inflammation:
Periosteal reaction on the cranial vault. May be related to normal nonadult bone growth.
Congenital: None.
Other: None.

(JG2)66
Grid square: JG2 **Grave:** 175 **Skeleton:** 66 **EA Number:** 96629
Skeletal sex: male? **Age:** 20+ years **Stature:** -
Preservation:
Taphonomic score: poor *Cortical surface score:* 4 *Completeness*: 37%

Inventory:

Skull (%)	Dentition (%)	Vertebrae (%)	Ribs/sternum (%)	Upper limbs (%)	Hands (%)	Pelvis (%)	Lower limbs (%)	Feet (%)
75	15	25	10	20	15	25	75	70

Palaeopathology:
Dental disease:
Antemortem tooth loss: ULI1.
Joint disease:
Osteoarthritis: right mandibular condyle, distal joint of the right clavicle, glenohumeral joint of the right scapula, right acetabulum, trochlear notch and distal radioulnar articulation on the right ulna, medial and lateral condyles of both the right femur and tibia, patellofemoral joint of the right patella, proximal tibiofibular joint of the right tibia, metacarpophalangeal joint of one right metacarpal, articular facets between the right medial cuneiform and first metatarsal, metatarsophalangeal joint of the first right metatarsal.
Vertebral disease:
Osteoarthritis of articular facets: C4, T12, L1, L2.
Osteophytes: C3, C4, T12, L2 through to S1.
Intervertebral disc disease: C3, C4.
Trauma:
Healed fracture of the shaft of a left middle rib.
Healed fracture on the proximal base of the right second metatarsal.
Healed misaligned fracture of the shaft of the right second metacarpal.
Inflammation:
Inflammatory bone changes within the left maxillary sinus.
Periosteal reaction on the medial aspect of the left tibial shaft.
Congenital: None.
Other: None.

(JG2)67
Grid square: JG2 **Grave:** 282 **Skeleton:** 67 **EA Number:** 96634
Skeletal sex: undetermined **Age:** 0-1 years **Stature:** -
Preservation:
Taphonomic score: poor *Cortical surface score:* 5 *Completeness*: 3%
Inventory:

Skull (%)	Dentition (%)	Vertebrae (%)	Ribs/sternum (%)	Upper limbs (%)	Hands (%)	Pelvis (%)	Lower limbs (%)	Feet (%)
0	0	0	0	0	0	0	20	5

Palaeopathology:
Dental disease: None.
Joint disease: None.
Vertebral disease: None.
Trauma: None.
Inflammation:
Periosteal reaction on the right tibial shaft. May be related to normal nonadult bone growth.
Congenital: None.
Other: None.

(JG2)215
Grid square: JG2 **Grave:** 171 **Skeleton:** 215 **EA Number:** 96628
Skeletal sex: male **Age:** 35-49 years **Stature:** 169.2cm $^{+}$/- 2.9cm (tibia$_{m}$)
Preservation:
Taphonomic score: good *Cortical surface score:* 4 *Completeness*: 91%
Inventory:

Skull (%)	Dentition (%)	Vertebrae (%)	Ribs/sternum (%)	Upper limbs (%)	Hands (%)	Pelvis (%)	Lower limbs (%)	Feet (%)
95	90	100	90	95	100	95	85	70

Palaeopathology:
Dental disease:
Caries: ULM2 and LRM2.
Antemortem tooth loss: URI2.

Joint disease:
Osteoarthritis: distal joints of both clavicles, acromioclavicular joints of both scapulae.
Vertebral disease:
Osteoarthritis of articular facets: T11.
Osteophytes: C2 through to T6, T8 through to S1.
Intervertebral disc disease: C3 through to C7, T5, T6, T11, T12, L2, L3.
Trauma:
Healed fracture of the shaft of the proximal phalanx of the right first foot digit.
Inflammation:
Inflammatory bone changes within the right maxillary sinus.
Periosteal reaction on the shafts of the right second and fifth metatarsals.
Congenital:
Sutural agenesis/craniosynostosis of the sagittal suture, with cranial scaphocephaly (elongation of the cranium anterior-posteriorly).
Other:
Pressure defects of the right transverse foramen of C4 and the left transverse foramen of C5.

(JG2)251
Grid square: JG2 **Grave:** 231 **Skeleton:** 251 **EA Number:** 96630
Skeletal sex: undetermined **Age:** 2-5 years **Stature:** -
Preservation:
Taphonomic score: fair *Cortical surface score:* 5 *Completeness*: 48%
Inventory:

Skull (%)	Dentition (%)	Vertebrae (%)	Ribs/sternum (%)	Upper limbs (%)	Hands (%)	Pelvis (%)	Lower limbs (%)	Feet (%)
55	25	70	50	40	15	70	65	40

Palaeopathology:
Dental disease:
Enamel hypoplasia observable on the unerupted crowns of URC, ULC and ULI2.
Joint disease: None.
Vertebral disease: None.
Trauma:
Possible traumatic injury to the left radius, resulting in slight misalignment of the radial head and bone remodelling in regions of muscle attachment on the proximal radius. No evidence for a fracture.
Inflammation: None.
Congenital: None.
Other:
Porosity on both orbital roofs.

(JG2)312
Grid square: JG2 **Grave:** 244 **Skeleton:** 312 **EA Number:** 96631
Skeletal sex: male **Age:** 35-49 years **Stature:** 176.5 $^{+}$/- 3.4cm (humerus $_{m}$ + radius $_{m}$)
Preservation:
Taphonomic score: poor *Cortical surface score:* 3 *Completeness*: 92%
Inventory:

Skull (%)	Dentition (%)	Vertebrae (%)	Ribs/sternum (%)	Upper limbs (%)	Hands (%)	Pelvis (%)	Lower limbs (%)	Feet (%)
90	95	95	70	95	95	95	95	100

Palaeopathology:
Dental disease:
Congenital absence of LLP2 and LRP2 and retention of dLLM2 and dLRM2.
Joint disease:
Osteoarthritis: distal joint of the left clavicle.
Osteophyte formation in the retroauricular area of both ilia, suggesting initiation of bilateral fusion of the sacroiliac joint.
Vertebral disease:
Osteoarthritis of articular facets: T3, L5.
Osteophytes: T8, T9.
Schmorl's nodes: T11 through to L4.
Pitting on the posterior surface of the vertebral bodies of C6 and C7.
Enlargement of the basivertebral foramen of L3.

Possible remodelled lytic lesion on the superior surface of the vertebral body of T7.
Trauma: None.
Inflammation:
Inflammatory bone changes within the right maxillary sinus.
Porous new bone formation on the anterior surface of the left zygomatic.
Congenital:
Craniosynostosis/agenesis of the sagittal and temporal sutures, with cranial scaphocephaly (elongation of the cranium anterior-posteriorly)
Other: None.

(JG2)313
Grid square: JG2 **Grave:** 244 **Skeleton:** 313 **EA Number:** 96632
Skeletal sex: male **Age:** 20-34 years **Stature:** 163.4cm $^{+}$/- 3.4cm (humerus$_{m}$ + radius$_{m}$)
Preservation:
Taphonomic score: good *Cortical surface score:* 3 *Completeness*: 92%
Inventory:

Skull (%)	Dentition (%)	Vertebrae (%)	Ribs/sternum (%)	Upper limbs (%)	Hands (%)	Pelvis (%)	Lower limbs (%)	Feet (%)
90	75	100	95	95	95	95	100	80

Palaeopathology:
Dental disease:
Antemortem tooth loss: URI2.
Joint disease: None.
Vertebral disease:
Osteoarthritis of articular facets: T3, T4, T10.
Schmorl's nodes: L1.
Slight asymmetry in lateral vertebral body height of T10, resulting in mild scoliosis.
Trauma: None.
Inflammation:
Inflammatory bone changes within the left maxillary sinus.
Congenital: None.
Other:
Small lesions of granular new bone embedded within the posterior surface of the frontal process of the left maxilla and within the medial wall of the right maxilla.

(JG2)314
Grid square: JG2 **Grave:** 244 **Skeleton:** 314 **EA Number:** 96633
Skeletal sex: intermediate (femoral and humeral head measurements: female)
Age: 20-34 years **Stature:** female: 159.4cm $^{+}$/- 2.7cm; male: 165cm $^{+}$/- 4.2cm (humerus$_{m}$)
Preservation:
Taphonomic score: fair *Cortical surface score:* 3 *Completeness*: 96%
Inventory:

Skull (%)	Dentition (%)	Vertebrae (%)	Ribs/sternum (%)	Upper limbs (%)	Hands (%)	Pelvis (%)	Lower limbs (%)	Feet (%)
90	95	100	95	100	100	95	100	85

Palaeopathology:
Dental disease:
Caries: LLM1, LRM1, LRM3.
Antemortem tooth loss: ULI1.
Joint disease:
Osteoarthritis: sternal joint of the right clavicle, distal joint of the left clavicle, costovertebral facets of the thoracic vertebrae.
Vertebral disease:
Osteoarthritis of articular facets: T1, T4, T6, T7.
Osteophytes: T2, T3, T4, T9, L4.
Intervertebral disc disease: T2, T3, L4.
Schmorl's nodes: T8 through to L3.
Trauma: None.
Inflammation: None.
Congenital:
Symphalangism of the distal interphalangeal joints of both fifth foot digits.

Other:
Accessory facet on the conoid tubercle of the clavicle.

Grid square JG3

(JG3)13
Grid square: JG3 **Grave:** 6 **Skeleton:** 13 **EA Number:** 96635
Skeletal sex: female **Age:** 20-34 years **Stature:** 154.4cm $^{+}$/- 4.1cm (radius $_{m}$)
Preservation:
Taphonomic score: good *Cortical surface score:* 5 *Completeness*: 73%
Inventory:

Skull (%)	Dentition (%)	Vertebrae (%)	Ribs/sternum (%)	Upper limbs (%)	Hands (%)	Pelvis (%)	Lower limbs (%)	Feet (%)
90	90	100	50	90	60	75	60	40

Palaeopathology:
Dental disease: None
Joint disease: None.
Vertebral disease:
Osteoarthritis of articular facets: T10.
Schmorl's node: L3.
Trauma:
Multiple instances of possible perimortem trauma.
Possible small perimortem depressed fracture/'bone chip' on the posterior aspect of the medial clavicle shaft, possibly as a result of projectile trauma. Measuring approximately 5mm in diameter and less than 1mm deep.
Possible perimortem blunt force fracture to the anterior margins of the glenoid fossa.
Possible perimortem projectile trauma to the right parietal. A puncture defect with bevelled margins, similar to a 'keyhole' wound seen in ballistics, is present near the lambdoid and mastoparietal sutures. Measuring approximately 11mm in length, ranging in width from 2mm to 7mm.
Possible perimortem trauma to the left iliac blade. Large perforation of the blade, with slight bevelling. Circular defect measures approximately 12mm to 14mm in diameter.
All instances of trauma may be taphonomic, inflicted during looting of the grave.
Inflammation:
Inflammatory bone changes within both maxillary sinuses.
Periosteal reaction on the visceral surfaces of multiple right ribs.
Periosteal reaction on the lateral aspect of the left tibial shaft.
Congenital:
Cranial vertebral border shift, with partial lumbarisation of T12.
Other:
Dense granular new bone formation embedded within the left side of the mandibular canal, only observable due to taphonomic breakage.
Accessory pseudofacet between the left navicular and calcaneus causing bone remodelling. Lytic lesion present on the pseudofacets on both the navicular and calcaneus.
Cyst-like lytic lesion, with sharp margins, on the sternal joint surface of the left clavicle.

(JG3)14
Grid square: JG3 **Grave:** 6 **Skeleton:** 14 **EA Number:** 96636
Skeletal sex: undetermined **Age:** 6-10 years **Stature:** -
Preservation:
Taphonomic score: fair *Cortical surface score:* 5 *Completeness*: 72%
Inventory:

Skull (%)	Dentition (%)	Vertebrae (%)	Ribs/sternum (%)	Upper limbs (%)	Hands (%)	Pelvis (%)	Lower limbs (%)	Feet (%)
65	90	60	65	85	65	65	70	80

Palaeopathology:
Dental disease: None.
Joint disease: None.
Vertebral disease: None.
Trauma: None.
Inflammation: None.

Congenital:
Symphalangism of the distal interphalangeal joint of the right fifth foot digit.
Other:
Porosity on both orbital roofs.

(JG3)21
Grid square: JG3 **Grave:** 23 **Skeleton:** 21 **EA Number:** 96637
Skeletal sex: undetermined (femoral head measurement: male)
Age: 20+ years **Stature:** -
Preservation:
Taphonomic score: fair *Cortical surface score:* 5 *Completeness*: 41%
Inventory:

Skull (%)	Dentition (%)	Vertebrae (%)	Ribs/sternum (%)	Upper limbs (%)	Hands (%)	Pelvis (%)	Lower limbs (%)	Feet (%)
25	20	10	5	35	85	10	85	95

Palaeopathology:
Dental disease: None.
Joint disease: None.
Vertebral disease:
Osteophytes: L4, L5.
Intervertebral disc disease: L4, L5.
Trauma:
Possible fracture of the shaft of the proximal phalanx of the left third foot digit.
Inflammation:
Inflammatory bone changes within the maxillary, frontal, and sphenoidal sinuses.
Periosteal reaction on the shaft of the proximal phalanx of the second right foot digit.
Congenital:
Absence of the styloid process of the left third metacarpal.
Symphalangism of the distal interphalangeal joints of both fifth foot digits.
Other:
Porosity on the ectocranial surface of the occipital, parietals, and frontal.

Grid square JH3

(JH3)74
Grid square: JH3 **Grave:** 11 **Skeleton:** 74 **EA Number:** 96642
Skeletal sex: undetermined **Age:** 16-19 years **Stature:** -
Preservation:
Taphonomic score: fair *Cortical surface score:* 3 *Completeness*: 69%
Inventory:

Skull (%)	Dentition (%)	Vertebrae (%)	Ribs/sternum (%)	Upper limbs (%)	Hands (%)	Pelvis (%)	Lower limbs (%)	Feet (%)
95	95	60	35	85	75	60	55	65

Palaeopathology:
Dental disease:
LRC has a double root (non-metric trait). LRP2 is rotated.
Joint disease: None.
Vertebral disease: None.
Trauma: None.
Inflammation:
Inflammatory bone changes within both maxillary sinuses.
Congenital: None.
Other: None.

(JH3)80
Grid square: JH3 **Grave:** 5 **Skeleton:** 80 **EA Number:** 96638
Skeletal sex: undetermined **Age:** 2-5 years **Stature:** -
Preservation:
Taphonomic score: fair *Cortical surface score:* 5 *Completeness*: 65%

Inventory:

Skull (%)	Dentition (%)	Vertebrae (%)	Ribs/sternum (%)	Upper limbs (%)	Hands (%)	Pelvis (%)	Lower limbs (%)	Feet (%)
60	75	45	40	75	70	75	85	60

Palaeopathology:
Dental disease:
Double-rooted upper deciduous canines (non-metric trait).
Joint disease: None.
Vertebral disease: None.
Trauma: None.
Inflammation: None.
Congenital: None.
Other:
Porosity on the left orbital roof.

(JH3)82
Grid square: JH3 **Grave:** 21 **Skeleton:** 8 **EA Number:** 96643
Skeletal sex: male? **Age:** 20-34 years **Stature:** 165.3cm $^{+}$/- 4.2cm (humerus $_{m}$)
Preservation:
Taphonomic score: fair *Cortical surface score:* 5 *Completeness*: 78%
Inventory:

Skull (%)	Dentition (%)	Vertebrae (%)	Ribs/sternum (%)	Upper limbs (%)	Hands (%)	Pelvis (%)	Lower limbs (%)	Feet (%)
75	95	85	60	75	85	70	75	80

Palaeopathology:
Dental disease: None.
Joint disease:
Osteoarthritis: proximal interphalangeal joint of the intermediate phalanx of the left fifth foot digit.
Vertebral disease: None.
Trauma:
Healed fracture of the distal shaft of the right tibia.
Healed misaligned fracture of the midshaft of the right fibula.
Inflammation:
Periosteal reaction on the proximal shaft of the left tibia.
Periosteal reaction on the distal shaft of the left fibula.
Congenital:
Symphalangism of the distal interphalangeal joints of both fifth foot digits.
Other:
Porosity of both orbital roofs.
Porosity on the posterior aspect of the ectocranial surface of the skull, involving the parietals and occipital, and in the region of the glabella and supraorbital margins of the frontal.

(JH3)90
Grid square: JH3 **Grave:** 9 **Skeleton:** 90 **EA Number:** 96639
Skeletal sex: undetermined **Age:** 6-10 years **Stature:** -
Preservation:
Taphonomic score: fair *Cortical surface score:* 3 *Completeness*: 59%
Inventory:

Skull (%)	Dentition (%)	Vertebrae (%)	Ribs/sternum (%)	Upper limbs (%)	Hands (%)	Pelvis (%)	Lower limbs (%)	Feet (%)
50	100	60	10	90	55	80	60	30

Palaeopathology:
Dental disease:
Caries: dLLM1 following antemortem tooth chip on the distal surface.
Enamel hypoplasia on the incisal edge of URI2, URI1, and ULI1.
Joint disease: None.
Vertebral disease: None.
Trauma: None.

Inflammation:
Inflammatory bone changes within the right maxillary sinus.
Congenital: None.
Other: None.

(JH3)99
Grid square: JH3 **Grave:** 9 **Skeleton:** 99 **EA Number:** 96640
Skeletal sex: undetermined **Age:** 2-5 years **Stature:** -
Preservation:
Taphonomic score: fair *Cortical surface score:* 4 *Completeness*: 34%
Inventory:

Skull (%)	Dentition (%)	Vertebrae (%)	Ribs/sternum (%)	Upper limbs (%)	Hands (%)	Pelvis (%)	Lower limbs (%)	Feet (%)
10	50	10	40	60	0	40	90	5

Palaeopathology:
Dental disease: None.
Joint disease: None.
Vertebral disease: None.
Trauma: None.
Inflammation: None.
Congenital: None.
Other: None.

(JH3)123
Grid square: JH3 **Grave:** 114 **Skeleton:** 123 **EA Number:** 96651
Skeletal sex: female? **Age:** 20-34 years **Stature:** 161.1cm $^{+}$/- 2.7cm (humerus $_{m}$)
Preservation:
Taphonomic score: fair *Cortical surface score:* 5 *Completeness*: 71%
Inventory:

Skull (%)	Dentition (%)	Vertebrae (%)	Ribs/sternum (%)	Upper limbs (%)	Hands (%)	Pelvis (%)	Lower limbs (%)	Feet (%)
85	80	75	70	80	70	30	60	85

Palaeopathology:
Dental disease:
Caries: ULP1, ULP2, ULM3, LLM3, LLM2, LRM2, LRM3.
Periapical lesion: LRM1.
Joint disease: None.
Vertebral disease:
Osteophytes: T8, T9.
Trauma:
Possible healed fracture of the proximal interphalangeal joint of the proximal phalanx of the left fifth foot digit.
Inflammation:
Inflammatory bone changes within the left maxillary sinus and sphenoidal sinus.
Congenital: None.
Other: None.

(JH3)125
Grid square: JH3 **Grave:** 39 **Skeleton:** 125 **EA Number:** 96645
Skeletal sex: undetermined (humeral and femoral head measurements: male)
Age: 35-49 years **Stature:** female: 159cm $^{+}$/- 4.1cm; male: 166.4cm $^{+}$/- 3.7cm (radius $_{m}$)
Preservation:
Taphonomic score: fair *Cortical surface score:* 5 *Completeness*: 58%
Inventory:

Skull (%)	Dentition (%)	Vertebrae (%)	Ribs/sternum (%)	Upper limbs (%)	Hands (%)	Pelvis (%)	Lower limbs (%)	Feet (%)
5	5	95	70	45	95	40	75	95

Palaeopathology:
Dental disease: None.
Joint disease:
Osteoarthritis: left acetabulum.

Secondary osteoarthritis present on the proximal interphalangeal joint of the intermediate phalanx of the left third foot digit, likely related to a fracture on the joint.
Vertebral disease:
Osteoarthritis of articular facets: C3, C4.
Osteophytes: C2, C5, C6, C7, T4 through to T11, L1 through to S1.
Schmorl's nodes: C3, C4, C5, T8 through to T11, L1, L2.
Pitting and slight destruction along the anterior margins of the body of S1.
Trauma:
Fracture on the proximal interphalangeal joint surface of the intermediate phalanx of the left third foot digit.
Healed fractures of the sternal ends of right ribs 2 and 4 and on the shaft of left rib 2.
Possible incomplete perimortem fracture of the neural arch of L4 across the superior facets. May be taphonomic.
Inflammation:
Periosteal reaction on the visceral surface of the shafts of left rib 6 and right rib 4. Lytic lesions, with possible cloaca, on the visceral and external surfaces of the shaft of right rib 8 and left rib 6.
Congenital: None.
Other:
Pronounced groove for peroneus longus/brevis tendon on both the right fibula and right calcaneus. Remodelling present on the dorsal aspect of the base of the fifth right metatarsal where peroneus brevis attaches. Possibly indicative of traumatic injury to the tendons.

(JH3)126
Grid square: JH3 **Grave:** 36 **Skeleton:** 126 **EA Number:** 96644
Skeletal sex: female? **Age:** 20-34 years **Stature:** 158.6cm $^{+}$/- 2.7cm (humerus$_{m}$)
Preservation:
Taphonomic score: poor *Cortical surface score:* 4 *Completeness*: 53%
Inventory:

Skull (%)	Dentition (%)	Vertebrae (%)	Ribs/sternum (%)	Upper limbs (%)	Hands (%)	Pelvis (%)	Lower limbs (%)	Feet (%)
60	65	60	35	70	25	65	70	25

Palaeopathology:
Dental disease: None.
Joint disease: None.
Vertebral disease:
Schmorl's nodes: L2, L3.
Trauma: None.
Inflammation:
Inflammatory bone changes within the right maxillary sinus.
Possible woven bone formation in the retroauricular area of the right ilium.
Congenital: None.
Other: None.

(JH3)133
Grid square: JH3 **Grave:** 116 **Skeleton:** 133 **EA Number:** 96652
Skeletal sex: female? **Age:** 35-49 years **Stature:** 160.7cm $^{+}$/- 2.5cm (femur$_{m}$)
Preservation:
Taphonomic score: poor *Cortical surface score:* 2 *Completeness*: 83%
Inventory:

Skull (%)	Dentition (%)	Vertebrae (%)	Ribs/sternum (%)	Upper limbs (%)	Hands (%)	Pelvis (%)	Lower limbs (%)	Feet (%)
80	100	100	75	95	95	90	50	65

Palaeopathology:
Dental disease: None.
Joint disease:
Osteoarthritis: distal joint of left clavicle.
Vertebral disease:
Osteophytes: C3, C5, C6, T3, T11, T12, L4.
Intervertebral disc disease: C5, C6, T11.
Trauma:
Possible small perimortem fracture of the left gonial angle of the mandible with cortical bone 'peeling' at the fracture margins. May be taphonomic.

Inflammation:
Inflammatory bone changes within both maxillary sinuses.
Congenital: None.
Other:
Slight thickening of the cranial vault in the region of the parietals and frontal due to expansion of the diploë.

(JH3)136
Grid square: JH3 **Grave:** 110 **Skeleton:** 136 **EA Number:** 96650
Skeletal sex: undetermined **Age:** 6-10 years **Stature:** -
Preservation:
Taphonomic score: fair *Cortical surface score:* 3 *Completeness*: 88%
Inventory:

Skull (%)	Dentition (%)	Vertebrae (%)	Ribs/sternum (%)	Upper limbs (%)	Hands (%)	Pelvis (%)	Lower limbs (%)	Feet (%)
90	100	90	95	90	70	90	90	80

Palaeopathology:
Dental disease:
Caries: dURM2, dURM1, dULC, dULM1, dULM2, dLRM2, ULM1, LLM1, LRM1.
Joint disease: None.
Vertebral disease: None.
Trauma: None.
Inflammation:
Inflammatory bone changes within the left sphenoidal sinus.
Periosteal reaction on the right femoral shaft.
Congenital: None.
Other: None.

(JH3)140
Grid square: JH3 **Grave:** 9 **Skeleton:** 140 **EA Number:** 96641
Skeletal sex: undetermined **Age:** 2-5 years **Stature:** -
Preservation:
Taphonomic score: fair *Cortical surface score:* 5 *Completeness*: 36%
Inventory:

Skull (%)	Dentition (%)	Vertebrae (%)	Ribs/sternum (%)	Upper limbs (%)	Hands (%)	Pelvis (%)	Lower limbs (%)	Feet (%)
40	75	10	5	40	5	50	80	20

Palaeopathology:
Dental disease: None.
Joint disease: None.
Vertebral disease: None.
Trauma: None.
Inflammation: None.
Congenital: None.
Other: None.

(JH3)141
Grid square: JH3 **Grave:** 43 **Skeleton:** 141 **EA Number:** 96646
Skeletal sex: undetermined **Age:** 20-34 years **Stature:** -
Preservation:
Taphonomic score: poor *Cortical surface score:* 5 *Completeness*: 43%
Inventory:

Skull (%)	Dentition (%)	Vertebrae (%)	Ribs/sternum (%)	Upper limbs (%)	Hands (%)	Pelvis (%)	Lower limbs (%)	Feet (%)
30	45	50	10	50	60	25	75	40

Palaeopathology:
Dental disease:
Periapical lesion: ULP1.
Unusual wear on the lingual surfaces of the upper incisors, canines, and premolars, and on the lower incisors. Possibly the result of non-masticatory wear.
Joint disease: None.

Vertebral disease:
Osteophytes: C5, C6, C7, L4.
Intervertebral disc disease: C5, C6, C7, L4.
Schmorl's nodes: T11, T12, L3.
Trauma: None.
Inflammation:
Inflammatory bone changes within the left maxillary sinus.
Periosteal reaction on the visceral surface of left rib 10.
Congenital: None.
Other:
Porosity on both orbital roofs.

(JH3)142
Grid square: JH3 **Grave:** 43 **Skeleton:** 142 **EA Number:** 96647
Skeletal sex: undetermined **Age:** 6-15 years **Stature:** -
Preservation:
Taphonomic score: fragments *Cortical surface score:* 5 *Completeness*: 7%
Inventory:

Skull (%)	Dentition (%)	Vertebrae (%)	Ribs/sternum (%)	Upper limbs (%)	Hands (%)	Pelvis (%)	Lower limbs (%)	Feet (%)
5	0	0	0	10	0	0	40	5

Palaeopathology:
Dental disease: None.
Joint disease: None.
Vertebral disease: None.
Trauma: None.
Inflammation: None.
Congenital: None.
Other: None.

(JH3)143
Grid square: JH3 **Grave:** 69 **Skeleton:** 143 **EA Number:** 96648
Skeletal sex: undetermined **Age:** 20+ **Stature:** -
Preservation:
Taphonomic score: good *Cortical surface score:* 3 *Completeness*: 4%
Inventory:

Skull (%)	Dentition (%)	Vertebrae (%)	Ribs/sternum (%)	Upper limbs (%)	Hands (%)	Pelvis (%)	Lower limbs (%)	Feet (%)
5	10	0	5	15	0	0	0	0

Palaeopathology:
Dental disease:
Possible non-masticatory wear of the labial surface of URI1.
Joint disease: None.
Vertebral disease: None.
Trauma: None.
Inflammation: None.
Congenital: None.
Other: None.

(JH3)144
Grid square: JH3 **Grave:** 69 **Skeleton:** 144 **EA Number:** 96649
Skeletal sex: undetermined **Age:** 0-1 years **Stature:** -
Preservation:
Taphonomic score: good *Cortical surface score:* 5 *Completeness*: 3%
Inventory:

Skull (%)	Dentition (%)	Vertebrae (%)	Ribs/sternum (%)	Upper limbs (%)	Hands (%)	Pelvis (%)	Lower limbs (%)	Feet (%)
5	10	0	0	0	10	0	0	0

Palaeopathology:
Dental disease: None.

Joint disease: None.
Vertebral disease: None.
Trauma: None.
Inflammation: None.
Congenital: None.
Other: None.

Grid square JH4

(JH4)3
Grid square: JH4 **Grave:** 2 **Skeleton:** 3 **EA Number:** 96653
Skeletal sex: undetermined **Age:** 11-15 years **Stature:** -
Preservation:
Taphonomic score: poor *Cortical surface score:* 4 *Completeness*: 8%
Inventory:

Skull (%)	Dentition (%)	Vertebrae (%)	Ribs/sternum (%)	Upper limbs (%)	Hands (%)	Pelvis (%)	Lower limbs (%)	Feet (%)
5	5	5	0	10	5	5	15	20

Palaeopathology:
Dental disease: None.
Joint disease: None.
Vertebral disease: None.
Trauma: None.
Inflammation:
Periosteal reaction on the lateral aspect of the right calcaneus.
Congenital: None.
Other: None.

(JH4)6
Grid square: JH4 **Grave:** 4 **Skeleton:** 6 **EA Number:** 96654
Skeletal sex: undetermined **Age:** 35-49 years **Stature:** -
Preservation:
Taphonomic score: poor *Cortical surface score:* 4 *Completeness*: 25%
Inventory:

Skull (%)	Dentition (%)	Vertebrae (%)	Ribs/sternum (%)	Upper limbs (%)	Hands (%)	Pelvis (%)	Lower limbs (%)	Feet (%)
50	5	20	15	55	45	25	0	10

Palaeopathology:
Dental disease: None.
Joint disease: None.
Vertebral disease:
Osteophytes: S1.
Intervertebral disc disease: S1.
Trauma:
Partially healed fractures to the proximal bases of two intermediate and one distal phalanx of the left hand.
Inflammation: None.
Congenital:
Symphalangism of the distal interphalangeal joint of one unsided foot digit.
Other: None.

(JH4)19
Grid square: JH4 **Grave:** 8 **Skeleton:** 19 **EA Number:** 96655
Skeletal sex: intermediate **Age:** 35-49 years **Stature:** female: 159cm $^{+}$/- 3.2cm;
male: 165.6cm $^{+}$/- 3.4cm (humerus$_{m}$ + radius$_{m}$)
Preservation:
Taphonomic score: fair *Cortical surface score:* 5 *Completeness*: 75%
Inventory:

Skull (%)	Dentition (%)	Vertebrae (%)	Ribs/sternum (%)	Upper limbs (%)	Hands (%)	Pelvis (%)	Lower limbs (%)	Feet (%)
75	90	95	85	85	85	25	50	85

Palaeopathology:
Dental disease:
Caries: URM2, URP2, URP1, LLM3, LLM2.
Periapical lesion: URP1, ULM1, LLM1, LRP1.
Antemortem tooth loss: LRM1, LRM2.
Joint disease:
Osteoarthritis: right mandibular condyle, distal joint of left clavicle, acromioclavicular joint of left scapula, metatarso-phalangeal joints of both first metatarsals.
Vertebral disease:
Osteoarthritis of atlantoaxial joint: C1, C2.
Osteoarthritis of articular facets: C7, T1, T4, T5.
Osteophytes: C3, C4, T4, T5, T7, T8, T9, T11, L1 through to S1.
Intervertebral disc disease: C4, C5, T11, L3.
Schmorl's nodes: L1 through to L4.
Trauma:
Possible depression trauma on the ectocranial surface of the parietal.
Inflammation:
Inflammatory bone changes within the right maxillary sinus.
Periosteal reaction on the visceral surface of the shaft of right rib 9.
Periosteal reaction on the greater trochanter of the left femur.
Congenital: None.
Other:
Small cyst-like lytic lesion embedded within the trabecular bone of the shaft of right rib 5 (only observable due to taphonomic damage).

(JH4)22
Grid square: JH4 **Grave:** 47 **Skeleton:** 22 **EA Number:** 96661
Skeletal sex: undetermined **Age:** 0-1 years **Stature:** -
Preservation:
Taphonomic score: fair *Cortical surface score:* 5 *Completeness*: 77%
Inventory:

Skull (%)	Dentition (%)	Vertebrae (%)	Ribs/sternum (%)	Upper limbs (%)	Hands (%)	Pelvis (%)	Lower limbs (%)	Feet (%)
75	100	55	70	80	75	70	95	70

Palaeopathology:
Dental disease: None.
Joint disease: None.
Vertebral disease: None.
Trauma: None.
Inflammation: None.
Congenital: None.
Other: None.

(JH4)50
Grid square: JH4 **Grave:** 35 **Skeleton:** 50 **EA Number:** 96658
Skeletal sex: female? **Age:** 35-49 **Stature:** 157.7cm $^{+}$/- 2.7cm (humerus $_{m}$)
Preservation:
Taphonomic score: fair *Cortical surface score:* 4 *Completeness*: 61%
Inventory:

Skull (%)	Dentition (%)	Vertebrae (%)	Ribs/sternum (%)	Upper limbs (%)	Hands (%)	Pelvis (%)	Lower limbs (%)	Feet (%)
90	35	55	60	85	80	70	30	40

Palaeopathology:
Dental disease:
Caries: URC, ULC, ULM3, LLM2, LLP2, LRM2.
Periapical lesion: ULP2, LLC
Antemortem tooth loss: URP2, URP1, ULM1, LLM3, LLM1, LLI2, LRI2, LRM3.
Joint disease: None.
Vertebral disease:
Osteoarthritis of articular facets: C7 through to T3.

Trauma:
Healed fracture on the distal interphalangeal joint surface of the distal phalanx of the left third hand digit.
Two possible depression fractures on the ectocranial surface of the left parietal.
Inflammation:
Inflammatory bone changes within both maxillary sinuses.
Congenital:
Ankylosis, with minimal new bone formation, of the distal interphalangeal joint of the right fourth hand digit and of the right intercarpal joint between the lunate and the triquetral. Likely congenital.
Other:
Enlarged arachnoid granulations along the sagittal sulcus of both parietals. Enlarged meningeal vessels also present on the parietals.

(JH4)51
Grid square: JH4 **Grave:** 24 **Skeleton:** 51 **EA Number:** 96657
Skeletal sex: female **Age:** 50+ years **Stature:** -
Preservation:
Taphonomic score: poor *Cortical surface score:* 5 *Completeness*: 69%
Inventory:

Skull (%)	Dentition (%)	Vertebrae (%)	Ribs/sternum (%)	Upper limbs (%)	Hands (%)	Pelvis (%)	Lower limbs (%)	Feet (%)
70	100	30	40	80	90	60	70	80

Palaeopathology:
Dental disease:
Caries: URP1, LLM1, LRM2.
Periapical lesion: LLM1.
Wear present on buccal tooth root surfaces of URM1, URP2, and URP1.
Joint disease:
Osteoarthritis: all temporomandibular joints on both temporals and mandible, distal joints of both clavicles, glenohumeral joint of right scapula, both acetabula, both femoral heads, joint surface between left lateral cuneiform and third metatarsal.
Irregular osteophyte formation on the dorsal margins of both right and left intertarsal joints of the naviculars and all cuneiforms, possibly indicating the early stages of joint ankylosis.
Vertebral disease:
Osteoarthritis of atlantoaxial joint: C1, C2.
Osteoarthritis of articular facets: C3, C4, C6, L2 through to L5, unidentified vertebral articular facet fragments.
Osteophytes: C4, C5, C7, S1, unidentified vertebral body fragments.
Intervertebral disc disease: C4, C7.
Trauma:
Fracture on the proximal interphalangeal joint surface of the proximal phalanx of the right fifth foot digit.
Partially healed fracture on an unidentified right rib shaft fragment.
Inflammation:
Inflammatory bone changes within the left maxillary sinus and right frontal sinus.
Congenital: None.
Other:
Intracarpal cysts on the lateral aspects of the right scaphoid and capitate.
Calcified elements recovered with the skeleton, including small nodular shaped calcifications and arteriosclerotic plaques (calcified arterial structures).

(JH4)52
Grid square: JH4 **Grave:** 36 **Skeleton:** 52 **EA Number:** 96659
Skeletal sex: undetermined **Age:** 6-10 years **Stature:** -
Preservation:
Taphonomic score: poor *Cortical surface score:* 5 *Completeness*: 39%
Inventory:

Skull (%)	Dentition (%)	Vertebrae (%)	Ribs/sternum (%)	Upper limbs (%)	Hands (%)	Pelvis (%)	Lower limbs (%)	Feet (%)
5	35	20	20	40	55	75	50	55

Palaeopathology:
Dental disease: None.
Joint disease: None.
Vertebral disease: None.

Trauma: None.
Inflammation: None.
Congenital: None.
Other: None.

(JH4)55
Grid square: JH4 **Grave:** 53 **Skeleton:** 55 **EA Number:** 96662
Skeletal sex: undetermined **Age:** 20+ years **Stature:** female: 156.2cm $^{+}$/- 4.1cm; 163.5cm $^{+}$/- 3.7cm (radius $_{m}$)

Preservation:
Taphonomic score: good *Cortical surface score:* 5 *Completeness*: 32%
Inventory:

Skull (%)	Dentition (%)	Vertebrae (%)	Ribs/sternum (%)	Upper limbs (%)	Hands (%)	Pelvis (%)	Lower limbs (%)	Feet (%)
0	0	70	50	40	70	0	15	40

Palaeopathology:
Dental disease: None.
Joint disease: None.
Vertebral disease: None.
Trauma: None.
Inflammation:
Periosteal reaction on the visceral surface of the shaft of left rib 1.
Periosteal reaction on the distal shaft of the right fibula.
Congenital:
Symphalangism of the distal interphalangeal joint of an unsided fifth foot digit.
Other: None.

(JH4)56
Grid square: JH4 **Grave:** 36 **Skeleton:** 56 **EA Number:** 96660
Skeletal sex: undetermined **Age:** 11-15 years **Stature:** -
Preservation:
Taphonomic score: poor *Cortical surface score:* 5 *Completeness*: 49%
Inventory:

Skull (%)	Dentition (%)	Vertebrae (%)	Ribs/sternum (%)	Upper limbs (%)	Hands (%)	Pelvis (%)	Lower limbs (%)	Feet (%)
10	30	35	50	75	85	60	45	50

Palaeopathology:
Dental disease:
Enamel hypoplasia on the LRM2 crown.
Joint disease: None.
Vertebral disease: None.
Trauma: None.
Inflammation: None.
Congenital: None.
Other: None.

(JH4)61
Grid square: JH4 **Grave:** 12 **Skeleton:** 61 **EA Number:** 96656
Skeletal sex: undetermined **Age:** undetermined nonadult **Stature:** -
Preservation:
Taphonomic score: fair *Cortical surface score:* 5 *Completeness*: 2%
Inventory:

Skull (%)	Dentition (%)	Vertebrae (%)	Ribs/sternum (%)	Upper limbs (%)	Hands (%)	Pelvis (%)	Lower limbs (%)	Feet (%)
0	0	0	0	5	5	0	0	5

Palaeopathology:
Dental disease: None.
Joint disease: None.
Vertebral disease: None.
Trauma: None.

Inflammation: None.
Congenital: None.
Other: None.

(JH4)108
Grid square: JH4 **Grave:** 106 **Skeleton:** 108 **EA Number:** 96663
Skeletal sex: intermediate (humeral and femoral head measurements: male)
Age: 20-34 years **Stature:** -
Preservation:
Taphonomic score: poor *Cortical surface score:* 3 *Completeness*: 55%
Inventory:

Skull (%)	Dentition (%)	Vertebrae (%)	Ribs/sternum (%)	Upper limbs (%)	Hands (%)	Pelvis (%)	Lower limbs (%)	Feet (%)
0	0	95	20	60	80	80	85	75

Palaeopathology:
Dental disease: None.
Joint disease: None.
Vertebral disease:
Osteoarthritis of articular facets: T3, T4.
Osteophytes: T9, L4.
Intervertebral disc disease: L4.
Pitting/porosity of the anterior margin of the superior surface of the vertebral body of L4, which extends onto the anterior surface of the vertebral body.
Trauma: None.
Inflammation:
Thick periosteal reaction on the distal shafts of both tibiae.
Thick periosteal reaction on the shafts of both fibulae.
Congenital:
Cranial vertebral border shift, resulting in partial lumbarisation of T12 and reduction in twelfth rib size.
Other: None.

(JH4)113
Grid square: JH4 **Grave:** 106 **Skeleton:** 113 **EA Number:** 96664
Skeletal sex: undetermined **Age:** 6-10 years **Stature:** -
Preservation:
Taphonomic score: poor *Cortical surface score:* 5 *Completeness*: 16%
Inventory:

Skull (%)	Dentition (%)	Vertebrae (%)	Ribs/sternum (%)	Upper limbs (%)	Hands (%)	Pelvis (%)	Lower limbs (%)	Feet (%)
5	30	10	5	20	50	5	10	10

Palaeopathology:
Dental disease: None.
Joint disease: None.
Vertebral disease: None.
Trauma: None.
Inflammation: None.
Congenital: None.
Other: None.

Grid square JI4

(JI4)2
Grid square: JI4 **Grave:** 1 **Skeleton:** 2 **EA Number:** 96665
Skeletal sex: undetermined **Age:** 2-5 years **Stature:** -
Preservation:
Taphonomic score: poor *Cortical surface score:* 4 *Completeness*: 22%
Inventory:

Skull (%)	Dentition (%)	Vertebrae (%)	Ribs/sternum (%)	Upper limbs (%)	Hands (%)	Pelvis (%)	Lower limbs (%)	Feet (%)
5	30	30	20	15	25	20	30	25

Palaeopathology:
Dental disease: None.
Joint disease: None.
Vertebral disease: None.
Trauma: None.
Inflammation: None.
Congenital: None.
Other: None.

Grid square FP6 in the town

(FP6)30
Grid square: FP6 **Building:** F1 **Room:** VI **Context:** 30 **EA Number:** 96660
Skeletal sex: undetermined (femoral head measurement: male)
Age: 20-34 **Stature:** -
Preservation:
Taphonomic score: fair *Cortical surface score:* 5 *Completeness*: 12%
Inventory:

Skull (%)	Dentition (%)	Vertebrae (%)	Ribs/sternum (%)	Upper limbs (%)	Hands (%)	Pelvis (%)	Lower limbs (%)	Feet (%)
0	0	30	0	0	0	60	20	0

Palaeopathology:
Dental disease: None.
Joint disease: None.
Vertebral disease:
Schmorl's node: L5.
Extensive ossification of the ligamentum flavum from T9 to L5 and lateral asymmetry of the inferior articular facets of the lumbar vertebrae.
Trauma: None.
Inflammation: None.
Congenital: None.
Other: None.

TABLE 2.1. THE AVERAGE PERCENTAGE OF COMPLETENESS FOR EACH SKELETAL ELEMENT GROUP AND FOR THE OVERALL COMPLETENESS OF EACH INDIVIDUAL.

Skull	Dentition	Vertebrae	Ribs/Sternum	Upper limbs	Hands	Pelvis	Lower limbs	Feet		Overall completeness
56%	58%	60%	49%	65%	58%	54%	66%	51%		57%

TABLE 2.2. THE PROPORTION OF INDIVIDUALS ALLOCATED EACH TAPHONOMIC SCORE AND THE AVERAGE SCORE ACROSS THE ENTIRE ASSEMBLAGE.

1 (Excellent)	2 (Good)	3 (Fair)	4 (Poor)	5 (Fragments)		Average score
3%	24.4%	43%	26.7%	3%		3
(4/135)	(33/135)	(58/135)	(36/135)	(4/135)		

TABLE 2.3. THE PROPORTION OF INDIVIDUALS ALLOCATED EACH CORTICAL SURFACE PRESERVATION SCORE AND THE AVERAGE SCORE ACROSS THE ENTIRE ASSEMBLAGE.

1 (0%)	2 (1-24%)	3 (25-49%)	4 (50-74%)	5 (75-99%)	6 (100%)		Average score
0%	2.2%	10.4%	17.8%	68.9%	0.7%		4.6
(0/135)	(3/135)	(14/135)	(24/135)	(93/135)	(1/135)		

TABLE 2.4. THE PROPORTION OF INDIVIDUALS IN EACH NONADULT AGE CATEGORY.

Preterm	Fullterm	Infancy	Early childhood	Late childhood	Puberty	Adolescence	Undetermined nonadult
0%	3.4%	29.3%	20.7%	19%	10.3%	10.3%	6.9%
(0/58)	(2/58)	(17/58)	(12/58)	(11/58)	(6/58)	(6/58)	(4/58)

TABLE 2.5. THE PROPORTION OF INDIVIDUALS IN EACH ADULT AGE CATEGORY.

Adolescence/ Young adult	Young adult	Middle adult	Old adult	Undetermined adult
1.3%	32.5%	40.3%	1.3%	24.7%
(1/77)	(25/77)	(31/77)	(1/77)	(19/77)

TABLE 2.6. THE PROPORTION OF ADULTS IN EACH SKELETAL SEX CATEGORY, ACCORDING TO AGE GROUP.

	Male	Male?	Intermediate	Female?	Female	Undetermined sex
Adolescence/ young adult	0%	0%	0%	0%	6.3%	0%
	(0/17)	(0/10)	(0/6)	(0/12)	(1/16)	(0/16)
Young adult	29.4%	40%	33.3%	50%	43.8%	6.3%
	(5/17)	(4/10)	(2/6)	(6/12)	(7/16)	(1/16)
Middle adult	58.8%	20%	50%	41.7%	43.8%	25%
	(10/17)	(2/10)	(3/6)	(5/12)	(7/16)	(4/16)
Old adult	0%	0%	0%	0%	6.3%	0%
	(0/17)	(0/10)	(0/6)	(0/12)	(1/16)	(0/16)
Undetermined adult	11.8%	40%	16.7%	8.3%	0%	68.8%
	(2/17)	(4/10)	(1/6)	(1/12)	(0/16)	(11/16)
Total	22.1%	13%	7.8%	15.6%	20.8%	20.8%
	(17/77)	(10/77)	(6/77)	(12/77)	(16/77)	(16/77)

TABLE 2.7. MORPHOLOGICAL DESCRIPTIONS OF NON-METRIC TRAITS AND THEIR SCORES.

Bone	Trait	Description
Frontal	Metopic suture	Persistence of the interfrontal (metopic) suture at the midline of the frontal bone.
	Supraorbital notch	Supraorbital notch on the supraorbital margin of the frontal bone present. Score 1: notch less than half occluded Score 2: notch greater than half occluded Score 3: degree of occlusion unknown Score 4: multiple notches present
	Supraorbital foramen	Supraorbital foramen on the supraorbital margin of the frontal bone present. Score 1: one foramen present. Score 2: multiple foramina present
	Frontal grooves	The presence of a groove or two grooves extending from the supraorbital region to the temporal line.
Parietal	Parietal foramen	Foramen present on the posterior half of the parietal bone, close to the sagittal suture. Score 1: on the parietal bone Score 2: on the suture
	Divided parietal bone	A division of the parietal bone in half by the presence of an accessory suture.
Occipital	Condylar canal	Canal present within the condylar fossa, posterior to the occipital condyles.
	Divided hypoglossal canal	Presence of a division of the hypoglossal canal by bony spines, located within the canal or at the internal opening of the canal. Score 1: partial division of the internal opening of the canal Score 2: partial division within the canal Score 3: complete division of the internal opening of the canal Score 4: complete division within the canal
	Double condylar facet	Division of the condylar facets of the occipital.
	Flexure of sagittal sulcus	Direction of flexure of the superior sagittal sulcus. Score 1: right Score 2: left Score 3: bifurcated
Sphenoid	Foramen ovale incompleteness	Foramen ovale incompletely formed. Score 1: partial formation of the foramen present Score 2: no definition of the foramen present
	Foramen spinosum incompleteness	Foramen spinosum incompletely formed. Score 1: partial formation of the foramen present Score 2: no definition of the foramen present
	Pterygo-spinous bridging	Bridge or spur of bone between the lateral pterygoid plate & the spina angularis of the sphenoid. Score 1: trace spur of bone present Score 2: partial bridging present Score 3: complete bridging present
	Pterygo-alar bridging	Bridge or spur of bone between the lateral pterygoid plate & inferior surface of the greater wing of the sphenoid. Score 1: trace spur of bone present Score 2: partial bridging present Score 3: complete bridging present
	Clinoid bridging	The presence of bridges or spurs of bone between the anterior, middle, or posterior clinoid processes of the sphenoid.

TABLE 2.7. MORPHOLOGICAL DESCRIPTIONS OF NON-METRIC TRAITS AND THEIR SCORES (CONT).

Bone	Trait	Description
Temporal	Auditory exostosis	A bony nodule or torus present within the internal auditory meatus. Score 1: less than one-third of the canal occluded Score 2: one- to two-thirds of the canal occluded Score 3: greater than two-thirds of the canal occluded
	Tympanic dehiscence	The presence of incomplete closure of the tympanic plate on the temporal bone, posterior to the mandibular fossa. Score 1: small foramen only Score 2: full defect
	Mastoid foramen location	The presence of a foramen located posteriorly to the mastoid process. Most often located on the temporal bone, but sometimes occurring within the occipito-mastoid suture or on the occipital itself. Score 1: located on the temporal Score 2: located on the occipito-mastoid suture Score 3: located on the occipital Score 4: located on both the temporal bone & occipo-mastoid suture. Score 5: located on both the temporal bone & on the occipital
	Mastoid foramen no.	The number of mastoid foramina present. Score 1: one foramen present Score 2: two foramina present Score 3: more than two foramina present
Zygomatic	Zygomaticofacial foramen	Size & number of foramina on the facial surface of the zygomatic bone. Score 1: one large foramen Score 2: one large foramen & one small foramen Score 3: two large foramina Score 4: multiple large & small foramina Score 5: one small foramen Score 6: multiple small foramina
	Os japonicum	The division of the zygomatic bone into two halves by an accessory suture.
Maxilla	Infraorbital suture	The presence of a suture extending from the orbital margin to the infraorbital foramen. Score 1: incomplete extension of the suture Score 2: complete extension of suture
	Multiple infraorbital foramina	Multiple infraorbital foramina present in the region of the infraorbital margin of the maxilla. Score 1: internal division of one foramen Score 2: two foramina present Score 3: more than two foramina present
	Torus	The presence of thickening or a ridge at the centre of the palate on the maxilla. Score 1: trace of a ridge present Score 2: moderate ridge of 2-5mm in extension present Score 3: marked ridge of more than 5mm in extension present
Palatine	Torus	The presence of thickening or a ridge at the centre of the palate on the palatine. Score 1: trace of a ridge present Score 2: moderate ridge of 2-5mm in extension present Score 3: marked ridge of more than 5mm in extension present

TABLE 2.7. MORPHOLOGICAL DESCRIPTIONS OF NON-METRIC TRAITS AND THEIR SCORES (CONT).

Bone	Trait	Description
Mandible	Mental foramen	The number of mental foramina present on the lateral aspects of the mandibular body. Score 1: one foramen present Score 2: two foramina present Score 3: more than two foramina present
	Torus	The presence of a bony ridge on the lingual aspect of the mandibular body. Score 1: trace of a ridge present Score 2: moderate ridge of 2-5mm in extension present Score 3: marked ridge of more than 5mm in extension present
	Mylohyoid bridge	The presence of a bridge of bone over the mylohyoid canal of the mandible, either located near the mandibular foramen or in the centre of the mylohyoid groove. Score 1: bridging located near the mandibular foramen Score 2: bridging located at the centre of the groove Score 3: bridging present at both locations with a hiatus between them Score 4: bridging present at both locations with no hiatus
	Mylohyoid bridge degree	The degree of mylohyoid bridging present. Score 1: partial bridging present Score 2: complete bridging present
	Rocker mandible	Curvature of the inferior surface of the mandibular ramus.
C1	Lateral bridging	Bridging uniting the lateral aspect of the superior articular facet with the lateral mass. Score 1: partial bridging present Score 2: complete bridging present
	Posterior bridging	Bridging uniting the posterior aspect of the superior articular facet with the posterior arch. Score 1: partial bridging present Score 2: complete bridging present
Cervical vertebrae	Accessory transverse foramen	Division of the transverse foramen by bony spicules. Score 1: partial bridging present Score 2: complete bridging present
Scapula	Suprascapular foramen	Bridging of the suprascapular notch to produce a foramen. Score 1: partial bridging present Score 2: complete bridging present
	Accessory acromial articular facet	An accessory articular facet located on the inferior surface of the acromion process.
	Unfused acromial epiphysis	Persistence of the acromial epiphysis in individuals older than 25 years, known as os acromiale.
	Glenoid fossa extension	Extension of the joint surface at the posterior-superior aspect of the glenoid fossa.
Sternum	Sternal foramen	Aperture present within the body of the sternum.
Humerus	Septal aperture	Aperture between the olecranon fossa & coronoid fossa on the distal humerus. Score 1: small pinhole present Score 2: true perforation present
	Supratrochlear spur	Spall spur of bone present on the medial supracondylar ridge.
Ulna	Two faceted trochlear notch form	Division of the trochlear notch into two discrete facets.
Os Coxa	Accessory sacro-iliac articulation	Accessory facet located posterior-superior to the sacroiliac joint on the retroauricular area.
	Acetabular crease	Notch or hiatus of the acetabular joint facet located on the superior region of the joint surface.

TABLE 2.7. MORPHOLOGICAL DESCRIPTIONS OF NON-METRIC TRAITS AND THEIR SCORES (CONT).

Bone	Trait	Description
Femur	Poirier's facet	Extension of the articular facet from the head onto the anterior-superior aspect of the neck.
	Femoral plaque	Area of raised irregular bone on the anterior-superior aspect of the femoral neck.
	Allen's fossa	Cortical discontinuity, exposing the trabeculae, on the anterior-superior aspect of the femoral neck.
	Third trochanter	Tuberosity located on the superior aspect of the gluteal crest.
Patella	Vastus notch	A notch located at the superior-lateral aspect of the patella.
Tibia	Medial squatting facet	Extension of the talocrural joint facet onto the anterior-medial aspect of the distal tibial metaphysis.
	Lateral squatting facet	Extension of the talocrural joint facet onto the anterior-lateral aspect of the distal tibial metaphysis.
Talus	Squatting facet	Extension of the talocrural joint facet onto the superior surface of the talus.
	Os trigonum	Accessory ossification centre located at the posterior aspect of the talus.
	Inferior articular surface double facet	Presence of two discrete facets on the inferior-anterior articular surface of the talus.
Calcaneus	Shape of superior articular facets	Morphology of the superior articular facets of the calcaneus. Score 1: three discrete facets Score 2: anterior & middle facets are joined Score 3: all facets are joined
	Anterior facet absent	Absence of the anterior calcaneal facet.

TABLE 2.8. THE PREVALENCE OF CRANIAL AND MANDIBULAR NON-METRIC TRAITS. PREVALENCE ACCORDING TO SCORE ARE PROVIDED FOR THOSE TRAITS WITH SCORING SYSTEMS OTHER THAN PRESENCE/ABSENCE, AS INDICATED BY NUMERICAL SCORES IN BOLD. MORPHOLOGICAL DESCRIPTIONS FOR EACH NUMERICAL SCORE ARE PRESENTED IN TABLE 2.7.

Bone	Trait	Left					Right			
Frontal	Metopic suture	0%								
		(0/54)								
	Supraorbital notch	1	2	3	4		1	2	3	4
		60.5%	18.6%	0%	0%		58.5%	19.5%	4.9%	0%
		(26/43)	(8/43)	(0/43)	(0/43)		(24/41)	(8/41)	(2/41)	(0/41)
	Supraorbital foramen	1		2			1		2	
		28.9%		4.4%			31.7%		7.3%	
		(13/45)		(2/45)			(13/41)		(3/41)	
	Frontal grooves	25.6%					24.3%			
		(10/39)					(9/37)			
Parietal	Parietal foramen	1		2			1		2	
		43.9%		0%			48.8%		4.7%	
		(19/41)		(0/41)			(21/43)		(2/43)	
	Divided parietal bone	0%					0%			
		(0/47)					(0/47)			
Occipital	Condylar canal	72.7%					66.7%			
		(13/18)					(12/18)			
	Divided hypoglossal canal	1	2	3	4		1	2	3	4
		4.8%	2.4%	9.5%	0%		5.1%	0%	10.3%	0%
		(2/42)	(1/42)	(4/42)	(0/42)		(2/39)	(0/39)	(4/39)	(0/39)
	Double condylar facet	0%					0%			
		(0/41)					(0/42)			
	Flexure of sagittal sulcus	1		2			3			
		71.1%		13.3%			6.7%			
		(32/45)		(6/45)			(3/45)			
Sphenoid	Foramen ovale incompleteness	1		2			1		2	
		5.7%		0%			2.6%		0%	
		(2/35)		(0/35)			(1/39)		(0/39)	
	Foramen spinosum incompleteness	1		2			1		2	
		40.7%		0%			23.5%		0%	
		(11/27)		(0/29)			(8/34)		(0/34)	
	Pterygo-spinous bridging	1	2	3			1	2	3	
		25%	0%	0%			25%	16.7%	0%	
		(3/12)	(0/12)	(0/12)			(3/12)	(2/12)	(0/12)	
	Pterygo-alar bridging	1	2	3			1	2	3	
		8.3%	8.3%	0%			9.1%	9.1%	0%	
		(1/12)	(1/12)	(0/12)			(1/11)	(1/11)	(0/11)	
	Clinoid bridging	33.3%					28.6%			
		(2/6)					(2/7)			

TABLE 2.8. THE PREVALENCE OF CRANIAL AND MANDIBULAR NON-METRIC TRAITS (CONT.).

Bone	Trait	Left				Right		
Temporal	Auditory exostosis	1	2	3		1	2	3
		0%	0%	0%		0%	0%	0%
		(0/38)	(0/38)	(0/38)		(0/47)	(0/47)	(0/47)
	Tympanic dehiscence	1		2		1		2
		10.3%		2.6%		5.1%		5.1%
		(4/39)		(1/39)		(2/39)		(2/39)
	Mastoid foramen location	1	2	3		1	2	3
		55.9%	5.9%	2.9%		58.1%	6.5%	3.2%
		(19/34)	(2/34)	(1/34)		(18/31)	(2/31)	(1/31)
		4		5		4		5
		8.8%		5.9%		9.7%		3.2%
		(3/34)		(2/34)		(3/31)		(1/31)
	Mastoid foramen no.	1	2	3		1	2	3
		41.4%	34.5%	10.3%		52%	20%	16%
		(12/29)	(10/29)	(3/29)		(13/25)	(5/25)	(4/25)
Zygomatic	Zygomaticofacial foramen	1	2	3		1	2	3
		19.1%	19.1%	10.6%		31.8%	9.1%	13.6%
		(9/47)	(9/47)	(5/47)		(14/44)	(4/44)	(6/44)
		4	5	6		4	5	6
		4.3%	8.5%	17%		11.4%	11.4%	11.4%
		(2/47)	(4/47)	(8/47)		(5/44)	(5/44)	(5/44)
	Os japonicum	0%				0%		
		(0/51)				(0/48)		
Maxilla	Infraorbital suture	1		2		1		2
		15.8%		5.3%		15%		20%
		(3/19)		(1/19)		(3/20)		(4/20)
	Multiple infraorbital foramina	1	2	3		1	2	3
		0%	5.6%	0%		5.9%	0%	0%
		(0/18)	(1/18)	(0/18)		(1/17)	(0/17)	(0/17)
	Torus	1	2	3		1	2	3
		14.3%	2.9%	0%		18.8%	3.1%	0%
		(5/35)	(1/35)	(0/35)		(6/32)	(1/32)	(0/32)
Palatine	Torus	1		2		3		
		27.8%		11.1%		0%		
		(5/18)		(2/18)		(0/18)		

TABLE 2.8. THE PREVALENCE OF CRANIAL AND MANDIBULAR NON-METRIC TRAITS (CONT.).

Bone	Trait	Left					Right			
Mandible	Mental foramen	1	2	3			1	2	3	
		100%	0%	0%			96.4%	3.6%	0%	
		(57/57)	(0/57)	(0/57)			(53/55)	(2/55)	(0/55)	
	Torus	1	2	3			1	2	3	
		21.2%	5.8%	0%			28.6%	2%	0%	
		(11/52)	(3/52)	(0/52)			(14/49)	(1/49)	(0/49)	
	Mylohyoid bridge	1	2	3	4		1	2	3	4
		0%	4.4%	2.2%	0%		2.1%	2.1%	4.2%	0%
		(0/45)	(2/45)	(1/45)	(0/45)		(1/48)	(1/48)	(2/48)	(0/48)
	Mylohyoid bridge degree	1		2			1		2	
		0%		100%			50%		50%	
		(0/3)		(3/3)			(2/4)		(2/4)	
	Rocker mandible	15.6%								
		(5/32)								

TABLE 2.9. THE PREVALENCE OF ACCESSORY CRANIAL SUTURAL BONES.

Sutural bone	Left		Right
Epipteric bone	7.7%		6.7%
	(1/13)		(1/15)
Bregmatic bone	0%		
	(0/33)		
Apical bone	10.4%		
	(5/48)		
Inca bone	0%		
	(0/45)		
Asterionic bone	3.6%		10.7%
	(1/28)		(3/28)
Occipito-mastoid bone	4.5%		4.2%
	(1/22)		(1/24)
Parietal notch bone	18.5%		11.5%
	(5/27)		(3/26)
Coronal ossicle	8.3%		7.4%
	(2/24)		(2/27)
Sagittal ossicle	6.5%		
	(2/31)		
Lambdoidal ossicle	35.5%		23.3%
	(11/31)		(7/30)

TABLE 2.10. THE PREVALENCE OF POST-CRANIAL NON-METRIC TRAITS. PREVALENCE ACCORDING TO SCORE IS PROVIDED FOR THOSE TRAITS WITH SCORING SYSTEMS OTHER THAN PRESENCE/ABSENCE, AS INDICATED BY NUMERICAL SCORES IN BOLD. MORPHOLOGICAL DESCRIPTIONS FOR EACH NUMERICAL SCORE ARE PRESENTED IN TABLE 2.7.

Bone	Trait	Left			Right	
C1	Lateral bridging	1	2		1	2
		0%	2.4%		0%	0%
		(0/42)	(1/42)		(0/38)	(0/38)
	Posterior bridging	1	2		1	2
		9.8%	9.8%		13.5%	5.4%
		(4/41)	(4/41)		(5/37)	(2/37)
C3	Accessory transverse foramen	1	2		1	2
		0%	0%		3.1%	0%
		(0/29)	(0/29)		(1/32)	(0/32)
C4	Accessory transverse foramen	1	2		1	2
		3.2%	3.2%		14.3%	5.7%
		(1/31)	(1/31)		(5/35)	(2/35)
C5	Accessory transverse foramen	1	2		1	2
		6.5%	22.6%		25.8%	9.7%
		(2/31)	(7/31)		(8/31)	(3/31)
C6	Accessory transverse foramen	1	2		1	2
		25%	29.2%		20%	56%
		(6/24)	(7/24)		(5/25)	(14/25)
C7	Accessory transverse foramen	1	2		1	2
		19%	9.5%		13.3%	13.3%
		(4/21)	(2/21)		(2/15)	(2/15)
Scapula	Suprascapular foramen	1	2		1	2
		30%	0%		14.3%	0%
		(3/10)	(0/10)		(2/14)	(0/14)
	Accessory acromial articular facet	2.2%			2.2%	
		(1/46)			(1/46)	
	Unfused acromial epiphysis	6.3%			2%	
		(3/48)			(1/50)	
	Glenoid fossa extension	7.1%			14.3%	
		(3/42)			(7/49)	
Sternum	Sternal foramen	5.9%				
		(1/17)				
Humerus	Septal aperture	1	2		1	2
		21.6%	35.3%		22.4%	26.5%
		(11/51)	(18/51)		(11/49)	(13/49)
	Supratrochlear spur	0%			0%	
		(0/53)			(0/51)	
Ulna	Two faceted trochlear notch form	8.9%			6.1%	
		(4/45)			(3/49)	
Os Coxa	Accessory sacro-iliac articulation	20.7%			8.6%	
		(6/29)			(3/35)	
	Acetabular crease	2.2%			2.2%	
		(1/45)			(1/45)	

TABLE 2.10. THE PREVALENCE OF POST-CRANIAL NON-METRIC TRAITS (CONT.).

Bone	Trait	Left				Right		
Femur	Poirier's facet	18.8%				7.5%		
		(6/32)				(3/40)		
	Femoral plaque	28.1%				29.3%		
		(9/32)				(12/41)		
	Allen's fossa	21.2%				19.5%		
		(7/33)				(8/41)		
	Third trochanter	12.2%				13%		
		(5/41)				(6/46)		
Patella	Vastus notch	36.4%				32.7%		
		(20/55)				(18/55)		
Tibia	Medial squatting facet	12.1%				10.5%		
		(4/33)				(4/38)		
	Lateral squatting facet	67.5%				70.5%		
		(27/40)				(31/44)		
Talus	Squatting facet	36.4%				38%		
		(16/44)				(19/50)		
	Os trigonum	0%				0%		
		(0/52)				(0/54)		
	Inferior articular surface double facet	25%				27.3%		
		(13/52)				(15/55)		
Calcaneus	Shape of superior articular facets	1	2	3		1	2	3
		37%	60.9%	2.2%		23.4%	70.2%	4.3%
		(17/46)	(28/46)	(1/46)		(11/47)	(33/47)	(2/47)
	Anterior facet absent	4.1%				8%		
		(2/49)				(4/50)		

TABLE 2.11. METRIC MEASUREMENTS (MM) FOR ADULT INDIVIDUALS, AFTER BUIKSTRA AND UBELAKER (1994, 69-84).

Skeleton	Maximum cranial length	Maximum cranial breadth	Bizygomatic diameter	Basion-bregma height	Cranial base length	Basion-prosthion length	Maxillo-alveolar breadth	Maxillo-alveolar length	Biauricular breadth	Upper facial height	Minimum frontal breadth	Upper facial breadth	Nasal height	Nasal breadth	Orbital breadth	Orbital height	Biorbital breadth	Interorbital breadth	Frontal chord	Parietal chord	Occipital chord	Foramen magnum length	Foramen magnum breadth	Mastoid length	Chin height	Mandibular body height	Mandibular body breadth	Mandibular bigonial width	Mandibular bicondylar breadth	Minimum ramus breadth	Maximum ramus breadth
533(30)																								25		32	14			29	40
561(21)																											8			30	44
561(24)											90	98							106	119	99			30		33	11			30	42
561(25)																								32	38	34	10			31	45
1052(3)																								42	35	31	14			36	47
1066(8)																															
1075(9)																								41	30	27	10			32	44
1075(11)																								28		27	10				
1075(16)																										28	11			31	
1083(5)																										31	10			27	38
1083(11)											90								103	112					29	30	10			29	39
1083(15)																										30	11			29	42
1093(8)																															
GD3(61)																								32	32	33	14			33	41
GD3(27)																									22	19					
GD3(146)	180	125		132	97	91	60	54	111	65	95	101	46	24		32		20	112	118	96	35	26	27		25	9			26	39
GD3(69)																								28	24	30	10			35	45
GD3(106)																									30	28	11	95	113	33	43
GD3(81)	194	136		133	106	101	60	58	122	68	90	103	50	20	40	32	97	22	108	112	107	37	32	35	34	34	13			33	44
GD3(78)																								27	34	34	11			35	
GD3(127)											100	99												31	29	30	12			27	40
GD3(89)	170	125		126	139				122		91	95				36		21	105	107	93	37	33	33		25	12	84	111	33	45
GD3(152)																								40						39	52
GD3(108)																															
GD3(115)																											11			32	
GD3(132)		130									96	105							117	119	91			25	32	33	13			38	46
GD3(151)																									37	35	13				
HA2(209)	184	122					65	52		68	100	110		27	38	30	98	27						37	33	33	13			34	48

TABLE 2.11. METRIC MEASUREMENTS (MM) FOR ADULT INDIVIDUALS (CONT.).

Skeleton	Maximum cranial length	Maximum cranial breadth	Bizygomatic diameter	Basion-bregma height	Cranial base length	Basion-prosthion length	Maxillo-alveolar breadth	Maxillo-alveolar length	Biauricular breadth	Upper facial height	Minimum frontal breadth	Upper facial breadth	Nasal height	Nasal breadth	Orbital breadth	Orbital height	Biorbital breadth	Interorbital breadth	Frontal chord	Parietal chord	Occipital chord	Foramen magnum length	Foramen magnum breadth	Mastoid length	Chin height	Mandibular body height	Mandibular body breadth	Mandibular bigonial width	Mandibular bicondylar breadth	Minimum ramus breadth	Maximum ramus breadth
HA2(142)																				113	100			30		31	10			32	44
HA2(259)																								40	35	31	13			37	49
HA2(280)																										35	11			38	50
HA2(192)																															
HA2(278)																															
HA2(195)																								34	23	24	10			30	45
HA2(232)																								38							
HA2(265)																															
HA2(198)	182	132	115	130	98	95	63	51	113	69	104	107	48	23	41	33	107	27	113	110	96	35	28	29	31	29	12	88	108	29	40
HA2(168)																										31	11				
HA2(169)											94	107							102												
HA2(164)																								30						31	44
HA2(171)																								41	29	31	14			31	41
HA2(172)																									28	29	12			31	40
HA2(155)																								32							
HA2(124)								59			92	104						26	109	103	100			38		35	16			37	45
HA2(193)	177	133							124		95	109							110	125	98			41		34	14			39	51
HA2(237)																															
HA2(257)	181	125					59	52		69	87		47	24	37	34		19	101	116	101				31	31	12			32	46
HA2(255)																								37	33	32	11			33	46
JE3(195)																								34							
JE3(185)																										27	9			32	42
JE3(186)																								33		32	12			31	
JF2(64)																								35	28	31	12			33	45
JG1(51)																															
JG2(23)																								29							
JG2(43)	184	140									96								112	157				33		35	11	101	121	32	44
JG2(64)																									35						

TABLE 2.11. METRIC MEASUREMENTS (MM) FOR ADULT INDIVIDUALS (CONT.).

Skeleton	Maximum cranial length	Maximum cranial breadth	Bizygomatic diameter	Basion-bregma height	Cranial base length	Basion-prosthion length	Maxillo-alveolar breadth	Maxillo-alveolar length	Biauricular breadth	Upper facial height	Minimum frontal breadth	Upper facial breadth	Nasal height	Nasal breadth	Orbital breadth	Orbital height	Biorbital breadth	Interorbital breadth	Frontal chord	Parietal chord	Occipital chord	Foramen magnum length	Foramen magnum breadth	Mastoid length	Chin height	Mandibular body height	Mandibular body breadth	Mandibular bigonial width	Mandibular bicondylar breadth	Minimum ramus breadth	Maximum ramus breadth
JG2(215)	192	133		137	112				123		105							27	112	125	95	39	31	28		31	12			35	
JG2(66)																								28			12			35	49
JG2(312)																				133				21	33	32	12			36	52
JG2(313)																								32	39	32	11			32	43
JG2(314)	161										91	97						21	110	95	96				36	30	11			33	38
JG3(13)											88	95												27	33	30	10	95		31	39
JG3(21)																								30							
JH3(82)																								29	27	28	11			29	40
JH3(126)											98	103							106						23						
JH3(125)																															
JH3(141)																								33						30	
JH3(123)	177	127																	105	111				28	31	31	12		108	32	36
JH3(133)																									25	24	11			30	43
JH4(6)																								23							
JH4(19)																								29	34	35	11			35	44
JH4(51)																									32	32	10			29	40
JH4(50)																															
JH4(55)																															
JH4(108)																															
FP6(30)																															

TABLE 2.11. METRIC MEASUREMENTS (MM) FOR ADULT INDIVIDUALS (CONT.).

Skeleton	Maximum ramus height	Mandibular length	Mandibular angle	Clavicular maximum length	Clavicular anterior-posterior diameter	Clavicular superior-inferior diameter	Scapular height	Scapular breadth	Humeral maximum length	Humeral epicondylar breadth	Humeral head vertical diameter	Humeral midshaft maximum diameter	Humeral midshaft minimum diameter	Radial maximum length	Radial midshaft anterior-posterior diameter	Radial midshaft medial-lateral diameter	Ulnar maximum length	Ulnar anterior-posterior diameter	Ulnar medial-lateral diameter	Ulnar physiological length	Pelvis height	Iliac breadth	Pubic length	Ischial length	Sacral anterior length	Sacral anterior-superior breadth	Sacrum maximum transverse diameter of base	Femoral maximum length	Femoral bicondylar length	Femoral epicondylar breadth
533(30)	53	74																												
561(21)	61									62																				
561(24)	62			129	12	10			328	57	44	21	17	250	12	13	275	15	12	247	189	144		79	93		46	444	443	78
561(25)	58			146	14	14				67	51				12	17	287	14	16	258		158	74			112	54			
1052(3)	70		88	143	12	11				62	45	22	19	246	11	15	271	13	17	240							53			84
1066(8)																														
1075(9)	54	78									35	16	13																	
1075(11)										56																				
1075(16)	65				10	8			302	52	39	15	13		8	12		13	9			138								
1083(5)	45																													
1083(11)	48	75								54		17	12																	
1083(15)	57			140	9	8			307	55	40	20	15																	
1093(8)																														
GD3(61)	57			141	11	9			295	54	39	19	14		10	14	244	13	11	216	188	149		81	102	106	38			
GD3(27)					9	8				53		18	12		9	11		10	11											
GD3(146)	54			144	11	9	133	107	300	55	38	20	14	232	10	11	249	14	11	225		141			117	119	53	429	428	72
GD3(69)	62			149	12	11				63		21	16		12	16	268	15	13	245			81	83			46			
GD3(106)	58	74	115	131	11	8	149	92	296	62	40	20	15	232	11	14	251	15	13	221	190	134	77	68	99	90	47	406	404	73
GD3(81)	73	81	122	157	15	11	158	110	330	65	48	25	18	261	13	17	287	19	14	256	208	151	96	95	93	102	54	472	467	84
GD3(78)					12	13								237	13	16	261	15	14	230								421	423	
GD3(127)	52			158	11	10		104	295	63	41	19	15	232	12	14	253	12	12	228	192	148	78	83	100	103	49	419	416	77
GD3(89)	53	75			10	8									10	14		11	15											
GD3(152)	63			147	10	8	142	104	313	54	39	20	16	244	11	12	264	13	11	239						112	42	430	427	72
GD3(108)										61					12	14		14	13	242						102	58			
GD3(115)										65																	51			
GD3(132)	60	84		159	14	10			343	64	45	20	17	257	13	16	279	14	14	250	211	161	82	92	124	97	51	478	476	80
GD3(151)										62	42	22	18										63	74			56			

TABLE 2.11. METRIC MEASUREMENTS (MM) FOR ADULT INDIVIDUALS (CONT.).

Skeleton	Maximum ramus height	Mandibular length	Mandibular angle	Clavicular maximum length	Clavicular anterior-posterior diameter	Clavicular superior-inferior diameter	Scapular height	Scapular breadth	Humeral maximum length	Humeral epicondylar breadth	Humeral head vertical diameter	Humeral midshaft maximum diameter	Humeral midshaft minimum diameter	Radial maximum length	Radial midshaft anterior-posterior diameter	Radial midshaft medial-lateral diameter	Ulnar maximum length	Ulnar anterior-posterior diameter	Ulnar medial-lateral diameter	Ulnar physiological length	Pelvis height	Iliac breadth	Pubic length	Ischial length	Sacral anterior length	Sacral anterior-superior breadth	Sacrum maximum transverse diameter of base	Femoral maximum length	Femoral bicondylar length	Femoral epicondylar breadth
HA2(209)	64	85		168	13	9			329	64	47	21	17	270	11	14	289	13	13	262			89				53			78
HA2(142)	55	87								53		19	13	210	9	11	227	10	13	201								388	388	71
HA2(259)	55	87		145	13	9			315	65	45	21	17	247	12	15		14	15						111		50			79
HA2(280)	50	75													10	12		10	13											
HA2(192)					9	11																					46			
HA2(278)																		13	15								44			
HA2(195)	51	69			8	8				52	35									207								411	409	72
HA2(232)				127	8	9				54							231	10	13	209										
HA2(265)				132	9	10								211	10	12										110	48	408	405	69
HA2(198)	47			140	12	10			318	54	41	19	17	241	11	14	262	12	13	236						105	47	445	444	76
HA2(168)										58				223	10	13														77
HA2(169)				136	12	10				63								13	15								49	411	409	83
HA2(164)	56			144	8	9			312	55	40	20	14	241	10	12		10	13	236							54			76
HA2(171)	64			138		9												11	16											
HA2(172)	56			142	12	8			296	58	37	18	15	227	10	13	242	10	15	219						110	53	397	395	73
HA2(155)				118	9	9					35																			
HA2(124)	58				13	11			319	56	39	20	17	258	12	15	279	13	14	250		140	68		97	101	43	468	463	71
HA2(193)	59			157	14	10			312	61	45	22	19	242	13	18	266	14	15	242	207	162	76	82	92	105	49	430	429	80
HA2(237)				136	10	8				62	45	20	14	256	11	13		13	13	237										76
HA2(257)	56			126	10	7				54	39	19	14		9	13	234	10	14	210						115	50			
HA2(255)	58			148	11	9				61	45	20	14	255	11	13	276	12	14	248										
JE3(195)											46																			
JE3(185)	59			137	11	9			317	58	39	18	15		11	14	263	14	11	236		139				115	49			
JE3(186)	66	73	108	135	13	11			318	64	49	23	19		13	16		17	13											
JF2(64)	56				12	9				57		21	15		9	11		10	15											
JG1(51)																														
JG2(23)																														

TABLE 2.11. METRIC MEASUREMENTS (MM) FOR ADULT INDIVIDUALS (CONT.).

Skeleton	Maximum ramus height	Mandibular length	Mandibular angle	Clavicular maximum length	Clavicular anterior-posterior diameter	Clavicular superior-inferior diameter	Scapular height	Scapular breadth	Humeral maximum length	Humeral epicondylar breadth	Humeral head vertical diameter	Humeral midshaft maximum diameter	Humeral midshaft minimum diameter	Radial maximum length	Radial midshaft anterior-posterior diameter	Radial midshaft medial-lateral diameter	Ulnar maximum length	Ulnar anterior-posterior diameter	Ulnar medial-lateral diameter	Ulnar physiological length	Pelvis height	Iliac breadth	Pubic length	Ischial length	Sacral anterior length	Sacral anterior-superior breadth	Sacrum maximum transverse diameter of base	Femoral maximum length	Femoral bicondylar length	Femoral epicondylar breadth
JG2(43)	38	79		159	13	10				62		23	17		11	17		13	14											76
JG2(64)										62		23	18					18	16							88				
JG2(215)					15	12				67	49	25	19		13	16		16	20						106	108	49	458	457	84
JG2(66)	61	77			12	14												20	16											
JG2(312)	70			155	14	12			356	63	50	23	18	281	13	16	304	14	14	271						124	59			87
JG2(313)	58	79		136	11	11			303	58	44	19	16	244	12	15	262	14	13	233		146				102	44			74
JG2(314)	50			155	12	12			313	54	39	19	18		12	14		12	13			140				102	43			74
JG3(13)	52	72		129	10	8				56		20	16	230	11	13		12	11					74			38			
JG3(21)															13	15		13	16	268										
JH3(82)	55	70		132	12	9			314	58	40	19	15		10	13		14	12											74
JH3(126)					10	10			310	52	34	17	13		9	11		13	9	246		129								
JH3(125)					13					58	43	21	17	248	11	14		13	14	239		154					53			
JH3(141)					13	11						19	17		13	14		15	15								42			
JH3(123)	56				9	7			319	55	39	19	13	245	10	12	267	14	10	237										
JH3(133)	45	80		149	11	8			311	54	38	19	16		10	13									116	109	48	443	435	
JH4(6)												19	13		10	13		12	10											
JH4(19)	55	70		149	10	8			305	57	40	21	15	257	11	12	279	12	11	251							47			
JH4(51)	62				12	8									10	12		14	11											
JH4(50)				139	9	7			307	54	40	19	14		13	11	249	13	13	228										
JH4(55)				152	10	11								237	12	17														
JH4(108)					13	10				63	46															88	46			
FP6(30)																											52			

TABLE 2.11. METRIC MEASUREMENTS (MM) FOR ADULT INDIVIDUALS (CONT.).

Skeleton	Femoral maximum head diameter	Femoral subtrochanteric anterior-posterior diameter	Femoral subtrochanteric medial-lateral diameter	Femoral midshaft anterior-posterior diameter	Femoral midshaft medial-lateral diameter	Tibial maximum length	Tibial physiological length	Tibial maximum proximal epiphyseal breadth	Tibial maximum distal epiphyseal breadth	Tibial maximum diameter at nutrient foramen	Tibial medial-lateral diameter at nutrient foramen	Fibular maximum length	Fibular maximum midshaft diameter	Calcaneal maximum length	Calcaneal middle breadth	Second metacarpal midline length	First metatarsal maximum length	Second metatarsal maximum length	Third metatarsal maximum length	Fourth metatarsal maximum length
533(30)																				
561(21)	40	22	30	25	26	401	388	70	45	34	21			78	38	66	62			72
561(24)	43	28	27	26	24			75	48				15	74	43	67	63	79	72	70
561(25)	49	24	38			410	400	81	50	36	25					67		82		75
1052(3)	46	31	35	30	27	384		78	51	38	27		17	89	43	69	65	79	73	71
1066(8)		21	29													63				
1075(9)		22	27						47											
1075(11)	39	22	26											73	32	58	58			
1075(16)	37	22	27													60	58	68	65	65
1083(5)	39																	74	70	67
1083(11)	37	21	25						42	26	18		12							
1083(15)																66				
1093(8)										28	19				41					69
GD3(61)	41	25	30	26	24				45				12	72	44	64	59	74	69	67
GD3(27)	37	21	24	24	22					26	19		12				52			61
GD3(146)	39	23	29	30	24	372	361	67	46	30	21	355	14	72	37		59	74	69	66
GD3(69)	45	25	30	30	26	364	349		51	36	22		13	82	44		64	75	70	
GD3(106)	43	22	26	31	23	348	337	71	48	28	22	339	16	78	40	63	60	74	69	68
GD3(81)	48	29	31	32	35	389	380	77	54	39	24		15	85	46	69	69	82	78	
GD3(78)	46	25	31	28	24					31	24		17	75	39	65				
GD3(127)	41	23	28	27	26	367	355	72	48	32	11		14	77	40	59	59	72	67	65
GD3(89)										26	18		11	75	38		63	80		
GD3(152)	38	22	26	26	24	368	364	68	44	32	22	362	14	75	35	65	62			
GD3(108)	46	24	33						51				15	81	40	65	59	74		68
GD3(115)	48	23	32							33	28			82	44	69	70		75	

TABLE 2.11. METRIC MEASUREMENTS (MM) FOR ADULT INDIVIDUALS (CONT.).

Skeleton	Femoral maximum head diameter	Femoral subtrochanteric anterior-posterior diameter	Femoral subtrochanteric medial-lateral diameter	Femoral midshaft anterior-posterior diameter	Femoral midshaft medial-lateral diameter	Tibial maximum length	Tibial physiological length	Tibial maximum proximal epiphyseal breadth	Tibial maximum distal epiphyseal breadth	Tibial maximum diameter at nutrient foramen	Tibial medial-lateral diameter at nutrient foramen	Fibular maximum length	Fibular maximum midshaft diameter	Calcaneal maximum length	Calcaneal middle breadth	Second metacarpal midline length	First metatarsal maximum length	Second metatarsal maximum length	Third metatarsal maximum length	Fourth metatarsal maximum length
GD3(132)	44	25	30	32	28	382	374	76	47	35	24	384	14	78	40	62	67	79	75	73
GD3(151)	46	27	33	32	27				48	39	24		15	85	40	66			71	70
HA2(209)	47	26	31						51				13	81	41	71	69	80		
HA2(142)	40	21	28	24	24	313	304	67	40	29	18		12			57	54			
HA2(259)	44	25	31						48			360	15	78	40	63				
HA2(280)																				
HA2(192)		21	29							30	18									
HA2(278)																			68	
HA2(195)	38	22	29	23	25			69	48								63	74	71	68
HA2(232)		21	28					64	44	29	22			73	38	59	60	67	63	61
HA2(265)		21	27	27	24	333	323	65	42	29	20	327	14	68	35	59	61	70	66	63
HA2(198)	40	26	29	30	26	381		67	43	31	23			73	36	61			69	65
HA2(168)	41	26	29						45	33	22			74	41	65	60			
HA2(169)	45	26	29	27	25					33	24			76	44	58	59	69		
HA2(164)	42	22	29			374	368	72	47	30	20		14	76	39	66	66	76	74	71
HA2(171)	43	25	33													69	66	76		70
HA2(172)		24	28	25	25	349	344	68	46	30	22		13	74	38	64	63	72	69	70
HA2(155)	37	19	26																	
HA2(124)	40	25	26	28	22	395	382	70	43	33	23	377	17	84	40	66	66	76	71	
HA2(193)	45	27	36	31	29			77	49	35	23			78	39	67	60	78	72	71
HA2(237)	46	20	28					72	50	32	23			75	42	64	67	74	67	
HA2(257)	41	22	30						46	26	21		12	68	37	58		66		61
HA2(255)	44	26	30						53	32	23			81	45	67	66	80		71
JE3(195)		27	31																	
JE3(185)	40	23	31	24	26				43								67		71	69

TABLE 2.11. METRIC MEASUREMENTS (MM) FOR ADULT INDIVIDUALS (CONT.).

Skeleton	Femoral maximum head diameter	Femoral subtrochanteric anterior-posterior diameter	Femoral subtrochanteric medial-lateral diameter	Femoral midshaft anteri-or-posterior diameter	Femoral midshaft medial-lateral diameter	Tibial maximum length	Tibial physiological length	Tibial maximum proximal epiphyseal breadth	Tibial maximum distal epiphyseal breadth	Tibial maximum diameter at nutrient foramen	Tibial medial-lateral diam-eter at nutrient foramen	Fibular maximum length	Fibular maximum midshaft diameter	Calcaneal maximum length	Calcaneal middle breadth	Second metacarpal midline length	First metatarsal maximum length	Second metatarsal maximum length	Third metatarsal maximum length	Fourth metatarsal maximum length
JE3(186)	49	32	31						43					83	42	62	63		69	67
JF2(64)	38	18	26					62		26	17		12	72	36	65				
JG1(51)	40	24	27					64						76	39	69	64	81	76	72
JG2(23)																				
JG2(43)	47	27	27	31	26											67				
JG2(64)	44									35	28			79		74				
JG2(215)	48	27	35	29	30	399	395	78	54	35	23		17	84	44	75	73	85		79
JG2(66)	47	29	32	35	28			85			24						67	78	74	74
JG2(312)	50	29	37	37	27			81	56	40	26		17	86		72	70	83	77	80
JG2(313)	41	24	30	32	24			70	46	33	24		15	70		65	62	73	68	65
JG2(314)	39	25	27	27	25			68	45	35	20		15	75	35	69	58	73	69	67
JG3(13)	41	26	25	31	21									83			65	75		
JG3(21)	46												15					82	78	79
JH3(82)	41	23	29	26	24											63		76		
JH3(126)	37	24	25	27	20								14			64				
JH3(125)	45	28	32	28	28				45				16	76	37	65	63	72	64	65
JH3(141)	42	24	27	27	26				43	31	22			83						
JH3(123)	40			26	24				40	29	19		13	76	42	67	63	74	71	71
JH3(133)	39	24	27	28	25									75	37	64				
JH4(6)																				
JH4(19)	41	23	30	26	24									81	43	72		78	77	75
JH4(51)	38	23	32							30	19					65	57			68
JH4(50)																				
JH4(55)													15			61				
JH4(108)	44							76	42	28	23				41	70	66		72	
FP6(30)	44	24	29	24	24															

TABLE 2.12. METRIC MEASUREMENTS (MM) FOR NONADULT INDIVIDUALS, AFTER BUIKSTRA AND UBELAKER (1994, 45-46).

Skeleton	Sphenoidal left lesser wing length	Sphenoidal right lesser wing length	Sphenoidal left lesser wing width	Sphenoidal right lesser wing width	Sphenoidal left greater wing length	Sphenoidal right greater wing length	Sphenoidal left greater wing width	Sphenoid right greater wing width	Sphenoidal body length	Sphenoidal body width	Basilar length	Basilar width	Left petrous length	Right petrous length	Left petrous width	Right petrous width	Left zygomatic length	Right zygomatic length	Left zygomatic width	Right zygomatic width	Left maxillary length	Right maxillary length	Left maxillary height	Right maxillary height	Left maxillary width	Right maxillary width	Left mandibular length	Right mandibular length	Left mandibular width	Right mandibular width	Left mandibular full length	Right mandibular full length
(1058)8																																
(1059)8																																
(1084)8																																
(1096)7											12	20																				
(1097)7											17																					
(GD3)26											14	17																				
(GD3)30		29	23	24	49				14	23	18	28			22	19	41	38	33	33	41	40	46		39	37			35	34		
(GD3)62		26		15		39		25	10	21	16	17					30		25	26				28								
(GD3)65											17	23					29	34	27	29	38	38		44	34	34			24	25		
(GD3)86																																
(GD3)114																																
(GD3)154	17	17	14	14							15	21						30		26		28		38		33	43	44	25		66	68
(HA2)230																																
(HA2)281																																
(HA2)154																																
(HA2)165																																
(HA2)102											17	25							33		33	34			38			55		29		83
(HA2)129											17	24								27	57											
(HA2)247																																
(JE2)33																																
(JE3)88						28		13	11		13	16		37		16		16		15												
(JE3)89															17					17												
(JE3)90	12		9	8	30	32	24		10	6	12	16	39	39	17	18	21	21	17	19	20		21		26			36				
(JE3)184																		40		34												
(JE3)188												21																				
(JE3)189																													35			
(JE3)190																		37		34												

TABLE 2.12. METRIC MEASUREMENTS (MM) FOR NONADULT INDIVIDUALS (CONT.).

Skeleton	Sphenoidal left lesser wing length	Sphenoidal right lesser wing length	Sphenoidal left lesser wing width	Sphenoidal right lesser wing width	Sphenoidal left greater wing length	Sphenoidal right greater wing length	Sphenoidal left greater wing width	Sphenoid right greater wing width	Sphenoidal body length	Sphenoidal body width	Basilar length	Basilar width	Left petrous length	Right petrous length	Left petrous width	Right petrous width	Left zygomatic length	Right zygomatic length	Left zygomatic width	Right zygomatic width	Left maxillary length	Right maxillary length	Left maxillary height	Right maxillary height	Left maxillary width	Right maxillary width	Left mandibular length	Right mandibular length	Left mandibular width	Right mandibular width	Left mandibular full length	Right mandibular full length
(JF2)91																																
(JF2)75											15	20																				
(JF2)88											16	22					32		30													
(JG2)35																17																
(JG2)65																																
(JG2)251											16	23																				
(JG2)67																																
(JG3)14																	38		33													
(JH3)80											19	26					27		30													
(JH3)90																																
(JH3)99																																
(JH3)140																																
(JH3)74																																
(JH3)142																																
(JH3)136																																
(JH4)3																																
(JH4)52																	35		31													
(JH4)56																																
(JH4)22											15																					

TABLE 2.12. METRIC MEASUREMENTS (MM) FOR NONADULT INDIVIDUALS (CONT.).

Skeleton	Left scapular length	Right scapular length	Left scapular width	Right scapular width	Left scapular spine	Right scapular spine	Left clavicular length	Right clavicular length	Left clavicular midshaft diameter	Right clavicular midshaft diameter	Left iliac length	Right iliac length	Left iliac width	Right iliac width	Left ischial length	Right ischial length	Left ischial width	Right ischial width	Left pubic length	Right pubic length	Left humeral length	Right humeral length	Left humeral distal width	Right humeral distal width	Left humeral midshaft diameter	Right humeral midshaft diameter	Left ulnar length	Right ulnar length	Left ulnar midshaft diameter	Right ulnar midshaft diameter	Left radial length	Right radial length
(1058)8							95	93	8	9	98	100	85	82								203		38		13						
(1059)8							112	110	10	10	104	107	99				45	44	51	49	235		41		17		212		13		183	
(1084)8									4												78		7		19							
(1096)7			37					60		5	52													22		8		84		6		74
(1097)7										6				63			28	26											9			
(GD3)26							53		5																	6	68		4	4		
(GD3)30	73			45		62	85	84	6	6	75	74	72	72	47	46	29	31	37	37	166		32	31	10		142		8		130	
(GD3)62															25	24		17			83		20	19	7				5			
(GD3)65		54		38		46	61	63	5	5	58	59	56	55	31	31	21	22	27	26	109	109	23	22	9	9	96	95	6	5	84	84
(GD3)86	129	130	93	90	112	112	123	122	12	11		127										286	52	53	17	19		257		12		230
(GD3)114		91	62	60		74		89		7	96	95	82	85							182	186	36	36	13	12	156	158	9	9	138	140
(GD3)154	47	46	38	37	44		53	52	4	5	48	48	43			22	19	18	24	23	94	94		23	10	10		84		6	73	73
(HA2)230							118		11	11	121	121							56	57												
(HA2)281								45	4	3												67		17		6					54	
(HA2)154								93		7					49		38	35	35	34	180	182	34		12	12	156	156	9	9	139	140
(HA2)165							110		10													230	44	43	15	15		206	11	11		185
(HA2)102								73	7	6	68	68	62	64																		
(HA2)129							62		5												109				10						85	
(HA2)247							132	137		11											305				20		265		14			
(JE2)33							146	145		11													58	59								
(JE3)88												33	28	30	18	18	12	12	15	15	64		16	17	6					4		55
(JE3)89										4																				4		
(JE3)90		33		28		30	44		4	4														18	6	6						54
(JE3)184											86								48			203		38		14				11		
(JE3)188																																
(JE3)189									8									41		48			35									
(JE3)190										8										39			33								138	
(JF2)91								98		8			99	100	60	59				45	215	215	35		13	14		181		10	164	167

TABLE 2.12. METRIC MEASUREMENTS (MM) FOR NONADULT INDIVIDUALS (CONT.).

Skeleton	Left scapular length	Right scapular length	Left scapular width	Right scapular width	Left scapular spine	Right scapular spine	Left clavicular length	Right clavicular length	Left clavicular midshaft diameter	Right clavicular midshaft diameter	Left iliac length	Right iliac length	Left iliac width	Right iliac width	Left ischial length	Right ischial length	Left ischial width	Right ischial width	Left pubic length	Right pubic length	Left humeral length	Right humeral length	Left humeral distal width	Right humeral distal width	Left humeral midshaft diameter	Right humeral midshaft diameter	Left ulnar length	Right ulnar length	Left ulnar midshaft diameter	Right ulnar midshaft diameter	Left radial length	Right radial length
(JF2)75										6																						
(JF2)88										7																						
(JG2)35										5							17			23			20		8				5			
(JG2)65										6																						
(JG2)251									5	5															10		101		7		90	
(JG2)67																																
(JG3)14									6	6						54	43	41		46		214		38		13	177	180	10	10		159
(JH3)80																38		25	32					29		10	118	117	8	8		107
(JH3)90																			47					38	13			184	10			
(JH3)99									6																9			125	8			
(JH3)140																																
(JH3)74									10	10														55		17			13	13		
(JH3)142																																
(JH3)136							101		8	8		99		87			36				209		37		14	13			10		167	
(JH4)3																																
(JH4)52								85		7									36	36				36		13		152		10		135
(JH4)56										9									51	51		239		41		15		201	10	9		185
(JH4)22				37													20					103		23		9		91		5	81	82

TABLE 2.12. METRIC MEASUREMENTS (MM) FOR NONADULT INDIVIDUALS (CONT.).

Skeleton	Left radial midshaft diameter	Right radial midshaft diameter	Left femoral length	Right femoral length	Left femoral distal width	Right femoral distal width	Left femoral midshaft diameter	Right femoral midshaft diameter	Left tibial length	Right tibial length	Left tibial midshaft diameter	Right tibial midshaft diameter	Left fibular length	Right fibular length	Left fibular midshaft diameter	Right fibular midshaft diameter
(1058)8						53		18								
(1059)8	12			337	51			19							10	
(1084)8																
(1096)7		5														
(1097)7			189	186			13	13	156	155	14	13			7	7
(GD3)26		4				21		7			8	8			4	4
(GD3)30	7	7	224	226	45	44	12	12	192	194	14	14	185		6	7
(GD3)62							8		78		7		79		4	
(GD3)65	6	6	142	141	27	28	10	10	119	119	9	9	113	113	5	5
(GD3)86		13		402	67	68	25	24	347	350	27	25	332	335	11	11
(GD3)114	8	9	264		52	55	16	17	217		16		210		10	10
(GD3)154	6	7	115	116	26		10	9	98	98	9	9				5
(HA2)230																
(HA2)281	4		78		20		7			68		7				
(HA2)154	8	9	250	250		50	15	15		217		17	207		8	
(HA2)165	9	10											276		10	
(HA2)102		8	185				14		157		14	13			6	6
(HA2)129	6															
(HA2)247			442		65	67	27		351	369	26				14	16
(JE2)33		14				73		25								
(JE3)88		3		74		17	7	7			7	7			4	
(JE3)89						18		7				7			4	4
(JE3)90		4					6				6				4	4
(JE3)184		10						18			20	20				
(JE3)188																
(JE3)189							18	18		240		19			10	
(JE3)190	9						15									
(JF2)91	9	9			52	53		18	264		19	19			9	9
(JF2)75																
(JF2)88				135		31		10	116		9					4
(JG2)35		5						8							5	
(JG2)65												10				6
(JG2)251	7		151		33		12	12			12					
(JG2)67												7			4	4
(JG3)14	9	9									18	18		244	10	10
(JH3)80	6	6	172		40		10	11		147	11	12	143		6	5
(JH3)90		10			52											
(JH3)99				185			13	13								
(JH3)140												12				
(JH3)74	12	13													14	
(JH3)142	9											19				10
(JH3)136	10	9			54						18				10	10
(JH4)3	9	9														
(JH4)52		10	243		52		16	16			16		205		8	8
(JH4)56	11	11		345		54		23							10	10
(JH4)22	6	6	133				10	11	112	112	9	9				

TABLE 2.13. THE RANGE AND MEAN VALUES FOR CRANIAL AND MANDIBULAR MEASUREMENTS (MM) IN FEMALES AND MALES. VALUES IN BRACKETS INDICATE THE NUMBER OF SKELETAL ELEMENTS MEASURED.

Cranial Measurement	Female			Male	
	Range	Mean		Range	Mean
Maximum cranial length	170-182 (4)	177		177-194 (5)	186
Maximum cranial breadth	125-132 (4)	127		122-140 (6)	132
Bizygomatic diameter	115 (1)	-		(0)	-
Basion-bregma height	126-132 (3)	129		133-137 (2)	135
Cranial base length	97-139 (3)	111		106-112 (2)	109
Basion-prosthion length	91-95 (2)	93		101 (1)	-
Maxillo-alveolar breadth	60-63 (2)	62		60-65 (2)	63
Maxillo-alveolar length	51-54 (2)	53		52-59 (3)	56
Biauricular breadth	111-122 (3)	115		122-124 (3)	123
Upper facial height	65-69 (2)	67		68 (2)	68
Minimum frontal breadth	88-104 (6)	94		90-105 (10)	96
Upper facial breadth	95-107 (5)	100		98-110 (8)	104
Nasal height	46-48 (2)	47		50 (1)	-
Nasal breadth	23-24 (2)	24		20-27 (2)	24
Orbital breadth	41 (1)	-		38-40 (2)	39
Orbital height	32-36 (3)	34		30-32 (2)	31
Biorbital breadth	107 (1)	-		97-98 (2)	98
Interorbital breadth	20-27 (3)	23		22-27 (4)	26
Frontal chord	103-113 (6)	107		102-117 (8)	110
Parietal chord	107-118 (6)	112		103-157 (8)	124
Occipital chord	93-100 (4)	96		91-107 (6)	98

TABLE 2.13. THE RANGE AND MEAN VALUES FOR CRANIAL AND MANDIBULAR MEASUREMENTS (MM) IN FEMALES AND MALES (CONT.).

Cranial Measurement	Female			Male	
	Range	Mean		Range	Mean
Foramen magnum length	35-37 (3)	36		37-39 (2)	38
Foramen magnum breadth	26-33 (3)	29		31-32 (2)	32
Mastoid length	27-41 (14)	32		21-42 (20)	32
Chin height	22-33 (13)	28		24-39 (16)	33
Height of mandibular body	19-33 (19)	28		28-35 (21)	32
Breadth of mandibular body	8-14 (19)	11		10-16 (22)	12
Bigonial width	84-95 (3)	89		95-101 (2)	98
Bicondylar breadth	108-111 (3)	109		113-121 (2)	117
Minimum ramus breadth	26-39 (20)	31		27-39 (21)	34
Maximum ramus breadth	36-52 (19)	42		40-52 (18)	46
Maximum ramus height	45-65 (20)	55		38-73 (19)	60

TABLE 2.14. THE RANGE AND MEAN VALUES FOR POSTCRANIAL MEASUREMENTS (MM) IN FEMALES AND MALES. VALUES IN BRACKETS INDICATE THE NUMBER OF SKELETAL ELEMENTS MEASURED.

Bone	Measurement	Female		Male	
		Range	Mean	Range	Mean
Clavicle	Maximum length	127-149 (12)	139	129-168 (19)	146
	Anterior-posterior diameter at midshaft	8-12 (21)	10	10-15 (23)	13
	Superior-inferior diameter at midshaft	7-11 (21)	9	8-14 (23)	11
Scapula	Height	133-142 (2)	138	149-158 (2)	154
	Breadth	104-107 (2)	106	92-110 (3)	102
Humerus	Maximum length	295-319 (12)	308	295-356 (13)	320
	Epicondylar breadth	52-62 (21)	55	56-67 (24)	62
	Vertical diameter of head	34-41 (14)	38	39-51 (19)	45
	Maximum diameter at midshaft	15-21 (18)	19	19-25 (21)	21
	Minimum diameter at midshaft	12-17 (18)	14	14-19 (21)	17
Radius	Maximum length	210-245 (10)	230	232-281 (15)	251
	Anterior-posterior diameter at midshaft	8-13 (20)	10	10-13 (22)	12
	Medial-lateral diameter at midshaft	11-14 (20)	12	13-18 (22)	15
Ulna	Maximum length	227-267 (10)	250	251-304 (15)	274
	Anterior-posterior diameter at midshaft	10-14 (18)	12	12-20 (25)	15
	Medial-lateral diameter at midshaft	9-15 (18)	12	12-20 (25)	14
	Physiological length	201-246 (13)	226	221-271 (17)	245
Sacrum	Anterior length	102-117 (3)	112	92-124 (9)	102
	Anterior superior breadth	105-119 (8)	111	88-124 (12)	103
	Maximum transverse diameter of base	38-54 (11)	47	43-59 (18)	51

TABLE 2.14. THE RANGE AND MEAN VALUES FOR POSTCRANIAL MEASUREMENTS (MM) IN FEMALES AND MALES (CONT.).

Bone	Measurement	Female		Male	
		Range	Mean	Range	Mean
Os coxa	Height	188 (1)	-	189-211 (6)	200
	Iliac breadth	129-149 (5)	139	134-162 (9)	149
	Pubis length	(0)	-	63-96 (10)	78
	Ischium length	74-81 (2)	78	68-95 (8)	82
Femur	Maximum length	388-445 (8)	419	406-478 (10)	441
	Bicondylar length	388-444 (8)	416	404-476 (10)	439
	Epicondylar breadth	69-77 (9)	73	71-87 (17)	79
	Maximum head diameter	37-42 (20)	39	40-50 (27)	45
	Anterior-posterior subtrochanteric diameter	18-26 (23)	23	20-32 (26)	26
	Medial-lateral subtrochanteric diameter	24-32 (23)	28	26-38 (26)	31
	Anterior-posterior midshaft diameter	23-31 (15)	26	26-37 (18)	30
	Medial-lateral midshaft diameter	20-26 (15)	24	22-35 (18)	26
Tibia	Length	313-401 (8)	361	348-410 (9)	382
	Maximum proximal epiphyseal breadth	62-72 (11)	67	64-85 (15)	75
	Maximum distal epiphyseal breadth	40-48 (16)	44	43-56 (20)	49
	Maximum diameter at the nutrient foramen	26-34 (17)	29	28-40 (18)	35
	Medial-lateral diameter at the nutrient foramen	17-23 (17)	20	11-28 (19)	23
Fibula	Maximum length	327-362 (3)	348	339-384 (4)	365
	Maximum diameter at the midshaft	11-14 (13)	13	13-17 (16)	15
Calcaneus	Maximum length	68-83 (15)	74	70-89 (23)	80
	Middle breadth	35-44 (14)	38	39-46 (20)	42

TABLE 2.14. THE RANGE AND MEAN VALUES FOR POSTCRANIAL MEASUREMENTS (MM) IN FEMALES AND MALES (CONT.).

Bone	Measurement	Female		Male	
		Range	Mean	Range	Mean
Second metacarpal	Midline length	57-67 (16)	63	58-75 (25)	66
Metatarsals	MT1 maximum length	52-67 (18)	61	59-73 (20)	65
	MT2 maximum length	67-80 (12)	73	69-85 (21)	78
	MT3 maximum length	63-74 (12)	69	67-78 (16)	72
	MT4 maximum length	61-72 (15)	67	65-80 (16)	72

TABLE 2.15. STATURE REGRESSION FORMULAE (IN CM) USED TO ESTIMATE STATURE IN ADULTS FROM KAWA (PRODUCED USING ANCIENT EGYPTIAN POPULATIONS BY RAXTER *ET AL*. 2008). $_M$ = MAXIMUM LENGTH.

Sex	Skeletal element	Formula	Standard error
Male	$Femur_m$	$2.257(femur_m) + 63.93$	+/- 3.218
	$Tibia_m$	$2.554(tibia_m) + 69.21$	+/- 3.002
	$Femur_m + tibia_m$	$1.282(femur_m + tibia_m) + 59.35$	+/- 2.851
	$Humerus_m$	$2.594(humerus_m) + 83.85$	+/- 4.218
	$Radius_m$	$2.641(radius_m) + 100.91$	+/- 3.731
	$Humerus_m + radius_m$	$1.456(humerus_m + radius_m) + 83.76$	+/- 3.353
Female	$Femur_m$	$2.340(femur_m) + 56.99$	+/- 2.517
	$Tibia_m$	$2.699(tibia_m) + 61.08$	+/- 1.921
	$Femur_m + tibia_m$	$1.313(femur_m + tibia_m) + 54.36$	+/- 1.968
	$Humerus_m$	$2.827(humerus_m) + 70.94$	+/- 2.732
	$Radius_m$	$2.509(radius_m) + 96.73$	+/- 4.057
	$Humerus_m + radius_m$	$1.291(humerus_m + radius_m) + 86.41$	+/- 3.247

TABLE 2.16. STATURE ESTIMATES (CM) FOR INDIVIDUALS WITH FEMORAL, TIBIAL, HUMERAL, OR RADIAL MEASUREMENTS ($_M$ = MAXIMUM LENGTH). THE BONE MEASUREMENTS USED TO CALCULATE STATURE FOR EACH INDIVIDUAL ARE HIGHLIGHTED IN BOLD, PREFERENTIALLY USING THE BONE MEASUREMENT RELATED TO THE EQUATION WITH THE SMALLEST STANDARD ERROR.

Skeleton	Skeletal sex		Long bone length (cm)					Stature (+/- standard error)
			$Femur_m$	$Tibia_m$	$Humerus_m$	$Radius_m$		
(GD3)61	Female		-	-	**29.5**	-		154.3 (+/- 2.7)
(GD3)146	Female		42.9	**37.2**	30	23.2		161.5 (+/- 1.9)
(GD3)152	Female		43	**36.8**	31.3	24.4		160.4 (+/- 1.9)
(HA2)195	Female		**41.1**	-	-	-		153.2 (+/- 2.5)
(HA2)265	Female		40.8	**33.3**	-	21.1		151.0(+/- 1.9)
(HA2)198	Female		44.5	**38.1**	31.8	24.1		163.9 (+/- 1.9)
(HA2)172	Female		39.7	**34.9**	29.6	22.7		155.3 (+/- 1.9)
(JG3)13	Female		-	**-**	-	**23**		154.4 (+/- 4.1)
(561)21	Female?		-	**40.1**	-	-		169.3 (+/- 1.9)
(1075)16	Female?		-	-	**30.2**	-		156.3 (+/- 2.7)
(HA2)142	Female?		38.8	**31.3**	-	21		145.6 (+/- 1.9)
(HA2)164	Female?		-	**37.4**	31.2	24.1		162.0 (+/- 1.9)
(HA2)168	Female?		-	**-**	-	22.3		152.7 (+/- 4.1)
(JE3)185	Female?		-	-	**31.7**	-		160.6 (+/- 2.7)
(JH3)126	Female?		-	-	**31**	-		158.6 (+/- 2.7)
(JH3)123	Female?			-	**31.9**	24.5		161.1 (+/- 2.7)
(JH3)133	Female?		**44.3**	-	31.1	-		160.7 (+/- 2.5)
(JH4)50	Female?		-	-	**30.7**	-		157.7 (+/- 2.7)
(561)24	Male		**44.4**	-	32.8	25		164.1 (+/- 3.2)
(561)25	Male		-	**41**	-	-		173.9 (+/- 3.0)
(1052)3	Male		-	**38.4**	-	24.6		167.3 (+/- 3.0)
(GD3)69	Male		-	**36.4**		-		162.2 (+/- 3.0)
(GD3)106	Male		**40.6**	**34.8**	29.6	23.2		156.0 (+/- 2.9)
(GD3)81	Male		**47.2**	**38.9**	33	26.1		169.7 (+/- 2.9)
(GD3)132	Male		**47.8**	**38.2**	34.3	25.7		169.6 (+/- 2.9)
(HA2)209	Male		-	-	**32.9**	**27**		171.0 (+/- 3.4)
(HA2)259	Male		-	-	**31.5**	**24.7**		165.6 (+/- 3.4)
(HA2)169	Male		**41.1**	-	-	-		156.7 (+/- 3.2)
(HA2)124	Male		**46.8**	**39.5**	31.9	25.8		170.0 (+/- 2.9)
(HA2)193	Male		**43**	-	31.2	24.2		161.0 (+/- 3.2)
(JE3)186	Male		-	-	**31.8**	-		166.3 (+/- 4.2)
(JG2)215	Male		**45.8**	**39.9**	-	-		169.2 (+/- 2.9)
(JG2)312	Male		-	-	**35.6**	**28.1**		176.5 (+/- 3.4)
(JG2)313	Male		-	-	**30.3**	**24.4**		163.4 (+/- 3.4)
(GD3)78	Male?		**42.1**	-	-	23.7		158.9 (+/- 3.2)
(GD3)127	Male?		**41.9**	**36.7**	29.5	23.2		160.1 (+/- 2.9)
(HA2)237	Male?		**-**	**-**	-	**25.6**		168.5 (+/- 3.7)
(HA2)255	Male?		**-**	**-**	-	**25.5**		168.3 (+/- 3.7)
(JH3)82	Male?		-	-	**31.4**	-		165.3 (+/- 4.2)
(1083)15	Undetermined		-	-	**30.7**	-		Female:157.7 (+/- 2.7) Male: 163.5 (+/- 4.2)
(JH3)125	Undetermined		-	-	**-**	**24.8**		Female: 159.0 (+/- 4.1) Male: 166.4 (+/- 3.7)
(JH4)55	Undetermined		-	-	**-**	**23.7**		Female: 156.2 (+/- 4.1) Male: 163.5 (+/- 3.7)
(JG2)314	Intermediate		-	-	**31.3**	-		Female: 159.4 (+/- 2.7) Male: 165.0 (+/- 4.2)
(JH4)19	Intermediate		-	-	**30.5**	**25.7**		Female: 159.0 (+/- 3.2) Male: 165.6 (+/- 3.4)

TABLE 2.17. THE PREVALENCE OF OSTEOARTHRITIS ON DIFFERENT JOINT SURFACES ACCORDING TO MALE AND FEMALE SEX GROUPS, YOUNG AND MIDDLE ADULT AGE GROUPS, AND IN ALL ADULTS (CALCULATED FOR ALL OBSERVABLE JOINT SURFACES WITH A COMPLETENESS OF 25% OR MORE).

Joint	Bone	Female		Male		Young adult		Middle adult		All adults	
		Left	Right	Left	Right	Left	Right	Left	Right	Left	Right
Temporomandibular joint	Temporal	5.3%	4.2%	10%	4.8%	0%	0%	9.1%	4.2%	8.2%	8.6%
		(1/19)	(1/24)	(2/20)	(1/21)	(0/16)	(0/19)	(2/22)	(1/24)	(4/49)	(5/58)
	Mandible	15%	20%	9.5%	15.8%	0%	0%	18.2%	27.3%	12.8%	19.1%
		(3/20)	(4/20)	(2/21)	(3/19)	(0/17)	(0/17)	(4/22)	(6/22)	(6/47)	(9/47)
Sternoclavicular joint	Clavicle	0%	5.3%	11.1%	16.7%	0%	12.5%	4.8%	9.5%	6.7%	11.4%
		(0/17)	(1/19)	(2/18)	(3/18)	(0/16)	(2/16)	(1/21)	(2/21)	(3/45)	(5/44)
	Sternum	0%	0%	0%	13.3%	0%	0%	0%	11.8%	2.9%	6.5%
		(0/11)	(0/11)	(0/17)	(2/15)	(0/13)	(0/12)	(0/18)	(2/17)	(1/34)	(2/31)
Acromioclavicular joint	Clavicle	33.3%	20%	60%	50%	14.3%	9.1%	63.6%	40.9%	47.8%	35.7%
		(5/15)	(3/15)	(12/20)	(9/18)	(2/14)	(1/11)	(14/22)	(9/22)	(22/46)	(15/42)
	Scapula	0%	10.5%	50%	44.4%	7.1%	0%	43.5%	45.5%	31.1%	25%
		(0/16)	(2/19)	(11/22)	(8/18)	(1/14)	(0/18)	(10/23)	(10/22)	(14/45)	(12/48)
Glenohumeral joint	Scapula	13.6%	15.4%	21.7%	20.8%	4.8%	4.5%	20%	13.8%	15.5%	17.2%
		(3/22)	(4/26)	(5/23)	(5/24)	(1/21)	(1/22)	(5/25)	(4/29)	(9/58)	(11/64)
	Humerus	9.5%	4.2%	9.5%	8.7%	6.3%	0%	7.1%	7.4%	7.5%	5.1%
		(2/21)	(1/24)	(2/21)	(2/23)	(1/16)	(0/22)	(2/28)	(2/27)	(4/53)	(3/59)
Humeroradial joint	Humerus	0%	0%	0%	0%	0%	0%	0%	0%	0%	0%
		(0/19)	(0/20)	(0/22)	(0/22)	(0/20)	(0/17)	(0/24)	(0/26)	(0/50)	(0/52)
	Radius	0%	0%	0%	0%	0%	0%	0%	4%	0%	1.7%
		(0/19)	(0/24)	(0/23)	(0/23)	(0/21)	(0/21)	(0/25)	(1/25)	(0/57)	(1/58)
Humeroulnar joint	Humerus	0%	4.2%	8.7%	0%	0%	0%	7.7%	0%	3.6%	0%
		(0/20)	(1/24)	(2/23)	(0/23)	(0/21)	(0/22)	(2/26)	(0/28)	(2/56)	(0/59)
	Ulna	4.2%	0%	8.3%	4%	0%	0%	7.1%	0%	4.7%	1.6%
		(1/24)	(0/23)	(2/24)	(1/25)	(0/23)	(0/21)	(2/28)	(0/28)	(3/64)	(1/62)
Proximal radioulnar joint	Radius	0%	5.3%	0%	0%	0%	0%	0%	4.3%	0%	2.2%
		(0/17)	(1/19)	(0/20)	(0/18)	(0/17)	(0/15)	(0/22)	(1/23)	(0/47)	(1/46)
	Ulna	0%	0%	0%	0%	0%	0%	0%	0%	0%	0%
		(0/22)	(0/19)	(0/21)	(0/23)	(0/22)	(0/15)	(0/27)	(0/28)	(0/58)	(0/53)
Distal radioulnar joint	Radius	0%	0%	0%	0%	0%	0%	0%	0%	0%	0%
		(0/14)	(0/19)	(0/21)	(0/24)	(0/15)	(0/19)	(0/22)	(0/25)	(0/45)	(0/50)
	Ulna	0%	5.6%	11.8%	8.7%	0%	0%	9.5%	9.1%	5%	6.3%
		(0/15)	(1/18)	(2/17)	(2/23)	(0/14)	(0/17)	(2/21)	(2/22)	(2/40)	(3/48)
Radioscaphoid joint	Radius	0%	0%	0%	0%	0%	0%	0%	0%	0%	0%
		(0/17)	(0/21)	(0/20)	(0/25)	(0/17)	(0/21)	(0/24)	(0/26)	(0/49)	(0/54)
Radiolunate joint	Radius	0%	0%	0%	0%	0%	0%	0%	0%	0%	0%
		(0/17)	(0/21)	(0/23)	(0/25)	(0/17)	(0/18)	(0/26)	(0/25)	(0/51)	(0/50)
Femoroacetabular joint	Os coxa	18.2%	21.7%	12.5%	26.9%	9.1%	9.1%	19.2%	28%	17.9%	22.8%
		(4/22)	(5/23)	(3/24)	(7/26)	(2/22)	(2/22)	(5/26)	(7/25)	(10/56)	(13/57)
	Femur	4.3%	11.1%	4%	4%	0%	0%	6.9%	10.7%	4.8%	6.3%
		(1/23)	(3/27)	(1/25)	(1/25)	(0/20)	(0/26)	(2/29)	(3/28)	(3/62)	(4/64)
Patellofemoral joint	Femur	5%	4.2%	4.8%	10%	0%	0%	8%	7.7%	4%	5.7%
		(1/20)	(1/24)	(1/21)	(2/20)	(0/16)	(0/19)	(2/25)	(2/26)	(2/50)	(3/53)
	Patella	18.2%	27.8%	13.6%	28%	4.3%	5.6%	23.1%	32.1%	15.5%	26.3%
		(4/22)	(5/18)	(3/22)	(7/25)	(1/23)	(1/18)	(6/26)	(9/28)	(9/58)	(15/57)

TABLE 2.17. THE PREVALENCE OF OSTEOARTHRITIS ON DIFFERENT JOINT SURFACES (CONT.).

Joint	Bone	Female		Male		Young adult		Middle adult		All adults	
		Left	Right	Left	Right	Left	Right	Left	Right	Left	Right
Medial tibiofemoral joint	Femur	4.5%	4.2%	4.2%	18.2%	5.3%	5%	3.6%	11.1%	5.4%	12.1%
		(1/22)	(1/24)	(1/24)	(4/22)	(1/19)	(1/20)	(1/28)	(3/27)	(3/56)	(7/68)
	Tibia	5%	0%	4%	13.6%	0%	0%	8%	8.7%	3.8%	6.1%
		(1/20)	(0/17)	(1/25)	(3/22)	(0/20)	(0/19)	(2/25)	(2/23)	(2/52)	(3/49)
Lateral tibiofemoral joint	Femur	10%	4.5%	8.7%	7.7%	5.9%	0%	14.8%	10.7%	9.6%	6.8%
		(2/20)	(1/22)	(2/23)	(2/26)	(1/17)	(0/21)	(4/27)	(3/28)	(5/52)	(4/59)
	Tibia	11.1%	5.9%	4.2%	9.1%	5.6%	5.6%	8.7%	4.8%	5.8%	6.4%
		(2/18)	(1/13)	(1/24)	(2/22)	(1/18)	(1/18)	(2/23)	(1/21)	(3/52)	(3/47)
Proximal tibiofibular joint	Tibia	7.7%	0%	0%	5.3%	0%	0%	5.3%	0%	2.6%	2.8%
		(1/13)	(0/11)	(0/19)	(1/19)	(0/14)	(0/13)	(1/19)	(0/16)	(1/38)	(1/36)
	Fibula	0%	0%	0%	5%	0%	0%	0%	5%	0%	2.6%
		(0/11)	(0/13)	(0/12)	(1/20)	(0/12)	(0/14)	(0/14)	(1/20)	(0/28)	(1/38)
Talocrural joint	Tibia	4.2%	0%	0%	0%	4.3%	0%	0%	0%	2.6%	0%
		(1/24)	(0/22)	(0/24)	(0/23)	(1/23)	(0/21)	(0/25)	(0/25)	(1/57)	(0/56)
	Fibula	0%	0%	0%	4.2%	0%	0%	0%	3.8%	0%	1.7%
		(0/21)	(0/23)	(0/23)	(1/24)	(0/21)	(0/21)	(0/22)	(1/26)	(0/55)	(1/59)

TABLE 2.18. THE PREVALENCE OF VERTEBRAL PATHOLOGY IN ALL ADULTS, CONSISTING OF PREVALENCE RATES FOR OSTEOARTHRITIS, OSTEOPHYTES, VERTEBRAL FUSION, INTERVERTEBRAL DISC DISEASE, SCHMORL'S NODES AND OSSIFICATION OF THE LIGAMENTUM FLAVUM.

Vertebra	Osteoarthritis		Osteophytes	Fusion	Intervertebral disc disease	Schmorl's nodes	Ligamentum flavum ossification
	Articular facets	Atlantoaxial joint					
Occipital condyles	2%	-	-	0%	-	-	-
	(1/51)			(0/51)			
C1	0%	18.9%	-	0%	-	-	0%
	(0/55)	(10/53)		(0/55)			(0/43)
C2	14.5%	15%	11.7%	0%	0%	1.7%	0%
	(9/62)	(9/60)	(7/60)	(0/61)	(0/60)	(1/60)	(0/51)
C3	20.4%	-	22.2%	1.8%	11.5%	5.7%	2.4%
	(11/54)		(12/54)	(1/55)	(6/52)	(3/53)	(1/42)
C4	23.2%	-	33.3%	1.7%	25%	5.3%	2.1%
	(13/56)		(19/57)	(1/58)	(14/56)	(3/57)	(1/48)
C5	19.6%	-	48.3%	1.7%	32.2%	3.4%	6%
	(11/56)		(28/58)	(1/69)	(19/59)	(2/59)	(3/50)
C6	7.8%	-	43.4%	1.9%	34%	0%	4.2%
	(4/51)		(23/53)	(1/55)	(18/53)	(0/53)	(2/48)
C7	20.7%	-	30.9%	0%	17.9%	0%	5.5%
	(12/58)		(17/55)	(0/60)	(10/56)	(0/53)	(3/55)
T1	18.5%	-	3.6%	0%	0%	0%	34.6%
	(10/54)		(2/56)	(0/56)	(0/55)	(0/55)	(18/52)
T2	9.8%	-	8%	0%	1.9%	0%	49%
	(5/51)		(4/50)	(0/53)	(1/53)	(0/52)	(25/51)
T3	15.2%	-	23.3%	2.2%	4.4%	0%	59.5%
	(7/46)		(10/43)	(1/46)	(2/45)	(0/44)	(25/42)
T4	21.1%	-	32.5%	2.3%	5.1%	0%	71.1%
	(8/38)		(13/40)	(1/43)	(2/39)	(0/40)	(27/38)
T5	19.5%	-	24.4%	4.3%	9.1%	0%	73.2%
	(8/41)		(11/45)	(2/47)	(4/44)	(0/45)	(30/41)
T6	15%	-	23.3%	2.2%	9.5%	2.3%	81%
	(6/40)		(10/43)	(1/46)	(4/42)	(1/43)	(34/42)
T7	9.3%	-	41.3%	2.1%	6.7%	0%	88.6%
	(4/43)		(19/46)	(1/48)	(3/45)	(0/44)	(39/44)
T8	11.9%	-	50%	4.3%	13.6%	15.2%	85.4%
	(5/42)		(23/46)	(2/46)	(6/44)	(7/46)	(35/41)
T9	14%	-	46.7%	4.3%	10.6%	12.8%	83.7%
	(6/43)		(21/45)	(2/47)	(5/47)	(6/47)	(36/43)
T10	17.4%	-	46.5%	0%	9.3%	6.8%	85.7%
	(8/46)		(20/43)	(0/46)	(4/43)	(3/44)	(36/42)
T11	10.4%	-	47.8%	4.3%	21.7%	18.8%	86.4%
	(5/48)		(22/46)	(2/47)	(10/46)	(9/48)	(38/44)
T12	14.6%	-	38.3%	6%	13%	17%	77.8%
	(7/48)		(18/47)	(3/50)	(6/46)	(8/47)	(35/45)
L1	13.7%	-	27.7%	2.1%	2.2%	12.5%	66.7%
	(7/51)		(13/47)	(1/48)	(1/46)	(6/48)	(32/48)
L2	13.5%	-	42.6%	1.9%	16.7%	16%	47.9%
	(7/52)		(20/47)	(1/52)	(8/48)	(8/50)	(23/48)

TABLE 2.18. THE PREVALENCE OF VERTEBRAL PATHOLOGY IN ALL ADULTS (CONT.).

Vertebra	Osteoarthritis		Osteophytes	Fusion	Intervertebral disc disease	Schmorl's nodes	Ligamentum flavum ossification
	Articular facets	Atlantoaxial joint					
L3	15.7%	-	53.1%	2.1%	21.7%	25.5%	44.2%
	(8/51)		(26/49)	(1/48)	(10/46)	(12/47)	(19/43)
L4	15.1%	-	67.3%	2%	25.5%	12.5%	29.8%
	(8/53)		(33/49)	(1/51)	(12/47)	(6/48)	(14/47)
L5	17.5%	-	58.8%	3.8%	24%	6%	25.5%
	(10/57)		(30/51)	(2/53)	(12/50)	(3/50)	(12/47)
L6	33.3%	-	100%	0%	50%	0%	0%
	(1/3)		(2/2)	(0/2)	(1/2)	(0/2)	(0/3)
S1	9.3%	-	41.3%	1.8%	12.5%	2.1%	9.7%
	(4/43)		(19/46)	(1/56)	(6/48)	(1/48)	(3/31)

TABLE 2.19. A COMPARISON OF THE PREVALENCE OF VERTEBRAL PATHOLOGY IN YOUNG AND MIDDLE ADULTS, CONSISTING OF PREVALENCE RATES FOR OSTEOARTHRITIS, OSTEOPHYTES, VERTEBRAL FUSION, INTERVERTEBRAL DISC DISEASE, SCHMORL'S NODES, AND OSSIFICATION OF THE LIGAMENTUM FLAVUM.

Vertebra	Osteoarthritis				Osteophytes		Fusion		Intervertebral disc disease		Schmorl's nodes		Ligamentum flavum ossification	
	Articular facets		Atlantoaxial joint											
	Young adult	Middle adult	Young adult	Middle adult	Young adult	Middle adult	Young adult	Middle adult	Young adult	Middle adult	Young adult	Middle adult	Young adult	Middle adult
Occipital condyles	0%	4.8%	-	-	-	-	0%	0%	-	-	-	-	-	-
	(0/17)	(1/21)					(0/17)	(0/21)						
C1	0%	0%	11.1%	16%	-	-	0%	0%	-	-	-	-	0%	0%
	(0/19)	(0/26)	(2/18)	(4/25)			(0/19)	(0/26)					(0/17)	(0/24)
C2	4.8%	21.4%	10.5%	10.7%	0%	14.8%	9%	0%	0%	0%	5%	0%	0%	0%
	(1/21)	(6/28)	(2/19)	(3/28)	(0/20)	(4/27)	(9/21)	(0/27)	(0/20)	(0/27)	(1/20)	(0/27)	(0/17)	(0/19)
C3	5.3%	22.2%	-	-	9.5%	28%	0%	3.8%	10%	8%	4.8%	8%	0%	0%
	(1/19)	(6/27)			(2/21)	(7/25)	(0/21)	(1/26)	(2/20)	(2/25)	(1/21)	(2/25)	(0/14)	(0/24)
C4	5.3%	32%	-	-	15.8%	34.6%	0%	3.7%	16.7%	23.1%	5.3%	7.7%	0%	4.5%
	(1/19)	(8/25)			(3/19)	(9/26)	(0/19)	(1/27)	(3/18)	(6/26)	(1/19)	(2/26)	(0/15)	(1/22)
C5	10%	20.8%	-	-	15.8%	66.7%	0%	0%	15%	44.4%	0%	7.4%	0%	0%
	(2/20)	(5/24)			(3/19)	(18/27)	(0/20)	(0/27)	(3/20)	(12/27)	(0/20)	(2/27)	(0/16)	(0/23)
C6	0%	8%	-	-	12.5%	57.1%	0%	0%	12.5%	39.3%	0%	0%	0%	8.3%
	(0/16)	(2/25)			(2/16)	(16/28)	(0/16)	(0/28)	(2/16)	(11/28)	(0/16)	(0/28)	(0/13)	(2/24)
C7	10%	22.2%	-	-	17.6%	38.5%	0%	0%	5.9%	22.2%	0%	0%	5.6%	3.8%
	(2/20)	(6/27)			(3/17)	(10/26)	(0/20)	(0/28)	(1/17)	(6/27)	(0/17)	(0/25)	(1/18)	(1/26)
T1	15%	23.1%	-	-	0%	8%	0%	0%	0%	0%	0%	0%	44.4%	3.8%
	(3/20)	(6/26)			(0/21)	(2/25)	(0/21)	(0/25)	(0/20)	(0/24)	(0/19)	(0/25)	(8/18)	(1/26)
T2	0%	20%	-	-	5%	13%	0%	0%	5%	0%	0%	0%	40%	30.8%
	(0/19)	(5/25)			(1/20)	(3/23)	(0/21)	(0/25)	(1/20)	(0/25)	(0/20)	(0/25)	(8/20)	(8/26)
T3	12.5%	21.7%	-	-	20%	17.4%	6.3%	0%	13.3%	0%	0%	0%	57.1%	56%
	(2/16)	(5/23)			(3/15)	(4/23)	(1/16)	(0/24)	(2/15)	(0/24)	(0/15)	(0/24)	(8/14)	(14/25)
T4	20%	25%	-	-	25%	35%	5.9%	0%	0%	4.8%	0%	0%	85.7%	58.3%
	(3/15)	(5/20)			(4/16)	(7/20)	(1/17)	(0/22)	(0/14)	(1/21)	(0/14)	(0/22)	(12/14)	(14/24)
T5	5.9%	33.3%	-	-	5.6%	30.4%	5.3%	0%	0%	13%	0%	0%	81.3%	61.9%
	(1/17)	(7/21)			(1/18)	(7/23)	(1/19)	(0/24)	(0/18)	(3/23)	(0/18)	(0/23)	(13/16)	(13/21)

TABLE 2.19. A COMPARISON OF THE PREVALENCE OF VERTEBRAL PATHOLOGY IN YOUNG AND MIDDLE ADULTS (CONT.).

Vertebra	Osteoarthritis				Osteophytes		Fusion		Intervertebral disc disease		Schmorl's nodes		Ligamentum flavum ossification	
	Articular facets		Atlantoaxial joint											
	Young adult	Middle adult	Young adult	Middle adult	Young adult	Middle adult	Young adult	Middle adult	Young adult	Middle adult	Young adult	Middle adult	Young adult	Middle adult
T6	17.6%	10%	-	-	0%	34.8%	0%	0%	0%	19%	0%	4.8%	100%	66.7%
	(3/17)	(2/20)			(0/16)	(8/23)	(0/17)	(0/24)	(0/16)	(4/21)	(0/17)	(1/21)	(16/16)	(14/21)
T7	10%	10.5%	-	-	11.1%	59.1%	0%	4.3%	5.6%	9.5%	0%	0%	94.7%	63.6%
	(2/20)	(2/19)			(2/18)	(13/22)	(0/19)	(1/23)	(1/18)	(2/21)	(0/17)	(0/21)	(18/19)	(14/22)
T8	0%	23.8%	-	-	21.1%	72.7%	0%	4.5%	11.1%	14.3%	15.8%	14.3%	93.8%	80%
	(0/17)	(5/21)			(4/19)	(16/22)	(0/18)	(1/22)	(2/18)	(3/21)	(3/19)	(3/21)	(15/16)	(16/20)
T9	0%	27.3%	-	-	21.1%	66.7%	0%	4.5%	0%	18.2%	10%	13.6%	89.5%	75%
	(0/17)	(6/22)			(4/19)	(14/21)	(0/20)	(1/22)	(0/20)	(4/22)	(2/20)	(3/22)	(17/19)	(15/20)
T10	11.1%	26.1%	-	-	11.8%	66.7%	0%	0%	0%	14.3%	5.6%	9.5%	88.9%	77.3%
	(2/18)	(6/23)			(2/17)	(14/21)	(0/19)	(0/21)	(0/17)	(3/21)	(1/18)	(2/21)	(16/18)	(17/22)
T11	0%	20%	-	-	22.2%	72.7%	0%	4.5%	11.1%	36.4%	20%	22.7%	84.2%	80%
	(0/18)	(5/25)			(4/18)	(16/22)	(0/19)	(1/22)	(2/18)	(8/22)	(4/20)	(5/22)	(16/19)	(16/20)
T12	0%	27.3%	-	-	15%	55%	0%	9.5%	5%	20%	23.8%	15%	78.9%	90.5%
	(0/21)	(6/22)			(3/20)	(11/20)	(0/22)	(2/21)	(1/20)	(4/20)	(5/21)	(3/20)	(15/19)	(19/21)
L1	5%	20.8%	-	-	5.3%	47.6%	0%	4.8%	0%	5%	14.3%	15%	68.4%	75%
	(1/20)	(5/24)			(1/19)	(10/21)	(0/21)	(1/21)	(0/19)	(1/20)	(3/21)	(3/20)	(13/19)	(15/20)
L2	9.5%	9.1%	-	-	23.8%	65%	0%	0%	14.3%	25%	21.7%	15%	45%	63.6%
	(2/21)	(2/22)			(5/21)	(13/20)	(0/23)	(0/22)	(3/21)	(5/20)	(5/23)	(3/20)	(9/20)	(14/22)
L3	9.5%	13.6%	-	-	28.6%	71.4%	0%	0%	14.3%	35%	31.8%	25%	47.1%	47.6%
	(2/21)	(3/22)			(6/21)	(15/21)	(0/21)	(0/22)	(3/21)	(7/20)	(7/22)	(5/20)	(8/17)	(10/21)
L4	10.5%	11.5%	-	-	50%	82.6%	0%	4.2%	26.3%	26.1%	15%	13%	26.3%	40%
	(2/19)	(3/26)			(10/20)	(19/23)	(0/21)	(1/24)	(5/19)	(6/23)	(3/20)	(3/23)	(5/19)	(8/20)
L5	13%	20.8%	-	-	38.1%	78.3%	0%	8.7%	19%	31.8%	10%	4.5%	35.3%	29.2%
	(3/23)	(5/24)			(8/21)	(18/23)	(0/21)	(2/23)	(4/21)	(7/22)	(2/20)	(1/22)	(6/17)	(7/24)
L6	-	33.3%	-	-	-	100%	-	0%	-	50%	-	0%	-	17.4%
	(0/0)	(1/3)			(0/0)	(2/2)	(0/0)	(0/2)	(0/0)	(1/2)	(0/0)	(0/2)	(0/0)	(4/23)
S1	6.3%	13.6%	-	-	5.9%	54.2%	0%	3.6%	0%	24%	5.6%	0%	18.2%	0%
	(1/16)	(3/22)			(1/17)	(13/24)	(0/20)	(1/28)	(0/18)	(6/25)	(1/18)	(0/24)	(2/11)	(0/3)

TABLE 2.20. A COMPARISON OF THE PREVALENCE OF VERTEBRAL PATHOLOGY IN MALE AND FEMALE SEX GROUPS, CONSISTING OF PREVALENCE RATES FOR OSTEOARTHRITIS, OSTEOPHYTES, VERTEBRAL FUSION, INTERVERTEBRAL DISC DISEASE, SCHMORL'S NODES, AND OSSIFICATION OF THE LIGAMENTUM FLAVUM.

Vertebra	Osteoarthritis				Osteophytes		Fusion		Intervertebral disc disease		Schmorl's nodes		Ligamentum flavum ossification	
	Articular facets		Atlantoaxial joint											
	Female	Male	Female	Male	Female	Male	Female	Male	Female	Male	Female	Male	Female	Male
Occipital condyles	0%	0%	-	-	-	-	0%	0%	-	-	-	-	-	-
	(0/20)	(0/20)					(0/20)	(0/20)						
C1	0%	0%	22.7%	15%	-	-	0%	0%	-	-	-	-	0%	0%
	(0/21)	(0/21)	(5/22)	(3/20)			(0/21)	(0/21)					(0/17)	(0/19)
C2	4.3%	29.2%	13%	13%	4.5%	16.7%	0%	0%	0%	0%	0%	4.2%	0%	0%
	(1/23)	(7/24)	(3/23)	(3/23)	(1/22)	(4/24)	(0/23)	(0/24)	(0/22)	(0/24)	(0/22)	(1/24)	(0/20)	(0/22)
C3	10%	27.3%	-	-	14.3%	33.3%	0%	4.8%	4.8%	19%	0%	9.5%	0%	0%
	(2/20)	(6/22)			(3/21)	(7/21)	(0/22)	(1/21)	(1/21)	(4/21)	(0/21)	(2/21)	(0/16)	(0/18)
C4	21.1%	20.8%	-	-	25%	41.7%	0%	4.2%	26.3%	25%	0%	8.3%	0%	4.8%
	(4/19)	(5/24)			(5/20)	(10/24)	(0/21)	(1/24)	(5/19)	(6/24)	(0/20)	(2/24)	(0/16)	(1/21)
C5	15.8%	21.7%	-	-	28.6%	60.9%	0%	4.3%	18.2%	34.8%	0%	4.3%	0%	8.7%
	(3/19)	(5/23)			(6/21)	(14/23)	(0/22)	(1/23)	(4/22)	(8/23)	(0/22)	(1/23)	(0/16)	(2/23)
C6	5%	15%	-	-	30%	50%	0%	4.8%	25%	40%	0%	0%	0%	0%
	(1/20)	(3/20)			(6/20)	(10/20)	(0/21)	(1/21)	(5/20)	(8/20)	(0/20)	(0/20)	(0/18)	(0/20)
C7	9.5%	25%	-	-	10.5%	52.2%	0%	0%	5%	30.4%	0%	0%	5%	4.3%
	(2/21)	(6/24)			(2/19)	(12/23)	(0/22)	(0/24)	(1/20)	(7/23)	(0/18)	(0/23)	(1/20)	(1/23)
T1	10%	22.7%	-	-	5%	4.5%	0%	0%	0%	0%	0%	0%	36.8%	31.8%
	(2/20)	(5/22)			(1/20)	(1/22)	(0/20)	(0/22)	(0/20)	(0/22)	(0/19)	(0/22)	(7/19)	(7/22)
T2	20%	5%	-	-	5.6%	9.5%	0%	0%	0%	0%	0%	0%	33.3%	55%
	(4/20)	(1/20)			(1/18)	(2/21)	(0/20)	(0/22)	(0/19)	(0/23)	(0/19)	(0/22)	(7/21)	(11/20)
T3	11.8%	10.5%	-	-	21.4%	23.8%	6.3%	0%	6.7%	0%	0%	0%	43.8%	65%
	(2/17)	(2/19)			(3/14)	(5/21)	(1/16)	(0/21)	(1/15)	(0/22)	(0/15)	(0/21)	(7/16)	(13/20)
T4	7.7%	11.1%	-	-	38.5%	15.8%	6.7%	0%	0%	5.6%	0%	0%	58.3%	78.9%
	(1/13)	(2/18)			(5/13)	(3/19)	(1/15)	(0/20)	(0/13)	(1/18)	(0/13)	(0/19)	(7/12)	(15/19)
T5	18.8%	21.1%	-	-	18.8%	19%	5.9%	4.5%	6.3%	9.5%	0%	0%	60%	84.2%
	(3/16)	(4/19)			(3/16)	(4/21)	(1/17)	(1/22)	(1/16)	(2/21)	(0/16)	(0/21)	(9/15)	(16/19)

TABLE 2.20. A COMPARISON OF THE PREVALENCE OF VERTEBRAL PATHOLOGY IN MALE AND FEMALE SEX GROUPS (CONT.).

Vertebra	Osteoarthritis				Osteophytes		Fusion		Intervertebral disc disease		Schmorl's nodes		Ligamentum flavum ossification	
	Articular facets		Atlantoaxial joint											
	Female	Male	Female	Male	Female	Male	Female	Male	Female	Male	Female	Male	Female	Male
T6	23.5%	5.6%	-	-	13.3%	25%	0%	5%	7.1%	10%	0%	5%	82.4%	80%
	(4/17)	(1/18)			(2/15)	(5/20)	(0/17)	(1/20)	(1/14)	(2/20)	(0/15)	(1/20)	(14/17)	(16/20)
T7	11.8%	5%	-	-	40%	34.8%	0%	4.3%	7.1%	4.3%	0%	0%	94.1%	80.0%
	(2/17)	(1/20)			(6/15)	(8/23)	(0/16)	(1/23)	(1/14)	(1/23)	(0/13)	(0/23)	(16/17)	(16/20)
T8	6.7%	19%	-	-	46.7%	50%	0%	8.7%	15.4%	9.1%	7.7%	13%	76.9%	85.7%
	(1/15)	(4/21)			(7/15)	(11/22)	(0/14)	(2/23)	(2/13)	(2/22)	(1/13)	(3/23)	(10/13)	(18/21)
T9	6.7%	20%	-	-	33.3%	47.6%	0%	9.5%	6.3%	14.3%	0%	19%	87.5%	81.0%
	(1/15)	(4/20)			(5/15)	(10/21)	(0/16)	(2/21)	(1/16)	(3/21)	(0/16)	(4/21)	(14/16)	(17/21)
T10	13.3%	22.7%	-	-	46.2%	42.9%	0%	0%	0%	9.5%	0%	4.8%	78.6%	85.7%
	(2/15)	(5/22)			(6/13)	(9/21)	(0/14)	(0/22)	(0/13)	(2/21)	(0/14)	(1/21)	(11/14)	(18/21)
T11	0%	18.2%	-	-	50%	52.4%	0%	8.7%	26.7%	22.7%	6.7%	21.7%	86.7%	85.7%
	(0/18)	(4/22)			(8/16)	(11/21)	(0/15)	(2/23)	(4/15)	(5/22)	(1/15)	(5/23)	(13/15)	(18/21)
T12	5.9%	22.7%	-	-	33.3%	50%	0%	13%	6.7%	19%	0%	27.3%	62.5%	90%
	(1/17)	(5/22)			(5/15)	(11/22)	(0/16)	(3/23)	(1/15)	(4/21)	(0/15)	(6/22)	(10/16)	(18/20)
L1	5.6%	26.1%	-	-	6.7%	45.5%	0%	4.8%	0%	4.8%	0%	13.6%	41.2%	85.7%
	(1/18)	(6/23)			(1/15)	(10/22)	(0/17)	(1/21)	(0/15)	(1/21)	(0/16)	(3/22)	(7/17)	(18/21)
L2	15.8%	18.2%	-	-	31.3%	54.5%	0%	4.2%	18.8%	21.7%	6.3%	20.8%	33.3%	57.9%
	(3/19)	(4/22)			(5/16)	(12/22)	(0/18)	(1/24)	(3/16)	(5/23)	(1/16)	(5/24)	(6/18)	(11/19)
L3	11.1%	27.3%	-	-	56.3%	59.1%	0%	4.5%	26.7%	23.8%	20%	22.7%	29.4%	52.6%
	(2/18)	(6/22)			(9/16)	(13/22)	(0/17)	(1/22)	(4/15)	(5/21)	(3/15)	(5/22)	(5/17)	(10/19)
L4	10.5%	21.7%	-	-	68.8%	60.9%	0%	0%	20%	22.7%	0%	21.7%	12.5%	27.3%
	(2/19)	(5/23)			(11/16)	(14/23)	(0/17)	(0/25)	(3/15)	(5/22)	(0/15)	(5/23)	(2/16)	(6/22)
L5	19%	20.8%	-	-	58.8%	62.5%	0%	3.8%	25%	29.2%	0%	9.1%	16.7%	25%
	(4/21)	(5/24)			(10/17)	(15/24)	(0/18)	(1/26)	(4/16)	(7/24)	(0/18)	(2/22)	(3/18)	(5/20)
L6	-	50%	-	-	-	100%	-	0%	-	50%	-	0%	-	0%
	(0/0)	(1/2)			(0/0)	(2/2)	(0/0)	(0/2)	(0/0)	(1/2)	(0/0)	(0/2)	(0/0)	(0/2)
S1	6.7%	14.3%	-	-	41.2%	42.1%	0%	4.3%	11.8%	15.8%	0%	5.3%	20	5.9%
	(1/15)	(3/21)			(7/17)	(8/19)	(0/22)	(1/23)	(2/17)	(3/19)	(0/18)	(1/19)	(2/10)	(1/17)

TABLE 2.21. THE PREVALENCE OF SKULL FRACTURES WITH REMODELLING IN ADULTS (CALCULATED FOR ALL BONES WITH A COMPLETENESS OF OVER 25%).

Bone	Left	Right
Frontal	10.5%	
	(6/57)	
Parietal	5.3%	1.8%
	(3/57)	(1/56)
Occipital	0%	
	(0/59)	
Temporal	3.8%	0%
	(2/53)	(0/60)
Zygomatic	0%	0%
	(0/54)	(0/53)
Nasal	6.9%	3.2%
	(2/29)	(1/31)
Maxilla	0%	0%
	(0/44)	(0/41)
Mandible	0%	0%
	(0/60)	(0/57)

TABLE 2.22. THE PREVALENCE OF PATELLAE, HAND AND FOOT FRACTURES WITH REMODELLING IN ADULTS (CALCULATED FOR ALL BONES WITH A COMPLETENESS OF OVER 25%).

Hands	Left	Right		Patellae & feet	Left	Right
Scaphoid	0%	0%		Patellae	0%	0%
	(0/56)	(0/54)			(0/57)	(0/59)
Lunate	0%	0%		Talus	0%	0%
	(0/52)	(0/56)			(0/67)	(0/63)
Triquetral	0%	0%		Calcaneus	0%	0%
	(0/39)	(0/51)			(0/58)	(0/57)
Pisiform	0%	0%		Cuboid	0%	1.9%
	(0/43)	(0/49)			(0/54)	(1/53)
Trapezium	0%	0%		Navicular	0%	0%
	(0/51)	(0/51)			(0/55)	(0/49)
Trapezoid	0%	0%		Medial cuneiform	0%	0%
	(0/50)	(0/47)			(0/53)	(0/53)
Capitate	0%	0%		Intermediate cuneiform	0%	0%
	(0/55)	(0/59)			(0/52)	(0/52)
Hamate	0%	0%		Lateral cuneiform	0%	0%
	(0/51)	(0/57)			(0/53)	(0/54)
First metacarpal	0%	0%		First metatarsal	0%	0%
	(0/52)	(0/55)			(0/53)	(0/50)
Second metacarpal	1.6%	1.8%		Second metatarsal	1.9%	1.8%
	(1/61)	(1/56)			(1/53)	(1/56)
Third metacarpal	3.1%	1.7%		Third metatarsal	0%	0%
	(2/65)	(1/60)			(0/55)	(0/49)
Fourth metacarpal	3.4%	0%		Fourth metatarsal	0%	0%
	(2/58)	(0/57)			(0/50)	(0/51)
Fifth Metacarpal	1.8%	3.7%		Fifth metatarsal	0%	1.9%
	(1/55)	(2/54)			(0/58)	(1/54)
Proximal phalanges	2%			Proximal phalanges	2.4%	
	(12/594)				(12/506)	
Intermediate phalanges	1.6%			Intermediate phalanges	1.8%	
	(7/432)				(5/281)	
Distal phalanges	0.7%			Distal phalanges	1.5%	
	(3/442)				(5/331)	

TABLE 2.23. THE PREVALENCE OF LONG BONE FRACTURES WITH REMODELLING IN ADULTS (CALCULATED FOR ALL BONE SECTIONS WITH A COMPLETENESS OF OVER 25%).

Bone	Left						Right				
	Proximal epiphysis	Proximal shaft	Middle shaft	Distal shaft	Distal epiphysis		Proximal epiphysis	Proximal shaft	Middle shaft	Distal shaft	Distal epiphysis
Clavicle	0%	1.9%	0%	0%	0%		0%	0%	0%	0%	0%
	(0/48)	(1/54)	(0/58)	(0/63)	(0/47)		(0/45)	(0/55)	(0/57)	(0/58)	(0/46)
Humerus	0%	0%	1.7%	0%	0%		0%	0%	0%	0%	0%
	(0/53)	(0/55)	(1/60)	(0/58)	(0/57)		(0/60)	(0/54)	(0/62)	(0/59)	(0/60)
Radius	0%	0%	0%	0%	0%		0%	0%	0%	0%	0%
	(0/54)	(0/60)	(0/61)	(0/59)	(0/53)		(0/58)	(0/62)	(0/61)	(0/54)	(0/53)
Ulna	1.6%	0%	0%	1.8%	0%		0%	0%	0%	0%	1.9%%
	(1/64)	(0/65)	(0/65)	(1/57)	(0/41)		(0/65)	(0/61)	(0/64)	(0/58)	(1/53)
Femur	0%	0%	0%	0%	0%		0%	0%	0%	0%	0%
	(0/67)	(0/64)	(0/66)	(0/54)	(0/58)		(0/64)	(0/65)	(0/67)	(0/60)	(0/63)
Tibia	0%	1.9%	0%	1.9%	0%		2.1%	0%	0%	1.9%	0%
	(0/52)	(1/52)	(0/61)	(1/54)	(0/56)		(1/47)	(0/47)	(0/46)	(1/52)	(0/59)
Fibula	3.1%	3.4%	0%	0%	0%		0%	0%	1.6%	0%	0%
	(1/32)	(2/58)	(0/62)	(0/61)	(0/56)		(0/37)	(0/63)	(1/61)	(0/65)	(0/62)

TABLE 2.24. THE PREVALENCE OF POST-CRANIAL AXIAL SKELETAL FRACTURES WITH REMODELLING IN ADULTS (CALCULATED FOR ALL BONES WITH A COMPLETENESS OF OVER 25%).

Bone	Left	Right
Manubrium	0%	
	(0/30)	
Sternal body	9.1%	
	(3/33)	
Scapula	0%	0%
	(0/50)	(0/56)
Ilium	0%	0%
	(0/50)	(0/51)
Ischium	0%	0%
	(0/54)	(0/53)
Pubis	0%	0%
	(0/35)	(0/36)

TABLE 2.25. THE PREVALENCE OF PERIOSTEAL REACTION ON LONG BONES IN ADULTS (CALCULATED FOR ALL BONE SECTIONS WITH A COMPLETENESS OF OVER 25%).

Bone	Left				Right		
	Proximal shaft	Middle shaft	Distal shaft		Proximal shaft	Middle shaft	Distal shaft
Clavicle	0%	0%	0%		0%	0%	0%
	(0/54)	(0/58)	(0/63)		(0/55)	(0/57)	(0/58)
Humerus	0%	0%	0%		0%	0%	0%
	(0/55)	(0/60)	(0/58)		(0/54)	(0/62)	(0/59)
Radius	0%	0%	1.7%		0%	0%	0%
	(0/60)	(0/61)	(1/59)		(0/62)	(0/61)	(0/54)
Ulna	0%	0%	1.8%		0%	0%	0%
	(0/65)	(0/65)	(1/57)		(0/61)	(0/64)	(0/58)
Femur	1.6%	1.5%	1.9%		0%	1.5%	3.3%
	(1/64)	(1/66)	(1/54)		(0/65)	(1/67)	(2/60)
Tibia	5.8%	13.1%	9.3%		8.5%	16.4%	7.7%
	(3/52)	(8/61)	(5/54)		(4/47)	(9/46)	(4/52)
Fibula	1.7%	14.5%	11.5%		0%	8.2%	7.7%
	(1/58)	(9/62)	(7/61)		(0/63)	(5/61)	(5/65)

TABLE 2.26. THE PREVALENCE OF PERIOSTEAL REACTION ON LONG BONES IN NONADULTS (CALCULATED FOR ALL BONE SECTIONS WITH A COMPLETENESS OF OVER 25%).

Bone	Left				Right		
	Proximal shaft	Middle shaft	Distal shaft		Proximal shaft	Middle shaft	Distal shaft
Clavicle	0%	0%	0%		2.8%	2.5%	2.6%
	(0/35	(0/39)	(0/39)		(1/36)	(1/40)	(1/39)
Humerus	0%	2.9%	2.9%		0%	0%	0%
	(0/35)	(1/34)	(1/35)		(0/36)	(0/37)	(0/40)
Radius	0%	0%	2.8%		0%	0%	0%
	(0/36)	(0/36)	(1/36)		(0/38)	(0/41)	(0/36)
Ulna	0%	0%	0%		0%	0%	0%
	(0/37)	(0/35)	(0/33)		(0/42)	(0/40)	(0/39)
Femur	4.7%	5%	0%		5%	7.9%	2.8%
	(2/43)	(2/40)	(0/38)		(2/40)	(3/38)	(1/36)
Tibia	2.7%	5.3%	0%		2.6%	7.1%	2.6%
	(1/37)	(2/38)	(0/38)		(1/39)	(3/42)	(1/38)
Fibula	0%	0%	0%		2.8%	2.4%	2.6%
	(0/39)	(0/43)	(0/39)		(1/36)	(1/41)	(1/38)

TABLE 2.27, THE PREVALENCE OF ENDOCRANIAL AND ECTOCRANIAL LESIONS IN ADULTS (CALCULATED FOR ALL BONES WITH A COMPLETENESS OF OVER 25%).

Bone	Endocranial			Ectocranial	
	Left	Right		Left	Right
Frontal	5.3%			7%	
	(3/57)			(4/57)	
Parietal	0%	0%		15.8%	16.1%
	(0/57)	(0/56)		(9/57)	(9/56)
Occipital	3.4%			16.9%	
	(2/59)			(10/59)	
Temporal	1.9%	1.7%		0%	0%
	(1/53)	(1/60)		(0/53)	(0/60)

TABLE 2.28, THE PREVALENCE OF ENDOCRANIAL AND ECTOCRANIAL LESIONS IN NONADULTS (CALCULATED FOR ALL BONES WITH A COMPLETENESS OF OVER 25%).

Bone	Endocranial			Ectocranial	
	Left	Right		Left	Right
Frontal	9.4%			3.1%	
	(3/32)			(1/32)	
Parietal	3.2%	3.6%		6.5%	7.1%
	(1/31)	(1/28)		(2/31)	(2/28)
Occipital	11.8%			2.9%	
	(4/34)			(1/34)	
Temporal	0%	0%		0%	0%
	(0/37)	(0/37)		(0/37)	(0/37)
Maxilla	-	-		12%	11.1%
				(3/25)	(3/27)
Mandible	-	-		6.1%	5.4%
				(2/33)	(2/37)

TABLE 2.29. THE PROPORTION OF TEETH IN DIFFERENT TOOTH PRESENCE CATEGORIES IN NON-ADULTS, ACCORDING TO AGE GROUP AND TOOTH TYPE (DECIDUOUS OR PERMANENT).

Category		Tooth type	Age group					
			Fullterm	Infancy	Early childhood	Late childhood	Puberty	Adolescence
Present	1 (Non-occluded)	Deciduous	50%	28.3%	0%	0%	-	-
			(2/4)	(53/187)	(0/158)	(0/87)	(0/0)	(0/0)
		Permanent	-	77.3%	47.2%	32.3%	8.3%	2.5%
			(0/0)	(51/66)	(60/127)	(89/276)	(12/144)	(4/162)
	2 (Occluded)	Deciduous	0%	25.1%	63.3%	70.1%	-	-
			(0/4)	(47/187)	(100/158)	(61/87)	(0/0)	(0/0)
		Permanent	-	0%	0%	40.9%	84.7%	84.6%
			(0/0)	(0/66)	(0/127)	(113/276)	(122/144)	(137/162)
	7 (Damaged)	Deciduous	0%	20.9%	22.8%	25.3%	-	-
			(0/4)	(39/187)	(36/158)	(22/87)	(0/0)	(0/0)
		Permanent	-	0%	2.4%	5.8%	1.4%	9.3%
			(0/0)	(0/66)	(3/127)	(16/276)	(2/144)	(15/162)
	8 (Unobservable)	Deciduous	0%	4.3%	0%	0%	-	-
			(0/4)	(8/187)	(0/158)	(0/87)	(0/0)	(0/0)
		Permanent	-	22.7%	48%	15.2%	4.2%	0%
			(0/0)	(15/66)	(61/127)	(42/276)	(6/144)	(0/162)
Absent	4 (Antemortem tooth loss)	Deciduous	0%	0%	1.3%	0%	-	-
			(0/4)	(0/187)	(2/158)	(0/87)	(0/0)	(0/0)
		Permanent	-	0%	0%	0%	0%	0%
			(0/0)	(0/66)	(0/127)	(0/276)	(0/144)	(0/162)
	5 (Postmortem tooth loss)	Deciduous	50%	21.4%	12.7%	4.6%	-	-
			(2/4)	(40/187)	(20/158)	(4/87)	(0/0)	(0/0)
		Permanent	-	0%	2.4%	5.8%	1.4%	3.7%
			(0/0)	(0/66)	(3/127)	(16/276)	(2/144)	(6/162)
	6 (Congenital absence)	Deciduous	0%	4.3%	0%	0%	-	-
			(0/4)	(8/187)	(0/158)	(0/87)	(0/0)	(0/0)
		Permanent	-	0%	0%	0%	0%	0%
			(0/0)	(0/66)	(0/127)	(0/276)	(0/144)	(0/162)

TABLE 2.30. THE PREVALENCE OF ANTEMORTEM TOOTH LOSS BY TOOTH SITE IN ADULTS.

Tooth	Upper			Lower	
	Left	Right		Left	Right
M3	2.6%	2.6%		12.5%	7.8%
	(1/38)	(1/39)		(6/48)	(4/51)
M2	2.1%	2.1%		10%	8.3%
	(1/47)	(1/47)		(6/60)	(5/60)
M1	7.7%	6%		16.4%	17.5%
	(4/52)	(3/50)		(10/61)	(10/57)
P2	1.8%	9.4%		11.5%	7.3%
	(1/57)	(5/53)		(7/61)	(4/55)
P1	3.6%	7%		6.5%	5.2%
	(2/55)	(4/57)		(4/62)	(3/58)
C	0%	1.7%		4.9%	3.3%
	(0/54)	(1/58)		(3/61)	(2/60)
I2	9.1%	11.7%		6.9%	10.3%
	(5/55)	(7/60)		(4/58)	(6/58)
I1	8.9%	8.5%		16.4%	20%
	(5/56)	(5/59)		(9/55)	(11/55)
Total	4.6%	6.4%		10.5%	9.9%
	(19/414)	(27/423)		(49/466)	(45/454)
	5.5%			10.2%	
	(46/837)			(94/920)	
	8%				
	(140/1757)				

TABLE 2.31. AVERAGE WEAR SCORES FOR EACH OF THE ANTERIOR TEETH ACCORDING TO MALE AND FEMALE SEX GROUPS, YOUNG AND MIDDLE ADULT AGE GROUPS, AND IN ALL ADULTS. THE NUMBER OF TEETH OBSERVED FOR WEAR IN EACH TOOTH CLASS IS PRESENTED IN BRACKETS.

Tooth	Female	Male		Young adult	Middle adult		All adults
URP2	4.9	5.2		4.2	5.6		5.1
	(18)	(19)		(18)	(19)		(43)
URP1	4.7	5.3		4.2	5.9		5.2
	(17)	(17)		(17)	(19)		(42)
URC	4.5	5.1		4.2	5.2		4.8
	(19)	(16)		(14)	(20)		(42)
URI2	3.7	4.2		3.8	3.8		4
	(16)	(12)		(16)	(13)		(35)
URI1	3.8	5.1		3.9	4.1		4.3
	(17)	(7)		(13)	(10)		(28)
ULI1	4	4.7		4.1	4.3		4.3
	(17)	(7)		(11)	(13)		(29)
ULI2	3.9	3.8		3.6	4.2		4
	(15)	(8)		(12)	(11)		(29)
ULC	4.1	4.9		3.8	4.7		4.6
	(18)	(16)		(12)	(18)		(38)
ULP1	4.5	5.2		3.9	5.6		5
	(19)	(13)		(16)	(15)		(41)
ULP2	4.2	5.1		3.8	5.4		4.8
	(20)	(17)		(16)	(18)		(46)
LLP2	4.4	4.4		3.2	5.2		4.4
	(13)	(18)		(12)	(17)		(39)
LLP1	4.3	4.6		3.9	5.1		4.5
	(14)	(17)		(16)	(16)		(39)
LLC	4.4	5		4.2	5.4		5
	(12)	(12)		(10)	(15)		(31)
LLI2	4.1	4.3		3.8	4.9		4.5
	(13)	(15)		(14)	(16)		(36)
LLI1	4.3	5.5		4.2	5.5		5.1
	(11)	(11)		(11)	(13)		(30)
LRI1	4.6	4.8		4.3	5.2		4.9
	(9)	(12)		(10)	(12)		(27)
LRI2	4	4.9		4	5		4.6
	(14)	(14)		(15)	(12)		(35)
LRC	4.1	4.6		4.2	4.7		4.7
	(14)	(16)		(16)	(14)		(39)
LRP1	4.2	4.8		3.7	5.5		4.7
	(16)	(18)		(18)	(17)		(41)
LRP2	4.1	4.9		3.8	5.2		4.6
	(18)	(19)		(18)	(16)		(45)
Total	4.2	4.8		3.9	5		4.7
	(310)	(284)		(285)	(304)		(735)

TABLE 2.32. AVERAGE WEAR SCORES FOR EACH OF THE MOLARS ACCORDING TO MALE AND FEMALE SEX GROUPS, YOUNG AND MIDDLE ADULT AGE GROUPS AND IN ALL ADULTS. THE NUMBER OF TEETH OBSERVED FOR WEAR IN EACH TOOTH CLASS IS PRESENTED IN BRACKETS

Tooth	Female	Male		Young adult	Middle adult		All adults
URM3	11.9	13.4		10.6	16.9		14.1
	(15)	(14)		(15)	(14)		(37)
URM2	19.5	18.4		15.8	21.9		18.7
	(16)	(15)		(15)	(16)		(40)
URM1	25.1	26.5		22.8	29		24.4
	(15)	(13)		(15)	(14)		(37)
ULM1	24.8	25.5		22.1	28.6		24.7
	(18)	(14)		(16)	(14)		(42)
ULM2	19.4	18.9		16.5	22.1		17.8
	(16)	(13)		(15)	(12)		(37)
ULM3	15.3	12.7		11.8	17.3		14.7
	(14)	(15)		(13)	(15)		(33)
LLM3	12.8	15.4		11.4	17.9		14.6
	(16)	(17)		(16)	(16)		(39)
LLM2	19.3	21.2		16.9	23.8		20.9
	(20)	(20)		(18)	(19)		(49)
LLM1	24.8	26		23.3	29.2		23.9
	(12)	(17)		(16)	(14)		(43)
LRM1	27.5	23.9		25.1	27.3		24.1
	(17)	(14)		(17)	(12)		(40)
LRM2	20.1	18.9		17.7	21.6		19.5
	(20)	(15)		(18)	(16)		(49)
LRM3	11.4	13.5		11.6	17.6		14.8
	(16)	(14)		(17)	(14)		(41)
Total	19.3	19.5		17.1	22.8		20.1
	(195)	(181)		(191)	(176)		(487)

TABLE 2.33. THE PREVALENCE OF CARIOUS LESIONS BY TOOTH ACCORDING TO MALE AND FEMALE SEX GROUPS, YOUNG AND MIDDLE ADULT AGE GROUPS AND IN ALL ADULTS.

Tooth	Female	Male		Young adult	Middle adult		All adults
URM3	20%	0%		6.7%	14.3%		11.1%
	(3/15)	(0/15)		(1/15)	(2/14)		(4/36)
URM2	16.7%	6.3%		12.5%	16.7%		17.5%
	(3/18)	(1/16)		(2/16)	(3/18)		(7/40)
URM1	6.3%	6.7%		6.3%	6.3%		8.3%
	(1/16)	(1/15)		(1/16)	(1/16)		(3/36)
URP2	11.1%	21.1%		5.6%	25%		18.6%
	(2/18)	(4/19)		(1/18)	(5/20)		(8/43)
URP1	5.9%	15%		5.9%	13.6%		15.2%
	(1/17)	(3/20)		(1/17)	(3/22)		(7/46)
URC	5%	0%		0%	4.8%		7%
	(1/20)	(0/16)		(0/14)	(1/21)		(3/43)
URI2	5%	0%		0%	5.9%		7.7%
	(1/20)	(0/12)		(0/16)	(1/17)		(3/39)
URI1	0%	0%		0%	0%		0%
	(0/19)	(0/9)		(0/14)	(0/14)		(0/34)
ULI1	0%	0%		0%	0%		0%
	(0/19)	(0/9)		(0/13)	(0/15)		(0/33)
ULI2	0%	0%		0%	0%		0%
	(0/16)	(0/9)		(0/12)	(0/13)		(0/30)
ULC	5.3%	0%		0%	5.3%		5.1%
	(1/19)	(0/15)		(0/13)	(1/19)		(2/39)
ULP1	5.3%	12.5%		6.3%	11.1%		9.3%
	(1/19)	(2/16)		(1/16)	(2/18)		(4/43)
ULP2	4.5%	6.3%		5.9%	5.6%		8.7%
	(1/22)	(1/16)		(1/17)	(1/18)		(4/46)
ULM1	10.5%	6.7%		6.7%	11.1%		16.7%
	(2/19)	(1/15)		(1/15)	(2/18)		(7/42)
ULM2	17.6%	11.8%		20%	12.5%		13.5%
	(3/17)	(2/17)		(3/15)	(2/16)		(5/37)
ULM3	30.8%	16.7%		15.4%	25%		23.5%
	(4/13)	(3/18)		(2/13)	(4/16)		(8/34)
LLM3	18.8%	0%		11.8%	12.5%		10.3%
	(3/16)	(0/18)		(2/17)	(2/16)		(4/39)
LLM2	42.1%	13.6%		22.2%	28.6%		25.5%
	(8/19)	(3/22)		(4/18)	(6/21)		(13/51)
LLM1	17.6%	17.6%		18.8%	18.8%		21.4%
	(3/17)	(3/17)		(3/16)	(3/16)		(9/42)
LLP2	7.7%	5.6%		0%	11.8%		7.9%
	(1/13)	(1/18)		(0/12)	(2/17)		(3/38)
LLP1	0%	5.3%		0%	5.3%		2.3%
	(0/17)	(1/19)		(0/16)	(1/19)		(1/43)
LLC	7.1%	0%		9.1%	0%		8.1%
	(1/14)	(0/14)		(1/11)	(0/19)		(3/37)
LLI2	0%	0%		0%	0%		2.8%
	(0/14)	(0/15)		(0/14)	(0/17)		(1/36)

TABLE 2.33. THE PREVALENCE OF CARIOUS LESIONS BY TOOTH (CONT.)

Tooth	Female	Male		Young adult	Middle adult		All adults
LLI1	0%	0%		0%	0%		0%
	(0/12)	(0/12)		(0/13)	(0/14)		(0/31)
LRI1	0%	0%		0%	0%		0%
	(0/9)	(0/15)		(0/11)	(0/14)		(0/30)
LRI2	6.3%	0%		6.3%	0%		2.7%
	(1/16)	(0/15)		(1/16)	(0/14)		(1/37)
LRC	5.9%	5.9%		5.9%	11.8%		11.6%
	(1/17)	(1/17)		(1/17)	(2/17)		(5/43)
LRP1	0%	0%		0%	5.6%		4.8%
	(0/16)	(0/18)		(0/18)	(1/18)		(2/42)
LRP2	5.6%	11.1%		5.6%	12.5%		11.4%
	(1/18)	(2/18)		(1/18)	(2/16)		(5/44)
LRM1	15.8%	20%		22.2%	21.4%		17.9%
	(3/19)	(3/15)		(4/18)	(3/14)		(7/39)
LRM2	40%	40%		33.3%	30%		36.7%
	(8/20)	(8/20)		(6/18)	(6/20)		(18/49)
LRM3	38.9%	18.8%		36.8%	12.5%		25%
	(7/18)	(3/16)		(7/19)	(2/16)		(11/44)
Total	11.3%	8.5%		8.9%	10.7%		11.7%
	(61/542)	(43/506)		(44/492)	(58/543)		(148/1266)

TABLE 2.34. THE PREVALENCE OF CARIOUS LESIONS BY DECIDUOUS TOOTH IN INFANCY, EARLY CHILDHOOD AND LATE CHILDHOOD AGE GROUPS, AND IN ALL NONADULTS.

Deciduous tooth	Infancy	Early childhood	Late childhood		All nonadults
URM2	0%	0%	20%		7.1%
	(0/2)	(0/7)	(1/5)		(1/14)
URM1	0%	0%	25%		7.7%
	(0/3)	(0/6)	(1/4)		(1/13)
URC	0%	14.3%	0%		7.1%
	(0/1)	(1/7)	(0/6)		(1/14)
URI2	14.3%	0%	-		8.3%
	(1/7)	(0/5)	(0/0)		(1/12)
URI1	0%	16.7%	-		8.3%
	(0/6)	(1/6)	(0/0)		(1/12)
ULI1	0%	0%	0%		0%
	(0/6)	(0/4)	(0/1)		(0/11)
ULI2	20%	0%	0%		9.1%
	(1/5)	(0/5)	(0/1)		(1/11)
ULC	0%	0%	25%		10%
	(0/1)	(0/5)	(1/4)		(1/10)
ULM1	0%	0%	50%		7.7%
	(0/4)	(0/7)	(1/2)		(1/13)
ULM2	0%	0%	33.3%		9.1%
	(0/1)	(0/7)	(1/3)		(1/11)
LLM2	0%	0%	0%		0%
	(0/1)	(0/6)	(0/9)		(0/16)
LLM1	20%	0%	20%		12.5%
	(1/5)	(0/6)	(1/5)		(2/16)
LLC	0%	0%	0%		0%
	(0/2)	(0/6)	(0/5)		(0/13)
LLI2	0%	0%	-		0%
	(0/5)	(0/4)	(0/0)		(0/9)
LLI1	0%	0%	-		0%
	(0/3)	(0/4)	(0/0)		(0/7)
LRI1	20%	0%	-		12.5%
	(1/5)	(0/3)	(0/0)		(1/8)
LRI2	0%	0%	-		0%
	(0/5)	(0/4)	(0/0)		(0/9)
LRC	0%	0%	0%		0%
	(0/1)	(0/5)	(0/6)		(0/12)
LRM1	33.3%	16.7%	0%		12.5%
	(1/3)	(1/6)	(0/7)		(2/16)
LRM2	0%	16.7%	28.6%		21.4%
	(0/1)	(1/6)	(2/7)		(3/14)
Total	7.5%	3.7%	12.3%		7.1%
	(5/67)	(4/109)	(8/65)		(17/241)

TABLE 2.35. THE PREVALENCE OF CARIOUS LESIONS BY PERMANENT TOOTH IN LATE CHILDHOOD, PUBERTY AND ADOLESCENCE AGE GROUPS AND IN ALL NONADULTS.

Permanent tooth	Late childhood	Puberty	Adolescence		All nonadults
URM3	-	0%	25%		14.3%
		(0/2)	(1/4)		(1/7)
URM2	0%	20%	0%		8.3%
	(0/1)	(1/5)	(0/5)		(1/12)
URM1	10%	20%	0%		9.1%
	(1/10)	(1/5)	(0/5)		(2/22)
URP2	0%	0%	0%		0%
	(0/2)	(0/5)	(0/5)		(0/13)
URP1	0%	0%	0%		0%
	(0/3)	(0/5)	(0/5)		(0/14)
URC	0%	0%	0%		0%
	(0/1)	(0/5)	(0/3)		(0/10)
URI2	0%	0%	0%		0%
	(0/7)	(0/4)	(0/4)		(0/16)
URI1	0%	0%	0%		0%
	(0/8)	(0/5)	(0/5)		(0/19)
ULI1	0%	0%	0%		0%
	(0/7)	(0/5)	(0/4)		(0/17)
ULI2	0%	0%	0%		0%
	(0/7)	(0/4)	(0/4)		(0/15)
ULC	0%	0%	0%		0%
	(0/2)	(0/4)	(0/5)		(0/12)
ULP1	0%	0%	0%		0%
	(0/2)	(0/4)	(0/3)		(0/10)
ULP2	0%	0%	0%		0%
	(0/2)	(0/4)	(0/5)		(0/12)
ULM1	14.3%	0%	0%		5.9%
	(1/7)	(0/4)	(0/5)		(1/17)
ULM2	50%	0%	0%		9.1%
	(1/2)	(0/4)	(0/4)		(1/11)
ULM3	-	0%	25%		16.7%
		(0/1)	(0/4)		(1/6)
LLM3	-	0%	66.7%		50%
		(0/2)	(2/3)		(3/6)
LLM2	0%	0%	0%		0%
	(0/1)	(0/4)	(0/5)		(0/11)
LLM1	25%	0%	0%		11.1%
	(2/8)	(0/4)	(0/5)		(2/18)
LLP2	0%	0%	0%		0%
	(0/1)	(0/4)	(0/5)		(0/11)
LLP1	0%	0%	0%		0%
	(0/2)	(0/4)	(0/5)		(0/12)
LLC	0%	0%	0%		0%
	(0/2)	(0/4)	(0/4)		(0/11)
LLI2	0%	0%	0%		0%
	(0/7)	(0/5)	(0/5)		(0/17)

TABLE 2.35. THE PREVALENCE OF CARIOUS LESIONS BY PERMANENT TOOTH (CONT.).

Permanent tooth	Late childhood	Puberty	Adolescence		All nonadults
LLI1	0%	0%	0%		0%
	(0/6)	(0/4)	(0/4)		(0/15)
LRI1	0%	0%	0%		0%
	(0/9)	(0/4)	(0/5)		(0/19)
LRI2	0%	0%	0%		0%
	(0/7)	(0/4)	(0/5)		(0/16)
LRC	0%	0%	0%		0%
	(0/3)	(0/4)	(0/5)		(0/12)
LRP1	0%	0%	20%		7.1%
	(0/4)	(0/4)	(1/5)		(1/14)
LRP2	0%	0%	0%		0%
	(0/2)	(0/4)	(0/5)		(0/12)
LRM1	20%	0%	0%		10%
	(2/10)	(0/4)	(0/5)		(2/20)
LRM2	0%	20%	20%		15.4%
	(0/2)	(1/5)	(1/5)		(2/13)
LRM3	-	0%	50%		33.3%
		(0/1)	(2/4)		(2/6)
Total	5.6%	2.4%	5.5%		4.5%
	(7/125)	(3/127)	(8/145)		(19/426)

TABLE 2.36. THE PERCENTAGE OF INDIVIDUALS WITH AT LEAST ONE OBSERVABLE TOOTH WITH CALCULUS PRESENT, ACCORDING TO PERMANENT OR DECIDUOUS DENTITION AND AGE GROUP.

Dentition type	Nonadult							Adults				Total
	Infant	Early childhood	Late childhood	Puberty	Adolescence	All nonadults		Young adult	Middle adult	All adults		
Deciduous	0%	36.4%	60%	-	-	35.7%		-	-	-		35.7%
	(0/7)	(7/11)	(4/10)			(10/28)						(10/28)
Permanent	-	-	54.5%	80%	83.3%	69.6%		95.2%	100%	98.5%		91%
			(6/11)	(4/5)	(5/6)	(16/23)		(20/21)	(29/29)	(65/66)		(81/89)

TABLE 2.37. THE PREVALENCE OF PERIODONTAL DISEASE SCORES IN ALL ADULTS ACCORDING TO POSITION OF THE ALVEOLAR CREST.

Alveolar crest	Score										
	Upper						Lower				
	1	2	3	4	5		1	2	3	4	5
RM3-M2	21.7%	17.4%	30.4%	13%	17.4%		21.4%	17.9%	17.9%	35.7%	7.1%
	(5/23)	(4/23)	(7/23)	(3/23)	(4/23)		(6/28)	(5/28)	(5/28)	(10/28)	(2/28)
RM2-M1	24%	32%	28%	12%	4%		14.3%	39.3%	21.4%	25%	0%
	(6/25)	(8/25)	(7/25)	(3/25)	(1/25)		(4/28)	(11/28)	(6/28)	(7/28)	(0/28)
RM1-P2	15.2%	54.5%	21.2%	6.1%	3%		16%	56%	24%	0%	4%
	(5/33)	(18/33)	(7/33)	(2/33)	(1/33)		(4/25)	(14/25)	(6/25)	(0/25)	(1/25)
RP2-P1	22.2%	58.3%	16.7%	0%	2.8%		33.3%	53.3%	6.7%	3.3%	3.3%
	(8/36)	(21/36)	(6/36)	(0/36)	(1/36)		(10/30)	(16/30)	(2/30)	(1/30)	(1/30)
RP1-C	28.6%	54.3%	11.4%	2.9%	2.9%		60.7%	32.1%	7.1%	0%	0%
	(10/35)	(19/35)	(4/35)	(1/35)	(1/35)		(17/28)	(9/28)	(2/28)	(0/28)	(0/28)
RC-I2	40.9%	40.9%	18.2%	0%	0%		47.8%	26.1%	26.1%	0%	0%
	(9/22)	(9/22)	(4/22)	(0/22)	(0/22)		(11/23)	(6/23)	(6/23)	(0/23)	(0/23)
RI2-I1	35%	35%	30%	0%	0%		31.3%	25%	43.8%	0%	0%
	(7/20)	(7/20)	(6/10)	(0/20)	(0/20)		(5/16)	(4/16)	(7/16)	(0/16)	(0/16)
RI1-LI1	57.1%	28.6%	14.3%	0%	0%		26.7%	46.7%	26.7%	0%	0%
	(8/14)	(4/14)	(2/14)	(0/14)	(0/14)		(4/15)	(7/15)	(4/15)	(0/15)	(0/15)
LI1-I2	35.7%	21.4%	42.9%	0%	0%		31.3%	37.5%	25%	6.3%	0%
	(5/14)	(3/14)	(6/14)	(0/14)	(0/14)		(5/16)	(6/16)	(4/16)	(1/16)	(0/16)
LI2-C	30.8%	42.3%	26.9%	0%	0%		33.3%	33.3%	28.6%	4.8%	0%
	(8/26)	(11/26)	(7/26)	(0/26)	(0/26)		(7/21)	(7/21)	(6/21)	(1/21)	(0/21)
LC-P1	26.7%	53.3%	20%	0%	0%		43.3%	33.3%	16.7%	3.3%	3.3%
	(8/30)	(16/30)	(6/30)	(0/30)	(0/30)		(13/30)	(10/30)	(5/30)	(1/30)	(1/30)
LP1-P2	23.7%	52.6%	23.7%	0%	0%		48.6%	34.3%	11.4%	5.7%	0%
	(9/38)	(20/38)	(9/38)	(0/38)	(0/38)		(17/35)	(12/35)	(4/35)	(2/35)	(0/35)
LP2-M1	17.2%	55.2%	24.1%	3.4%	0%		10.7%	57.1%	14.3%	10.7%	7.1%
	(5/29)	(16/29)	(7/29)	(1/29)	(0/29)		(3/28)	(16/28)	(4/28)	(3/28)	(2/28)
LM1-M2	18.5%	40.7%	22.2%	11.1%	7.4%		13.5%	21.6%	35.1%	24.3%	5.4%
	(5/27)	(11/27)	(6/27)	(3/27)	(2/27)		(5/37)	(8/37)	(13/37)	(9/37)	(2/37)
LM2-M3	23.8%	19%	23.8%	19%	14.3%		12.1%	15.2%	27.3%	45.5%	0%
	(5/21)	(4/21)	(5/21)	(4/21)	(3/21)		(4/33)	(5/33)	(9/33)	(15/33)	(0/33)

TABLE 2.38. THE PREVALENCE OF PERIODONTAL DISEASE SCORES IN MALE AND FEMALE SEX GROUPS ACCORDING TO POSITION OF THE ALVEOLAR CREST.

Alveolar crest	Female					Male				
	1	2	3	4	5	1	2	3	4	5
URM3-M2	22.2%	22.2%	33.3%	0%	22.2%	25%	8.3%	25%	25%	16.7%
	(2/9)	(2/9)	(3/9)	(0/9)	(2/9)	(3/12)	(1/12)	(3/12)	(3/12)	(2/12)
URM2-M1	30%	40%	20%	10%	0%	21.4%	21.4%	35.7%	14.3%	7.1%
	(3/10)	(4/10)	(2/10)	(1/10)	(0/10)	(3/14)	(3/14)	(5/14)	(2/14)	(1/14)
URM1-P2	21.4%	28.6%	35.7%	7.1%	7.1%	6.7%	86.7%	0%	6.7%	0%
	(3/14)	(4/14)	(5/14)	(1/14)	(1/14)	(1/15)	(13/15)	(0/15)	(1/15)	(0/15)
URP2-P1	25%	56.3%	12.5%	0%	6.3%	18.8%	62.5%	18.8%	0%	0%
	(4/16)	(9/16)	(2/16)	(0/16)	(1/16)	(3/16)	(10/16)	(3/16)	(0/16)	(0/16)
URP1-C	31.3%	50%	6.3%	6.3%	6.3%	25%	66.7%	8.3%	0%	0%
	(5/16)	(8/16)	(1/16)	(1/16)	(1/16)	(3/12)	(8/12)	(1/12)	(0/12)	(0/12)
URC-I2	54.5%	36.4%	9.1%	0%	0%	30%	50%	20%	0%	0%
	(6/11)	(4/11)	(1/11)	(0/11)	(0/11)	(3/10)	(5/10)	(2/10)	(0/10)	(0/10)
URI2-I1	44.4%	33.3%	22.2%	0%	0%	22.2%	44.4%	33.3%	0%	0%
	(4/9)	(3/9)	(2/9)	(0/9)	(0/9)	(2/9)	(4/9)	(3/9)	(0/9)	(0/9)
URI1-ULI1	42.9%	42.9%	14.3%	0%	0%	60%	20%	20%	0%	0%
	(3/7)	(3/7)	(1/7)	(0/7)	(0/7)	(3/5)	(1/5)	(1/5)	(0/5)	(0/5)
ULI1-I2	33.3%	33.3%	33.3%	0%	0%	33.3%	16.7%	50%	0%	0%
	(2/6)	(2/6)	(2/6)	(0/6)	(0/6)	(2/6)	(1/6)	(3/6)	(0/6)	(0/6)
ULI2-C	27.3%	54.5%	18.2%	0%	0%	45.5%	36.4%	18.2%	0%	0%
	(3/11)	(6/11)	(2/11)	(0/11)	(0/11)	(5/11)	(4/11)	(2/11)	(0/11)	(0/11)
ULC-P1	23.1%	61.5%	15.4%	0%	0%	41.7%	41.7%	16.7%	0%	0%
	(3/13)	(8/13)	(2/13)	(0/13)	(0/13)	(5/12)	(5/12)	(2/12)	(0/12)	(0/12)
ULP1-P2	40%	40%	20%	0%	0%	11.8%	58.8%	29.4%	0%	0%
	(6/15)	(6/15)	(3/15)	(0/15)	(0/15)	(2/17)	(10/17)	(5/17)	(0/17)	(0/17)
ULP2-M1	15.4%	53.8%	23.1%	7.7%	0%	23.1%	53.8%	23.1%	0%	0%
	(2/13)	(7/13)	(3/13)	(1/13)	(0/13)	(3/13)	(7/13)	(3/13)	(0/13)	(0/13)
ULM1-M2	18.2%	54.5%	18.2%	9.1%	0%	23.1%	30.8%	23.1%	15.4%	7.7%
	(2/11)	(6/11)	(2/11)	(1/11)	(0/11)	(3/13)	(4/13)	(3/13)	(2/13)	(1/13)
ULM2-M3	14.3%	42.9%	14.3%	0%	28.6%	30.8%	0%	30.8%	30.8%	7.7%
	(1/7)	(3/7)	(1/7)	(0/7)	(2/7)	(4/13)	(0/13)	(4/13)	(4/13)	(1/13)
LLM3-M2	18.2%	27.3%	0%	54.5%	0%	10.5%	10.5%	36.8%	42.1%	0%
	(2/11)	(3/11)	(0/11)	(6/11)	(0/11)	(2/19)	(2/19)	(7/19)	(8/19)	(0/19)
LLM2-M1	7.7%	30.8%	30.8%	30.8%	0%	16.7%	16.7%	38.9%	22.2%	5.6%
	(1/13)	(4/13)	(4/13)	(4/13)	(0/13)	(3/18)	(3/18)	(7/18)	(4/18)	(1/18)
LLM1-P2	10%	60%	20%	10%	0%	7.7%	61.5%	15.4%	7.7%	7.7%
	(1/10)	(6/10)	(2/10)	(1/10)	(0/10)	(1/13)	(8/13)	(2/13)	(1/13)	(1/13)
LLP2-P1	58.3%	41.7%	0%	0%	0%	47.1%	29.4%	11.8%	11.8%	0%
	(7/12)	(5/12)	(0/12)	(0/12)	(0/12)	(8/17)	(5/17)	(2/17)	(2/17)	(0/17)
LLP1-C	36.4%	27.3%	27.3%	0%	9.1%	50%	28.6%	14.3%	7.1%	0%
	(4/11)	(3/11)	(3/11)	(0/11)	(1/11)	(7/14)	(4/14)	(2/14)	(1/14)	(0/14)
LLC-I2	44.4%	22.2%	22.2%	11.1%	0%	33.3%	44.4%	22.2%	0%	0%
	(4/9)	(2/9)	(2/9)	(1/9)	(0/9)	(3/9)	(4/9)	(2/9)	(0/9)	(0/9)
LLI2-I1	20%	60%	0%	20%	0%	33.3%	22.2%	44.4%	0%	0%
	(1/5)	(3/5)	(0/5)	(1/5)	(0/5)	(3/9)	(2/9)	(4/9)	(0/9)	(0/9)
LLI1-LRI1	40%	40%	20%	0%	0%	0%	50%	50%	0%	0%
	(2/5)	(2/5)	(1/5)	(0/5)	(0/5)	(0/6)	(3/6)	(3/6)	(0/6)	(0/6)

TABLE 2.38. THE PREVALENCE OF PERIODONTAL DISEASE SCORES IN MALE AND FEMALE SEX GROUPS (CONT.)

Alveolar crest	Female					Male				
	1	2	3	4	5	1	2	3	4	5
LRI1-I2	28.6%	28.6%	42.9%	0%	0%	14.3%	28.6%	57.1%	0%	0%
	(2/7)	(2/7)	(3/7)	(0/7)	(0/7)	(1/7)	(2/7)	(4/7)	(0/7)	(0/7)
LRI2-C	70%	20%	10%	0%	0%	18.2%	36.4%	45.5%	0%	0%
	(7/10)	(2/10)	(1/10)	(0/10)	(0/10)	(2/11)	(4/11)	(5/11)	(0/11)	(0/11)
LRC-P1	54.5%	45.5%	0%	0%	0%	76.9%	15.4%	7.7%	0%	0%
	(6/11)	(5/11)	(0/11)	(0/11)	(0/11)	(10/13)	(2/13)	(1/13)	(0/13)	(0/13)
LRP1-P2	41.7%	41.7%	8.3%	8.3%	0%	33.3%	53.3%	6.7%	0%	6.7%
	(5/12)	(5/12)	(1/12)	(1/12)	(0/12)	(5/15)	(8/15)	(1/15)	(0/15)	(1/15)
LRP2-M1	30%	40%	30%	0%	0%	8.3%	66.7%	25%	0%	0%
	(3/10)	(4/10)	(3/10)	(0/10)	(0/10)	(1/12)	(8/12)	(3/12)	(0/12)	(0/12)
LRM1-M2	14.3%	28.6%	21.4%	35.7%	0%	16.7%	41.7%	25%	16.7%	0%
	(2/14)	(4/14)	(3/14)	(5/14)	(0/14)	(2/12)	(5/12)	(3/12)	(2/12)	(0/12)
LRM2-M3	36.4%	18.2%	9.1%	27.3%	9.1%	14.3%	7.1%	21.4%	50%	7.1%
	(4/11)	(2/11)	(1/11)	(3/11)	(1/11)	(2/14)	(1/14)	(3/14)	(7/14)	(1/14)

TABLE 2.39. THE PREVALENCE OF PERIODONTAL DISEASE SCORES IN YOUNG ADULT AND MIDDLE ADULT AGE GROUPS ACCORDING TO POSITION OF THE ALVEOLAR CREST.

Alveolar crest	Young adult						Middle adult				
	1	2	3	4	5		1	2	3	4	5
URM3-M2	30%	10%	20%	20%	20%		10%	30%	30%	10%	20%
	(3/10)	(1/10)	(2/10)	(2/10)	(2/10)		(1/10)	(3/10)	(3/10)	(1/10)	(2/10)
URM2-M1	33.3%	25%	33.3%	8.3%	0%		9.1%	36.4%	27.3%	18.2%	9.1%
	(4/12)	(3/12)	(4/12)	(1/12)	(0/12)		(1/11)	(4/11)	(3/11)	(2/11)	(1/11)
URM1-P2	21.4%	57.1%	21.4%	0%	0%		7.1%	57.1%	21.4%	14.3%	0%
	(3/14)	(8/14)	(3/14)	(0/14)	(0/14)		(1/14)	(8/14)	(3/14)	(2/14)	(0/14)
URP2-P1	38.5%	46.2%	7.7%	0%	7.7%		11.1%	61.1%	27.8%	0%	0%
	(5/13)	(6/13)	(1/13)	(0/13)	(1/13)		(2/18)	(11/18)	(5/18)	(0/18)	(0/18)
URP1-C	41.7%	41.7%	8.3%	0%	8.3%		22.2%	55.6%	16.7%	5.6%	0%
	(5/12)	(5/12)	(1/12)	(0/12)	(1/12)		(4/18)	(10/18)	(3/18)	(1/18)	(0/18)
URC-I2	37.5%	37.5%	25%	0%	0%		40%	50%	10%	0%	0%
	(3/8)	(3/8)	(2/8)	(0/8)	(0/8)		(4/10)	(5/10)	(1/10)	(0/10)	(0/10)
URI2-I1	33.3%	50%	16.7%	0%	0%		27.3%	36.4%	36.4%	0%	0%
	(2/6)	(3/6)	(1/6)	(0/6)	(0/6)		(3/11)	(4/11)	(4/11)	(0/11)	(0/11)
URI1-ULI1	50%	25%	25%	0%	0%		55.6%	33.3%	11.1%	0%	0%
	(2/4)	(1/4)	(1/4)	(0/4)	(0/4)		(5/9)	(3/9)	(1/9)	(0/9)	(0/9)
ULI1-I2	20%	20%	60%	0%	0%		28.6%	28.6%	42.9%	0%	0%
	(1/5)	(1/5)	(3/5)	(0/5)	(0/5)		(2/7)	(2/7)	(3/7)	(0/7)	(0/7)
ULI2-C	33.3%	50%	16.7%	0%	0%		25%	41.7%	33.3%	0%	0%
	(4/12)	(6/12)	(2/12)	(0/12)	(0/12)		(3/12)	(5/12)	(4/12)	(0/12)	(0/12)
ULC-P1	41.7%	33.3%	25%	0%	0%		14.3%	71.4%	14.3%	0%	0%
	(5/12)	(4/12)	(3/12)	(0/12)	(0/12)		(2/14)	(10/14)	(2/14)	(0/14)	(0/14)
ULP1-P2	33.3%	53.3%	13.3%	0%	0%		11.1%	50%	38.9%	0%	0%
	(5/15)	(8/15)	(2/15)	(0/15)	(0/15)		(2/18)	(9/18)	(7/18)	(0/18)	(0/18)
ULP2-M1	25%	50%	16.7%	8.3%	0%		7.1%	57.1%	35.7%	0%	0%
	(3/12)	(6/12)	(2/12)	(1/12)	(0/12)		(1/14)	(8/14)	(5/14)	(0/14)	(0/14)
ULM1-M2	33.3%	33.3%	25%	8.3%	0%		0%	45.5%	27.3%	18.2%	9.1%
	(4/12)	(4/12)	(3/12)	(1/12)	(0/12)		(0/11)	(5/11)	(3/11)	(2/11)	(1/11)
ULM2-M3	25%	25%	25%	25%	0%		20%	20%	20%	20%	20%
	(2/8)	(2/8)	(2/8)	(2/8)	(0/8)		(2/10)	(2/10)	(2/10)	(2/10)	(2/10)
LLM3-M2	20%	13.3%	26.7%	40%	0%		0%	15.4%	38.5%	46.2%	0%
	(3/15)	(2/15)	(4/15)	(6/15)	(0/15)		(0/13)	(2/13)	(5/13)	(6/13)	(0/13)
LLM2-M1	12.5%	25%	31.3%	25%	6.3%		6.7%	26.7%	46.7%	20%	0%
	(2/16)	(4/16)	(5/16)	(4/16)	(1/16)		(1/15)	(4/15)	(7/15)	(3/15)	(0/15)
LLM1-P2	6.7%	80%	6.7%	0%	6.7%		11.1%	33.3%	33.3%	22.2%	0%
	(1/15)	(12/15)	(1/15)	(0/15)	(1/15)		(1/9)	(3/9)	(3/9)	(2/9)	(0/9)
LLP2-P1	60%	40%	0%	0%	0%		40%	33.3%	13.3%	13.3%	0%
	(9/15)	(6/15)	(0/15)	(0/15)	(0/15)		(6/15)	(5/15)	(2/15)	(2/15)	(0/15)
LLP1-C	57.1%	35.7%	7.1%	0%	0%		23.1%	30.8%	30.8%	7.7%	7.7%
	(8/14)	(5/14)	(1/14)	(0/14)	(0/14)		(3/13)	(4/13)	(4/13)	(1/13)	(1/13)
LLC-I2	50%	30%	10%	10%	10%		22.2%	33.3%	44.4%	0%	0%
	(5/10)	(3/10)	(1/10)	(1/10)	(1/10)		(2/9)	(3/9)	(4/9)	(0/9)	(0/9)
LLI2-I1	42.9%	42.9%	0%	14.3%	0%		28.6%	28.6%	42.9%	0%	0%
	(3/7)	(3/7)	(0/7)	(1/7)	(0/7)		(2/7)	(2/7)	(3/7)	(0/7)	(0/7)
LLI1-LRI1	33.3%	33.3%	33.3%	0%	0%		28.6%	42.9%	28.6%	0%	0%
	(2/6)	(2/6)	(2/6)	(0/6)	(0/6)		(2/7)	(3/7)	(2/7)	(0/7)	(0/7)

TABLE 2.39. THE PREVALENCE OF PERIODONTAL DISEASE SCORES IN YOUNG ADULT AND MIDDLE ADULT AGE GROUPS (CONT.).

Alveolar crest	Young adult						Middle adult				
	1	2	3	4	5		1	2	3	4	5
LRI1-I2	16.7%	50%	33.3%	0%	0%		44.4%	0%	55.6%	0%	0%
	(1/6)	(3/6)	(2/6)	(0/6)	(0/6)		(4/9)	(0/9)	(5/9)	(0/9)	(0/9)
LRI2-C	70%	20%	10%	0%	0%		36.4%	27.3%	36.4%	0%	0%
	(7/10)	(2/10)	(1/10)	(0/10)	(0/10)		(4/11)	(3/11)	(4/11)	(0/11)	(0/11)
LRC-P1	83.3%	16.7%	0%	0%	0%		42.9%	42.9%	14.3%	0%	0%
	(10/12)	(2/12)	(0/12)	(0/12)	(0/12)		(6/14)	(6/14)	(2/14)	(0/14)	(0/14)
LRP1-P2	46.2%	38.5%	15.4%	0%	0%		14.3%	71.4%	0%	7.1%	7.1%
	(6/13)	(5/13)	(2/13)	(0/13)	(0/13)		(2/14)	(10/14)	(0/14)	(1/14)	(1/14)
LRP2-M1	16.7%	75%	8.3%	0%	0%		11.1%	44.4%	44.4%	0%	0%
	(2/12)	(9/12)	(1/12)	(0/12)	(0/12)		(1/9)	(4/9)	(4/9)	(0/9)	(0/9)
LRM1-M2	23.1%	46.2%	23.1%	7.7%	0%		0%	36.4%	18.2%	45.5%	0%
	(3/13)	(6/13)	(3/13)	(1/13)	(0/13)		(0/11)	(4/11)	(2/11)	(5/11)	(0/11)
LRM2-M3	40%	10%	10%	30%	10%		8.3%	25%	25%	33.3%	8.3%
	(4/10)	(1/10)	(1/10)	(3/10)	(1/10)		(1/12)	(3/12)	(3/12)	(4/12)	(1/12)

TABLE 2.40. THE PREVALENCE OF PERIAPICAL LESIONS IN ADULTS ACCORDING TO MALE AND FEMALE SEX GROUPS, YOUNG AND MIDDLE ADULT AGE GROUPS AND IN ALL ADULTS.
1 = SMOOTH-WALLED CAVITY; 2 = ROUGH-WALLED CAVITY.

Tooth socket	Female		Male		Young adult		Middle adult		All adults	
	1	2	1	2	1	2	1	2	1	2
URM3	0%	0%	0%	0%	0%	0%	0%	0%	0%	0%
	(0/6)	(0/6)	(0/6)	(0/6)	(0/5)	(0/5)	(0/7)	(0/7)	(0/16)	(0/16)
URM2	28.6%	0%	0%	0%	25%	0%	14.3%	0%	11.1%	0%
	(2/7)	(0/7)	(0/8)	(0/8)	(1/4)	(0/4)	(1/7)	(0/7)	(2/18)	(0/18)
URM1	16.7%	33.3%	0%	12.5%	20%	0%	0%	40%	6.3%	25%
	(1/6)	(2/6)	(0/8)	(1/8)	(1/5)	(0/5)	(0/5)	(2/5)	(1/16)	(4/16)
URP2	0%	0%	0%	11.1%	0%	0%	0%	10%	5.6%	5.6%
	(0/8)	(0/8)	(0/9)	(1/9)	(0/3)	(0/3)	(0/10)	(1/10)	(1/18)	(1/18)
URP1	14.3%	0%	12.5%	12.5%	25%	0%	11.1%	22.2%	15.8%	15.8%
	(1/7)	(0/7)	(1/8)	(1/8)	(1/4)	(0/4)	(1/9)	(2/9)	(3/19)	(3/19)
URC	0%	0%	7.1%	0%	0%	0%	5.9%	0%	8.3%	0%
	(0/15)	(0/15)	(1/14)	(0/14)	(0/10)	(0/10)	(1/17)	(0/17)	(3/36)	(0/36)
URI2	0%	0%	0%	0%	0%	0%	0%	0%	0%	0%
	(0/17)	(0/17)	(0/11)	(0/11)	(0/13)	(0/13)	(0/12)	(0/12)	(0/34)	(0/34)
URI1	0%	0%	0%	7.7%	0%	0%	0%	5.6%	0%	2.4%
	(0/20)	(0/20)	(0/13)	(1/13)	(0/16)	(0/16)	(0/18)	(1/18)	(0/41)	(1/41)
ULI1	0%	6.3%	0%	0%	0%	0%	0%	6.7%	0%	2.9%
	(0/16)	(1/16)	(0/12)	(0/12)	(0/11)	(0/11)	(0/15)	(1/15)	(0/35)	(1/35)
ULI2	0%	0%	0%	0%	0%	0%	0%	0%	0%	0%
	(0/15)	(0/15)	(0/10)	(0/10)	(0/12)	(0/12)	(0/15)	(0/15)	(0/31)	(0/31)
ULC	5.6%	0%	0%	0%	0%	0%	5.3%	0%	5.3%	0%
	(1/18)	(0/18)	(0/14)	(0/14)	(0/11)	(0/11)	(1/19)	(0/19)	(2/38)	(0/38)
ULP1	0%	0%	14.3%	14.3%	25%	0%	12.5%	12.5%	11.8%	5.9%
	(0/7)	(0/7)	(1/7)	(1/7)	(1/4)	(0/4)	(1/8)	(1/8)	(2/17)	(1/17)
ULP2	10%	0%	0%	8.3%	0%	0%	7.7%	7.7%	4%	8%
	(1/10)	(0/10)	(0/12)	(1/12)	(0/7)	(0/7)	(1/13)	(1/13)	(1/25)	(2/25)
ULM1	25%	50%	0%	16.7%	0%	66.7%	16.7%	16.7%	8.3%	41.7%
	(1/4)	(2/4)	(0/6)	(1/6)	(0/3)	(2/3)	(1/6)	(1/6)	(1/12)	(5/12)
ULM2	33.3%	0%	0%	0%	16.7%	0%	0%	0%	6.7%	6.7%
	(1/3)	(0/3)	(0/9)	(0/9)	(1/6)	(0/6)	(0/4)	(0/4)	(1/15)	(1/15)
ULM3	0%	0%	0%	0%	0%	0%	0%	0%	0%	0%
	(0/5)	(0/5)	(0/8)	(0/8)	(0/4)	(0/4)	(0/7)	(0/7)	(0/13)	(0/13)
LLM3	0%	0%	0%	0%	0%	0%	0%	0%	0%	0%
	(0/4)	(0/4)	(0/9)	(0/9)	(0/6)	(0/6)	(0/7)	(0/7)	(0/15)	(0/15)
LLM2	0%	0%	0%	0%	0%	0%	0%	0%	0%	6.7%
	(0/4)	(0/4)	(0/7)	(0/7)	(0/5)	(0/5)	(0/6)	(0/6)	(0/15)	(1/15)
LLM1	0%	33.3%	0%	0%	0%	0%	50%	0%	9.1%	18.2%
	(0/3)	(1/3)	(0/3)	(0/3)	(0/3)	(0/3)	(1/2)	(0/2)	(1/11)	(2/11)
LLP2	0%	0%	0%	12.5%	0%	0%	8.3%	8.3%	4.5%	4.5%
	(0/9)	(0/9)	(0/8)	(1/8)	(0/6)	(0/6)	(1/12)	(1/12)	(1/22)	(1/22)
LLP1	0%	6.7%	10%	0%	0%	0%	5.6%	5.6%	3%	3%
	(0/15)	(1/15)	(1/10)	(0/10)	(0/7)	(0/7)	(1/18)	(1/18)	(1/33)	(1/33)
LLC	5.9%	0%	0%	2%	0%	6.3%	6.7%	6.7%	2.6%	10.3%
	(1/17)	(0/17)	(0/14)	(2/14)	(0/16)	(1/16)	(1/15)	(1/15)	(1/39)	(4/39)

TABLE 2.40. THE PREVALENCE OF PERIAPICAL LESIONS IN ADULTS (CONT.).

Tooth socket	Female		Male		Young adult		Middle adult		All adults	
	1	2	1	2	1	2	1	2	1	2
LLI2	0%	7.1%	0%	0%	0%	0%	0%	7.7%	0%	9.4%
	(0/14)	(1/14)	(0/11)	(0/11)	(0/12)	(0/12)	(0/13)	(1/13)	(0/32)	(3/32)
LLI1	0%	0%	0%	8.3%	0%	0%	0%	10%	0%	7.1%
	(0/10)	(0/10)	(0/12)	(1/12)	(0/12)	(0/12)	(0/10)	(1/10)	(0/28)	(2/28)
LRI1	10%	0%	0%	7.7%	0%	0%	10%	10%	3.7%	3.7%
	(0/10)	(0/10)	(0/13)	(1/13)	(0/10)	(0/10)	(1/10)	(1/10)	(1/27)	(1/27)
LRI2	0%	0%	0%	9.1%	0%	0%	0%	9.1%	3.4%	6.9%
	(0/11)	(0/11)	(0/11)	(1/11)	(0/11)	(0/11)	(0/11)	(1/11)	(1/29)	(2/29)
LRC	0%	0%	0%	0%	0%	0%	8.3%	0%	5.7%	2.9%
	(0/14)	(0/14)	(0/14)	(0/14)	(0/14)	(0/14)	(1/12)	(0/12)	(2/35)	(1/35)
LRP1	16.7%	0%	0%	0%	0%	0%	16.7%	8.3%	7.1%	3.6%
	(2/12)	(0/12)	(0/11)	(0/11)	(0/11)	(0/11)	(2/12)	(1/12)	(2/28)	(1/28)
LRP2	0%	0%	0%	0%	0%	0%	0%	0%	0%	0%
	(0/12)	(0/12)	(0/6)	(0/6)	(0/9)	(0/9)	(0/9)	(0/9)	(0/24)	(0/24)
LRM1	40%	20%	33.3%	0%	25%	25%	33.3%	0%	27.3%	9.1%
	(2/5)	(1/5)	(1/3)	(0/3)	(1/4)	(1/4)	(2/6)	(0/6)	(3/11)	(1/11)
LRM2	0%	0%	16.7%	16.7%	0%	25%	14.3%	0%	15.4%	7.7%
	(0/4)	(0/4)	(1/6)	(1/6)	(0/4)	(1/4)	(1/7)	(0/7)	(2/13)	(1/13)
LRM3	0%	0%	0%	0%	0%	0%	0%	0%	0%	0%
	(0/3)	(0/3)	(0/10)	(0/10)	(0/5)	(0/5)	(0/6)	(0/6)	(0/14)	(0/14)
Total	4.5%	2.9%	2%	4.6%	2.4%	2%	5.5%	5.5%	4.2%	5.3%
	(14/311)	(9/311)	(6/303)	(14/303)	(6/253)	(5/253)	(18/328)	(18/328)	(32/760)	(40/760)
	7.4%		6.6%		4.3%		11%		9.5%	
	(23/311)		(20/303)		(11/253)		(36/328)		(72/760)	

TABLE 2.41. DESCRIPTIONS OF DISARTICULATED REMAINS RECOVERED FROM KAWA.

* Grave numbers are given where there is a possibility that remains are associated with a burial intended for a particular grave.

Area/ Grid square	Grave*	Level	MNI	Description	Comments
561?			2	Cranial, appendicular, axial & dental fragments from at least one probable adult & a nonadult.	
561		20	1	Axial & appendicular fragments from at least one probable adult.	
1052?			1	Axial & cranial fragments from at least one probable adult.	
1055			2	Axial & appendicular fragments from at least one probable adult & a nonadult.	
1088		1	2	Axial & appendicular fragments from at least one adult, & axial fragments from at least one nonadult.	
1098		2	1	Several small fragments of unidentified bone, possibly long bone, from a probable adult.	
1098		7	1	Small fragment of rib, only, from a probable adult.	
GD3		Feature 3?	2	Appendicular, cranial & axial fragments from at least one nonadult, probably between 11-15 years, & a cranial fragment from an older individual, probably adult.	
GD3		1	4	Very fragmentary & weathered remains of at least four individuals, two probable adults, one infant (probably between 0-1 year), & one older nonadult.	
GD3		8	1	Cranial, axial & appendicular fragments from at least one probable adult.	
GD3		10	1	Cranial, axial & appendicular fragments from at least one nonadult.	
GD3		14	1	Cranial fragments from at least on probable adult.	
GD3		21	4	Cranial & appendicular fragment from a probable adult, & cranial, axial & appendicular fragments from three nonadults, an 11–15-year-old, a neonate & an individual around 1 year of age.	
GD3		23	1	Very weathered unidentified cranial fragments from a nonadult.	
GD3		25	1	Unidentified bone fragments from at least one adult or nonadult.	
GD3		32	2	Cranial, axial, dental & appendicular fragments from at least one adult & one nonadult aged between 0-1 year.	
GD3		34	2	Appendicular & axial fragments from at least one nonadult aged between 12-20 years, & appendicular & axial fragments from at least one nonadult aged 0-1 year.	
GD3		39	1	Unidentified bone fragments from at least one adult or nonadult.	
GD3		40	2	Femoral fragments from at least one adult, & cranial & appendicular fragments from at least one nonadult, probably between 6-15 years.	
GD3		44	2	Cranial, axial, dental & appendicular remains from at least two probable adults, one a probable female aged between 20-34 years.	Dental caries on the worn occlusal surface of the lower left first molar.
GD3		42	1	Axial & appendicular remains from at least one adult, probably aged between 20-34 years.	

TABLE 2.41. DESCRIPTIONS OF DISARTICULATED REMAINS RECOVERED FROM KAWA (CONT.).

Area/ Grid square	Grave*	Level	MNI	Description	Comments
GD3	45?	46	3	Cranial & axial fragments from at least one probable adult, & cranial & appendicular remains from at least two nonadults, one between 1-3 years & one probably younger.	
GD3		48	1	Cranial & axial fragments from at least one probable adult, & cranial & axial fragments from at least one nonadult, probably between 2-10 years.	
GD3		52	1	Cranial & appendicular fragments from at least one adult.	
GD3		53	1	Cranial, axial & appendicular fragments from at least one adult.	Proximal foot phalanx present with a flat plate of new bone on the side of the proximal articulation, possibly as a reaction to trauma in this region.
GD3		54	1	Left femur of an adult, only.	
GD3		74	1	Cranial fragments from at least one nonadult.	
GD3		74	2	Cranial, axial & appendicular fragments from at least one younger nonadult & one adult/older nonadult.	
GD3		91	2	Cranial, axial & appendicular fragments from at least one young adult or older nonadult, & cranial remains from a young nonadult, probably in infancy.	
GD3		92	1	Axial, appendicular & dental fragments from at least one probable adult.	A healed fracture is present on a right femur near the proximal end of the shaft. This consists of a large swelling of disorganised bone, accompanied by apparent shortening of the bone. Nonmasticatory wear, in the form of an interproximal groove, is present on the distal upper right first molar.
GD3		94	1	Appendicular fragments from at least one adult.	
GD3		115	2	Cranial, axial, dental, & appendicular fragments from at least one nonadult & one adult.	
GD3		116	2	Cranial, axial, dental & appendicular fragments from at least one nonadult & one adult.	Adult remains of a left maxilla demonstrate a periapical lesion on the alveolar bone in the region of the left first premolar socket. Nonmasticatory wear present on the disto-lingual interproximal region of the upper left second premolar. A large (*c*. 1cm) lytic lesion is present on the distal articular surface of the fifth metatarsal.
GD3		117	1	Cranial, axial, dental & appendicular fragments from at least one adult.	
GD3		125	3	Cranial, axial, dental & appendicular fragments from at least one younger nonadult between 2-4 years of age, one older nonadult, & one adult.	

TABLE 2.41. DESCRIPTIONS OF DISARTICULATED REMAINS RECOVERED FROM KAWA (CONT.).

Area/ Grid square	Grave*	Level	MNI	Description	Comments
GD3		132	1	Appendicular & dental fragments from at least one adult.	
GD3		135	1	Appendicular fragments from at least one nonadult, probably aged 3-7 years.	
GD3		139	1	Cranial bones from one adult individual.	
GD3		141	1	Axial & appendicular remains from at least one adult.	
HA1		20	1	Fragments from the feet of at least one probable adult.	
HA2		2	1	Fragments of frontal bone from a probable adult.	
HA2		3	1	Cranial & appendicular fragments from at least one probable adult.	
HA2		12	1	Axial & appendicular fragments from at least one probable adult.	
HA2	64	1	1	Axial & appendicular fragments from at least one probable adult.	
HA2	64	45	1	Trapezoid & food phalanx from at least one probable adult.	
HA2	64	66	1	Second & third right metatarsals from a single probable adult.	
HA2	46	3	1	Appendicular fragments from at least one probable adult.	
HA2	50	1	3	Vertebral fragments from an adult, cranial, axial & appendicular fragments from at least two nonadults, & mandibular & dental fragments which can be assigned to two nonadults of 2-5 years of age.	The adult vertebrae show evidence for osteoarthritis on the vertebral facets.
HA2	31	12/15/ 31/35/ 36/45	2	Appendicular, axial, dental, & cranial fragments from at least two probable adults.	Evidence for osteoarthritis present on lumbar vertebrae. Carious lesion present on a lower left third molar at the cemento-enamel junction. A lytic lesion is present on a broken section of rib surface.
HA2	23	25	1	Tarsal & vertebral fragments from at least one probable adult.	
HA2	55	45	2	Axial, cranial & appendicular fragments from at least one non adult & one adult.	
HA2	71	72	1	Ribs, humeral head & right scapula, only, belonging to at least one probable adult.	
HA2		188	1	Right fifth metatarsal & proximal foot phalanx from at least one probable adult.	
HA2	39?	38/40/ 52	1	Cranial, appendicular, axial & dental fragments from at least one probable adult.	
HA2	80/72?	45	2	Appendicular, axial & cranial fragments from at least one probable adult & one nonadult.	
HA2	20	46/17	1	Rib, vertebral & clavicular fragments from at least one probable adult.	
HA2	51	59/60/ 75	1	Axial, appendicular & dental remains from at least one probable adult between 35-49 years of age.	
HA2		78	2	Axial & cranial fragments from at least one probable adult, & a radius & ulna from a nonadult between 0-1 years in age.	

TABLE 2.41. DESCRIPTIONS OF DISARTICULATED REMAINS RECOVERED FROM KAWA (CONT.).

Area/ Grid square	Grave*	Level	MNI	Description	Comments
HA2		87	1	Several fragments of foot bones from at least one probable adult.	Label with the remains notes: 'bone from coffin'.
HA2	90	93	1	Right zygomatic bone from a probable adult.	
HA2	94		2	Cranial & axial fragments from at least two probable adults.	
HA2	94?	95	1	Unidentifiable bone fragments, possibly human/ animal.	
HA2	100?	99	2	Appendicular & cranial fragments from at least one probable adult & a nonadult.	
HA2		102?	1	Appendicular, axial, dental, & cranial fragments from at least one probable adult.	
HA2	94	139/ 150	2	Cranial, dental, axial, & appendicular fragments from at least two probable adults.	
HA2	94	146/ 151	1	Appendicular & axial fragments from at least one probable adult.	
HA2		197	2	Cranial, axial, & appendicular remains from at least two probable adults.	
JC2		1	2	Cranial fragment from one probable adult, & cranial fragments from a nonadult.	
JC2		3	1	Right ulna from a probable adult.	
JC2		25	1	Unidentifiable fragments, could be human or animal.	
JC3	12?	2	1	Cranial, axial, dental, & appendicular fragments from probably a single adult individual, likely less than 25-30 years of age as the proximal clavicle epiphysis is unfused.	Several ivory pieces including cut rhomboid sections were found in levels 4 & 8.
		4			
		8			
JC3	12?	10	1	Cranial, axial, dental, & appendicular fragments from probably a single adult individual.	
		14			
JD2		Unstratified	1	Upper left first molar, several unidentified fragments of bone, & a partial hand phalanx from at least one adult individual.	
JD2		1	2	Hand phalanx & metatarsal from at least one probable adult, & dental fragment from at least one nonadult.	
JD2		2	1	Unidentified appendicular fragments, could be human or animal.	
JD2		10	1	Cranial fragments from a nonadult.	
JD2		16	0/1	Unidentified weathered fragments, could be human or animal.	
JD2		18	1	Unidentified cranial & appendicular fragments, could be human or animal.	
JD2		19	1	Unidentified appendicular fragments, could be human or animal.	
JD2		80	1	Unidentified appendicular fragments, could be human or animal.	
JD3		1	1	Cranial & dental fragments, & one metacarpal from at least one individual.	
JD3		2	2	Cranial, appendicular, axial, & dental fragments from at least one young adult between 20-34 years of age, & a metatarsal from another adult of unknown age.	
JD3		4	1	Fifth metatarsal from a probable adult.	

TABLE 2.41. DESCRIPTIONS OF DISARTICULATED REMAINS RECOVERED FROM KAWA (CONT.).

Area/ Grid square	Grave*	Level	MNI	Description	Comments
JD3		21	1	Appendicular fragments & a rib head from at least one probable adult.	
JD3		25	1	Cranial, appendicular, axial, & dental fragments from at least one probable adult.	
JD3		30	1	Cranial, appendicular, axial, & dental fragments from at least one probable adult.	
JE1		1	1	Cranial & long bone fragments from at least one probable adult.	
JE2	14	15	1	Unidentified human bone fragment.	
JE2		17	1	Appendicular fragments from at least one nonadult between the age of 11-15 years	Humeral & femoral fragments demonstrate a layer of diffuse woven bone on the cortical surfaces.
JE3		1	2	Axial & cranial fragments from at least one probable adult & one nonadult.	Marked woven bone on the endocranial surface belonging to the nonadult.
JE3		2	1	Cranial fragments from at least one probable adult.	
JE3		13	1	Axial, cranial, & dental fragments from at least one probable adult.	
JE3		24	1	Axial fragments from at least one probable adult.	
JE3		133	1	Cranial fragments from at least one nonadult.	
JE3	69	35	2	Axial & dental fragments from at least one probable adult & one nonadult.	
JE3	115	26,28,45, 113,114, 120,123, 124	2	Axial, cranial, & dental fragments from at least two probable adults.	
JE3	132	132	1	Axial & appendicular fragments from at least one probable adult.	
JE3	132	171	1	Nonadult metacarpal, only.	
JE3	132	178	2	Cranial & appendicular fragments from at least one probable adult & one nonadult.	
JE3	132	184	2	Axial & appendicular fragments from at least one probable adult & at least one nonadult.	
JE3	132	186	2	Axial & appendicular fragments from at least one probable adult & one nonadult.	
JE3	132	187	2	Axial & appendicular fragments from at least one probable adult & nonadult.	
JE3	132	188	2	Appendicular fragments from at least one probable adult & one nonadult.	
JE3	132	189	2	Axial & appendicular fragments from at least one probable adult & one nonadult.	
JE3	132	184/189	2	Axial & appendicular fragments from at least one probable adult & one nonadult.	
JE3	132	190	1	Appendicular fragments from at least one probable adult.	
JE3	132	193	1	Appendicular fragments from at least one probable adult.	
JE3	132	194	1	Axial fragments from at least one nonadult.	
JF1		1	1	Left talus from one probable adult.	
JF1		7	1	Nonadult cranial fragment.	

TABLE 2.41. DESCRIPTIONS OF DISARTICULATED REMAINS RECOVERED FROM KAWA (CONT.).

Area/ Grid square	Grave*	Level	MNI	Description	Comments
JF2		1	1	Nonadult cranial fragment.	
JF2		28	1	Nonadult sacral fragment.	
JF2	20	39	1	Cranial fragments from a nonadult, probably between 0-1 year of age.	
JF2	20	60	2	Cranial fragments from a nonadult, probably between 0-1 year of age, & one long bone fragment from a probable adult.	
JF2		57	1	Lower deciduous second premolar & unidentified bone fragments from at least one nonadult between the age of 2-5 years.	Includes animal bone.
JF2		83	1	Cranial & appendicular fragments from at least one nonadult, probably between 0-1 year of age.	
JF2	55	84	1	Cranial & appendicular fragments from at least one nonadult, probably between 0-1 year of age.	Includes animal bone.
JF2		89	0/1	Unidentified bone fragments, could be human.	
JG1		20	1	Axial & cranial fragments from at least one probable adult.	Includes animal bone.
JG2		1	1	Axial fragments (ribs, only) from at least one probable adult.	
JH3	21	52	1	Cranial, dental, & appendicular fragments from at least one nonadult, probably between 6-10 years of age.	
JI4	1		1	Dental fragments from one individual.	
-	-	-	2	Cranial, appendicular, axial, & dental fragments from at least one probable adult & one nonadult.	Unknown context.
Q3 AD5		246/247	1	Lower left third molar, only.	Root of molar not fully formed.

3. The Faunal Remains from Kawa

Pernille Bangsgaard

Introduction

The site of Kawa is located in the Dongola Reach in northern Sudan and the city contain substantial remains particularly from the Kushite Period. The analysis presented in this chapter is based on the faunal remains from several field seasons[1] by the SARS Kawa Excavation Project running from 2001 to 2015. A selection of this material has been studied at the Natural History Museum of Denmark, using the large comparative collections available there. However, the majority of the material presented here was studied on-site in Sudan, during the 2008-9 and 2010-2011 field season. Here a small collection of comparative skeletons was collected and prepared, including seven different species, covering all the main domesticates.

Faunal remains were recovered from all excavated areas across the site of Kawa. Recovery was exclusively by hand collection, as no large-scale sieving of excavated soil was carried out. Although the soil (sand) at Kawa should facilitate the recovery of many bones, including some smaller fragments, it must be assumed that the lack of sieving has affected the recovery of particularly the smallest fragments, such as smaller fish bones and bones from any micro fauna. This means that some of these smaller species may be underrepresented compared to the lager mammalian species.

The current study includes a substantial proportion of the excavated faunal material, but it does not cover the entire collection or all areas of excavation. However, the faunal material originates from some 13 different excavation areas and as such, the analysis should give a good and reliable indication of what the remaining collection may contain.

All faunal material included in the study was identified to skeletal element and species or to the nearest possible taxon (*order*, *family*, or *genus*) when possible. The registration of each bone also includes information on section of bone, side of body, and observation of various changes, whether human-induced or other, such as cut-marks, and burning. The bones are quantified by number of fragments, NISP (*number of identified specimens*), and long bone fragments were registered with age categories (*foetal*, *pullus*, *unfused*, and *fused*)[2]. All mandibles were registered with ontogenetic age[3], when that information was available and all measurements were taken according to Angela von den Driesch's *A Guide to the Measurement of Animal Bones from Archaeological Sites* (von den Driesch 1979).

The results

A total of 38,940 fragments (weighing approx. 278kg) was analysed in this study, the overwhelming majority of these belong to various mammalian species and of these the domesticated animals completely dominate. The state of preservation is generally poor to very poor, meaning that the original surface of the bones is in many instances affected by some changes or simply lost and post- or pre-excavation fragmentation is widespread. These factors likely influenced the identification of e.g. cut-marks and other minor changes to the bone. Despite this, it was still possible to detect nearly 1,400 cut and chop marks on the Kawa bones, which will be described in more detail below.

Further changes or damage to the bones includes various signs of burning and gnawing. The former is widespread in the Kawa collection, as more than a quarter of the collection show signs of burning (10,991 fragments). The majority of these were only partly burnt with smaller or larger patches of discolouration due to heat exposure. This type of burning may be the result of indirect heat exposure or a very limited heat exposure and as such could partly be related to the cooking process or to the disposal process where fragments may end up near a fire or near still-hot ashes. Among the burnt bones were also close to 500 completely-calcinated fragments with multiple fracturing and white colouring. Additionally, around 2,200 fragments are black to white burnt adding to the number of fragments that are likely to have been exposed to higher and/or direct burning and for a longer time. These are, therefore, unlikely to be related to food preparation but could be a result or a part of the disposal process. Gnawing is on the other hand not very often detected in the collection, only 52 fragments were registered with this type of changes. Most of this gnawing was inflicted by rodents (35), but evidence of carnivore (13) and ruminate (3) gnawing has been identified.

A single species, namely cattle (*Bos taurus*), dominates the collection from Kawa with 94% of the identified fragments (NISP 6,520) (see Table 3.1 for a full overview). That share would rise to 97% of the total collection if the remains identified to large ungulate were included (NISP 15,896). Other large ungulate species have been identified in the collection, but these amount to just 33 fragments in total and it must, therefore, be assumed that the overwhelming majority of the large ungulate bones belong to cattle. Mammalian species are by far the most common remains in the collection, but a few species of fish, bird and reptiles have also been identified, all will be described in the sections below.

Cattle

The 6,520 fragments of cattle bones identified in the collection weights almost 140kg and the remains represent the largest collection of bones from Kawa by a large margin. A further 9,376 fragments were identified only to large ruminate, but these probably also mainly represent cattle, as explained above.

Generally, the cattle remains are characterised by a high

[1] The 2001-2, 2007-2009, 2011 and 2014-15 seasons are all represented in the current study.

[2] Age estimation for fusion of limb bones according to Schmid 1972, Silver 1970 and collected by Reitz and Wing 1999.

[3] Sheep/goat according to Payne 1973, cattle according to Grant 1982 and Legge, 1992.

degree of fragmentation, which includes both pre- and post-depositional fractures. The former type is significantly more common, compared to any other species in the collection (based on a lack of colour variation between the fractures and bone surface). This is probably due to the larger size of the cattle body, skeleton, bones and attached muscle tissue, compared to, for example, sheep or goat, meaning that a higher degree of dismembering and carving is needed or desired to achieve a manageable size of cuts-of-meat from cattle.

The identified bones originate from across the body, representing all parts (see Table 3.2 & Figure 3.1 for an overview). The figure includes numbers for both cattle and the larger ruminates. The high number of body fragments from the latter mainly consist of rib and vertebrates. These are elements, which are difficult or impossible to identify to species level based on morphology, particularly when they

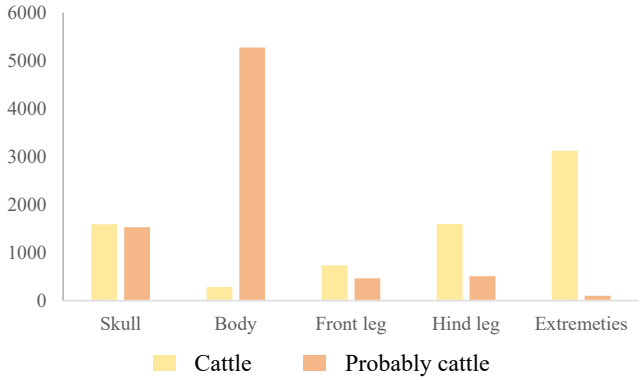

Figure 3.1. Distribution of body parts for cattle and large ungulate remains from Kawa.

are fragmented. Furthermore, there is a higher number of these elements in a single body compared to, for example, the long bones. Similarly, the relative high number of bones from the extremities are also consistent with a higher number of phalanges and carpal/tarsal bones in a single body. Regarding the extremities, the bones are also small and compact and thus do not suffer from the same high degree of fragmentation seen among the long bones, meaning that a higher percentage of the former is likely to be identified to species. The collection thus includes both bones associated with cuts of meat along with bones that are associated with the initial butchering and skinning of the animal, such as the phalanges. The pattern suggests that the identified bones represent both the initial kill and butchering of the animals, as well as the end-product of food consumption and disposal of household rubbish.

As mentioned on the previous page, nearly 1400 instances of cut- or chop-marks were registered for the Kawa collection and the overwhelming majority of these was found on cattle or large ruminate fragments. Only 60 were registered on other mammalian species, such as sheep/goat, dog and antelope. It therefore seems appropriate to discuss the results here (see Table 3.3 for an overview of types and the number of registered examples). Overall, the marks are evenly distributed between shallower cut-marks, which leave some form of a clear indentation or scar on the surface of the bone and chop-marks which severed the bone in two. The marks are widely and evenly distributed across the different parts of the body and between long bones. But there is an overrepresentation of marks on the ribs and first phalanges.

The first phalanges from cattle also display a very high degree of fragmentation, similarly to what was observed for the long bones and unlike the described pattern for small compact bones. The pattern of fractures suggests that the bones were hit centrally on the diafyse primarily on the dorsal side (in some instances leaving an identifiable chop-mark – PP4). In many cases the impact caused the bone to fracture in two or more fragments or it created a hole into the inner bone tissue (see Plate 3.1 for three examples of the latter). The most likely reason for the practice is extraction of the bone marrow, suggesting an intense and somewhat unusual use of this part of the skeleton. The other common

Plate 3.1. Three examples of fractured 1st phalanges from Kawa.

cut-mark on the first phalanges circles the proximal articulated surface and may well relate to the disarticulation of the phalanges from the upper part of the leg or extremities and may well have been in preparation for the fracturing of the bone for marrow extraction.

The marks on the ribs mainly include a cut/chop on the middle section of the rib body, suggesting a subdivision of this meat cut similarly to a back- or side-rib cut of beef. Based on location of marks the list appears to include marks related to both the initial butchering and skinning of the animals, followed by dismembering into body parts and a further division of the body into smaller meat cut along with a few likely filleting marks.

The overall impression based on the pattern of pre-deposition fracturing and the marks is one of uniformity and homogeneity, with a consistency in placement and in appearance. The pattern of fracturing suggests that most long bones were consistently chopped into at least two fragments or more. The evidence thus points to a uniform and consistent tradition of butchering and could suggest that these activities were carried out within a single tradition of butchery and of a similar skill level.

Due to the large collection of cattle remains, it was possible to use age distribution data from both teeth eruption and wear together with fusion data from the long bones. The former includes some 84 mandibles and suggests a primary kill-off interval during the second and third year of life,

with a smaller group of animals being killed both before and in the following three to four years after that period (see Figure 3.2). The data based on long bone fusion is less accurate than data based on teeth eruption and wear, but the former also include a lot more data (NISP 2,991) (see Table 3.4). The extensive dataset does to a large extent confirm the

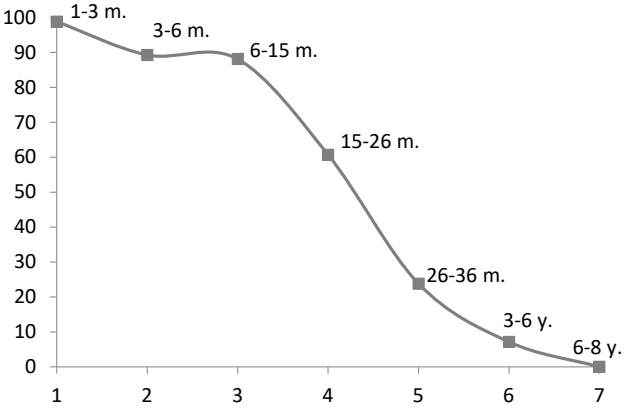

Figure 3.2. Kill-off profile for cattle based on tooth eruption and wear (NISP 84).

results from the teeth eruption and wear, with the majority of identified fusing bones group around two years and with the balance of unfused to fused changing during the medium fusion phase, which occurs between two and four years of age. Animals were clearly also butchered before and after this period and these appear to be more visible in the long bone fusion dataset. Included among these long bones are also a number of fragments, which could be attributed to either a pullus (13) or foetal (2) age category. The former may include animals that were intentionally butchered at a very early age, as two of the bones carry cut-marks and six have traces of burning on them. The latter category exclusively includes bones which are equal to or smaller than a newborn[4] and there is no sign of either cut-marks or burning on these two fragments. This confirms that the bones are likely to be from stillborn animals and, therefore, the bodies were probably not consumed. The presence of these bones does, however, suggest that at least some of the cattle bones found at Kawa represent local populations that were bred and kept in and around the city. But the low number (less than 0.01% of the total number of cattle and large ruminate bones) would suggest that a substantial part or most of the cattle populations were not present in Kawa itself for extended amounts of time before they were butchered. If the animals were mainly kept elsewhere, it would explain why hardly any bones from stillborn calves have been found in the archaeological record at Kawa.

Size distribution of the cattle remains comes mainly from the smaller compact bones due to the overall fragmentation of most long bones, leaving very few elements complete enough for any measurements to be taken (see Table 3.5 for the full overview). When bones are complete both fused and unfused were measured, and the state of fusion has, therefore, been registered when that information was available or relevant for the specific bone. A total of four metatarsal and one metacarpal was complete so a GL measurement could be taken: these gave a shoulder height of between 1.2m to 1.4m.[5] Generally the size of the cattle from Kawa appears to be comparable with the earlier cattle from the site of Kerma, where Louis Chaix has accumulated a very large corpus of osteometric data (Chaix 2007). The majority of these are based on the large scale deposits of cattle skulls in connection with burial rites, but some post-cranial data is available (see Table 3.6 for a direct comparison of measurement from adult metapodiums and calcaneus).

Horse/Donkey and Dromedary/Camel

Two further domesticated mammalian species belonging to the group of large ungulates were identified in the Kawa collections. Both were found in very limited numbers; 24 fragments were identified as equid (*Equus* sp.) and a further three were identified to dromedary/camel (*Camelus* sp.). Among the equid bones, a single distal tibia suggest that donkey (*Equus asinus*) is the probable species,[6] but the remaining fragments cannot be further identified to confirm this. Furthermore, the morphological criteria for species identification are not very strong for the tibia,[7] so only a probable identification is possible. The other fragments derive from the extremities, with just two limb bones represented and a significant number of tooth fragments (16), leaving an MNI of just one. When it is possible to identify the age category of the bone, they originate from an adult animal (3), suggesting that the animals were kept for secondary use such as beast of burden or similar. It was possible to measure four of the bones (see Table 3.7 for the result).

The three bones identified to dromedary/camel includes a pelvis, a scapula and an astragalus of which one is from an adult animal (with a fused diafyse). Unfortunately, none of these fragments were of a size or in a condition to make a species identification possible, but due to the geographical location and the time period in question they are very likely bones from a dromedary (*Camelus dromedarus*).[8] The very low number of dromedary remains fits well with results from other sites.[9] The pattern of very few dromedary bones and almost exclusively from adult animals, found in urban contexts, has elsewhere been interpreted as evidence for the animals primarily functioning in long distance caravan transport. They therefore rarely entered the urban centres and the bones only find their way into such contexts, when an animal was injured or old and subsequently was sold off for butchering and consumption.

None of the bones from dromedary or equids display any cut-marks, but two of the fragments identified to equid had been exposed to some heat and are registered as partly black burnt.

Caprines

The second largest group of bones originate from sheep (*Ovis aries*) and goat (*Capra hircus*). Most of these bones

[4] In comparison with a newborn calf present in the collection at the National Museum of Denmark – MK 495.

[5] Calculated according to Boessneck 1956.

[6] Species identification according to Johnstone 2004.

[7] Study of the different identification criteria.

[8] Species identification criteria was based on Steiger 1990.

[9] For example Studer and Schneider 2008.

could only be identified to sheep/goat (*Ovis/Capra* sp.) (201 fragments). However, a small portion of the bones could be identified to either sheep (4 fragments) or goat (59 fragments), meaning that there are nearly 15 goats to each identified sheep. Due to the much smaller collection of bones compared to cattle, less evidence is also available for the age distribution of these two species. The four fragments from sheep, included two fused elements (distal humerus and 2nd phalanges), which indicated a time-of-death above 3-13 months and 6-16 months, respectively. A second distal humerus was unfused, suggesting a very early time of death before the 3-13 months range.[10] The size of this bone is also comparable in size to a modern skeleton of a 10-day old sheep.[11] With no further evidence available for sheep, little can be concluded on the overall herding strategy at Kawa based on this very limited data.

For goat, more evidence is available and includes dental age data based on teeth eruption and wear stages, as well as much more data based on fusion categories for the post-cranial skeleton (see Table 3.8 for the latter). Two goat mandibles were determined to be 26-36 months old at time-of-death.[12] But as these are left/right sided and originate from a single context they could well represent a single individual.[13] Evidence from the long bone fusion categories is more substantial (NISP 55) and suggests that the overwhelming majority of the goats lived through their first year, but were butchered during their 2nd to 3rd year, with only some being killed slightly later. A somewhat similar pattern is seen among the sheep/goat remains (see Table 3.9) (NISP 58), with a lack of unfused remains in the youngest category and with a kill-off period during the 2nd and 3rd year. The sheep/goat evidence also suggest that a limited number of animals lived beyond the 3rd year, with a few fused elements in the late fusion category. The almost complete lack of evidence for butchering of goat (and sheep) during the first year of life and a primary kill-off period during the 2nd and 3rd year of life, suggest that the breeding and management of these animals at Kawa was primarily focused on a meat production strategy (Payne 1973). As a large urban centre, it could also be suggested that the observed pattern could be caused by some or many animals being brought into the town for slaughter and consumption and thus emphasizing the meat production profile, by only showing part of the full population profile. The complete lack of any foetal bones and the presence of only a single pullus bone in the Kawa collection could support this conclusion and, as such, this may only represent part of a more complex story of local production modes and populations of sheep and goat from a larger geographical area.

For the larger group of goat remains it was also possible to generate some size data on the bones. Apart from the very large collection of cattle, this was the only species where more than a single bone or two could be measured, (see Table 3.10). The majority of this osteometric data derives from the smaller and more compact bone. But based on the appearance of the fragmented long bones, that could not be measured, the caprines at Kawa appear to be similar to earlier population of Sudanese sheep and goat found at Kerma (Chaix and Grant 1987) and also at C-Group and Pangrave cemeteries (Bangsgaard 2010). These animals are characterised as being taller and more slender than their Levantine counterparts.

Gazelle and Antelope

The main group of wild mammalian or game species, includes antelope (*Oryx* sp.) and gazelle (*Gazella* sp.), but these are also found in very limited numbers. Antelope is represented by six fragments, which include elements from the skull, the hind legs and the extremities. Gazelle is represented by three fragments, all of which are from the extremity of the hind leg (carpals and metatarsal) and represent two different contexts. None of these fragments were complete enough or diagnostic enough for an identification to species level.

Carnivores

Carnivore remains include two domesticated or likely domesticated species, namely dog (*Canis familiaris*) and cat (*Felis* sp.). The bones from the latter could not be definitively identified as belonging to domesticated cat (*Felis domesticus*), but due to the size and morphology and the period of the site, that is likely to be the case. A total of 91 cat bones were identified in the Kawa collection. Despite the high number of remains, the MNI is only two. Four bones originate from three different contexts in Building F1 (contexts (FO6)77, (FP7)23 & (FP7)102), which are dated to periods 2 and 3. The remaining bones all belong to a single context, also in Building F1, but dated to period 3+ (context (FP7)82).[14] There is no overlap of elements among these bones and both morphology, size and age suggest that they represent a single juvenile animal (likely between 6 and 10 months old at time of dead).[15] No heat exposure or cut-marks of any kind including for skinning have been detected on the bones, suggesting that the cats at Kawa likely served for pest control or other activities, which would leave no evidence on the skeleton itself. A few of the bones from context (FP7)82 could be measured, along with two from (FP7)102, the results can be seen in Table 3.7.

Dog is represented by 14 fragments, found in four different areas[16] and representing an MNI of two individuals, but based on context and period three is probably more likely. The majority of the bones are from (AD5)/(AC5) and found inside Building A2, representing two animals based on the fusion data. The remainder of the bones are found in contexts from periods 1-3 and as such may represent more individuals. However, all the dog remains at Kawa appear to be from a medium to smallish-sized dog. It was possible

[10] Time-of-death age-categories are based on Schmid 1972 and Silver 1970, collected by Reitz & Wing 1999.

[11] Skeleton CN2208, in the Quaternary Zoological Collection, at the Natural History Museum of Denmark.

[12] Age determination based on Payne 1973.

[13] Grid square (ZH5), context 37, Building Z1.

[14] Period 1 – pre-Building F1; Period 2 – construction and use of the building; Period 3 – activities post-dating its abandonment.

[15] Among the remains the proximal metapodium, the distal humerus, proximal radius, scapula and the phalanges were fused and all other including tibia, ulna and femur were unfused. Age determination according to Smith 1969.

[16] Grid squares (AD5), (AC5), (FP6) and (FP7).

to measure two bones in the collection (see Table 3.7). A radius was complete enough to take a GL measurement (151mm), suggesting a shoulder height of 486mm.[17] This length and a Bd measure (20.7mm) from the same bones is consistent with a medium-sized dog of relative slender build. The bones are from across the body and apart from six bones which show limited signs of heat exposure, there are no signs of cut marks or other changes to the bones. The majority of bones are also from adult animals, the exception being an unfused proximal tibia (fusion around 1½ year) and a fusing proximal humerus (fusion around 1 year).[18] All in all the evidence is consistent with animals that likely served purposes which left no evidence on the bones themselves, such as guarding and herding dogs in and around the city of Kawa.

Two wild species of carnivores have been identified in the Kawa collection, namely a smaller fox (*Vulpes* sp.) with a single fragment (humerus) and a honey badger (*Mellivora capensis*), also represented by a single fragment (astragalus). Based on the size of the former, the bone represent one of the desert and mountain foxes of which there are three potential species (Rüppell's Sand fox, *Vulpes rueppelli*, Blandford's fox, *Vulpes cana* or Fennec fox, *Vulpes zerda*) based on the limited available modern habitat information (Aulagnier *et al.* 2009). Due to a lack of comparative skeletons and a similar size range between the species, it was not possible to identify this bone to species. However, all three species would be an indication that the desert hinterland of Kawa was also utilised by the inhabitants of Kawa.

An additional six bones have been attributed just to carnivore. These include ribs and vertebrates too fragmented or undiagnostic for species identification. All are from a medium-sized animal and could, therefore, belong to either badger, fox or a smallish dog.

Rodents

A single further mammalian species was identified at Kawa, namely a species of small rodent, represented by a single mandible without teeth present. The bone was registered in Sudan, where no comparative collection was available to aid identification, but based on the morphology and size of the mandible, it likely comes from a species of gerbil (*Gerbillinae*), of which there are multiple species represented in the general area today (Aulagnier *et al*. 2009).

Other fauna

The remaining collection from Kawa include at least a further seven species, distributed with a minimum of one species of amphibian, one species of reptiles, two species of birds and three species of fish (see Table 3.2 for an overview).

Most of these bones were identified in the Natural History Museum of Denmark, meaning that the large Quaternary Collections aided the identification to species for some bones, in other instances the bones could only be identified to family or genus, mainly due to a lack of the probable species needed for comparison. This is particularly the case for the freshwater fish where very little comparative material was available and as such these species cannot be either confirmed or excluded, leaving a genus or family identification.

Both the amphibian and reptile remains consist of just one bone each. The amphibian bone is a pelvis from a small frog or toad (*Anura*). The other fragment is another much larger pelvic fragment, which could be identified to Nile crocodile (*Crocodilus niloticus*).

The bird remains include a much larger group of bones, in total 42 fragments, of which 15 could be identified to near species or genus. The latter include a single tarsusmetatarsus from a small species of hawk (*Accipiter* sp.), which in size and morphology is consistent with the sparrow hawk (*Accipiter nisus*), making this the probable identification. However, as not all probable species were available in the collections, the identification is only the most likely. The remaining 14 identified bird fragments all belong to a large raven (*Corvus* sp.), leading to an identification to either common raven (*Corvus corax*) or thick-billed raven (*Corvus crassirostris*). All these raven bones are from a single building and appear to represent a single adult bird.[19] Among the remaining unidentified bird remains (in total 27), 12 are less diagnostic bones or smaller fragments of remains from the same context as the raven. These are consistent with the general size/morphology and are, therefore, likely to also be from the same single bird skeleton.

The final group of bones identified in the Kawa collection is the fish remains, a small group of 18 fragments of which over half could be identified to a specific family. The effort to identify the fish remains to species or genus was hampered by the lack of reference skeletons from all the freshwater species likely to be found in the Nile, as only a few representatives were available from each family, making it impossible to take the identification any further. All three families include one or more freshwater species, found in the Nile today. Two fragments (dentary and vertebrae) were identified to catfish (Bagridae), the size and morphology of the remains is consistent with an identification to a bayad (*Bagrus bayad*), but as other species could not be ruled out due to the mentioned lack of comparative skeletons, the identification is left as catfish. Seven vertebrates were identified to carp (Cyprinidae) and finally a single vertebra was identified to a species of lates perch (Latidae). The insignificant number of fish remains in the Kawa collection is notable and it must be assumed that part of the reason for this is the lack of fauna from sieved context in the current study,[20] particularly when the results are compared to evidence from other nearby sites.[21]

Fauna according to area of excavation

As mentioned in the introduction the faunal collection analysed from Kawa originate from 12 areas of excavation, but

[17] Calculation based on Koudalka 1885.

[18] Age determination according to Schmid 1972.

[19] Area (FP7), context 95 (and 93 for 1 bone), Building F1, room 1B

[20] A large number of samples was collected at Kawa for archaeobotanical analysis. When processed these samples should give an indication of what might have been missed from other contexts.

[21] See for example Osypińska 2014.

the number of bones from each of these vary considerably, as some are represented by under 100 fragments and for others more than 10,000 or even 25,000 fragments have been registered (see Table 3.11). This distribution poses potential problems regarding whether the smaller collections are representative for any given area and whether it is advisable to directly compare collections with such a variable number of bones. To counter this, collections have been grouped together for a visual representation of the distribution (see Figure 3.3 for the result). The collections were grouped according to geographic closeness, which left only two localities with very small collections, namely grid squares (FO6) and (BD2) with fewer than 100 bones each. The former collection originated from within a large administrative building (Building F1) and the latter originate from a single room in a multi-period dwellings (Building B14) (Welsby 2023e; 2023f).

Taking a closer look at the distribution of bones from within Area A, around 3,100 bones originate from the shrine, inside Building A2 around 29,300 bones were recovered, and finally from the two earlier buildings, Buildings A3 and A4, only around 1,500 bones and just over 800 fragments was found. It is likely that a substantial proportion of the bones recovered relate to the latest use phase of each building or as the building was going out of use, thus transforming the area into a convenient dumping ground for activities in surrounding rooms, buildings or areas. The the large collection of bones especially from Building A2 (Plates 3.2 & 3.3) however, is notable and hints at substantial meat processing or cooking activities going on inside or immediately around the building. The bones are almost exclusively from cattle with a smaller amount of sheep/goat[22] and the bones from cattle originate from across the body eliminating the possibility that they represent primary butchering debris where only extremities and possible skull fragments would be expected. It is possible that this large collection of cattle bones could be the result of, for example, feasting, sacrificial or communal eating activities related to the shrine next door (cf. Welsby 2023c, 37).

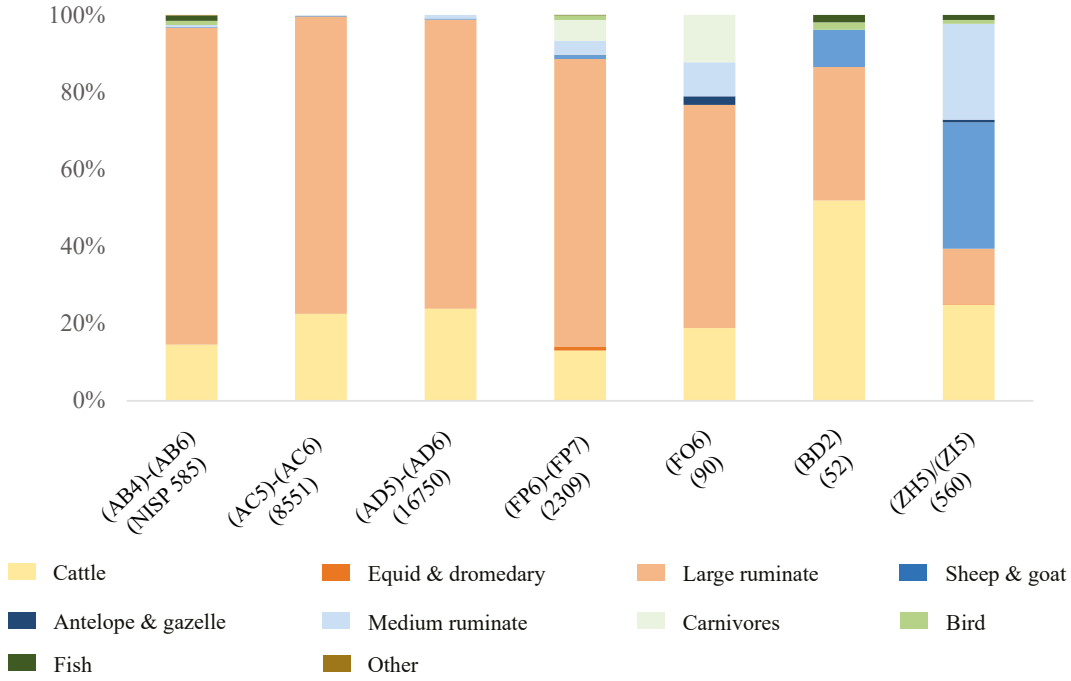

Figure 3.3. Distribution of species at Kawa according to excavation area. The carnivore group includes all dog and cat remains, the other group includes rodent, frog/toad and crocodile remains.

All the areas in grid squares (AB)-(AD) are heavily dominated by the cattle and large ruminate (probable cattle) remains, particularly for grid squares (AD5), (AD6), (AC5) and (AC6) where they probably contribute up to 99% of the bones. These areas also represented the most numerous collections and thus the main contributor to the overall distribution of faunal remains from the site. In grid squares (AB4), (AB5) and (AB6), cattle and probable-cattle "only" contributes 91%, of the total NISP, as the medium ruminates is proportionately more prominent and contributing with 7%. Area A include a series of buildings where the most prominent is Building A1, a shrine dated to the reign of Taharqo (represented by the collection from grid squares (AB4), (AB5) and (AB6)). Building A2 is located immediately next to the shrine and likely associated with it, whereas Buildings A3 and A4 are earlier buildings in the same location, one replacing the other (Welsby 2023d, 49ff.) and represented by the collection from (AC5), (AC6), (AD5) and (AD6).

One area does appear to display a significantly different distribution of faunal remains with many fewer cattle, namely the collection from (ZH5)-(ZI5), where the group of medium ruminates dominate the collection. Sheep and goat are represented by 183 elements, or 33% of the total NISP (560), which is clearly not a very large collection of bones and they all originate from inside or immediately around Building Z1, which is located at the northern edge of the site close to the riverbank. The specific use of the

[22] 4,958 cattle bones to fewer than 50 sheep/goat bones.

Plate 3.2. Animal bones in Building A2, Room II (photo: D. A. Welsby).

Plate 3.3. Animal bones within deposits seen in section in the doorway between Rooms VI and VII in Building A2 (photo: D. A. Welsby).

building is currently not clear, but the presence of many seal impressions could suggest some importance while other finds suggest a domestic function (Mahmoud Suliman Bashir and Welsby 2023).

Apart from the issue with smaller faunal collections potentially not being representative for the general activities of an entire area, there are also areas of Kawa that are not represented at all in this analysis. Future analysis of the large-scale collection from Kawa may produce new results, for example, from areas with a more varied distribution of species and/or from areas with other practices. Two such areas could be to the north east of Building F3 (rectangular kiln) and near the Eastern Kiosk. In both locations a dense spread of fragmented bones was visible on the present-day ground surface (Welsby 2023c, 41-42). The location of the faunal collection close to a kiln could reflect other types of activities, perhaps even relating to the use of the adjacent industrial installation.

Site R18

Excavations in the Kushite cemetery, site R18, at Kawa have added additional faunal material to the current collections. These remains were found among disarticulated human remains from several disturbed graves and tombs. Due to the burial context, these faunal remains may represent very different practices from those analysed above. It is, therefore, worth mentioning these bones despite this analysis being based purely on photographs of the remains that have only recently become available.

The small collection includes around 280 fragments with a majority being poorly preserved fragments of unidentified mammalian bone. The size and morphology suggest they originate from mainly large to medium mammals, which fits well with the species that could be identified, namely cattle[23] and a couple of possible sheep/goat/gazelle fragments.[24] The cattle remains are mainly small compact bones from the extremities, but a long bone (radius) was also identified, however the overrepresentation of the former type of bones could partly be due to their easier identification on the photographs. Among the large mammalian remains are also rib, skull and vertebrae fragments that could originate from cattle, suggesting that remains come from across the body.

One context [(JC2)2] includes up to 10 fragments of bird bones, representing at least three different bones (humerus, tibiatarsus, carpometacarpus). A near complete humerus suggests the presence of a likely new species in the collections, namely a dove (*Columba* sp.), the remaining bird bones may represent the same animal, but these cannot be morphologically identified.

The collection from site R18 includes several fragments which display signs of exposure to fire, some are burnt black others completely calcined. These remains are unidentified fragments as well as a few identified to cattle. Overall, the appearance of the collection with the species and bones identified, as well as the degree of fragmentation and signs of burning, appear similar in appearance to what is seen elsewhere at Kawa. This does not exclude that these particular remains were part of ritualised burial practices perhaps as food deposits inside the graves and tombs.

The excavations in the cemetery also uncovered *in-situ* faunal remains that provide evidence for the practice of faunal deposits. In grave (JG1)12 a cattle horn core was placed on the sloping surface of the descendary (Plate 3.4; Welsby 2023g, 321, pl. 11.229), whereas in grave (KE5)18 a lumbar vertebra, identified to hippopotamus or elephant, attests to the presence of non-domesticated species in the faunal deposits (Fathi Abdul Hamid Salih Khider 2001). But evidence from elsewhere suggests that the animal species present in such burial contexts often are the most common domesticated animals.[25]

Comparative faunal remains

An additional assemblage of bones has previously been studied from Kawa, originating from the 2000-2001 seasons and they were analysed by Kim Burrows.[26] The remains all originate from Areas A and B and although the analysis was never formally published, a report describes the preliminary results of the analysis. These mirror the findings from the

[23] Multiple fragments (radius, tarsals, carpals and phalanges) from (GD3)12, (GD3)92 and (GD3)125.

[24] Scapula fragment from (GD3)125 and possible tooth fragment from (JC3)1.

[25] See for example Osypińska 2007.

[26] Burrow unpublished.

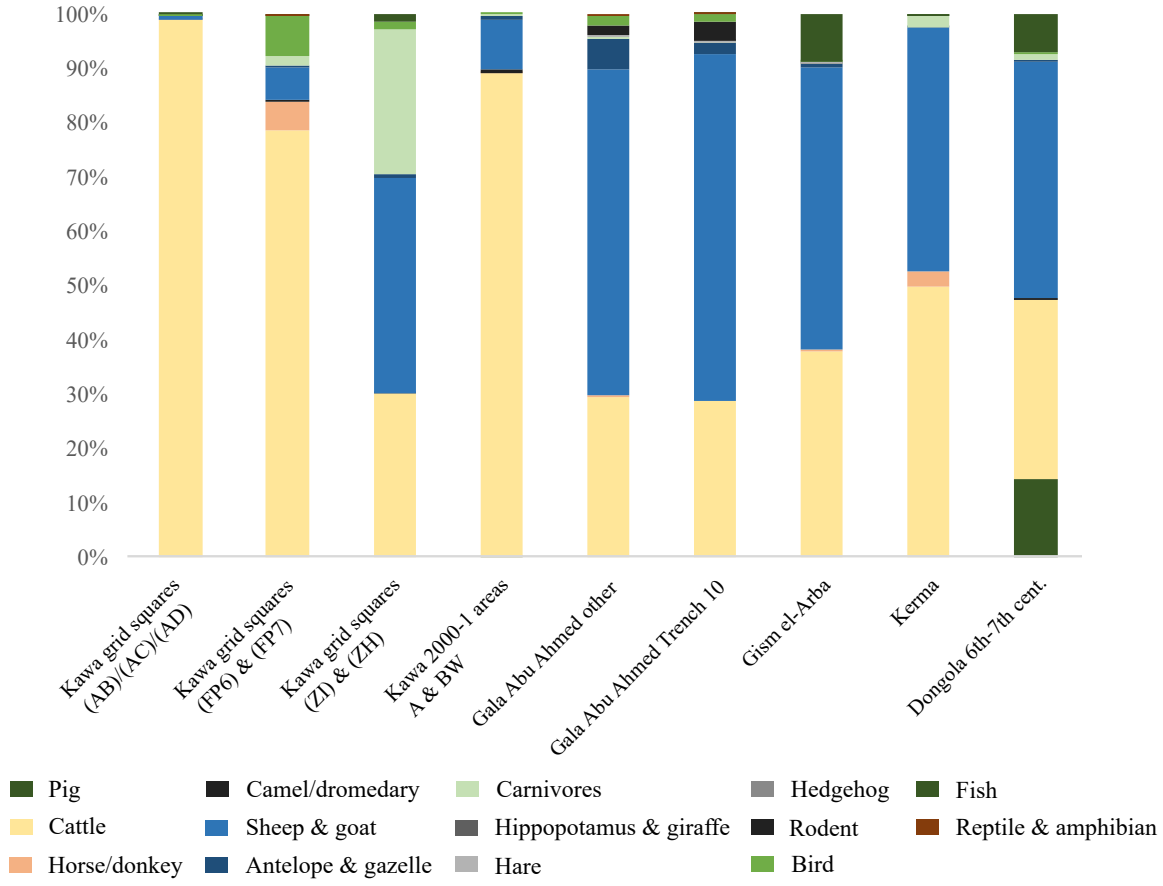

Figure 3.4. Distribution of species from comparative sites.

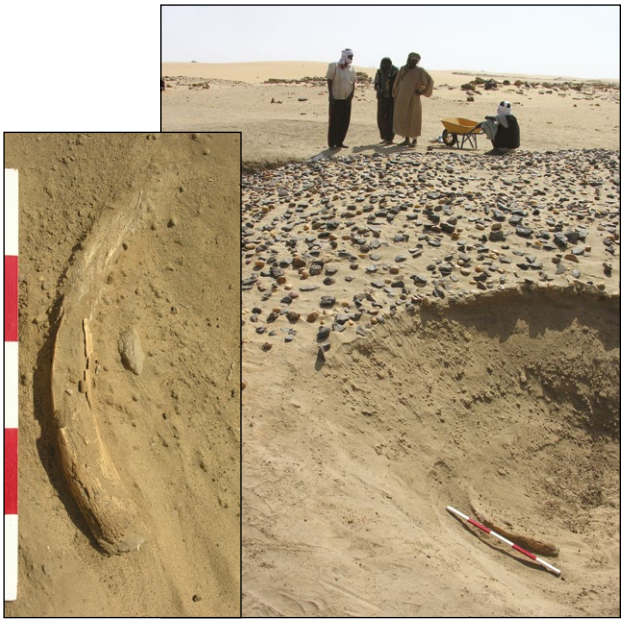

Plate 3.4. Cattle horn core resting on the sloping surface of the descendary in grave (JG1)12 (photos: D. A. Welsby).

current study as the collection is dominated by cattle with only some sheep and goat present (see Table 3.12 & Figure 3.4). But how do these faunal results from Kawa compare to results from elsewhere? Unfortunately, there is currently a limited number of published faunal analyses from the Kushite Period (Chaix 2008) and the majority of these include a much more limited number of bones, making it hard to reach any conclusions on the period in general.

Roughly contemporary to Kawa the southern pre-Napatan and Napatan fortress and likely trade post of Gala Abu Ahmed represents the single largest collection currently published from the period (NISP 16,645).[27] The site is not located in the Nile Valley proper, but around 110km to the west in the lower Wadi Howar. Multiple areas were excavated and these identified the large-scale fortifications, various buildings, storage facilities and structures for water management. The location away from the Valley is reflected through the high amount of wild fauna found here and mainly representing the local arid desert environment, such as fennec fox (*Vulpes zerda*) and dama gazelle (*Nanger dama*). In contrast to the Kawa collection, sheep and particularly goat dominates the assemblage, but with significant amounts of cattle still present. The authors suggest that the latter of the three species may have been brought in from the Nile Valley for slaughter, whereas sheep/goat were at least partly kept nearby due to the presence of neonate and infantile bones from these species. For cattle no such evidence for very young animals have been found at Gala Abu Ahmed (Linseele and Pöllath 2015). The largest trench (T10) uncovered a large complex structure and a substantial collection of fauna and as such Linseele and Pöllath separated that out from the rest of the collection, but the overall difference in distribution is limited for the main species (see Figure 3.4).

Louis Chaix has previously published a small Napatan

[27] This total number includes identified mollusc shells, which are not part of this study and thus not included in the table/figure.

TABLE 3.1. DISTRIBUTION OF MAMMALIAN SPECIES IDENTIFIED IN THE KAWA COLLECTION.

	Bos taurus	*Equus* sp.	*Camelus* sp.	*Oryx* sp.	Large ruminate	*Capra hircus*	*Ovis aries*	*Capra/Ovis* sp.	*Gazella* sp.	*Medium ruminate*	*Canis familiaris*	*Vulpes* sp	*Felissp.* (prob. *domesticus)*	*Mellivora capensis*	*Carnivora*	*Rodentia*	Large mammalia	Medium mammalia	Small mammalia	unidentified mammalia
Cranium	499			1	1232	3		30		50			21				180	8	1	2
Mandible	227				297	2		4		1	3		2			1	2			
Loose teeth	863	16		1	1427			8		24							14			1
Vertebrate	248				3187	1		47		25	1		29		5		1032	28	4	11
Ribs	25				2075			46		53			33		1		177	39	1	14
Sternum	7				8												5	2		
Scapula	122		1		228	4	1	2		5	1		1				11	1		
Humerus	208				154	6	2	4		1	1	1	2				22	2		
Radius	249	1			47	3		5		3	1		2				4			
rad uln	32				1			3									1			
Ulna	121				33	2		2					2				2			
Pelvis	302		1*		126	2		2			1		1				24	1		
Femur	246			1	210	5		6			2		2				15	6		
Tibia	167	1			169			8		3	3		2				11		1	
Patella	83				1			2			1		1							
Fibula													2					1		
Carpal/ Tarsal	852	4	1	1	22	4	1	20	2	3			2	1			1		1	
Metapo-dium	786	1		2	76	8		6	1	1			12				1			
Phalanges	1483	1			2	19		6					10							
Unidenti-fied					81												19941	326	6	467
Total	6520	24	3	6	9376	59	4	201	3	169	14	1	124	1	6	1	21443	414	14	495
Weight	138029	391	112	159	75778	406	25	696	5	296	126	2	85	1	6	0	61238	455	3	646

* probable identification

assemblage from the site of Kerma, which is mainly composed of cattle (78%) and caprines (17%), with dogs, equid, antelope and a galliform bird also represented. Enough cattle remains were found to suggest a main time of slaughter around 20 to 28 months, indicating an exploitation mainly aimed at meat (Chaix 1992). No NISP data has been published and it was, therefore, not possible to include the data in tables and figures.

Moving further back in time to the Kerma period further faunal data have been published by Louis Chaix, which include a large collection (NISP 7,614) from the rural site of Gism el-Arba. For comparative purposes the article also includes the then full basic faunal data set from the site of Kerma itself (NISP 35,142) (Chaix 2006), spanning a much longer and primarily earlier period than the above-mentioned data. At Kerma cattle dominates slightly over sheep and goat, whereas at Gism el-Arba the tables are turned slightly between the two groups. A somewhat similar distribution has been reported by Marta Osypińska from Makurite Dongola (NISP 3,436). In the early Makurian assemblage (6th – 7th century AD) sheep and goat dominate, again followed by cattle. The assemblage also includes a high number of fish, but the majority of these are described as "very small fish", so likely they represented a minor addition to the diet. The context is also a little unusual as all finds originate from the royal residence area (Osypińska 2014).

Concluding remarks

The current assemblage of fauna from Kawa represents a significant new contribution to our pool of information on animals and animal-use practices during the Kushite period. Previously only a single substantial collection has been published (Linseele and Pöllath 2015) along with a few other much smaller collections (see for example Chaix 1992), leaving a thin base for any meaningful

TABLE 3.2. DISTRIBUTION OF 0THER SPECIES IDENTIFIED IN THE KAWA COLLECTION.

	Anura	*Crocodilus niloticus*	*Accipeter sp. (nisus)*	*Corvus corax/crassirostris*	Unidentified birds	Bagridae	Cyprinidae	Latidae	Unidentified fish
Cranium									7
Dentary						1			
Vertebrate					2	1	7	1	
Spina									1
Humerus				1	2				
Radius				1	2				
Ulna				3	1				
Pelvis	1	1							
Femur				2	1				
Tibiatarsus					4				
Carpusmetacarpus				3	4				
Tarsusmetarsus			1	1					
Phalanges				3	3				
unidentifed					8				
Total	1	1	1	14	27	2	7	1	8
Weight	0	16	0	11	7	6	3	5	22

interpretations. Other large-scale datasets are available from both earlier and later periods,[28] however, it is entirely possible that faunal practices changed over time and between different geographical areas. The comparisons above certainly illustrate that there are significant species distribution differences between sites of the Kushite period as well as between earlier and later sites in the same region. In more recent times the final livestock count in 1963, before the completion of the Aswan Dam, states that there were 2,831 cattle, 19,335 sheep and 34,246 goats, a number of other domesticated mammals, birds and around 50,000 human inhabitants in that particular area of the Nile Valley which was about to be flooded (Adams 1977, 54).[29] It is worth noting the emphasis and dominant presence of sheep and goat when purely based on the number of animals, similar to what we see from most sites and periods

Most notable among the results from Kawa is, therefore, the high frequency of cattle compared to all other sites. Although cattle require frequent access to a good quality water source and, therefore, are not well adapted to very arid conditions, such as are found around Gala Abu Ahmed, there is still cattle present at all Kushite sites. Due to the desert conditions surrounding much of the northern part of the Nile Valley, it must be assumed that substantial cattle herds would have to be by or near to the Nile for good parts of the year. But Kawa is just one of many sites located along the river valley. It is also entirely possible that local environmental conditions changed over time, for example, with varying access to water based on fluctuations of the Nile floods and changes to the course of the river(s): in fact evidence suggests so (Macklin and Woodward 2001; Macklin *et al*. 2015; Sevara *et al*. 2023). Furthermore, to the north east of Kawa, the Seleim Basin (the southern extension of the Kerma Basin) could have created extensive grazing areas for livestock and smaller lakes for watering (Plate 3.5) through several months each year, particularly during years with higher Nile floods and improved environmental conditions (Macklin and Woodward 2001).

Changing environmental conditions do not necessarily explain the difference in distribution between Kawa and contemporary sites located in similar conditions. It might be suggested that part of the explanation for the extremely high amounts of cattle is instead to be found in the type of contexts that was included in the current analysis. At Kawa most of the faunal collection originates from area A and contexts near the shrine and particularly from the adjacent Building A2. If this building was in fact related to some form of large-scale feasting or offering and/or re-distribution of meat or prepared food activities, which likely related to the cult of the shrine, that might explain why cattle were found in such high concentrations here. Whatever was behind the accumulation and concentration of cattle remains, another interesting question relates to what practices would have to be in place to procure so many cattle. Were the animals brought in from a broader geographical area(s) or were they from local populations in the immediate hinterland of Kawa and what systems of trade and ownership was in place for this to be possible? We simply do not know enough about the Kushite context to answer those questions currently.

Plate 3.5. Sheep and goats grazing in the Seleim Basin with one of the seasonal lakes in the background (photo: D. A. Welsby).

Much of the other data generated from the Kawa collections regarding, for example, age distribution, size and

[28] See for example Chaix 2007; Bangsgaard 2010; Osypińska and Żurawski 2020.

[29] The other domesticated animals mentioned include 86 horses, 3,415 donkeys, 608 camels, 34,583 chickens, 27,520 pigeons and 1,564 ducks.

body-part distributions from the main species, along with the general list of species found at the site, appear to show a high degree of similarity with evidence from other sites. As such the evidence from Kawa is clearly set in the general Kushite context and studies in the future should make it possible to further our knowledge about the animal and animal-use practices during this period.

TABLE 3.3. DISTRIBUTION OF CUT- AND CHOP-MARKS IN THE KAWA COLLECTION ACCORDING TO BONE AND LOCATION.

Code	Description	Number
Cranium		
Ca1	Longitudinal cut on the concave side of hyale	3
Ca2	Transverse cut on ventral surface of atlas	1
Ca3	Transverse cut on the foramen magnum area, caudal end	1
Ca4	Dorsal-ventral cut across zygomaticus, immidate caudal of the orbit.	2
Ca5	Transverse (med-lat) cut into temporalis, near tuberculum articulare	1
Ca6	Transverse cut at the base of cornus	1
Mandible		
Ma1	Transverse cut on dorsal surface, between incisor and premolar	3
Ma2	Transverse cut caudal on ramus, below the condyle	5
Ma3	Transverse cut on the root of the incisor, caudal side	1
Cervical vertebrae		
Cv1	Transverse cut on top of arcus, next to a facet	10
Cv2	Transverse cut on axis, lateral-ventral side, near cranial articulated surface	9
Cv3	Transverse cut on middle corpus, ventral side	4
Cv4	Oblique cut on margin of cranial articulated surface of atlas	1
Cv5	Transverse cut on ventral surface of atlas	1
Cv6	Transverse-oblique chop through corpus	52
Thoracic vertebrae		
Tv1	Caudal-cranial or oblique cut at the base of the processus spinosus	27
Tv2	Transverse cut on the cranial articulated surface	6
Tv3	Transverse-oblique chop through corpus	20
Tv4	Transverse cut on middle corpus, ventral side	15
Lumbar vertebrae		
Lv1	Transverse cut on the top of arcus just caudal of the cranial facet	14
Lv2	Cranial-caudal cut along the base of the processus spinosus	1
Lv3	Transverse chop through caudal arcus	1
Lv4	Transverse cut on middle corpus, ventral side	31
Lv5	Transverse cut at base of processus spinosus	1
Lv6	Transverse-oblique chop through corpus	10
Sacrum vertebrae		
Sv1	Cranial-caudal cut on the transverse processes of the 1st sac. V	3
Sv2	Transverse cut on corpus ventral side	10
Ribs		
C1	Transverse cut on the rib head	14
C2	Transverse cut of the middle body	237
C3	Transverse cut immediately below the rib head	79
Scapula		
S1	Transverse cut along the neck of scapula	10
S2	Transverse cut at the start of spina scapulae	6
S3	Longitudinal cut along base of spine	10
Humerus		
H1	Transverse cut on the middle diafyse	10
H2	Transverse cut on anterior side of distal articulated surface	7
H3	Transverse cut on margin of olecranon fossa, medial side	6
H4	Transverse cut on margin of proximal articulated surface, anterior side	3
H5	Oblique-longitudal chop through lateral condyle	25

TABLE 3.3. DISTRIBUTION OF CUT- AND CHOP-MARKS IN THE KAWA COLLECTION ACCORDING TO BONE AND LOCATION. (CONT.).

Code	Description	Number
H6	Transverse cut on margin of olecranon fossa, lateral side	1
Radius & Ulna		
R1 rad	Transverse cut on anterior margin of radial tuberosity	14
R2 uln	Transverse cut on margin of the semi lunar notch	4
R3 uln	Transverse cut on distal tip of ulna	1
R4 rad	Transverse cut on distal diafyse, lateral-caudal side	7
R5 uln	Transverse cut on diaphyse	5
R6 uln	Transverse-oblique cut across the olecranon	3
R7 rad	Longitudial-oblique chop through diafyse	7
Pelvis		
P1	Transverse cut above the acetabulum on the ilium arm	20
P2	Transverse on the lip of acetabulum	7
P3	Transverse cut below the acetabulum on the pubis arm	18
P4	Transverse cut below the acetabulum on the ischium arm	6
P5	Transverse cut on the pubis arm, on opposite side from acetabulum	4
P6	Longitudinal cut (cranial-caudal) on lateral-dorsal side of the wing of sacrum	4
P7	Transverse-oblique cut on cranial side of sacrum, next to arcus articulated surface	8
P8	Transverse cut on the dorsal side of the ilium arm – opposite acetabulum	3
Femur		
F1	Oblique-longitudal chop, often start at distal condyles	22
F2	Transverse cut on the caudal diafyse, immediately above the distal epifyse	1
F3	Transverse cut on diafyse, caudal side	8
F4	Transverse and longitudinal cut in or on lip of caudal medial articulated surface	2
F5	Transverse cut on the neck of femur	2
F6	Cut on the ball of the femur head	2
Patella		
PA1	Longitudinal cut on anterior surface, proximal end	5
Tibia		
T1	Transverse cut on medial-caudal side, immediately above the distal articulated surface	6
T2	Oblique cut on the length of diafyse, caudal side	8
T3	Cut on or around the intercondylar tubercles	2
T4	Transverse cut on cranial side of the diaphyse at distal end of cristae tibiae	4
Astragalus		
A1	Transverse cut proximal, on the lateral condyle	3
Calcaneus		
CL1	Transverse cut on dorsal chest, midway between tuber calcis and articulated surface	4
CL2	Deep transverse cut on middle shaft, lateral side	2
CL3	Transverse cut on the ventral crest	2
CL4	Oblique cut on sus tali	1
Carpals & Tarsals		
TA1	Transverse cut on centrotarsale dorsal side	8
TA2	Transverse cut on tarsi sec et ter, dorsal side	1
TA3	Transverse cut on carpi quartum, volar side	1
TA4	Transverse cut on any tar car	28
Metapodium		
M1	Transverse cut on lateral and medial condyle of the distal articulated surface	6
M2	Transverse cut on the margin of the proximal articulated surface (cranial/lateral side)	44

TABLE 3.3. DISTRIBUTION OF CUT- AND CHOP-MARKS IN THE KAWA COLLECTION ACCORDING TO BONE AND LOCATION. (CONT.).

Code	Description	Number
M3	Transverse cut above/along distal articulated circumference, some circling the diaphyse	3
M4	Transverse cut on the cranial side of diafyse	22
M5	Transverse cut on the diaphyse below proximal articulated surface, caudal side	4
1st Phalanges		
PP1	Transverse cut immediately below proximal articulated surface, circling	10
PP2	Transverse cut on the proximal articulated surface.	153
PP3	Transverse cut circling the shaft, central or proximal of the distal articulated surface	11
PP4	Transverse-longitudial chop through the entire bone, angle-starting point varies	96
2nd Phalanges		
MP1	Transverse cut circling the shaft on middle shaft	1
MP2	Transverse cut on the caudal margin of proximal articulated surface	3
MP3	Transverse cut on caudal diafyse	3
MP4	Transverse cut on caudal-medial side of distal articulated surface	1
MP5	Transverse-longitudial chop through, angle and starting point varies	7
3rd Phalanges		
DP1	Transverse cut on middle of articulated surface	2

TABLE 3.4. DISTRIBUTION OF STATE-OF-FUSION FOR CATTLE LONG-BONES FROM KAWA.

Age is based on Schmid 1972 and Silver 1970, collected by Reitz & Wing 1999.

	Unfused	Fusing	Fused	Age Category
Early Fusion				
Metapodium proximal	3	-	287 (*)	Before birth
Pelvis	107	2	100	6-10 months
Scapula	16	2	70	7-10 months
Radius proximal	7 (^)	5	126	12-18 months
Humerus distal	37 (*)	21	94	12-18 months
Phalanges 1	174 (“)	16	413	18-24 months
Phalanges 2	54 (¤)	28	229	18-24 months
Medium Fusion				
Tibia distal	70	2	17	24-30 months
Metacarpal distal	213 (¤)	3	124	24-36 months
Calcaneus	73	2	11	36-42 months
Late Fusion				
Femur proximal	6	1	120	42 months
Humerus proximal	40	2	6	42-48 months
Radius distal	109 (*^)	2	9	42-48 months
Ulna proximal	38		4	42-48 months
Ulna distal	12	1	6	42-48 months
Femur distal	6	5	85	42-48 months
Tibia proximal	63	4	3	42-48 months
Vertebrates	100	3	60	84-108 months

The following symbols have been used:
(*) – 1 pullus, (¤) – 3 pullus, (“) – 4 pullus bones, (^) – 1 foetal bone

TABLE 3.5. ALL MEASUREMENTS TAKEN ON CATTLE REMAINS IN THE KAWA COLLECTION.

Humerus				
Fusion	Code	Measurement	Code	Measurement
u fus	Bd	80.7	BT	73.8
u fus	Bd	67	BT	63.9
u fus	Bd	90.2	BT	78.5
u fus	Bd	92	BT	86
u fus	Bd	91	BT	79.4
u fus	Bd	88.5	BT	81.3
u fus	Bd	82.8	BT	76.5
u fusi	Bd	72.7	BT	67.3
u fus	Bd	76.9	BT	73.2
u fus			BT	76.2
u fusi			BT	61
u fus			BT	73.4
u fus			BT	79.1
u fus			BT	75.3
u fus			BT	74.6
Radius				
Fusion	Code	Measurement	Code	Measurement
fus u	BP	74.7	BFp	69.2
fus u	BP	72.6	BFp	68
fus u	BP	75	BFp	68.5
fus u	BP	77.9	BFp	71.6
fus u	BP	67.9	BFp	65.3
fus u	Bp	90.6	BFp	83.4
fus u	Bp	85.9	BFp	78.1
fus u	Bp	88.1	BFp	81.7
fus u	Bp	78	BFp	72.2
fus u	Bp	86.6	BFp	77.8
fus u	Bp	73.4	BFp	68.8
fus u	Bp	79.5	BFp	72.7
fus u	Bp	64.3	BFp	60.8
fus u	Bp	82.6	BFp	75.5
fus u	Bp	74.45		
fusi u	Bp	71.5	BFp	67.2
u fus	Bd	87.1	BFd	807
u fus	Bd	76.4	BFd	70.8
u fus	Bd	79.3	BFd	65.1
u fus	Bd	73.4	BFd	66.4
u fus	Bd	72.3		
u unf	Bd	63.5	BFd	52
u unf	Bd	66.8	BFd	53.5
u unf	Bd	68.3	BFd	54
u unf	Bd	65.8	BFd	50.3
u unf	Bd	59.6	BFd	55.2
u unf	Bd	59.2	BFd	51
u unf	Bd	65.7	BFd	64.3
u unf	Bd	73.5	BFd	56.6
u unf	Bd	65.6	BFd	52

Fusion	Code	Measurement	Code	Measurement
u unf	Bd	65.7	BFd	58.8
u unf	Bd	82.7	BFd	76.1
u unf	Bd	72	BFd	64.2
u unf	Bd	66.2	BFd	56.6
u unf	Bd	71.6	BFd	68.3
u unf	Bd	65.5	BFd	55.6
u unf	Bd	63.7	BFd	57.8
u unf	Bd	74.6	BFd	59.1
u unf	Bd	74.2	BFd	60.2
u unf	Bd	70	BFd	56.5
u unf	Bd	72.8	BFd	66.3
u unf			BFd	56

Tibia

Fusion	Code	Measurement
u fus	Bd	67.1
u fus	Bd	64.3
u fus	Bd	63.9
u fus	Bd	75
u fusi	Bd	87.6
u unf	Bd	55
u unf	Bd	46.3
u unf	Bd	55.8

Astragalus

	Code	Measurement	Code	Measurement	Code	Measurement	Code	Measurement	Code	Measurement
	GLl	72.5	GLm	67.5	Dl	41.1	Dm	40.2	Bd	40.2
	GLl	64.6	GLm	58.3	Dl	33.2	Dm	32.6	Bd	39.4
	GLl	62.7	GLm	57.8	Dl	33.4	Dm	31.8	Bd	38
	GLl	66.5	GLm	59.6	Dl	36	Dm	34.7	Bd	40.8
	GLl	67.3	GLm	63	Dl	37	Dm	39.5	Bd	45.4
	GLl	69.8	GLm	61.9	Dl	36.9	Dm	36.8	Bd	49.9
	GLl	66	GLm	60.3	Dl	36.8	Dm	35.2	Bd	42.5
	GLl	63	GLm	58.3	Dl	33.4	Dm	34.2	Bd	38.9
	GLl	65.9	GLm	58.4	Dl	34.8	Dm	33.8	Bd	39.6
	GLl	58.3	GLm	53.3	Dl	29.9	Dm	29.5	Bd	32.6
	GLl	66.9	GLm	61.4	Dl	35.7	Dm	35.8	Bd	43
	GLl	66.3	GLm	59.4	Dl	37	Dm	36.9	Bd	43.2
	GLl	68.6	GLm	61.8	Dl	36.8	Dm	35.1	Bd	40.1
	GLl	67	GLm	61.8	Dl	36.2	Dm	35.8	Bd	37.8
	GLl	61.9	GLm	55.8	Dl	34.3	Dm	33	Bd	37.7
	GLl	64.1	GLm	58.3	Dl	33.4	Dm	34.2	Bd	39.2
	GLl	69.8	GLm	64.1	Dl	35.7	Dm	37.8	Bd	43.5
	DLl	67.1	DLm	61.9	DL	36	Dm	35.4	Bd	41.4
	GLl	64.6	GLm	59.7	Dl	33.3	Dm	33.4	Bd	37.8
	GLl	66.9	GLm	61.1	Dl	35.2	Dm	35.7	Bd	40.3
	GLl	68.5	GLm	62.7	Dl	38.1	Dm	31.5	Bd	43.9
	GLl	69.6	GLm	63.6	Dl	38.8	Dm	39	Bd	45
	GLl	68.9	GLm	62.9	Dl	38.5	Dm	39	Bd	41.9
	GLl	71.4	GLm	63.9	Dl	39.8	Dm	38.9	Bd	44.9
	GLl	66.4	GLm	59.3	Dl	37.1	Dm	36.1	Bd	41.1

	Code	Measurement	Code	Measurement	Code	Measurement	Code	Measurement	Code	Measurement
	GLl	68.5	GLm	61.9	Dl	37.7	Dm	37.9	Bd	42.6
	GLl	66.5	GLm	60.1	Dl	34.6	Dm	33.7	Bd	39.3
	GLl	72.6	GLm	66.1	Dl	38.2	Dm	38	Bd	43.6
	GLl	66.5	GLm	60.6	Dl	35.4	Dm	36.6	Bd	40
	GLl	69	GLm	61.8	Dl	37.6	Dm	37.2	Bd	41
	GLl	63.2	GLm	57.9	Dl	36.2	Dm	40.2	Bd	48.1
	GLl	66.3	GLm	61.8	Dl	36.6	Dm	35.4	Bd	39
	GLl	69.2	GLm	62.4	Dl	36.9	Dm	34.8	Bd	43.6
	GLl	73.4	GLm	65.2			Dm	37.5	Bd	45.5
	GLl	69.6	GLm	64			Dm	38.8	Bd	47
	GLl	65.9	GLm	60.6			Dm	35	Bd	38.3
	GLl	63	GLm	57.1	Dl	33.3			Bd	37.6
	GLl	67.6	GLm	61.7	Dl	36.4			Bd	41.6
	GLl	73.8	GLm	67.5	Dl	39.5			Bd	50.1
	GLl	64.5	GLm	60.3	Dl	33.5			Bd	37.8
	GLl	67.8	GLm	61.5	Dl	35.4			Bd	40.5
	GLl	63.7	GLm	60.2	Dl	33.4			Bd	37.9
	GLl	69.28	GLm	63.45	Dl	38.86			Bd	43.92
	GLl	68.6	GLm	60.8			Dm	34.8	Bd	40.8
	GLl	66.8			Dl	36.1			Bd	40.9
	GLl	68.4			Dl	37.8	Dm	37.6		
			GLm	67.3	Dl	40	Dm	40.8	Bd	46.6
			GLm	57.6			Dm	34.8	Bd	37.4
			GLm	58.1			Dm	34.6	Bd	42
			GLm	65			Dm	38.9	Bd	45.1

Calcaneus

Fusion	Code	Measurement	Code	Measurement
unf	GL	122.5	GB	39
unf	GL	118.9	GB	36
unf	GL	120.3	GB	43.3
unf	GL	136.2	GB	43.5
unf	GL	118.9	GB	41.5
fus	GL	125.4	GB	39.7
fus	GL	146.6	GB	47.8
fus	GL	129	GB	46
unf	GL	112.2	GB	36.5
unf	GL	95.5	GB	34.8

Metacarpal

Fusion	Code	Measurement	Code	Measurement
fus unf	GL	186.3	Bp	48.7
fus u			Bp	59.8
fus u			Bp	57.8
fus u			Bp	64.2
fus u			Bp	54.2
fus u			Bp	62.3
fus u			Bp	52.5
fus u			Bp	53
fus u			Bp	56.8
fus u			Bp	55.5

Fusion	Code	Measurement	Code	Measurement
fus u			Bp	57.3
fus u			Bp	49.8
fus u			Bp	53.6
fus u			Bp	67.8
fus u			Bp	57.3
fus u			Bp	57.3
fus u			Bp	56.1
fus u			Bp	63.2
fus u			Bp	62.7
fus u			Bp	59.5
fus u			Bp	62.6
fus u			Bp	53
fus u			Bp	64.7
fus u			Bp	63.7
fus u			Bp	49.4
fus u			Bp	49
fus u			Bp	53.8
fus u			Bp	50.7
fus u			Bp	58.7
fus u			Bp	65.7
fus u			Bp	57.3
fus u			Bp	50.3
fus u			Bp	57.3
fus u			Bp	51.8
fus u			Bp	64.6
fus u			Bp	51.8
fus u			Bp	63.9
fus u			Bp	68.1
fus u			Bp	50.9
fus u			Bp	60.9
fus u			Bp	66.4
fus u			Bp	55.8
fus u			Bp	66.9
fus u			Bp	70.4
fus u			Bp	57.4
fus u			Bp	61
fus u			Bp	63.2
fus u			Bp	55.6
fus u			Bp	64.1
fus u			Bp	69.2
fus u			Bp	57.5
fus u			Bp	58.9
fus u			Bp	49.3
fus u			Bp	52.7
fus u			Bp	62.9
fus u			Bp	60.3
u fus	DD	23.3	Bd	64.8
u fus	DD	24.8	Bd	63.1
u fus			Bd	57

	Code	Measurement	Code	Measurement
u fus			Bd	69.4
u fus			Bd	69.6
u fus			Bd	73.4
u fus			Bd	61
u fus			Bd	64.3
u fus			Bd	65.6
u fus			Bd	63.3
u fus			Bd	62.9
u fus			Bd	67.4
u fus			Bd	51.3
u fus			Bd	58.2
u fus			Bd	61.8
u fus			Bd	64
u fus			Bd	63
u fus			Bd	58.3
u fus			Bd	59.6
u fus			Bd	66.1
u fus			Bd	62.4
u fus			Bd	64.8
u fus			Bd	63.5
u fus			Bd	62.9
u fus			Bd	62.5
u fus			Bd	69.8
u fus			Bd	63.3
u fus			Bd	61.6
u fus			Bd	69.2
u fus			Bd	73.1
u fus			Bd	72.4
u fus			Bd	60.4
u fus			Bd	66
u fus			Bd	60.7
u unf	DD	19.9	Bd	57.3
u unf			Bd	62
u unf			Bd	55.4
u unf			Bd	62.8
u unf			Bd	56.8
u unf			Bd	50.8
u unf			Bd	55.3

Metatarsal

Fusion	Code	Measurement	Code	Measurement	Code	Measurement	Code	Measurement	Code	Measurement
fus fus	GL	244.7	Bp	49.3	SD	23.3	DD	25.6	Bd	58.2
fus unf	GL	232.1	Bp	41.2	SD	21	DD	22.4		
fus unf	GL	208.4	Bp	41.7	SD	18.6	DD	17.6	Bd	43.8
fus unf	GL	209	Bp	40.8	SD	18.4	DD	17.6	Bd	44.8
fus u			Bp	37.5	SD	20				
fus u			Bp	47.3	SD	27.4				
fus u			Bp	44.7						
fus u			Bp	44.7						
fus u			Bp	50.1						

Fusion	Code	Measurement	Code	Measurement	Code	Measurement	Code	Measurement	Code	Measurement
fus u			Bp	43.5						
fus u			Bp	39.5						
fus u			Bp	43.4						
fus u			Bp	44.6						
fus u			Bp	42.2						
fus u			Bp	43.8						
fus u			Bp	53						
fus u			Bp	51.4						
fus u			Bp	53.7						
fus u			Bp	52.2						
fus u			Bp	48.1						
fus u			Bp	49.2						
fus u			Bp	46.5						
fus u			Bp	45.9						
fus u			Bp	48.8						
fus u			Bp	45.1						
fus u			Bp	43.2						
fus u			Bp	49.2						
fus u			Bp	40.3						
fus u			Bp	50.8						
fus u			Bp	45						
fus u			Bp	49.9						
fus u			Bp	47.9						
fus u			Bp	51.7						
fus u			Bp	41.9						
fus u			Bp	41						
fus u			Bp	39						
fus u			Bp	43.8						
fus u			Bp	40.4						
fus u			Bp	42.7						
fus u			Bp	55.5						
fus u			Bp	51.5						
fus u			Bp	44.7						
fus u			Bp	51.9						
fus u			Bp	47.5						
fus u			Bp	44.3						
fus u			Bp	53.4						
fus u			Bp	48.8						
fus u			Bp	54.8						
fus u			Bp	55.8						
fus u			Bp	42.4						
fus u			Bp	50.3						
fus u			Bp	51						
fus u			Bp	44						
fus u			Bp	53.8						
fus u			Bp	55.6						
u fus							DD	26.9	Bd	61.9
u fus							DD	26.4	Bd	59.4
u fus							DD	28.8	Bd	66.7

Fusion	Code	Measurement	Code	Measurement	Code	Measurement	Code	Measurement	Code	Measurement
u fus							DD	28.6	Bd	62.5
u fus							DD	26.8	Bd	59.5
u fus							DD	24.7	Bd	54.2
u fus							DD	26.5	Bd	58.4
u fus							DD	24.3	Bd	58.2
u fus									Bd	62.4
u fus									Bd	57.9
u fus									Bd	63.9
u fus									Bd	56.9
u fus									Bd	59.5
u fus									Bd	66.2
u fus									Bd	65.9
u fus									Bd	59.1
u fus									Bd	56.7
u fus									Bd	60.9
u fus									Bd	60.8
u fus									Bd	64
u fus									Bd	58
u fus									Bd	58.6
u fus									Bd	64.3
u fus									Bd	56.1
u fus									Bd	65.7
u fus									Bd	65
u fus									Bd	61.8
u fus									Bd	61.2
u fus									Bd	64.2
u fus									Bd	64.7
u fus									Bd	58.3
u fus									Bd	53
u fus									Bd	60.1
u fus									Bd	58.5
u fus									Bd	60.7
u fus									Bd	56.3
u fus									Bd	61.8
u fus									Bd	64.2
u fus									Bd	63.4
u fus									Bd	60.3
u fus									Bd	68.2
u fus									Bd	59.7
u unf									Bd	52.5
u unf									Bd	51.7
u unf									Bd	40.9
u unf									Bd	50.3

Patella

	Code	Measurement	Code	Measurement
	GL	63.5	GB	52.3
	GL	62.6	GB	48
	GL	64.3	GB	51.2
	GL	62.2	GB	47.9

	Code	Measurement	Code	Measurement
	GL	60.4	GB	44.1
	GL	61	GB	44
	GL	55.3	GB	42.7
	GL	61.5	GB	49.8
	GL	70.4	GB	58.4
	GL	71.7	GB	61.6
	GL	66.3	GB	53.4
	GL	65.1	GB	46.5
	GL	57.7	GB	44.6
	GL	58.4	GB	43.1

1st Phalanges

Fusion	Code	Measurement	Code	Measurement	Code	Measurement	Code	Measurement	Code	Measurement
fus	GLpe	57.4	Bp	26.6	Dp	31.2	SD	21.6	Bd	25.7
fus	GLpe	63	Bp	31	Dp	37.3	SD	25.6	Bd	30.4
fus	GLpe	57.8	Bp	29.8	Dp	32.3	SD	25.1	Bd	28.8
fus	GLpe	58.4	Bp	25.6	Dp	30	SD	20.8	Bd	25.7
fus	GLpe	62.5	Bp	26.9	Dp	32.8	SD	23.2	Bd	27.3
fus	GLpe	57.1	Bp	25.5	Dp	29.3	SD	20.4	Bd	25.3
fus	GLpe	58.4	Bp	29.6	Dp	33.6	SD	24.7	Bd	27.5
fus	GLpe	62.8	Bp	31	Dp	36.3	SD	25.4	Bd	30.6
fus	GLpe	62.8	Bp	26.3	Dp	30.5	SD	22	Bd	25.7
fus	GLpe	60.6	Bp	26.5	Dp	31.2	SD	22.7	Bd	26.6
fus	GLpe	62.9	Bp	30.9	Dp	32.3	SD	27.3	Bd	29.6
fus	GLpe	66.2	Bp	29.2	Dp	35.6	SD	24.7	Bd	28.3
fus	GLpe	64.3	Bp	29.6	Dp	36.1	SD	25.8	Bd	29.9
fus	GLpe	61.6	Bp	29.8	Dp	34	SD	24.5	Bd	28.7
fus	GLpe	62.8	Bp	26.2	Dp	31.1	SD	22.6	Bd	27.1
fus	GLpe	64.7	Bp	30.3	Dp	34.7	SD	26.5	Bd	30.4
fus	GLpe	61.7	Bp	32.1	Dp	34	SD	27.1	Bd	31
fus	GLpe	60.8	Bp	29.2	Dp	33.1	SD	22.6	Bd	28.9
fus	GLpe	64.2	Bp	31.3	Dp	35.3	SD	26.4	Bd	29.5
fus	GLpe	60.2	Bp	28.8	Dp	32.5	SD	26.2	Bd	29.3
fus	GLpe	61.5	Bp	26.6	Dp	30.9	SD	21.1	Bd	23.5
fus	GLpe	63.2	Bp	31.9	Dp	33.3	SD	25	Bd	29.2
fus	GLpe	60.8	Bp	25.6	Dp	30.2	SD	21	Bd	25.9
fus	GLpe	63.2	Bp	27.8	Dp	33.6	SD	24.3	Bd	28.4
fus	GLpe	61.6	Bp	26.6	Dp	31.9	SD	22.2	Bd	26.9
fus	GLpe	63	Bp	27.4	Dp	32.6	SD	22.4	Bd	27
fus	GLpe	57.7	Bp	27.9	Dp	29.1	SD	22.7	Bd	25
fus	GLpe	60.1	Bp	28.4	Dp	29.8	SD	24.3	Bd	25.8
fus	GLpe	64.7	Bp	32.5	Dp	37.9	SD	26.5	Bd	29.8
fus	GLpe	63.4	Bp	27.2	Dp	30.9	SD	23.5	Bd	26.7
fus	GLpe	60.4	Bp	30.6	Dp	36.1	SD	26.7	Bd	31.3
fus	GLpe	67.7	Bp	34.2	Dp	37.9	SD	29.2	Bd	33
fus	GLpe	63.7	Bp	28.2	Dp	32.4	SD	24.7	Bd	29.7
fus	GLpe	54.5	Bp	26.2	Dp	27.7	SD	21.8	Bd	24.8
fus	GLpe	60.9	Bp	30.6	Dp	33.3	SD	24.8	Bd	28.6
fus	GLpe	61.6	Bp	27.5	Dp	29.8	SD	21.8	Bd	25.8
fus	GLpe	63.8	Bp	33.5	Dp	34.1	SD	26.5	Bd	30.9

	Code	Measurement	Code	Measurement	Code	Measurement	Code	Measurement	Code	Measurement
fus	GLpe	64.9	Bp	32.4	Dp	34.8	SD	26.2	Bd	31.6
fus	GLpe	57.3	Bp	27.5	Dp	29.8	SD	22.2	Bd	28.1
fus	GLpe	68.1	Bp	30	Dp	36.3	SD	25.4	Bd	29.9
fus	GLpe	62.3	Bp	30.5	Dp	36	SD	26.5	Bd	32.3
fus	GLpe	66.1	Bp	31.3	Dp	34.5	SD	26.5	Bd	31.6
fus	GLpe	66.1	Bp	31.5	Dp	35.8	SD	24.6	Bd	27.7
fusi	GLpe	54.7	Bp	22	Dp	26.5	SD	19	Bd	22.7
fusi	GLpe	59.2	Bp	25.4	Dp	30	SD	21.3	Bd	25.8
fusi	GLpe	60.5	Bp	27.2	Dp	33.4	SD	22.6	Bd	27.7
unf	GLpe	52.4	Bp	22.4	Dp	26.3	SD	18.3	Bd	22.4
unf	GLpe	54.5	Bp	22.2	Dp	26.6	SD	18.8	Bd	21.8
unf	GLpe	54.3	Bp	21.7	Dp	26.7	SD	19.1	Bd	22.5
unf	GLpe	58.7	Bp	24.2	Dp	29.4	SD	20.3	Bd	25.2
unf	GLpe	51.8	Bp	22.9	Dp	25.5	SD	19.5	Bd	23.7
fus	GLpe	63	Bp	29.5	Dp	34.4			Bd	28.7
fus	GLpe	56.6	Bp	28	Dp	30.8			Bd	27.6
fus	GLpe	59.3	Bp	31	Dp	32.5			Bd	29.8
fus	GLpe	66.78	Bp	31.59	SD	28.73			Bd	33.89
fus	GLpe	65.8			Dp	37.3	SD	27	Bd	31.2
unf	Glpe	59.7			Dp	31.3	SD	22.8	Bd	28
fus	GLpe	59.6	Bp	27.2	Dp	28.9	SD	22.8		
fus	GLpe	68.7	Bp	31.2	Dp	35.2	SD	27.2		
fus	GLpe	70.3	Bp	32.8	Dp	34.8	SD	26.5		
unf	GLpe	56.9	Bp	23.7	Dp	28.9	SD	22.2		
unf	GLpe	63.7	Bp	29.3	Dp	24.8	SD	27.5		
unf	GLpe	57.2	Bp	25.6	Dp	29.5	SD	21.3		
unf	GLpe	56.1	Bp	24.9	Dp	26.8	SD	21		
fus	GLpe	61.6	Bp	31.9	Dp	33.7				
fus	GLpe	56.5	Bp	30.6	Dp	28.4				
fus	GLpe	57.3	Bp	30	Dp	28.4				
fus	GLpe	58.6	Bp	29.6	Dp	30.6				
fus	GLpe	60.4	Bp	28.8	Dp	30.8				
fus	GLpe	57.8	Bp	29	Dp	32.6				
fus	GLpe	59	Bp	28.4	Dp	32				
fus	GLpe	59.1	Bp	29.1	Dp	31				
fus	GLpe	64.8	Bp	27.7	Dp	32.8				
fus	GLpe	58.5	Bp	28.4	Dp	30.7				
fus	GLpe	59.3	Bp	30.2	Dp	33.8				
fus	GLpe	60.4	Bp	26	Dp	30.9				
fus	GLpe	63.7	Bp	31.7	Dp	34.9				
fus	GLpe	62.8	Bp	26.3	Dp	32.7				
fus	GLpe	60	Bp	26.9	Dp	32.2				
fus	GLpe	60.3	Bp	26.2	Dp	31				
fus	GLpe	60.9	Bp	26.8	Dp	30.6				
fus	GLpe	58.2	Bp	30.6	Dp	33.8				
fus	GLpe	58.6	Bp	29.3	Dp	31.8				
fus	GLpe	56.8	Bp	26.6	Dp	31.2				
fus	GLpe	56.2	Bp	27.3	Dp	30.1				
fus	GLpe	61	Bp	24.1	Dp	29.1				

	Code	Measurement	Code	Measurement	Code	Measurement
fus	GLpe	63.8	Bp	25.2	Dp	31.6
fus	GLpe	64.9	Bp	31	Dp	35.7
fus	GLpe	61.8	Bp	28.8	Dp	34.4
fus	GLpe	58.4	Bp	27.3	Dp	30.5
fus	GLpe	54.8	Bp	24	Dp	27.1
fus	GLpe	62.3	Bp	29.7	Dp	34.9
fus	GLpe	58.6	Bp	27.6	Dp	31.5
fus	GLpe	60.4	Bp	28.77	Dp	32.7
fus	GLpe	58.1	Bp	27.9	Dp	31.1
fus	GLpe	56.9	Bp	26.4	Dp	30.8
fus	GLpe	58.1	Bp	27.5	Dp	31.5
fus	GLpe	59.7	Bp	26.8	Dp	30.1
fus	GLpe	64.9	Bp	28	Dp	31.9
fus	GLpe	62.1	Bp	29.3	Dp	31.1
fus	GLpe	61.3	Bp	28	Dp	31.5
fus	GLpe	58.3	Bp	31.2	Dp	34.8
fus	GLpe	60.9	Bp	25.6	Dp	30.8
fus	GLpe	60	Bp	26.7	Dp	31.3
fus	GLpe	62.1	Bp	28.5	Dp	33
fus	GLpe	60.5	Bp	27.3	Dp	32.1
fus	GLpe	64	Bp	27.2	Dp	31.8
fus	GLpe	59.8	Bp	28.8	Dp	33
fus	GLpe	61.9	Bp	29.4	Dp	34.4
fus	GLpe	65.8	Bp	29.8	Dp	37.5
fus	GLpe	56.2	Bp	28	Dp	30
fus	GLpe	57.6	Bp	26.9	Dp	29.4
fus	GLpe	54.2	Bp	25.6	Dp	27.8
fus	GLpe	61.2	Bp	28	Dp	32.8
fus	GLpe	59.4	Bp	28.6	Dp	30.6
fus	GLpe	59.9	Bp	28.1	Dp	31.6
fus	GLpe	57.9	Bp	27.5	Dp	30.5
fus	GLpe	61.3	Bp	28.6	Dp	31.7
fus	GLpe	58.8	Bp	30.2	Dp	32.5
fus	GLpe	57.4	Bp	26.2	Dp	29.6
fus	GLpe	60.3	Bp	27.4	Dp	31.6
fus	GLpe	59.5	Bp	28.9	Dp	32.4
fus	GLpe	61.7	Bp	29.1	Dp	32.9
fus	GLpe	64.3	Bp	29	Dp	34.8
fus	GLpe	63.4	Bp	33.4	Dp	37.3
fus	GLpe	62.4	Bp	26.4	Dp	31.6
fus	GLpe	60.4	Bp	30.7	Dp	31.7
fus	GLpe	62.3	Bp	27.2	Dp	33.5
fus	GLpe	61.6	Bp	27.9	Dp	31.3
fus	GLpe	58.7	Bp	27.8	Dp	32.1
fus	GLpe	60.9	Bp	27.8	Dp	31.1
fus	GLpe	61	Bp	25.2	Dp	32.8
fus	GLpe	57.3	Bp	27	Dp	30.4
fus	GLpe	56.8	Bp	27.6	Dp	31.4
fus	GLpe	57.2	Bp	25.8	Dp	30

Fusion	Code	Measurement	Code	Measurement	Code	Measurement
fus	GLpe	57.9	Bp	26.3	Dp	32
fus	GLpe	57.7	Bp	25.5	Dp	33.1
fus	GLpe	65.9	Bp	30.6	Dp	35.4
fus	GLpe	61.8	Bp	34.8	Dp	37
fus	GLpe	63.9	Bp	34.1	Dp	35.5
fus	GLpe	64.4	Bp	29.1	Dp	34.6
fus	GLpe	61.9	Bp	32.8	Dp	33.6
fus	GLpe	54.4	Bp	29.3	Dp	30.8
fus	GLpe	62.2	Bp	26.7	Dp	32
fus	GLpe	67.2	Bp	30.7	Dp	33
fus	GLpe	60.4	Bp	28.1	Dp	31.1
fus	GLpe	55	Bp	24.8	Dp	30.1
fus	GLpe	65.4	Bp	33.2	Dp	34.3
fus	GLpe	65.2	Bp	28.9	Dp	32.7
fus	GLpe	60.1	Bp	28.9	Dp	28.8
fus	GLpe	61.6	Bp	28.9	Dp	30.3
fus	GLpe	61.8	Bp	26.3	Dp	30.4
fus	GLpe	58.1	Bp	26.8	Dp	29.8
fus	GLpe	61.4	Bp	25.5	Dp	29.1
fus	GLpe	65.3	Bp	35.3	Dp	36.3
fus	GLpe	68.4	Bp	30.6	Dp	34.8
fus	GLpe	64.1	Bp	30.6	Dp	32.2
fus	GLpe	61.6	Bp	32.7	Dp	33.7
fus	GLpe	67.8	Bp	39.4	Dp	41.9
fus	GLpe	62.6	Bp	27.1	Dp	33.2
fus	GLpe	62.5	Bp	29.7	Dp	32
fus	GLpe	57.5	Bp	25.2	Dp	28.4
fus	GLpe	64	Bp	26.9	Dp	33.6
fus	GLpe	66.8	Bp	30.6	Bd	37.1
fus	GLpe	63.9	Bp	29.9	Dp	34.1
fusi	GLpe	60.9	Bp	25.4	Dp	31.5
unf	GLpe	49.9	Bp	23.5	Dp	26
unf	GLpe	58.1	Bp	25.6	Dp	29.6
unf	GLpe	60.1	Bp	28	Dp	33.1
unf	GLpe	60.4	Bp	28.7	Dp	33.2

2nd Phalanges

Fusion	Code	Measurement	Code	Measurement	Code	Measurement	Code	Measurement
fus	GL	37.4	Bp	23.6	SD	19	Bd	20.2
fus	GL	41.6	Bp	27.2	SD	21.2	Bd	22.9
fus	GL	46	Bp	30.8	SD	25.1	Bd	27.4
fus	GL	38.8	Bp	24.8	SD	20	Bd	21.3
fus	GL	40.8	Bp	27.4	SD	21.5	Bd	23.8
fus	GL	42.4	Bp	32.3	SD	26.2	Bd	26.6
fus	GL	40.2	Bp	28.3	SD	23.4	Bd	26.7
fus	GL	39.4	Bp	25.6	SD	20.3	Bd	21.9
fus	GL	45.1	Bp	32.6	SD	28.1	Bd	30
fus	GL	39.6	Bp	26.6	SD	23	Bd	24.3
fus	GL	48.3	Bp	31	SD	25	Bd	27

Fusion	Code	Measurement	Code	Measurement	Code	Measurement	Code	Measurement
fus	GL	42.2	Bp	32.2	SD	24.8	Bd	28.4
fus	GL	39.5	Bp	28.9	SD	23.3	Bd	25.5
fus	GL	40.4	Bp	30.2	SD	24.4	Bd	26.8
fus	GL	37	Bp	28.6	SD	22.1	Bd	23.6
fus	GL	42.4	Bp	27.8	SD	23	Bd	23.8
fus	GL	39.4	Bp	28.3	SD	23.4	Bd	26.2
fus	GL	41	Bp	26.6	SD	21.1	Bd	22.7
fus	GL	38	Bp	25.8	SD	21	Bd	22.4
fus	GL	39.4	Bp	24.9	SD	20.7	Bd	21.9
fus	GL	38.5	Bp	24.8	SD	20.2	Bd	21
fus	GL	38.7	Bp	29.1	SD	23.9	Bd	25.2
fus	GL	46.6	Bp	34.8	SD	29.3	Bd	29.9
fus	GL	41.5	Bp	25.5	SD	20.7	Bd	23.9
fus	GL	41.5	Bp	26.5	SD	21	Bd	22
fus	GL	37	Bp	24.4	SD	19.3	Bd	21.3
fus	GL	38.7	Bp	29.2	SD	23	Bd	25.2
fus	GL	39.7	Bp	27.7	SD	21.9	Bd	24.2
fus	GL	39.2	Bp	29	SD	24	Bd	25.2
fus	GL	40.9	Bp	26.3	SD	20.4	Bd	23.8
fus	GL	38.7	Bp	26.4	SD	20.2	Bd	22.3
fus	GL	39.2	Bp	29.7	SD	23.2	Bd	25.8
fus	GL	45	Bp	31	SD	25.3	Bd	28.3
fus	GL	38.2	Bp	27.3	SD	22.3	Bd	24.7
fus	GL	35	Bp	25.7	SD	20.5	Bd	22
fus	GL	38.2	Bp	24.9	SD	20.7	Bd	22.2
fus	GL	40.6	Bp	28.3	SD	23.6	Bd	24.6
fus	GL	40	Bp	27.9	SD	22.9	Bd	24.2
fus	GL	39.2	Bp	28	SD	22.3	Bd	23.5
fus	GL	40.3	Bp	27.5	SD	22	Bd	23.8
fus	GL	39.2	Bp	24.2	SD	19.4	Bd	21.6
fus	GL	43.8	Bp	28.9	SD	22.6	Bd	23.3
fus	GL	40.9	Bp	25.8	SD	22.2	Bd	23.4
fus	GL	40.8	Bp	27.2	SD	22.4	Bd	24.2
fus	GL	40.4	Bp	31.1	SD	25.1	Bd	26.7
fus	GL	35.7	Bp	28.4	SD	23.6	Bd	24.4
fus	GL	39.3	Bp	30.2	SD	24.4	Bd	25.8
fus	GL	42.1	Bp	28.7	SD	23.4	Bd	26
fus	GL	41.9	Bp	27.1	SD	21.5	Bd	22.9
fus	GL	41.4	Bp	26.2	SD	21.7	Bd	23.4
fus	GL	40.7	Bp	26.1	SD	22.5	Bd	23.9
fus	GL	44.7	Bp	31.1	SD	25.3	Bd	27.5
fus	GL	40.8	Bp	26.7	SD	21.8	Bd	23.7
fus	GL	39.1	Bp	27.9	SD	22.6	Bd	23.6
fus	GL	38.8	Bp	27	SD	21.8	Bd	22.4
fus	GL	39.8	Bp	26.8	SD	21.6	Bd	23.6
fus	GL	38.9	Bp	26.6	SD	21.9	Bd	22.8
fus	GL	39.2	Bp	28.8	SD	22.9	Bd	24.3
fus	GL	39.1	Bp	31.3	SD	24.1	Bd	26.8
fus	GL	39.3	Bp	27.1	SD	22.5	Bd	23

Fusion	Code	Measurement	Code	Measurement	Code	Measurement	Code	Measurement
fus	GL	38.3	Bp	27.6	SD	21.7	Bd	23.5
fus	GL	42.2	Bp	31	SD	25.9	Bd	26.7
fus	GL	38.8	Bp	30.6	SD	24.7	Bd	26.9
fus	GL	38.1	Bp	27.5	SD	20.4	Bd	21.9
fus	GL	39.1	Bp	26.1	SD	21.7	Bd	22.5
fus	GL	40.9	Bp	29.1	SD	24	Bd	23.7
fus	GL	39.9	Bp	29.5	SD	22.3	Bd	25.2
fus	GL	39.7	Bp	27.8	SD	22	Bd	25
fus	GL	40	Bp	25.8	SD	20.5	Bd	21.5
fus	GL	42.7	Bp	29	SD	23.8	Bd	27.1
fus	GL	43.4	Bp	28.8	SD	24.1	Bd	26.1
fus	GL	43.8	Bp	29.2	SD	25	Bd	24.9
fus	GL	41.8	Bp	31.4	SD	26.6	Bd	28.3
fus	GL	39.5	Bp	30.5	SD	24.6	Bd	28.7
fus	GL	37.4	Bp	28.2	SD	22.5	Bd	25
fus	GL	41.9	Bp	33.6	SD	27.8	Bd	31.3
fus	GL	39.4	Bp	27.8	SD	22.6	Bd	24.9
fus	GL	39.7	Bp	26	SD	21.8	Bd	24
fus	GL	43.8	Bp	29.8	SD	22.3	Bd	25.2
fus	GL	40.3	Bp	30.4	SD	25.3	Bd	27.7
fus	GL	44.2	Bp	28.1	SD	22.5	Bd	25.3
fus	GL	38.5	Bp	25	SD	20.3	Bd	21.2
fus	GL	39.3	Bp	27.2	SD	22.5	Bd	24
fus	GL	42.3	Bp	32.4	SD	26.9	Bd	30.6
fus	GL	44	Bp	32.1	SD	26.2	Bd	28.6
fus	GL	45.1	Bp	31.2	SD	25.5	Bd	28.4
fus	GL	42.2	Bp	30.7	SD	24	Bd	24.3
fus	GL	46.5	Bp	31.2	SD	27	Bd	27.9
fus	GL	48.7	Bp	31	SD	48.6	Bd	30
fus	GL	42.5	Bp	28.7	SD	24.3	Bd	24.7
fus	GL	42.6	Bp	30.9	SD	25	Bd	27.6
fus	GL	42.6	Bp	28	SD	23.1	Bd	25.5
fus	GL	45.6	Bp	31.7	SD	27.2	Bd	28
fus	GL	45.8	Bp	29.3	SD	25.4	Bd	26
fus	GL	38	Bp	27.7	SD	22.3	Bd	23.1
fus	GL	44.3	Bp	30.7	SD	23.7	Bd	26.2
fus	GL	46.3	Bp	30.1	SD	24.7	Bd	26.9
fus	GL	38.1	Bp	27	SD	22.3	Bd	24.1
fus	GL	48.1	Bp	30.5	SD	25.4	Bd	29.6
fus	GL	49.4	Bp	34.3	SD	29.3	Bd	32.6
fus	GL	40.1	Bp	26.5	SD	23.1	Bd	23.4
fus	GL	48.1	Bp	32.6	SD	28.3	Bd	29.6
fus	GL	42.4	Bp	28.6	SD	24.1	Bd	25.8
fus	GL	37.8	Bp	27	SD	21.1	Bd	22.8
fus	GL	41.7	Bp	29.5	SD	24.5	Bd	23.8
fus	GL	45.9	Bp	31.1	SD	26.3	Bd	27.9
fus	GL	40.4	Bp	28.7	SD	23.3	Bd	25.8
fus	GL	38.9	Bp	29.4	SD	25.3	Bd	24.4
fus	GL	41.4	Bp	30.4	SD	25.2	Bd	28.1

Fusion	Code	Measurement	Code	Measurement	Code	Measurement	Code	Measurement
fus	GL	45.6	Bp	29.1	SD	23.6	Bd	24.2
fus	GL	40.5	Bp	31.2	SD	25	Bd	27.2
fus	GL	46	Bp	29.5	SD	24.9	Bd	27.7
fus	GL	46.3	Bp	33.5	SD	27.9	Bd	28.3
fus	GL	40.9	Bp	30.6	SD	24.5	Bd	25.5
fus	GL	37.6	Bp	28.1	SD	22.6	Bd	25.1
fus	GL	40.8	Bp	28.8	SD	24.3	Bd	24.9
fus	GL	37.7	Bp	28.4	SD	21.8	Bd	24.7
fus	GL	42.9	Bp	28.2	SD	24.1	Bd	24.9
fus	GL	39.7	Bp	26.9	SD	21.3	Bd	22.8
fus	GL	37.31	Bp	26.18	SD	22.53	Bd	23.54
fus	GL	37.35	Bp	26.5	SD	23.07	Bd	23.86
fus	GL	40.93	Bp	31.05	SD	24.63	Bd	26.32
fus	GL	43.67	Bp	28.36	SD	24.41	Bd	27.59
fus	GL	47.07	Bp	34.01	SD	27.08	Bd	28.23
fus	GL	41.9	Bp	28.68	SD	22.92	Bd	24.6
fus	GL	38.17	Bp	26.79	SD	22.27	Bd	25.87
fus	GL	45.3	Bp	33.5	SD	25.4	Bd	26.5
fus	GL	45.9	Bp	29	SD	23.6	Bd	25.8
fus	GL	44.9	Bp	28.6	SD	22.9	Bd	22.5
fus	GL	43.6	Bp	29.1	SD	23.4	Bd	25.8
fus	GL	42	Bp	28.8	SD	23.1	Bd	25.3
fus	GL	41.8	Bp	29.2	SD	24.7	Bd	25.9
fus	GL	44	Bp	29.7	SD	25.3	Bd	26.9
fus	GL	39.7	Bp	27.9	SD	21.2	Bd	24.3
fus	GL	41.7	Bp	26	SD	20.5	Bd	22.6
fus	GL	40.2	Bp	28	SD	22.5	Bd	23.5
fus	GL	38.9	Bp	28	SD	24	Bd	24.8
fus	GL	40	Bp	305	SD	24.6	Bd	26
fus	GL	38.4	Bp	25.9	SD	21.2	Bd	23.4
fus	GL	41.8	Bp	32.3	SD	25.9	Bd	27.6
fus	GL	40.6	Bp	29.3	SD	24.7	Bd	25.2
fus	GL	44.9	Bp	30.6	SD	25	Bd	26.4
fus	GL	45.9	Bp	32	SD	25.6	Bd	25.9
fus	GL	39.5	Bp	29	SD	22.9	Bd	25.8
fus	GL	36.7	Bp	26.3	SD	20.9	Bd	23.4
fus	GL	37.7	Bp	25.6	SD	20.7	Bd	22.3
fus	GL	40.1	Bp	30.7	SD	24.8	Bd	25.8
fus	GL	42.6	Bp	30.7	SD	25	Bd	26.7
fus	GL	38.5	Bp	26.2	SD	20.6	Bd	23.1
fus	GL	35.3	Bp	25.7	SD	21.2	Bd	22.4
fus	GL	38.2	Bp	27.3	SD	21.5	Bd	23.4
fus	GL	39.2	Bp	26.1	SD	21.6	Bd	23
fus	GL	37.2	Bp	29.2	SD	24.3	Bd	26.2
fus	GL	42.8	Bp	31.9	SD	24.1	Bd	26
fus	GL	39.3	Bp	29.2	SD	22.5	Bd	22.9
fus	GL	43.4	Bp	30.1	SD	23.7	Bd	26.5
fus	GL	45	Bp	32.8	SD	26.3	Bd	29
fus	GL	44	Bp	28	SD	23.2	Bd	24.9

Fusion	Code	Measurement	Code	Measurement	Code	Measurement	Code	Measurement
fus	GL	39.8	Bp	29.6	SD	23.5	Bd	24.3
fus	GL	49	Bp	34.4	SD	25.8	Bd	27.7
fus	GL	43.8	Bp	33.9	SD	27.6	Bd	28.9
fus	GL	40.3	Bp	27.6	SD	22.66	Bd	24.9
fus	GL	42.5	Bp	30.9	SD	27	Bd	29.7
fus	GL	47.4	Bp	31.7	SD	28.4	Bd	28.6
fus	GL	46.9	Bp	31.4	SD	26.2	Bd	26.9
fus	GL	42.9	Bp	32.8	SD	27.4	Bd	29.3
fusi	GL	43.8	Bp	28	SD	23.3	Bd	24.1
fusi	GL	43.4	Bp	29.4	SD	23.3	Bd	24.2
fusi	GL	39.5	Bp	25.7	SD	21.2	Bd	22.6
fusi	GL	42.9	Bp	27.5	SD	23.5	Bd	23.6
fusi	GL	41.4	Bp	27.5	SD	22.2	Bd	23.6
fusi	GL	43.9	Bp	29.3	SD	24.5	Bd	25.2
fusi	GL	41.6	Bp	30.1	SD	23.3	Bd	24.5
fusi	GL	38.1	Bp	24.3	SD	19.4	Bd	21.2
fusi	GL	35.9	Bp	25.6	SD	19.8	Bd	23.4
fusi	GL	37.8	Bp	23.8	SD	17.7	Bd	19.8
fusi	GL	42.01	Bp	26.54	SD	21.01	Bd	22.66
fusi	GL	40.4	Bp	25.5	SD	20.4	Bd	23.2
fusi	GL	38.5	Bp	23.8	SD	20.3	Bd	20.5
fusi	GL	36.3	Bp	26	SD	19.2	Bd	21.4
fusi	GL	36.4	Bp	24.9	SD	20.6	Bd	22.2
fusi	GL	38.7	Bp	27.2	SD	22	Bd	22.3
fusi	GL	39.9	Bp	23.4	SD	19.1	Bd	20.8
fusi	GL	38.8	Bp	25.1	SD	20.5	Bd	24
fusi	GL	44.8	Bp	27.8	SD	22.3	Bd	24.7
fusi	GL	42	Bp	25.8	SD	21.4	Bd	22.8
fusi	GL	42	Bp	24.9	SD	19	Bd	21.9
unf	GL	39.5	Bp	24.1	SD	18.6	Bd	20.7
unf	GL	39.2	Bp	27	SD	21.2	Bd	23.2
unf	GL	41.7	Bp	25.3	SD	20.6	Bd	23.1

3rd Phalanges

	Code	Measurement	Code	Measurement	Code	Measurement
	DLS	55.2	Ld	44.2	MBS	20.4
	DLS	65.3	Ld	54	MBS	21.6
	DLS	53	Ld	42.9	MBS	17.3
	DLS	60.4	Ld	46.2	MBS	20.8
	DLS	60.2	Ld	46.3	MBS	19.5
	DLS	59.4	Ld	47.1	MBS	19
	DLS	55.9	Ld	47	MBS	17.8
	DLS	49.1	Ld	39.8	MBS	16
	DLS	70.9	Ld	52.6	MBS	23.1
	DLS	71.2	Ld	52.9	MBS	28.2
	DLS	51.9	Ld	40.9	MBS	15.4
	DLS	49.6	Ld	41.1	MBS	17.1
	DLS	54.3	Ld	46	MBS	17.6
	DLS	52.9	Ld	45.5	MBS	18.4
	DLS	54.6	Ld	46	MBS	18.3

	Code	Measurement	Code	Measurement	Code	Measurement
	DLS	50.2	Ld	39.2	MBS	15.7
	DLS	51.7	Ld	42.9	MBS	18.7
	DLS	56.2	Ld	46.8	MBS	19.9
	DLS	50.6	Ld	41.2	MBS	17.2
	DLS	60.6	Ld	47.3	MBS	21.1
	DLS	67.2	Ld	52.7	MBS	24.4
	DLS	64	Ld	49.6	MBS	23.8
	DLS	55.9	Ld	43.1	MBS	18.6
	DLS	54.1	Ld	45	MBS	19.8
	DLS	57.6	Ld	46.5	MBS	20.8
	DLS	67.2	Ld	55	MBS	21.2
	DLS	68.2	Ld	51	MBS	24.5
	DLS	55.2	Ld	41.9	MBS	19.7
	DLS	55.6	Ld	45.9	MBS	19.3
	DLS	57.6	Ld	45	MBS	17.6
	DLS	57.8	Ld	42.9	MBS	20.9
	DLS	61.9	Ld	47.8	MBS	19.3
	DLS	59.4	Ld	48.1	MBS	20
	DLS	56.1	Ld	43	MBS	19.2
	DLS	62	Ld	52.1	MBS	23.4
	DLS	56	Ld	47	MBS	16.9
	DLS	58.4	Ld	47.6	MBS	18.9
	DLS	58	Ld	49.5	MBS	19.3
	DLS	79	Ld	58.2	MBS	25.3
	DLS	78.2	Ld	60.4	MBS	29.6
	DLS	50	Ld	38	MBS	16.1
	DLS	65.5	Ld	49.4	MBS	23
	DLS	62.7	Ld	49.4	MBS	20.1
	DLS	65.3	Ld	51	MBS	21.3
	DLS	69	Ld	51.6	MBS	21.9
	DLS	60.4	Ld	43.7	MBS	20.3
	DLS	59.9	Ld	44.3	MBS	18.8
	DLS	62.2	Ld	51.6	MBS	21.3
	DLS	60.8	Ld	47.3	MBS	19.9
	DLS	64	Ld	53.1	MBS	21.1
	DLS	52.9	Ld	40.5	MBS	16.9
	DLS	73.6	Ld	56.6	MBS	24.2
	DLS	68.4	Ld	49.4	MBS	23.6
	DLS	68.7	Ld	53.3	MBS	27.5
	DLS	73.8	Ld	57.3	MBS	24
	DLS	82.9	Ld	61.5	MBS	32.3
	DLS	58.1	Ld	46.3	MBS	19.7
	DLS	73.7	Ld	56.9	MBS	24.8
	DLS	73.4	Ld	57.1	MBS	24.1
	DLS	57.8	Ld	48.8	MBS	18.6
	DLS	53.5	Ld	44.8	MBS	17.2
	DLS	62	Ld	53	MBS	20.4
	DLS	58.5	Ld	44.3	MBS	19.3
	DLS	62.4	Ld	51.2	MBS	21.1

	Code	Measurement	Code	Measurement	Code	Measurement
	DLS	55.7	Ld	47.2	MBS	18.7
	DLS	64.8	Ld	52.6	MBS	22
	DLS	77.5	Ld	60.1	MBS	24.8
	DLS	81.7	Ld	62.7	MBS	31
	DLS	77.9	Ld	59.6	MBS	25.8
	DLS	83.1	Ld	62.6	MBS	30.3
	DLS	51.1	Ld	42.3	MBS	17.4
	DLS	79.1	Ld	58.3	MBS	28.2
	DLS	61.6	Ld	50.7	MBS	21.5
	DLS	64.9	Ld	52.4	MBS	21.4
	DLS	72	Ld	53.8	MBS	24.2
	DLS	71.3	Ld	54.4	MBS	23.6
	DLS	50.7	Ld	41.3	MBS	16.3
	DLS	66	Ld	48.4	MBS	22
	DLS	90	Ld	67.4	MBS	30.5
	DLS	79.8	Ld	65.8	MBS	30.3
	DLS	82.1	Ld	58.7	MBS	27.4
	DLS	72.45	Ld	54.71	MBS	19.93
	DLS	84.77	Ld	62.88	MBS	29.7
	DLS	69.56	Ld	54.83	MBS	26.24
	DLS	56.18	Ld	56.06	MBS	17.3
	DLS	56.78	Ld	46.35	MBS	20.44

TABLE 3.6. DIRECT COMPARISON OF MEASUREMENTS OF THE METAPODIUMS AND CALCANEUS BETWEEN THE SITES OF KAWA AND KERMA. THE LATTER MEASUREMENTS ARE PUBLISHED BY LOUIS CHAIX (CHAIX 2007).

KAWA		mean	min.	max.	number
Metcarpal	Bp	58.55	49	70.4	55
	Bd	64.02	51.3	73.4	34
Metatarsal	GL	223.55	20.84	244.7	4
	Bp	46.91	39	55.8	55
	Bd	60.87	53	68.2	43
Calcaneus	GL	133.67	125.4	146.6	3
KERMA		mean	min.	max.	number
Metcarpal	Bp	59.46	52	67.2	13
	Bd	59.39	54.2	69	20
Metatarsal	GL	257	257	257	1
	Bp	50.51	43	56.2	15
	Bd	58.99	48.5	84.9	32
Calcaneus	GL	140.13	124.8	156	23

TABLE 3.7. ALL MEASUREMENTS TAKEN FROM OTHER SPECIES IN THE KAWA COLLECTION.

Ovis aries											
Bone	Fusion	Code	Measurement	Code	Measurement	Code	Measurement	Code	Measurement	Code	Measurement
2nd Phalanges	fus	GL	25.14	Bp	13.4	SD	10.33	Bd	9.81		
Equus sp											
Bone	Fusion	Code	Measurement	Code	Measurement	Code	Measurement	Code	Measurement	Code	Measurement
Astragalus	u	GH	44.86	BFd	35.69	LmT	43.32				
Astragalus	u	GH	45.3	BFd	34.21	LmT	42.93				
2nd Phalanges	fus	GL	35.26	Bp	35.88	BFp	33.61	Dp	22.94	Bd	33.7
Tibia	u fus	Bd	49.47	Dd	33.85						
Felis sp.											
Bone	Fusion	Code	Measurement	Code	Measurement	Code	Measurement	Code	Measurement	Code	Measurement
Astragalus		GL	26.68								
Mandible		1	53.76	2	51.11	5	20.1	7	7.16		
Humerus	unf fus	GL	94.14	GLC	92.58	Bp	14.37	SD	6.05	Bd	15.82
Radius	fus unf	GL	88.85	BP	7.22			SD	5.1		
Radius	fus unf	GL	88.98	BP	7.46			SD	5.09	Bd	11.12
Femur	unf	SD	7.81	Bd	17.79						
Tibia*	fus fus	GL	126.93	Bp	21.52	Bd	15.05				
Metatarsal III*	fus fus	GL	52.46	Bd	5.55						

*From context (FP7)102, the remaining bones all originate from context (FP7)82

Canis familiaris										
Bone	Fusion	Code	Measurement	Code	Measurement	Code	Measurement	Code	Measurement	
Radius	fusfus	GL	151	Bp	16.7	SD	11	Bd	20.7	
Femur	fus			Bp	32.2	DC	16.6			

TABLE 3.8. DISTRIBUTION OF STATE-OF-FUSION FOR GOAT (NISP 55) LONG BONES FROM KAWA.

For goat age is based on Noddle 1974, collected by Reitz and Wing 1999 and for sheep/goat age is based on Schmid 1972, Silver 1970 and Noddle 1974, collected by Reitz and Wing 1999.

	Unfused	Fusing	Fused	Age Category
Early Fusion				
Metapodium proximal	-	-	7	Before birth
Radius proximal	-	-	2	4-9 months
Humerus distal	-	-	4	11-13 months
Scapula	-	-	4	9-13 months
Phalanges 2	-	-	6	9-13 months
Phalanges 1	1	-	9	11-15 months
Medium Fusion				
Metapodium distal	4	1	2	23-36 months
Calcaneus	2	-	-	23-60 months
Late Fusion				
Femur distal	2	-	-	23-60 months
Humerus proximal	-	-	1	23-84 months
Femur proximal	4	-	1	23-84 months
Ulna proximal	2	-	-	24-84 months
Radius distal	3	-	-	33-84 months

TABLE 3.9. DISTRIBUTION OF STATE OF FUSION FOR SHEEP/GOAT (NISP 58) LONG BONES FROM KAWA.

For sheep/goat age is based on Schmid 1972, Silver 1970 and Noddle 1974, collected by Reitz and Wing 1999.

	Unfused	Fusing	Fused	Age Category
Early Fusion				
Metapodium proximal	-	-	1	Before birth
Radius proximal	-	-	2	3-10 months
Humerus distal	-	-	1	3-13 months
Scapula	-	-	2	6-13 months
Phalanges	-	-	2	6-16 months
Medium Fusion				
Tibia distal	2	1	1	15-24 months
Metapodium distal	2	-	-	18-36 months
Late Fusion				
Tibia proximal	2	-	-	23-60 months
Femur distal	3	-	1	23-60 months
Femur proximal	-	-	1	23-84 months
Radius, distal	1	-	-	33-84 months
Humerus proximal	1	-	-	23-84 months
Ulna proximal	1	-	-	24-84 months
Vertebrate	32	-	2	48-60 months

TABLE 3.10. ALL MEASUREMENTS TAKEN ON GOAT REMAINS IN THE KAWA COLLECTION.

Fusion	Code	Measurement	Code	Measurement	Code	Measurement	Code	Measurement	Code	Measurement
Astragalus										
	GLl	25.1	GLm	23.3	Dl	12.7	Bd	15.4		
	GLl	24.5	GLm	22.7	Dl	12.6	Bd	15.2		
Femur										
unf unf	GL	147.4	GLC	147	Bp	32.8	DC	16.8	Bd	28.1
unf unf			GLC	147.7	Bp	32.2	DC	16.8	Bd	28.8
unf u					Bp	33.3	DC	18.6		
Humerus										
u fus	Bd	24.9	BT	24.3						
u fus	Bd	25.5	BT	25.1						
u fus	Bd	23.1	BT	22.9						
u fus	Bd	24.7	BT	23.9						
u fus	Bd	24.2	BT	23.7						
Radius										
fus unf	GL	145.2	Bp	24.1	BFp	23.3	SD	12.9	Bd	22.9
fus unf	GL	143.7	Bp	23.8	BFp	23	SD	12.9	Bd	22.5
Metacarpus										
fus fusi	GL	100.3	Bp	19.5	SD	10.8	DD	7.2	Bd	22.3
Metatarsal										
fus fus	GL	113.2	Bp	16.8	SD	10	DD	7.9	Bd	20.4
fus unf	GL	112.1	Bp	16.9	SD	8.6	DD	7.5	Bd	19.8
fus unf			Bp	15.4	SD	8.2	DD	7.1		
fus unf			Bp	16.7	SD	8.5	DD	7.5		
1st Phalanges										
fus	GLpe	40.4	Bp	11.7	Dp	14.1	SD	9	Bd	11.4
fus	GLpe	33.7	Bp	11.1	Dp	12.5	SD	8.7	Bd	10.2
fus	GLpe	36	Bp	11.2	Dp	12.4	SD	8.8	Bd	10.8
fus	GLpe	32.6	Bp	10.4	Dp	11.9	SD	7.7	Bd	9.9
fus	GLpe	33.2	Bp	9.5	Dp	11.6	SD	7.7	Bd	9.5
fus	GLpe	33.4	Bp	9.5	Dp	11.6	SD	7.2	Bd	9.6
fus	GLpe	33.7	Bp	10.8	Dp	11.2	SD	8.8	Bd	11.3
fus	GLpe	33.9	Bp	10.9	Dp	11.7	SD	8.7	Bd	11.2
fus	GLpe	33.3	Bp	9.3	Dp	11			Bd	9.4
2nd Phalanges										
fus	GL	23	Bp	10.3	SD	7.3	Bd	8.3		
fus	GL	21.8	Bp	8.9	SD	6.3	Bd	7.5		
fus	GL	21.8	Bp	10.4	SD	7.4	Bd	8.7		
fus	GL	21.5	Bp	10.3	SD	7.2	Bd	8.2		
fus	GL	22.4	Bp	9	SD	6.1	Bd	7.3		
fus	GL	21.1	Bp	10.2	SD	7.2				

TABLE 3.11. DISTRIBUTION OF SPECIES AT KAWA ACCORDING TO EXCAVATION AREA.

	(AB4)	(AB5)	(AB6)	(AC5)	(AC6)	(AD5)	(AD6)	(BD2)	(FO6)	(FP6)	(FP7)	(ZH5)/(ZI5)
Cattle	6	79		1908	18	3914	100	27	17	204	97	139
Horse/donkey						1	1			20	2	
Camel/dromedary										2		1
Large ruminate	32	448		6576	12	12311	211	18	52	1245	476	81
Sheep & goat		1		8		42	1	5		15	8	183
Antelope & gazelle				1		1			2	1		4
Medium ruminate		3		19	2	158	2		8	63	23	139
Carnivores				6		6			11	1	122	
Bird			6	1		1		1			28	6
Fish	1	7						1			1	7
Rodent			1									
Reptile & amphibian						1				1		
Total	39	538	7	8519	32	16435	315	52	90	1552	757	560

TABLE 3.12. DISTRIBUTION OF SPECIES COMPARING FAUNAL RESULT FROM VARIOUS SITES.

Kawa 2000-1 result are from Burrow, unpublished report, Gala Abu Ahmed results are from Linseele and Pöllath 2015, Gism el-Arba and Kerma result are from Chaix 2006 and Dongola results are from Osypińska 2014.

	Kawa grid squares (AB)/ (AC)/(AD)	Kawa grid squares (FP6) & (FP7)	Kawa grid squares (ZI) & (ZH)	Kawa 2000-1 Areas A & B	Gala Abu Ahmed Other	Gala Abu Ahmed Trench 10	Gism el-Arba	Kerma	Dongola 6th-7th century AD
Pig				4					491
Cattle	6025	301	139	3376	916	3252	2856	17500	1140
Horse/donkey	2	20		6	6		30	1050	
Camel/dromedary		2	1	17					3
Sheep & goat	52	23	183	352	1868	7244	3901	15750	1495
Antelope & gazelle	2	1	4	30	181	222	45	16	17
Carnivores		6	123	4	11	32	7	700	31
Hippopotamus & giraffe							1	17	
Hare					1	28	8		
Hedgehog						3			
Rodent	1				58	394			
Bird	8	28	6	4	55	134	2	29	14
Fish	8	1	7			2	665	80	244
Reptile and amphibian		1			12	18			

4. Bibliography for Volume IV

Acsádi, G. Y. and J. Nemeskéri 1970. *History of human life span and mortality*. Budapest.

Adams, W. Y. 1977. *Nubia, Corridor to Africa*. London.

Agarwal, S. C. 2016. 'Bone morphologies and histories: Life course approaches in bioarchaeology', *American Journal of Physical Anthropology* 159, 130-149.

Alvrus, A. 1999. 'Fracture patterns among the Nubians of Semna South, Sudanese Nubia', *International Journal of Osteoarchaeology* 9, 417–429.

Antoine, D. and J. Ambers 2014. 'The Scientific Analysis of Human Remains from the British Museum Collection: Research Potential and Examples from the Nile Valley', in A. Fletcher, D. Antoine and J. D. Hill (eds), *Regarding the dead: human remains in the British Museum*. London, 20-30.

Antoine, D. and T. Waldron 2023. 'Abnormalities of the vertebral artery: are cervical pressure defects being overlooked in palaeopathology?', in M. Binder, C. A. Roberts and D. Antoine (eds), *The bioarchaeology of Cardiovascular Disease*. Cambridge, 174-201.

Armelagos, G. J. 1969. 'Disease in Ancient Nubia', *Science* 163, 255-259.

Aufderheide, A. C. and C. Rodriguez-Martin 1998. *The Cambridge encyclopedia of human paleopathology*. Cambridge.

Aulagnier, S. P. Haffner, A. J. Mitchell-Jones, F. Moutou and J. Zima 2009. *Mammals of Europe, North Africa and the Middle East*. Paris.

Baek, G. H. and H. J. Lee 2012. 'Classification and Surgical Treatment of Symphalangism in Interphalangeal Joints of the Hand', *Clinics in Orthopedic Surgery* 4, 58.

Bangsgaard, P. 2010. *Ritual Cows or just another flock of Sheep? Faunal Deposit practices at C-Group and Pangrave Cemeteries*. PhD dissertation, Copenhagen University.

Barnes, E. 2012. *Atlas of developmental field anomalies of the human skeleton: a paleopathology perspective*. Hoboken, N.J.

Bass, W. M. 2005. *Human osteology: a laboratory and field manual*. 5th edn. Special publication of the Missouri Archaeological Society, 2. Columbia, Mo.

Bebel, A. and A. Golijewskaja 2015. 'A case of Hyperostosis Frontalis Interna from Deir el-Bahari, Egypt', *Bioarchaeology of the Near East* 9, 45-54.

Behrensmeyer, A. K. 1978. 'Taphonomic and Ecologic Information from Bone Weathering', *Paleobiology* 4, 150-162.

Bell, J. E., A. Gordon and A. F. J. Maloney 1980. 'The Association of Hydrocephalus and Arnold-Chiari Malformation with Spina Bifida in the Fetus', *Neuropathology and Applied Neurobiology* 6, 29-39.

Bell, L. S. and K. Piper 2000. 'An introduction to palaeohistopathology', in M. Cox and S. Mays (eds), *Human osteology in archaeology and forensic science*. repr. Cambridge, 289-306.

Bello, S. M., A. Thomann, M. Signoli, O. Dutour and P. Andrews 2006. 'Age and sex bias in the reconstruction of past population structures', *American Journal of Physical Anthropology* 129, 24-38.

Berry, A. C. and R. J. Berry 1972. 'Origins and relationships of the ancient Egyptians. Based on a study of non-metrical variations in the skull', *Journal of Human Evolution* 1, 199-208.

Berryman, H. E., N. R. Shirley and A. K. Lanfear 2013. 'Low velocity trauma', in M. A. Tersigni-Tarrant and N. R. Shirley (eds), *Forensic anthropology: an introduction*. London, 271-290.

Binder, M. 2014. *Health and Diet in Upper Nubia through Climate and Political Change - A bioarchaeological investigation of health and living conditions at ancient Amara West between 1300 and 800BC*. PhD thesis. Durham University.

Binder, M., C. Roberts, N. Spencer, D. Antoine and C. Cartwright 2014. 'On the Antiquity of Cancer: Evidence for Metastatic Carcinoma in a Young Man from Ancient Nubia (c. 1200BC)', *PLOS ONE* 9(3), e90924.

Binder, M. and N. A. Spencer 2014. 'The bioarchaeology of Amara West in Nubia: Investigating the impacts of political, cultural and environmental change on health and diet', in A. Fletcher, D. Antoine and J. D. Hill (eds), R*egarding the dead: human remains in the British Museum*. The British Museum Research Publication, 197. London, 123-136.

Boessneck, J. 1956. 'Ein Beitrag zur Errechnung der Widerristhöhe nach Metapodienmaßen bei Rindern', *Zeitschrift für Tierzüchtung und Züchtungsbiologie* 68, Issue 1, 75-90.

Bolhofner, K. L. 2017. 'Identity Marker or Medicinal Treatment? An Exploration of the Practice and Purpose of Dental Ablation in Ancient Nubia', in S. E. Burnett and J. D. Irish (eds), *A World View of Bioculturally Modified Teeth*. Gainsville, Fl, 48-61.

Bonnet, C. 1982. 'Les fouilles archéologiques de Kerma (Soudan). Rapport préliminaire des campagnes de 1980-1981 et de 1981-1982', *Genava* n.s. 30, 29-53.

Botham, A. D. 2019. 'Unthinking empiricism and the overdiagnosis of nonlethal cranial injuries: An interdisciplinary review of diagnostic criteria for healing, depressed cranial fractures', *Journal of Archaeological Science*: Reports 27, 101939.

Boulle, E.-L. 2001. 'Evolution of two human skeletal markers of the squatting position: A diachronic study from antiquity to the modern age', *American Journal of Physical Anthropology* 115, 50-56.

Brickley, M. B. 2004. 'Determination of sex from archaeological skeletal material and assessment of parturition', in M. B. Brickley and J. I. McKinley (eds), *Guidelines to the standards for recording human remains*. IFA Paper, 7. Southampton; Reading, 23-25.

Brickley, M. B. 2018. 'Cribra orbitalia and porotic hyperostosis: A biological approach to diagnosis', *American Journal of Physical Anthropology* 167, 896-902.

Brickley, M. B. and R. Ives 2006. 'Skeletal manifestations of infantile scurvy', *American Journal of Physical Anthropology* 129, 163-172.

Brook, I. 2009. 'Sinusitis', *Periodontology 2000* 49, 126-139.

Brooks, S. and J. M. Suchey 1990. 'Skeletal age determination based on the os pubis: A comparison of the Acsádi-Nemeskéri and Suchey-Brooks methods', *Human Evolution* 5, 227-238.

Brothwell, D. R. 1981. *Digging up bones: the excavation, treatment and study of human skeletal remains*. 3rd ed. London.

Bruzek, J. 2002. 'A method for visual determination of sex, using the human hip bone', *American Journal of Physical Anthropology* 117, 157-168.

Buckley, S., D. Usai, T. Jakob, A. Radini and K. Hardy 2014. 'Dental Calculus Reveals Unique Insights into Food Items,

Cooking and Plant Processing in Prehistoric Central Sudan', *PLOS ONE* 9, e100808.

Buikstra, J. E. (ed.) 2019. *Ortner's Identification of Pathological Conditions in Human Skeletal Remains (Third Edition)*. San Diego.

Buikstra, J. E. and D. H. Ubelaker (eds) 1994. *Standards for data collection from human skeletal remains: Proceedings of a seminar at the Field Museum of Natural History, organized by Jonathan Haas*. Archaeological Survey Research Series, 44. Fayetteville, Ark.

Burrow, K. *The Animal Bone from Kawa, Interim Report: 2000-2001 Season*. Unpublished report. Sudan Archaeological Research Society Kawa Archive.

Byers, S., K. Akoshima and B. Curran 1989. 'Determination of adult stature from metatarsal length', *American Journal of Physical Anthropology* 79, 275-279.

Carlson, D. S., G. Armelagos and D. Van Gerven 1974. 'Factors influencing the etiology of cribra orbitalia in prehistoric Nubia', *Journal of Human Evolution* 3, 405-410.

Carson, E. A. 2006. 'Maximum-Likelihood Variance Components Analysis of Heritabilities of Cranial Nonmetric Traits', *Human Biology* 78, 383-402.

Case, D. T. and J. Heilman 2005. 'Pedal symphalangism in modern American and Japanese skeletons', *Homo: Internationale Zeitschrift Fur Die Vergleichende Forschung Am Menschen* 55, 251-262.

Chaix, L. 1992. 'La faune des édifices napatéens à Kerma', in Salah el-Din Mohamed Ahmed, *L'agglomération napatéenne de Kerma. Enquête archéologique et ethnographique en milieu urbain*. Paris, 121-122.

Chaix, L. 2006. 'New data about rural economy in the Kerma culture: the site of Gism el-Arba (Sudan), in K. Kroeper, M. Chłodnicki and M. Kobusiewicz (eds), *Archaeology of Early Northeastern Africa, Studies in African Archaeology vol. 9*, Poznan, 25-38.

Chaix, L. 2007. 'Contribution to the knowledge of domestic cattle in Africa: The osteometry of fossil Bos taurus L. from Kerma, Sudan (2050 – 1750 BC)', in G. Grupe and J. Peters (eds), *Skeletal series and their socio-economic context*. Rahden/ Westf., 69-248.

Chaix, L. and A. Grant 1987. 'A Study of a Prehistoric Population of Sheep (*Ovis aries L.*) from Kerma (Sudan) - Archaeozoological and Archaeological Implications', *Anthropozoologia,* 1(1), 77-92.

Chaudhary, M. and S. D. Chaudhary 2012. 'Osteosarcoma of jaws', *Journal of Oral and Maxillofacial Pathology: JOMFP* 16, 233-238.

Cohen, H., I. Sarie, B. Medlej, F. Bocquentin, T. Toledano, I. Hershkovitz and V. Slon 2014. 'Trauma to the Skull: A Historical Perspective from the Southern Levant (4300BCE-1917CE)', *International Journal of Osteoarchaeology* 24, 722-736.

Cordeiro, C., J. I. Muñoz-Barús, S. Wasterlain, E. Cunha and D. N. Vieira 2009. 'Predicting adult stature from metatarsal length in a Portuguese population', *Forensic Science International* 193, 131.e1-131.e4.

Cunningham, C., L. Scheuer and S. M. Black 2016. *Developmental juvenile osteology*. 2nd edition. Amsterdam.

Davies, W. V. 2001. 'The dynastic tombs at Hierakonpolis: the lower group and the artist Sedjemnetjeru', in W. V. Davies (ed.), *Colour and Painting in Ancient Egypt*. London, 113-125.

Davies-Barrett, A. M., D. Antoine and C. A. Roberts 2019. 'Inflammatory periosteal reaction on ribs associated with lower respiratory tract disease: A method for recording prevalence from sites with differing preservation', *American Journal of Physical Anthropology* 168, 530-542.

Davies-Barrett, A. M., D. Antoine and C. A. Roberts 2023. 'Desert dust and city smoke: investigating the impact of urbanisation and aridification on the prevalence of pulmonary/ pleural inflammation in the Middle Nile Valley (2500 BCE to 1500 CE)', *Bioarchaeology International* [Early view].

Davies-Barrett, A. M., C. A. Roberts and D. Antoine 2021. 'Time to be nosy: Evaluating the impact of environmental and sociocultural changes on maxillary sinusitis in the Middle Nile Valley (Neolithic to Medieval periods)', *International Journal of Paleopathology* 34, 182-196.

Daviet-Noual, V., A.-L. Ejeil, C. Gossiome, N. Moreau and B. Salmon 2017. 'Differentiating early stage florid osseous dysplasia from periapical endodontic lesions: a radiological-based diagnostic algorithm', *BMC oral health* 17, 161.

Derry, D. E. 1913. 'A Case of Hydrocephalus in an Egyptian of the Roman Period', *Journal of Anatomy and Physiology* 47, 436-458.

Driesch, A. von den. 1979. *A Guide to the Measurement of Animal Bones from Archaeological Sites*, Peabody Museum of Archaeology and Ethnology Bulletin, 1. Cambridge, MA.

Duray, S. M. and S. S. Martel 2006. 'A Quantitative Method for Estimation of Volume Changes in Arachnoid Foveae with Age', *Journal of Forensic Sciences* 51, 238-243.

El-Mofty, S. K. 2014. 'Fibro-osseous lesions of the craniofacial skeleton: an update', *Head and Neck Pathology* 8, 432-444.

Esche, E., A. Mummert, J. Robinson and G. Armelagos 2010. 'Cancer in Egypt and Nubia', *Anthropologie* 48, 133-139.

Faccia, K. J. and R. C. Williams 2008. 'Schmorl's nodes: clinical significance and implications for the bioarchaeological record', *International Journal of Osteoarchaeology* 18, 28-44.

Fathi Abdul Hamid Salih Khider 2001. 'Site R18', in D. A. Welsby, *Life on the Desert Edge. 7000 years of Settlement in the Northern Dongola Reach, Sudan*. Sudan Archaeological Research Society Publication 7. London, 224-227.

Fazekas, I. G. and Kósa, F. 1978. *Forensic fetal osteology*. Budapest.

Fernández-Moreno, M., I. Rego, V. Carreira-Garcia and F. J. Blanco 2008. 'Genetics in Osteoarthritis', *Current Genomics* 9, 542-547.

Filer, J. M. 1992. 'Head Injuries in Egypt and Nubia: A Comparison of Skulls from Giza and Kerma', *The Journal of Egyptian Archaeology* 78, 281-285.

Finnegan, M. 1978. 'Non-metric variation of the infracranial skeleton', *Journal of Anatomy* 125, 23-37.

Fuller, D. Q 2004. 'Early Kushite Agriculture: Archaeobotanical Evidence from Kawa', *Sudan & Nubia* 8, 70-74.

Garvin, H. M., S. B. Sholts and L. A. Mosca 2014. 'Sexual dimorphism in human cranial trait scores: Effects of population, age, and body size', *American Journal of Physical Anthropology* 154, 259-269.

Geber, J. and N. Hammer 2018. 'Ossification of the Ligamentum Flavum in a Nineteenth-Century Skeletal Population Sample from Ireland: Using Bioarchaeology to Reveal a Neglected Spine Pathology', *Scientific Reports* 8, 9313.

Goldberg, C. J., D. P. Moore, E. E. Fogarty and F. E. Dowling 2008. 'Scoliosis: a review', *Pediatric Surgery International* 24, 129-144.

Grant, E. M. 1982. 'The use of tooth wear as a guide to the age of domestic ungulates', in B. Wilson, C. Grigson and S. Payne (eds), *Aging and sexing animal bones from archaeological sites.* British Archaeological Reports British Series 109. Oxford, 91-108.

Hancock, S., C. Zinn and G. Schofield 2020. 'The consumption of processed sugar- and starch-containing foods, and dental caries: a systematic review', *European Journal of Oral Sciences* 128, 467-475.

Hansen, M. F., M. Seton and A. Merchant 2006. 'Osteosarcoma in Paget's disease of bone', *Journal of Bone and Mineral Research: The Official Journal of the American Society for Bone and Mineral Research* 21 Suppl. 2, 58-63.

Herbich, T. 2023. 'Magnetic survey at Kawa', in D. A. Welsby (ed.), *Gematon: living and dying in a Kushite town on the Nile. Volume I: Excavations at Kawa, 1997-2018*. Sudan Archaeological Research Society Publication 27. London, 390-404.

Hershkovitz, I., B. M. Rothschild, O. Dutour and C. Greenwald 1998. 'Clues to recognition of fungal origin of lytic skeletal lesions', *American Journal of Physical Anthropology* 106, 47-60.

Hillson, S. 2001. 'Recording dental caries in archaeological human remains', *International Journal of Osteoarchaeology* 11, 249-289.

Hillson, S. 2005. *Teeth*. 2nd edn. Cambridge Manuals in Archaeology. Cambridge.

Hixon, A. L. and L. M. Gibbs 2000. 'Osteochondritis dissecans: a diagnosis not to miss', *American Family Physician* 61, 151-156, 158.

Hoppa, R. D. 2000. 'Population variation in osteological aging criteria: An example from the pubic symphysis', *American Journal of Physical Anthropology* 111, 185-191.

Huber, A. R. and G. S. Folk 2009. 'Cementoblastoma', *Head and Neck Pathology* 3, 133-135.

Jiménez-Brobeil, S. A., Ph. du Souich and I. Al Oumaoui 2009. 'Possible relationship of cranial traumatic injuries with violence in the south-east Iberian Peninsula from the Neolithic to the Bronze Age', *American Journal of Physical Anthropology* 140, 465-475.

Jin, Y. and H.-K. Yip 2002. 'Supragingival Calculus: Formation and Control', *Critical Reviews in Oral Biology & Medicine* 13, 426-441.

Johnstone, C. J. 2004. *A Biometric Study of Equids in the Roman World*. PhD Thesis, University of York, York.

Judd, M. A. 2001. 'The human remains', in D. A. Welsby (ed.), *Life on the desert edge: seven thousand years of settlement in the Northern Dongola Reach, Sudan*. Sudan Archaeological Research Society Publication No. 7. London, 458-543.

Judd, M. A. 2006. 'Continuity of interpersonal violence between Nubian communities', *American Journal of Physical Anthropology* 131, 324-333.

Judd, M. A. 2012. *Gabati: a Meroitic, post-Meroitic and medieval cemetery in central Sudan. Vol. 2: The Physical Anthropology*. Sudan Archaeological Research Society Publication no. 19. London.

Judd, M. A. and J. Irish 2009. 'Dying to serve: the mass burials at Kerma', *Antiquity* 83, 709-722.

Kaniewska, M., M. Haefeli, U. Laesser and T. Niemann 2017. 'That's my STYLEoideum - Symptomatic os styloideum in an adolescent male', *Journal of Radiology Case Reports* 11, 14-19.

Katz, D. and J. M. Suchey 1989. 'Race differences in pubic symphyseal aging patterns in the male', *American Journal of Physical Anthropology* 80, 167-172.

Kaufman, M. H., D. Whitaker and J. McTavish 1997. 'Differential Diagnosis of Holes in the Calvarium: Application of Modern Clinical Data to Palaeopathology', *Journal of Archaeological Science* 24, 193-218.

Kemp, W. L. 2016. 'Postmortem Change and its Effect on Evaluation of Fractures', *Academic Forensic Pathology* 6, 28-44.

Kent, M. (ed.) 2006. *The Oxford dictionary of sports science & medicine*. 3rd ed. Oxford; New York.

Kerr, N. W. 1988. 'A method of assessing periodontal status in archaeologically derived skeletal material', *Journal of Paleopathology* 2, 67-78.

Klaus, H. D. 2018. 'Possible prostate cancer in northern Peru: Differential diagnosis, vascular anatomy, and molecular signaling in the paleopathology of metastatic bone disease', *International Journal of Paleopathology* 21, 147-157.

Klepinger, L. L., D. Katz, M. S. Micozzi and L. Carroll 1992. 'Evaluation of Cast Methods for Estimating Age from the *Os Pubis*', *Journal of Forensic Science* 37, 763-770.

Koudalka, F. 1885. 'Das Verhältnis der Ossa longa zur Skeletthöhe bei den Säugetieren', *Verhandl. D. Naturforsch. Ver. Brünn* 24, 127-153.

Kranioti, E. F. 2015. 'Forensic investigation of cranial injuries due to blunt force trauma: current best practice', *Research and Reports in Forensic Medical Science* 5, 25-37.

Kubicka, A. M., A. Myszka and J. Piontek 2015. 'Geometric Morphometrics: Does the Appearance of the Septal Aperture Depend on the Shape of Ulnar Processes?', *The Anatomical Record* 298, 2030-2038.

Lambert, P. M. 1997. 'Patterns of violence in prehistoric hunter-gatherer societies of coastal southern California', in D. L. Martin and D. W. Frayer (eds), *Troubled times: violence and warfare in the past*. War and society, v. 3. Amsterdam, 77-110.

Leden, I., K. Forslind, B. Svensson and BARFOT study group 2012. 'Ankylosis of wrist and small joints of the hand occurs in rheumatoid arthritis: Diagnostic implication in paleopathology', *International Journal of Paleopathology* 2, 249-251.

Legge, A. J. 1992. *Excavations at Grimes Graves, Norfolk, 1972-76: Animals, Environment and the Bronze Age Economy. Fascicule 4*. London.

Lewis, M. E. 2004. 'Endocranial lesions in non-adult skeletons: understanding their aetiology', *International Journal of Osteoarchaeology* 14, 82-97.

Lewis, M. E. 2007. *The bioarchaeology of children: perspectives from biological and forensic anthropology*. Cambridge studies in biological and evolutionary anthropology 50. Cambridge.

Lewis, M. E. 2019. 'Chapter 17 - Congenital and Neuromechanical Abnormalities of the Skeleton', in Buikstra (ed.), 585-613.

Lewis, M. E. and A. Flavel 2006. 'Age assessment of child skeletal remains in forensic contexts', in A. Schmitt, E. Cunha and J. Pinheiro (eds), *Forensic Anthropology and Medicine*. Totowa, NJ, 243-258.

Lieverse, A. R., D. H. Temple and V. I. Bazaliiskii 2014. 'Paleopathological Description and Diagnosis of Metastatic Carcinoma in an Early Bronze Age (4588+34 Cal. BP) Forager from the Cis-Baikal Region of Eastern Siberia', *PLOS ONE* 9, e113919.

Lingström, P., J. van Houte and S. Kashket 2000. 'Food starches and dental caries', *Critical Reviews in Oral Biology and Medicine: An Official Publication of the American Association of Oral Biologists* 11, 366-380.

Linseele, V. and N. Pöllath 2015. 'Local Foods and Traded Goods – the Faunal Remains from a Napatan Outpost at Gala Abu Ahmed (Sudan, first Millennium BC)', *African Archaeological Review* 32, 537-590.

Lovejoy, C. O., R. S. Meindl, T. R. Pryzbeck and R. P. Mensforth 1985. 'Chronological metamorphosis of the auricular surface of the ilium: A new method for the determination of adult skeletal age at death', *American Journal of Physical Anthropology* 68, 15-28.

Lovell, N. C. 1997. 'Trauma analysis in paleopathology', *American Journal of Physical Anthropology* 104, 139-170.

Mabrey, J. D. and R. D. Fitch 1989. 'Plastic deformation in pediatric fractures: mechanism and treatment', *Journal of Pediatric Orthopedics* 9, 310-314.

Macklin, M. G. and J. C. Woodward 2001. 'Holocene alluvial history and the palaeochannels of the River Nile in the Northern Dongola Reach', in D. A. Welsby, *Life on the Desert Edge: Seven Thousand Years of Human Settlement in the Northern Dongola Reach.* Sudan Archaeological Research Society Publication No. 7. London, 7-13.

Macklin, M. G.,W. H. J. Toonen, J. C. Woodward, M. A. J. Williams, C. Flaux, N. Marriner, K. Nicoll, G. Verstraeten, N. Spencer and D. Welsby 2015. 'A new model of river dynamics, hydroclimatic change and human settlement in the Nile Valley derived from meta-analysis of the Holocene fluvial archive', *Quaternary Science Reviews* 130, 109-123.

Mahmoud Suliman Bashir and D. A. Welsby 2023. 'Excavations of Building Z1', in Welsby (ed.) 2023a, 174-178.

Mallick, I. H., M. H. Thoufeeq and T. P. Rajendran 2004. 'Iliopsoas abscesses', *Postgraduate Medical Journal* 80, 459-462.

Mann, R. W. and D. R. Hunt 2005. *Photographic regional atlas of bone disease: a guide to pathologic and normal variation in the human skeleton*. 3rd ed. Springfield . Ill.

Marques, C. 2019. 'Chapter 19 - Tumors of Bone', in Buikstra (ed.), 639-717.

Marques, C., V. Matos and N. J. Meinzer 2018. 'Proliferative Periosteal Reactions: Assessment of Trends in Europe over the Past Two Millennia', in C. A. Roberts, C. S. Larsen, J. Baten and R. H. Steckel (eds), *The Backbone of Europe: Health, Diet, Work and Violence over Two Millennia*. Cambridge Studies in Biological and Evolutionary Anthropology. Cambridge, 137-174.

Mays, S. 2007. 'Lysis at the anterior vertebral body margin: evidence for brucellar spondylitis?', *International Journal of Osteoarchaeology* 17, 107-118.

Mays, S. 2008. 'Septal aperture of the humerus in a mediaeval human skeletal population', *American Journal of Physical Anthropology* 136, 432-440.

Mays, S., M. B. Brickley and R. Ives 2006. 'Skeletal manifestations of rickets in infants and young children in a historic population from England', *American Journal of Physical Anthropology* 129, 362-374.

McCarthy, E. F. and F. J. Frassica 2015. *Pathology of bone and joint disorders: With clinical and radiographic correlation*. 2nd ed. Cambridge.

Meadows, L. and R. L. Jantz 1992. 'Estimation of stature from metacarpal lengths', *Journal of Forensic Sciences* 37, 147-154.

Meindl, R. S., C. O. Lovejoy, R. P. Mensforth and L. D. Carlos 1985. 'Accuracy and direction of error in the sexing of the skeleton: Implications for paleodemography', *American Journal of Physical Anthropology* 68, 79-85.

Menge, T. J., R. E. Boykin, B. D. Bushnell and I. R. Byram 2014. 'Acromioclavicular osteoarthritis: a common cause of shoulder pain', *Southern Medical Journal* 107, 324-329.

Milner, G. R. and J. L. Boldsen 2012. 'Humeral and Femoral Head Diameters in Recent White American Skeletons', *Journal of Forensic Sciences* 57, 35-40.

Miranker, M. 2016. 'A Comparison of Different Age Estimation Methods of the Adult Pelvis', *Journal of Forensic Sciences* 61, 1173-1179.

Mittler, D. M. and D. P. Van Gerven 1994. 'Developmental, diachronic, and demographic analysis of cribra orbitalia in the medieval Christian populations of Kulubnarti', *American Journal of Physical Anthropology* 93, 287-297.

Molto, J. E., C. L. Kirkpatrick and J. Keron 2019. 'The paleoepidemiology of Sacral Spina Bifida Occulta in population samples from the Dakhleh Oasis, Egypt', *International Journal of Paleopathology* 26, 93-103.

Moore, W. J. and M. E. Corbett 1971. 'The distribution of dental caries in ancient British populations. 1. Anglo-saxon period', *Caries Research* 5, 151-168.

Moraitis, K., C. Eliopoulos and C. Spiliopoulou 2009. 'Fracture Characteristics of Perimortem Trauma in Skeletal Material', *The Internet Journal of Biological Anthropology* 3, 585.

Moraitis, K. and C. Spiliopoulou 2006. 'Identification and differential diagnosis of perimortem blunt force trauma in tubular long bones', *Forensic Science, Medicine, and Pathology* 2, 221-229.

Mutolo, M. J., L. L. Jenny, A. R. Buszek, T. W. Fenton and D. R. Foran 2012. 'Osteological and molecular identification of brucellosis in ancient Butrint, Albania', *American Journal of Physical Anthropology* 147, 254-263.

Niespodziewanski, E. 2014. 'Testing stature equations on a Medieval Upper Nubian skeletal sample.' *American Association of Physical Anthropologists 83rd Annual Meeting*, Calgary, Alberta, Canada. April.

Noddle, B. 1974. 'Ages of epiphyseal closure in feral and domesticated goats and ages of dental eruption', *Journal of Archaeological Science* 1, 195-204.

Osypińska, M. 2007. 'Animal bones remain from the cemetery in el-Zuma (2007 season)', *Polish Archaeology in the Mediterranean* XIX, 488-493.

Osypińska, M. 2014. 'Animal husbandry and meat consumption in Makurite Dongola, Sudan, faunal evidence from the royal residence area, 6th-17th century', *Archaeologia* 64, 67-81.

Osypińska, M. and B. T. Żurawski 2020. 'Pork for pilgrims: livestock breeding and meat consumption at medieval Banganarti, Nubia', *Antiquity* 94 (373), 164-178.

Palazzo, C., F. Sailhan and M. Revel 2014. 'Scheuermann's disease: an update', *Joint Bone Spine* 81, 209-214.

Park, S.-H., K.-S. Park, and J.-H. Hwang 2018. 'Arachnoid Granulations Mimicking Multiple Osteolytic Bone Lesions in the Occipital Bone', *Brain Tumor Research and Treatment* 6, 68-72.

Payne, S. 1973. 'Kill-Off patterns in Sheep and Goats: the mandibles from Aşvan Kale', *Anatolian Studies* 23, 281-303.

Peterson, H. A. 2007. *Epiphyseal growth Plate fractures*. Berlin.

Phenice, T. W. 1969. 'A newly developed visual method of sexing the os pubis', *American Journal of Physical Anthropology* 30, 297-301.

Pihlstrom, B. L., B. S. Michalowicz and N. W. Johnson 2005. 'Periodontal diseases', *Lancet* 366, 1809-1820.

Prowse, T. L. and N. C. Lovell 1995. 'Biological continuity between the A- and C-groups in lower Nubia: Evidence from cranial non-metric traits', *International Journal of Osteoarchaeology* 5, 103-114.

Radini, A., E. Nikita, S. Buckley, L. Copeland and K. Hardy 2017. 'Beyond food: The multiple pathways for inclusion of materials into ancient dental calculus', *American Journal of Physical Anthropology* 162, 71-83.

Ragsdale, B. D., R. A. Campbell and C. L. Kirkpatrick 2018. 'Neoplasm or not? General principles of morphologic analysis of dry bone specimens', *International Journal of Paleopathology* 21, 27-40.

Rahman, A. M. A., S. N. Madge, K. Billing, P. J. Anderson, I. Leibovitch, D. Selva and D. David 2009. 'Craniofacial fibrous dysplasia: clinical characteristics and long-term outcomes', *Eye (London, England)* 23, 2175-2181.

Raikos, A., G. K. Paraskevas, F. Yusuf, P. Kordali, S. Meditskou, A. Al-Haj and B. Brand-Saberi 2011. 'Etiopathogenesis of hyperostosis frontalis interna: a mystery still', *Annals of Anatomy - Anatomischer Anzeiger* 193, 453-458.

Ramachandran Nair, P. N. 1997. 'Apical periodontitis: a dynamic encounter between root canal infection and host response', *Periodontology 2000* 13, 121-148.

Rana, R. S., J. S. Wu and R. L. Eisenberg 2009. 'Periosteal Reaction', *American Journal of Roentgenology* 193, W259-W272.

Raxter, M. H., C. B. Ruff, A. Azab, M. Erfan, M. Soliman and A. El-Sawaf 2008. 'Stature estimation in ancient Egyptians: A new technique based on anatomical reconstruction of stature', *American Journal of Physical Anthropology* 136, 147-155.

Redfern, R. 2017. *Injury and trauma in bioarchaeology interpreting violence in past lives*. Cambridge

Reitz, E. J. and E. S. Wing 1999. *Zooarchaeology*. Cambridge Manuals in Archaeology, Cambridge.

Rekate, H. L. 2009. 'A contemporary definition and classification of hydrocephalus', *Seminars in Pediatric Neurology* 16, 9-15.

Resnick, D. 2002. *Diagnosis of bone and joint disorders*. 4th ed. Philadelphia.

Richards, G. D. and S. C. Anton 1991. 'Craniofacial configuration and postcranial development of a hydrocephalic child (ca. 2500 B.C.-500 A.D.): with a review of cases and comment on diagnostic criteria', *American Journal of Physical Anthropology* 85, 185-200.

Rittemard, C., A. Colombo, P. Desbarats, B. Dutailly, O. Dutour and H. Coqueugniot 2019. 'The periosteum dilemma in bioarcheology: Normal growth or pathological condition? - 3D discriminating microscopic approach', *Journal of Archaeological Science: Reports* 24, 236-243.

Roberts, C. A. 2007. 'A bioarcheological study of maxillary sinusitis', *American Journal of Physical Anthropology* 133, 792-807.

Roberts, C. A. 2016. 'Palaeopathology and its relevance to understanding health and disease today: the impact of the environment on health, past and present', *Anthropological Review* 79, 1-16.

Roberts, C. A. and J. E. Buikstra 2019. 'Chapter 11 - Bacterial Infections', in Buikstra (ed.), 321-439.

Roberts, C. A. and K. Manchester 2010. *The archaeology of disease*. 3rd ed. Stroud.

Rodríguez, S., X. Miguéns, M. S. Rodríguez-Calvo, M. Febrero-Bande and J. I. Muñoz-Barús 2013. 'Estimating adult stature from radiographically determined metatarsal length in a Spanish population', *Forensic Science International* 226, 297.e1-297.e4.

Rose, J. C., S. C. Anton, A. C. Aufderheide, J. E. Buikstra, L. Eisenberg, J. B.Gregg, E. E. Hunt, E. J. Neiburger and B. M. Rothschild 1991. *Skeletal database committee recommendations*. Detroit.

Ruff, C. B. and C. S. Larsen 2014. 'Long bone structural analyses and the reconstruction of past mobility: A historical review', in K. J. Carlson and D. Marchi (eds), *Reconstructing Mobility: Environmental, Behavioral, and Morphological Determinants*. Boston, MA, 13-29.

Rühli, F. J., T. Böni and M. Henneberg 2004. 'Hyperostosis frontalis interna: archaeological evidence of possible microevolution of human sex steroids?', *Homo: Internationale Zeitschrift Fur Die Vergleichende Forschung Am Menschen* 55, 91-99.

Sakaue, K. 2006. 'Application of the Suchey-Brooks system of pubic age estimation to recent Japanese skeletal material', *Anthropological Science* 114, 59-64.

Santos, A. L. 1996. 'How old is this pelvis? A comparison of age at death estimation using the auricular surface of the ilium and os pubis', in G. Pwiti and R. A. Soper (eds), *Aspects of African Archaeology: Papers from the 10th Congress of the PanAfrican Association for Prehistory and Related Studies*. *Aspects of African Archaeology: Papers from the 10th Congress of the PanAfrican Association for Prehistory and Related Studies*. Zinbabwe, 29-36.

Satinoff, M. I. 1972. 'Study of the squatting facets of the talus and tibia in ancient Egyptians', *Journal of Human Evolution* 1, 209-212.

Schaefer, M., L. Scheuer and S. M. Black 2009. *Juvenile osteology: a laboratory and field manual*. Amsterdam; Burlington, MA.

Schmitt, A. 2004. 'Age-at-death assessment using the os pubis and the auricular surface of the ilium: a test on an identified Asian sample', *International Journal of Osteoarchaeology* 14, 1-6.

Schmid, E. 1972. *Atlas of Animal Bones / Knochenatlas*. Amsterdam.

Schultz, M. 2001. 'Paleohistopathology of bone: A new approach to the study of ancient diseases', *American Journal of Physical Anthropology* 116, 106-147.

Scoles, P. V., B. M. Latimer, B. F. DigIovanni, E. Vargo, S. Bauza and L. M. Jellema 1991. 'Vertebral alterations in Scheuermann's kyphosis', *Spine* 16, 509-515.

Settecase, F., H. R. Harnsberger, M. A. Michel, P. Chapman and C. M. Glastonbury 2014. 'Spontaneous Lateral Sphenoid Cephaloceles: Anatomic Factors Contributing to Pathogenesis and Proposed Classification', *AJNR: American Journal of Neuroradiology* 35, 784-789.

Sevara, C., T. Kinnaird, Ahmed El-Ameen Ahmed El-Hassan (Sokhari) and S. Turner 2023. 'New work on landscapes of the Northern Dongola Reach', *Sudan & Nubia* 27, 86-106.

al-Shahed, M. S., H. S. Sharif, M. C. Haddad, M. Y. Aabed, B. M. Sammak and M. A. Mutairi 1994. 'Imaging features of musculoskeletal brucellosis', *RadioGraphics* 14, 333-348.

Shaw, B., C. L. Burrell, D. Green, A. Navarro-Martinez, D. Scott, A. Daroszewska, R. van't Hof, L. Smith, F. Hargrave, S. Mistry, A. Bottrill, B. M. Kessler, R. Fischer, A. Singh, T. Dalmay, W. D. Fraser, K. Henneberger, T. King, S. Gonzalez and R. Layfield 2019. 'Molecular insights into an ancient form of Paget's disease of bone', *Proceedings of the National Academy of Sciences of the United States of America* 116, 10463-10472.

Silver, I. A. 1970. 'The ageing of domestic mammals', in D. Brothwell and E. Higgs, *Science in Archaeology: A Survey of Progress and Research*. London, 283-302.

Simon, C., R. Menk and C. Kramar 2002. 'The human remains from Wadi Shaw (Sudan): a study of physical anthropology and paleopathology', in T. Lenssen-Erz, U. Tegtmeier, and S. Kröplin (eds), *Tides of the desert: contributions to the archaeology and environmental history of Africa in honour to Rudolf Kupfer*. Africa Praehistorica 14. Cologne, 257-276.

Šlaus, M., T. Cicvara-Pećina, I. Lucijanić, M. Pećina and D. Stilinović 2010. 'Osteochondritis dissecans of the knee in a subadult from a medieval (ninth century A.D.) site in Croatia', *Acta Clinica Croatica* 49, 189-195.

Šlaus, M., M. Novak, Ž. Bedić and D. Strinović 2012. 'Bone fractures as indicators of intentional violence in the eastern adriatic from the antique to the late medieval period (2nd-16th century AD)', *American Journal of Physical Anthropology* 149, 26-38.

Smith, R. N. 1969. 'Fusion of Ossification Centres in the Cat', *Journal of Small Animal Practice* 10, 523-530.

Smith-Guzmán, N. E. 2015a. 'Cribra orbitalia in the ancient Nile Valley and its connection to malaria', *International Journal of Paleopathology* 10, 1-12.

Smith-Guzmán, N. E. 2015b. 'The skeletal manifestation of malaria: An epidemiological approach using documented skeletal collections', *American Journal of Physical Anthropology* 158, 624-635.

Stark, R. J., J. S. Cybulski and T. A. Bács 2015. 'Iliacus-piriformis abscess and septic arthritis from Theban Tomb (TT) 65', *International Journal of Paleopathology* 8, 57-63.

Steiger C. 1990. *Vergleichende morphologische Untersuchungen an Einzelknochen des postkranialen Skeletts das Altweltkamele* [dissertation]. Institut für Paläoanatomie, Domestikationsforschung und Geshichte der Tiermedizin der Universität München.

Stenlund, B., I. Goldie, M. Hagberg, C. Hogstedt and O. Marions 1992. 'Radiographic osteoarthrosis in the acromioclavicular joint resulting from manual work or exposure to vibration', *British Journal of Industrial Medicine* 49, 588-593.

Steyn, M. and J. Buskes 2016. 'Skeletal manifestations of tuberculosis in modern human remains', *Clinical Anatomy* 29, 854-861.

Stojanowski, C. M. and M. A. Schillaci 2006. 'Phenotypic approaches for understanding patterns of intracemetery biological variation', *American Journal of Physical Anthropology* 131, 49-88.

Stull, K., L. E. Cirillo, S. J. Cole and C. N. Hulse 2020. 'Subadult sex estimation and KidStats', in, A. R. Klales (ed.), *Sex estimation of the human skeleton: history, methods, and emerging techniques*. 1st edn. Waltham, 219-242.

Studer, J. and A. Schneider 2008. 'Camel Use in the Petra Region, Jordan: 1st century BC to 4th Century AD', *Archaeozoology of the Near East* 8, 581-596.

Taylor, J. H. and D. Antoine 2014. *Ancient lives: new discoveries eight mummies, eight stories*. London.

Temple, D. H. 2016. 'Caries: the ancient scourge', in J. D. Irish and G. R. Scott (eds), *A companion to dental anthropology*. Wiley Blackwell companions to anthropology, 29. Chichester, 433-449.

Tipper, S. 2020. *A Bioarchaeological Analysis of Spinal Pathology across Ancient Nubia between 300 BC and 1500 AD*. PhD thesis. Durham University.

Trinkaus, E. 1975. 'Squatting among the neandertals: A problem in the behavioral interpretation of skeletal morphology', *Journal of Archaeological Science* 2, 327-351.

Trinkaus, E. 1978. 'Bilateral asymmetry of human skeletal non-metric traits', *American Journal of Physical Anthropology* 49, 315-318.

Tully, H. M. and W. B. Dobyns 2014. 'Infantile hydrocephalus: a review of epidemiology, classification and causes', *European Journal of Medical Genetics* 57, 359-368.

Tyrell, A. 2000. 'Skeletal non-metric traits and the assessment of inter- and intra-population diversity: past problems and future potential', in M. Cox and S. Mays (eds), *Human osteology in archaeology and forensic science*. Cambridge, 289-306.

Ubelaker, D. H. 1978. *Human skeletal remains: excavation, analysis, interpretation*. Chicago.

Üstündağ, H. and A. Deveci 2011. 'A possible case of Scheuermann's disease from Akarçay Höyük, Birecik (Şanlıurfa, Turkey)', *International Journal of Osteoarchaeology* 21, 187-196.

Waldron, T. 2021. *Palaeopathology*. 2nd edn. Cambridge manuals in archaeology. Cambridge; New York, NY.

Walker, P. L. 1989. 'Cranial injuries as evidence of violence in prehistoric southern California', *American Journal of Physical Anthropology* 80, 313-323.

Walker, P. L., R. R. Bathurst, R. Richman, T. Gjerdrum and V. A. Andrushko 2009. 'The causes of porotic hyperostosis and cribra orbitalia: a reappraisal of the iron-deficiency-anemia hypothesis', *American Journal of Physical Anthropology* 139, 109-125.

Wapler, U., E. Crubézy and M. Schultz 2004. 'Is cribra orbitalia synonymous with anemia? Analysis and interpretation of cranial pathology in Sudan', *American Journal of Physical Anthropology* 123, 333-339.

Weiss, E. and R. Jurmain 2007. 'Osteoarthritis revisited: a contemporary review of aetiology', *International Journal of Osteoarchaeology* 17, 437-450.

Welsby, D. A. 1996. *The Kingdom of Kush, the Napatan and Meroitic Empires.* London.

Welsby, D. A. 2000. 'The Kawa excavation project.', *Sudan & Nubia* 4, 5-10.

Welsby, D. A. 2011. 'Excavations in the Kushite town and cemetery at Kawa, 2010-11', *Sudan & Nubia :* 17, 437-450.

Welsby, D. A. (ed.) 2023a. *Gematon: Living and Dying in a Kushite Town on the Nile, Excavations at Kawa 1997-2018 vol. I*. Sudan Archaeological Research Society Publication 27. London.

Welsby, D. A. 2023b. 'Introduction', in Welsby (ed.) 2023a, 1-7.

Welsby, D. A. 2023c. 'The Kushite town of Gematon', in Welsby (ed.) 2023a, 8-43.

Welsby, D. A. 2023d. 'Excavations of the painted shrine and other buildings in Area A', in Welsby (ed.) 2023a, 44-78.

Welsby, D. A. 2023e. 'Excavations in Area B', in Welsby (ed.) 2023a, 79-113.

Welsby, D. A. 2023f. 'Excavations in Area F – Building F1, adjacent streets and Building F11', in Welsby (ed.) 2023a, 129-153.

Welsby, D. A. 2023g. 'Excavations within the Kushite cemetery at Gematon (site R18)', in Welsby (ed.) 2023a, 194-359.

Welsby, D. A. 2023h. 'The Kushite cemetery at Gematon (site R18)', in Welsby (ed.) 2023a, 360-389.

Welsby, D. A. and J. H. Taylor 2024. 'The Small Finds', in D. A. Welsby (ed.) *Gematon: Living and Dying in a Kushite Town on the Nile. Volume II. The Artefacts*. Sudan Archaeological Research Society Publication 28. London, 51-244.

Welsby Sjöström, I. 2023. *Gematon: Living and Dying in a Kushite Town on the Nile. Volume III: the pottery*. London.

Weston, D. A. 2008. 'Investigating the specificity of periosteal reactions in pathology museum specimens', *American Journal of Physical Anthropology* 137, 48-59.

Weston, D. A. 2012. 'Nonspecific infection in palaeopathology: interpreting periosteal reactions', in A. L. Grauer (ed.), *A companion to paleopathology*. Chichester, 492-512.

White, T. D., M. T. Black and P. A. Folkens 2012. *Human osteology*. 3rd ed. San Diego, California.

Whiting, R. 2018. 'The physical anthropology', in D. A. Welsby (ed.), *A* Kerma Ancien *cemetery in the northern Dongola reach: excavations at site H29*. Sudan Archaeological Research Society Publication 22. London, 149-201.

Whiting, R., D. Antoine and S. Hillson 2019. 'Periodontal disease and "oral health" in the past: new insights from ancient Sudan on a very modern problem', *Dental Anthropology Journal* 32, 30-50.

Whiting, R., E. L. W. Phillips, D. O'Flynn and D. Antoine 2022. 'Early evidence for cancer in Sudan: an advanced example of bone metastases from ancient Nubia (circa 2500–2050 BCE)', *The Lancet Oncology* 23, 992-994.

Wu, X.-J., L. A. Schepartz, W. Liu and E. Trinkaus 2011. 'Antemortem trauma and survival in the late Middle Pleistocene human cranium from Maba, South China', *Proceedings of the National Academy of Sciences* 108, 19558-19562.

Skeletons in the cemetery and a bucranium in Building F1.

Recent Publications of the Sudan Archaeological Research Society

GEMATON: LIVING AND DYING IN A KUSHITE TOWN ON THE NILE

Volume I. Excavations at Kawa, 1997-2018
edited by
D. A. Welsby 2023

GEMATON: LIVING AND DYING IN A KUSHITE TOWN ON THE NILE

Volume II. The Artefacts
edited by
D. A. Welsby 2024

SUDAN ARCHAEOLOGICAL RESEARCH SOCIETY

ARCHAEOPRESS www.archaeopress.com